

---

# **Molybdenum transport in plants**

A thesis submitted for the Degree of the Doctor of Philosophy

at

**The University of Adelaide**

Discipline of Wine and Horticulture,  
School of Agriculture, Food and Wine.

Submitted by

**Kate Louise Fitzpatrick**

April, 2008

---

# Table of Contents

---

<b>Table of Contents</b> .....	1
<b>List of Figures</b> .....	7
<b>List of Tables</b> .....	13
<b>Abstract</b> .....	15
<b>Declaration</b> .....	17
<b>Acknowledgments</b> .....	18
<b>Publications</b> .....	20
<b>Abbreviations</b> .....	21
<b>1. Chapter 1 – Literature review</b>	
1.1 Introduction.....	23
1.2 Molybdenum nutrition in plants.....	24
1.2.1 Soil factors affecting molybdenum uptake in plants.....	24
1.2.2 Molybdenum deficiency symptoms in plants.....	25
1.2.3 Effect of molybdenum deficiency amongst plant species.....	26
1.2.4 Molybdenum deficiency in <i>Vitis vinifera</i> cv. Merlot.....	27
1.3 Biochemical and physiological roles of molybdenum on plants.....	28
1.3.1 The molybdenum cofactor (Moco).....	28
1.4 Molybdenum containing enzymes.....	29
1.4.1 Nitrate reductase (NR) .....	29
1.4.2 Nitrogenase.....	30
1.4.3 Other molybdenum containing enzymes.....	31
1.5 Molybdenum transport in the model organism, <i>Escherichia coli</i> .....	32
1.5.1 The <i>Escherichia coli</i> ABC-MoO <sub>4</sub> <sup>2-</sup> transport system ( <i>modABCD</i> operon) .....	33
1.6 Mechanism for molybdenum uptake in plants.....	34
1.6.1 Plant phosphate transporters.....	34
1.6.2 Plant P-type ATPases.....	35
1.7 Plant sulfate transporters.....	36
1.7.1 Sulfur assimilation, reduction and metabolism.....	36
1.7.2 Phylogenetic analysis of plant sulfate transporters.....	36
1.7.3 Topology of plant sulfate transporters.....	37
1.7.4 Regulation of sulfate transporters.....	37

1.8 Sulfate transporters – the new molybdenum transport system?.....	38
1.8.1 Identification of sulfate transporters in <i>Saccharomyces cerevisiae</i> ...	40
1.8.2 Identification of <i>Stylosanthes hamata</i> sulfate transporters.....	41
1.8.3 Identification of putative sulfate transporters on the symbiotic membrane of nodules.....	42
1.9 General aims of thesis.....	42

## **Chapter 2 – Identification MoO<sub>4</sub><sup>2-</sup> transport proteins by functional yeast complementation**

2.1 Introduction.....	53
2.2 Methods.....	56
2.2.1 Mutant generation.....	56
2.2.1.1 Toxicity determination.....	56
2.2.1.2 EMS mutagenesis of wild type yeast Invsc1.....	56
2.2.2 Targeted gene approach to identify molybdenum transport proteins using the Low Mo assay.....	57
2.2.2.1 Molybdenum removal from media and glassware.....	57
2.2.3 Identification of putative MoO <sub>4</sub> <sup>2-</sup> and SO <sub>4</sub> <sup>2-</sup> transport proteins using functional yeast complementation.....	57
2.2.3.1 <i>Vitis vinifera</i> culture.....	57
2.2.3.2 Total and Poly (A) <sup>+</sup> RNA isolation.....	58
2.2.3.3 cDNA library construction.....	59
2.2.3.4 Ligation into pYES3 via Gateway® Technology.....	59
2.2.3.5 cDNA library amplification.....	59
2.2.3.6 Functional complementation of YSD1 with <i>Vitis vinifera</i> cDNA.....	60
2.2.3.7 Yeast plasmid isolation.....	61
2.2.3.8 DNA sequencing.....	61
2.3 Results.....	63
2.3.1 Determination of molybdenum toxicity to yeast.....	63
2.3.2 Identification of putative MoO <sub>4</sub> <sup>2-</sup> and SO <sub>4</sub> <sup>2-</sup> transport proteins using functional yeast complementation.....	63
2.3.2.1 cDNA library construction and ligation into pYES3 via Gateway® Technology.....	63

2.3.2.2 Functional complementation of YSD1 with <i>Vitis vinifera</i> cv. Pinot noir root cDNA's.....	63
2.4 Discussion.....	66

**Chapter 3 – Functional yeast complementation and characterisation of *Stylosanthes hamata* root cDNA SHST1 and *Glycine max* nodule cDNA GmNod70**

3.1 Introduction.....	76
3.2 Methods.....	76
3.2.1 Gene constructs of SHST1 and GmNod70.....	89
3.2.2 Transformation of YSD1 with SHST1 and GmNod70.....	79
3.2.3 Functional complementation of YSD1 with GmNod70.....	79
3.2.4 Functional complementation of YSD1 with SHST1 on the Low Mo Gal media assay.....	80
3.2.5 Functional expression of SHST1 and GmNod70 in YSD.....	80
3.2.5.1 Yeast cell growth and harvest.....	80
3.2.5.2 <sup>35</sup> SO <sub>4</sub> <sup>2-</sup> and <sup>99</sup> MoO <sub>4</sub> <sup>2-</sup> uptake in yeast.....	80
3.3 Results.....	82
3.3.1 GmNod70 analysis.....	82
3.3.2 Functional complementation of YSD1/GmNod70.....	82
3.3.3 <sup>35</sup> SO <sub>4</sub> <sup>2-</sup> accumulation by YSD1 cells containing GmNod70 or pYES3.....	82
3.3.4 Identification of pre-characterised sulfate transporter SHST1 through a targeted gene approach and functional yeast complementation using the Low Mo Gal media assay.....	83
3.3.5 <sup>35</sup> SO <sub>4</sub> <sup>2-</sup> accumulation by YSD1 cells containing SHST1 or pYES3...	83
3.3.6 <sup>99</sup> MoO <sub>4</sub> <sup>2-</sup> accumulation by YSD1 cells containing SHST1 or pYES3.	84
3.4 Discussion.....	86
3.4.1 Molybdenum transport through SHST1.....	86
3.4.2 GmNod70 properties.....	90

**Chapter 4 – <sup>99</sup>MoO<sub>4</sub><sup>2-</sup> uptake in *Vitis vinifera* L. rootlings and *Glycine max* nodule symbiosomes**

4.1 Introduction.....	116
4.1.1 Molybdenum uptake in <i>Vitis vinifera</i> .....	116
4.1.2 Molybdenum uptake in <i>Glycine max</i> symbiosomes.....	117

4.2 Methods.....	119
4.2.1 <i>Vitis vinifera</i> uptake assay.....	119
4.2.1.1 <i>Vitis vinifera</i> cv. Merlot and Chardonnay culture.....	119
4.2.1.2 $^{99}\text{MoO}_4^{2-}$ uptake assay and protocol for <i>Vitis vinifera</i> cv. Merlot and Chardonnay.....	119
4.2.2 <i>Glycine max</i> symbiosome assay.....	119
4.2.2.1 <i>Glycine max</i> culture.....	119
4.2.2.2 Aerobic <i>Glycine max</i> symbiosome isolation.....	120
4.2.2.3 $^{99}\text{MoO}_4^{2-}$ uptake assay and protocol for <i>Glycine max</i> symbiosomes.....	120
4.3 Results.....	122
4.3.1 $^{99}\text{MoO}_4^{2-}$ accumulation of <i>Vitis vinifera</i> cv. Merlot and Chardonnay plants.....	122
4.3.2 Uptake of $^{99}\text{MoO}_4^{2-}$ by <i>Glycine max</i> symbiosomes.....	122
4.4 Discussion.....	124
4.4.1 $^{99}\text{MoO}_4^{2-}$ accumulation of <i>Vitis vinifera</i> cv. Merlot and Chardonnay plants.....	124
4.4.2 Uptake of $^{99}\text{MoO}_4^{2-}$ by <i>Glycine max</i> symbiosomes.....	125

**Chapter 5 – Effects of foliar applied molybdenum on yield, yield components and quality parameters in *Vitis vinifera* cv. Merlot**

5.1 Introduction.....	135
5.2 Methods.....	138
5.2.1 McLaren Vale Visitor Centre Merlot trial.....	138
5.2.2 Molybdenum application.....	138
5.2.3 Petiole collection and analysis.....	139
5.2.4 Fruit set analysis.....	140
5.2.5 Bunch and berry sampling and analysis.....	140
5.2.6 Grape berry juice extraction.....	141
5.2.7 Total soluble solids (°Brix) determination.....	141
5.2.8 pH determination.....	141
5.2.9 Anthocyanin and total phenolics determination of grape berries.....	141
5.2.10 Climatic data.....	142
5.2.11 Statistical analysis.....	143
5.3 Results.....	144

5.3.1 Fruit set.....	144
5.3.1.1 Regression analysis of flower number and inflorescence length.....	144
5.3.1.2 Fruit set over 3 years.....	144
5.3.2 Yield components.....	144
5.3.2.1 Mean yield per vine.....	144
5.3.2.2 Mean bunches per vine.....	145
5.3.2.3 Mean bunch weight.....	145
5.3.2.4 Mean berries per bunch.....	145
5.3.2.5 Mean berry weight.....	146
5.3.2.6 Mean rachis weight.....	146
5.3.3 Climatic data.....	146
5.3.4 Berry quality.....	146
5.3.4.1 Total soluble solids and pH measurements of grape berry juice from the 2005/2006 growing season (Year 3) .....	146
5.3.4.2 Anthocyanin and total phenolics determination of grape berry juice from the 2005/2006 growing season (Year 3) .....	147
5.3.5 Petiole nutrients.....	147
5.3.5.1 Molybdenum petiole concentration.....	147
5.3.5.2 Sulfur petiole concentration.....	147
5.3.5.3 Total nitrogen petiole concentration.....	148
5.3.5.4 Copper petiole concentration.....	148
5.3.5.5 Potassium petiole concentration.....	148
5.3.5.6 Boron petiole concentration.....	149
5.3.5.7 Zinc petiole concentration.....	149
5.4 Discussion.....	150
5.4.1 Molybdenum transport and translocation within <i>Vitis</i> sp.....	150
5.4.2 Petiole nutrient profiles.....	152
5.4.3 Yield and yield component responses in relation to foliar application of molybdenum.....	153
5.4.4 Berry quality parameters.....	154

## **Chapter 6 – General discussion**

6.1 Identification of molybdenum transport proteins.....	194
--	-----

6.2 Functional complementation in yeast to identify molybdenum transport proteins in <i>Vitis vinifera</i> .....	195
6.3 SHST1 – the new molybdenum transport system.....	196
6.4 Molybdenum transport and translocation in plants.....	198
6.4.1 Molybdenum uptake in <i>Vitis vinifera</i> .....	198
6.4.2 Molybdenum uptake in <i>Glycine max</i> symbiosomes.....	200
6.5 The effects of foliar applied molybdenum on yield, yield components, quality parameters and petiole nutrient content in <i>Vitis vinifera</i> cv. Merlot.....	201
6.5.1 Molybdenum fertilisation and its effects on productivity in <i>Vitis vinifera</i> cv. Merlot.....	201
6.5.2 Petiole nutrient content.....	202
6.5.3 Yield and yield components responses to molybdenum sprays.....	202
6.5.4 Quality parameters.....	203
6.6 Future research directions.....	203
6.7 Conclusion.....	204
<b>Bibliography</b> .....	205
<b>Appendix 1</b> .....	219
<b>Appendix 2</b> .....	222
<b>Appendix 3</b> .....	223
<b>Appendix 4</b> .....	238

## List of Figures

---

Figure 1. Molybdenum deficiency responses in grapevines.....	44
Figure 1.2 Molybdenum deficiency phenotypes in <i>V.vinifera</i> cv. Merlot.....	45
Figure 1.3 The chemical structure of the molybdenum cofactor (Moco).....	46
Figure 1.4 The position in which Moco is found within the 4 plant enzymes (modified from Mendel and Hansch, 2002; Mendel and Bittner, 2006).....	47
Figure 1.5 Transmission electron micrograph showing a symbiosome isolated from a soybean root nodule infected cell. The bacterioids are contained within the peribacteriod space (PBS), which is enclosed by the peribacteriod membrane (PBM). ....	48
Figure 1.6 Molybdate transport in <i>E.coli</i> . ....	49
Figure 1.7 Phylogenetic analysis of plant sulfate transporters from <i>Arabidopsis thaliana</i> (At), <i>Vitis vinifera</i> EST's (Vv), <i>Oryza sativa</i> (Os) and <i>Stylosanthes hamata</i> (Sh), <i>Glycine max</i> (Gm) <i>Lotus japonicus</i> (Lj) and <i>Zea mays</i> (Zm). ....	50
Figure 1.8 Alignment of amino acid sequences of SHST1, SHST2 and SHST3.....	52
Figure 2.1 Yeast strain $\Sigma$ 1278b plated on varying concentrations of molybdenum to determine toxicity levels.....	67
Figure 2.2 Yeast strain S288c plated on varying concentrations of molybdate to determine toxicity levels.....	68
Figure 2.3 Yeast strain Invsc1 plated on varying concentrations of molybdate to determine toxicity levels.....	69
Figure 2.4 A schematic diagram of Gateway® cDNA library construction and Gateway® recombination reactions used in the Gateway cDNA library construction manual.....	70



Figure 2.5 Vector map of pDONR™222 (Invitrogen, 2006).....	72
Figure 2.6 Vector map of pYES3-DEST.....	73
Figure 2.7 Digest of inserts contained within <i>V.vinifera</i> cv. Pinot noir cDNA library.....	74
Figure 2.8 Low S (100 μM) Glu and Low S (100 μM) Gal plates containing putative sulfate transport proteins in YSD1.....	75
Figure 3.1 Kyte/Doolittle hydrophilicity analysis of GmN#70 and GmNod70.....	95
Figure 3.2 Multiple sequence alignment of amino acid sequences of LjSST1, AtSultr1;2, AtSultr1;2, SHST1, GmN#70 and GmNod70.....	96
Figure 3.3 Phylogenetic tree of sulfate transporters from <i>Arabidopsis thaliana</i> , <i>S. cerevisiae</i> , <i>Lotus japonicus</i> , <i>Stylosanthes hamata</i> , <i>Glycine max</i> and <i>Brassica</i> spp. with homology to GmNod70 cloned from this study in addition to GmN#70 identified by Kouchi and Shingo (1993).....	98
Figure 3.4 Growth of YSD1 and Invsc1 cells transformed with either the empty pYES3 vector, or pYES3 vectors containing either SHST1 or GmNOD70. 1=SHST1/pYES3 expressed in YSD1, 2=GmNod70/pYES3 expressed in YSD1, 3=pYES3 expressed in YSD1 4=pYES3 expressed in Invsc1. ....	99
Figure 3.5. Accumulation of <sup>35</sup> SO <sub>4</sub> <sup>2-</sup> by YSD1 cells containing GmNod70 or pYES3.....	100
Figure 3.6 Growth of YSD1 and Invsc1 cells transformed with either the empty pYES3 vector or the pYES3 vector containing SHST1 on various concentrations of molybdenum.....	101
Figure 3.7. Accumulation of <sup>35</sup> SO <sub>4</sub> <sup>2-</sup> YSD1 cells containing SHST1 or pYES3 grown in 2xTL Gal media.....	102

Figure 3.8 Accumulation of $^{35}\text{SO}_4^{2-}$ by YSD1 cells containing SHST1 or pYES3 grown in Low Mo Gal media.....	103
Figure 3.9 Competition of $^{35}\text{SO}_4^{2-}$ uptake in YSD1 cells containing SHST1 or pYES3 grown in 2xTL Gal.....	104
Figure 3.10 Competition of $^{35}\text{SO}_4^{2-}$ uptake in YSD1 cells containing SHST1 or pYES3 grown in Low Mo Gal.....	105
Figure 3.11 Competitive inhibition of $^{35}\text{SO}_4^{2-}$ uptake by YSD1 cells containing SHST1 grown in 2xTL Gal.....	107
Figure 3.12 Accumulation of $^{99}\text{MoO}_4^{2-}$ in YSD1 cells containing SHST1 or pYES3 grown in Low Mo Gal (10 nM $\text{MoO}_4^{2-}$ ).....	108
Figure 3.13 Accumulation of $^{99}\text{MoO}_4^{2-}$ in YSD1 cells containing SHST1 or pYES3 grown in Low Mo Gal (80 nM $\text{MoO}_4^{2-}$ ).....	109
Figure 3.14 Concentration dependent accumulation of $^{99}\text{MoO}_4^{2-}$ in YSD1 cells containing SHST1 or pYES3 grown in Low Mo Gal.....	110
Figure 3.15 Concentration dependent accumulation of $^{35}\text{SO}_4^{2-}$ in YSD1 cells containing SHST1 or pYES3 grown in 2xTL.....	113
Figure 3.16 Substrate competition of $^{99}\text{MoO}_4^{2-}$ uptake in YSD1 cells containing SHST1 or pYES3 grown in Low Mo Gal.....	114
Figure 3.17 Influence of external pH on the uptake of $^{99}\text{MoO}_4^{2-}$ YSD1 cells containing SHST1 or pYES3. ....	115
Figure 4.1 Accumulation of $^{99}\text{MoO}_4^{2-}$ over time in root tissue of Merlot and Chardonnay rootlings grown without molybdenum.....	128
Figure 4.2 Accumulation of $^{99}\text{MoO}_4^{2-}$ over time in root tissue of Merlot and Chardonnay rootlings grown with molybdenum.....	129

Figure 4.3 Concentration dependent accumulation of $^{99}\text{MoO}_4^{2-}$ in soybean symbiosomes from plants grown with and without molybdenum.....	130
Figure 4.4 A. Concentration dependent accumulation of $^{99}\text{MoO}_4^{2-}$ in soybean symbiosomes from plants grown without molybdenum and D. Concentration dependent accumulation of $^{99}\text{MoO}_4^{2-}$ in soybean symbiosomes from plants grown with molybdenum.....	133
Figure 5.1 Diagram showing grapevine shoot structure. ....	140
Figure 5.2. Regression analysis to determine number of flowers per inflorescence. ....	156
Figure 5.3 Mean % fruit set over the 3 year trial period for the 4 clones.....	157
Figure 5.4 Mean yield per vine (kg/vine) over the 3 year trial period for the 4 clones....	158
Figure 5.5 Mean bunch number per vine over the 3 year trial period for the 4 clones.....	159
Figure 5.6 Mean bunch weight (g) over the 3 year trial period for the 4 clones.....	160
Figure 5.7 Mean berry number per bunch over the 3 year trial period for the 4 clones...	161
Figure 5.8 Mean berry weight (g) over the 3 year trial period for the 4 clones.....	162
Figure 5.9 Mean rachis weight (g) over the 3 year trial period for the 4 clones.....	163
Figure 5.10 Mean monthly minimum, maximum and rainfall for years 2003 to 2006.....	164
Figure 5.11 Mean harvest total soluble solids ( $^{\circ}\text{Brix}$ ) from the 2005/2006 growing season.....	165
Figure 5.12 Mean harvest pH from the 2005/2006 growing season.....	166
Figure 5.13 Colour or anthocyanin (malvidin-3-glucose) of berries at harvest in 2005/2006 after 3 years of different molybdenum treatments. ....	167

Figure 5.14 Total phenolics of berries at harvest in 2005/2006 after 3 years of different molybdenum treatments. ....	168
Figure 5.15 Mean Mo (mg/kg) concentration in petioles at 50 – 80% flowering for clones D3V14 and Q45-14 over the 3 years of the trial. Suggested deficiency concentrations for molybdenum may occur between 0.05 – 0.09 mg/kg DW (Williams et. al., 2004). ....	169
Figure 5.16 Mean Mo (mg/kg) concentration in petioles at 50 – 80% flowering for clones 8R and 6R over the 3 years of the trial. Suggested deficiency concentrations for molybdenum may occur between 0.05 – 0.09 mg/kg DW (Williams et. al., 2004). ....	170
Figure 5.17 Mean S (g/kg DW) concentration in petioles at 50 – 80% flowering for clones D3V14 and Q45-14 over the 3 years of the trial. ....	175
Figure 5.18 Mean S (g/kg DW) concentration in petioles at 50 – 80% flowering for clones 8R and 6R over the 3 years of the trial. ....	175
Figure 5.19 Mean total N (% DW) concentration in petioles at 50 – 80% flowering for clones D3V14 and Q45-14 over the 3 years of the trial. Adequate levels of total N occur between 1.8 – 3% DW (Reuter and Robinson, 1997). ....	177
Figure 5.20 Mean total N (% DW) concentration in petioles at 50 – 80% flowering for clones 8R and 6R over the 3 years of the trial. Adequate levels of total N occur between 1.8 – 3% DW (Reuter and Robinson, 1997). ....	178
Figure 5.21 Mean Cu (mg/kg DW) concentration in petioles at 50 – 80% flowering for clones 8R and 6R over the 3 years of the trial. Adequate levels of Cu occur between 6 – 11 mg/kg DW (Reuter and Robinson, 1997). ....	181
Figure 5.22 Mean Cu (mg/kg DW) concentration in petioles at 50 – 80% flowering for clones 8R and 6R over the 3 years of the trial. Adequate levels of Cu occur between 6 – 11 mg/kg DW (Reuter and Robinson, 1997). ....	182

Figure 5.23 Mean K (% DW) concentration in petioles at 50 – 80% flowering for clones D3V14 and Q45-14 over the 3 years of the trial. Adequate levels of K occur between 1.8 – 3% DW (Reuter and Robinson, 1997). .....	184
Figure 5.24 Mean K (% DW) concentration in petioles at 50 – 80% flowering for clones 8R and 6R over the 3 years of the trial. Adequate levels of K occur between 1.8 – 3% DW (Reuter and Robinson, 1997). .....	185
Figure 5.25 Mean B (mg/kg DW) concentration in petioles at 50 – 80% flowering for clones D3V14 and Q45-14 over the 3 years of the trial. Adequate levels of B occur between 35 – 70 mg/kg DW (Reuter and Robinson, 1997). .....	188
Figure 5.26 Mean B (mg/kg DW) concentration in petioles at 50 – 80% flowering for clones 8R and 6R over the 3 years of the trial. Adequate levels of B occur between 35 – 70 mg/kg DW (Reuter and Robinson, 1997). .....	189
Figure 5.27 Mean Zn (mg/kg DW) concentration in petioles at 50 – 80% flowering for clones D3V14 and Q45-14 over the 3 years of the trial. Adequate levels of Zn occur at >26 mg/kg DW (Reuter and Robinson, 1997). .....	192
Figure 5.28 Mean Zn (mg/kg DW) concentration in petioles at 50 – 80% flowering for clones 8R and 6R over the 3 years of the trial. Adequate levels of Zn occur at >26 mg/kg DW (Reuter and Robinson, 1997). .....	193

## List of Tables

---

Table 3.1 Initial identification of GmN#70 (D13505) homologues through BLAST searches of the public protein databases. ....	92
Table 4.1 Statistical analyses of the concentrations in concentration dependent accumulation between 0 and 4000 nM of $^{99}\text{MoO}_4^{2-}$ in soybean symbiosomes isolated from plants grown from plants with and without molybdenum.....	131
Table 5.1 Molybdenum foliar spray regime for growing seasons 2003/2004 to 2005/2006.....	138
Table 5.2 Table of vineyard trial site and spray regime imposed. ....	155
Table 5.3 Treatment differences between the treatments for molybdenum petiole concentrations in years 1, 2 and 3 of the trial.....	171
Table 5.4 Clonal differences between the treatments for molybdenum petiole concentrations in years 1 and 3 of the trial. ....	173
Table 5. 5 Clonal differences between the treatments for sulfur petiole concentrations in year 1, 2 and 3 of the trial. ....	176
Table 5.6 Treatment differences between the treatments for nitrogen petiole concentrations in years 2 and 3 of the trial. ....	179
Table 5.7 Clonal differences between the treatments for nitrogen petiole concentrations in year 1, 2 and 3 of the trial. ....	180
Table 5.8 Treatment differences between the year and clones for copper petiole concentrations in years 1 and 2 of the trial. ....	183
Table 5.9 Treatment differences between the years and clones for potassium petiole concentrations in years 2 and 3 of the trial. ....	186

Table 5.10 Treatment differences between the years and clones for potassium petiole concentrations in years 2 and 3 of the trial. ....	187
Table 5. 11 Treatment differences between the years and clones for boron petiole concentrations in years 2 and 3 of the trial.....	190
Table 5. 12 Clonal differences between the years and treatment for boron petiole concentrations in years 1, 2 and 3 of the trial.....	191

Molybdenum (Mo) is an essential micronutrient required by plants. It is biologically inactive until bound in a pterin compound named the molybdenum cofactor (Moco) that binds to apoproteins used in both reductive and oxidative reactions such as nitrate reductase (NR), xanthine dehydrogenase (XDH), aldehyde oxidase (AO) and sulfite oxidase (SOX). In *Vitis vinifera* cv. Merlot, molybdenum deficiency is common amongst vines grown on own roots in acidic soils often resulting in yield reductions. Foliar application of molybdenum sprays increases yield and remedies deficiency indicating that Merlot grown on own roots has a reduced capacity for molybdenum uptake from the soil.

Molybdenum generally occurs as molybdate ( $\text{MoO}_4^{2-}$ ) within the soil solution. The mechanism(s) involved in molybdenum transport have recently been discovered in plants, although are well characterised within prokaryotic systems. Unfortunately, no homologues of prokaryotic genes involved in molybdate transport exist within eukaryotes. It has been suggested that molybdenum transport in plants may occur through other systems including sulfate transporters due to chemical similarities between sulfate and molybdate.

A yeast functional complementation approach using a sulfate transport mutant was initially used to identify novel putative plant molybdenum transport proteins. A cDNA library derived from Pinot noir roots starved of molybdenum was screened for transporters. Unfortunately, no cDNAs were identified that met the requirements of a molybdenum transporter when screened on media containing low amounts of molybdenum. However, a number of putative cDNA's partially complemented the yeast mutant YSD1, however none of these could be validated in second round screens.

A candidate gene approach was then initiated to identify pre-characterised genes that may also have capacity to transport molybdenum. The plant sulfate transporter, SHST1, restored growth of YSD1 on media containing low amounts of molybdenum. Kinetic analysis using  $^{99}\text{MoO}_4^{2-}$  to trace molybdenum transport in yeast cells demonstrated that SHST1 enhanced the uptake of molybdenum at nM concentrations. The uptake was not inhibited by sulfate, but the transport of sulfate was reduced with molybdenum. Further analysis demonstrated that SHST1 did prefer sulfate as the substrate but molybdenum could compete at higher concentrations. This result is the first measurement of molybdenum being transported through a pre characterised sulfate transport protein.



Whole plant experiments using rooted grapevine cuttings and  $^{99}\text{MoO}_4^{2-}$  to trace molybdenum movement into plants indicated that Merlot did not have reduced capacity to uptake molybdenum compared to other varieties that do not suffer from molybdenum deficiencies such as Chardonnay. When plants were grown with molybdenum, Merlot accumulated more molybdenum than Chardonnay, with the reverse being true when plants were grown without molybdenum. Similar experiments were performed on symbiosomes isolated from *Glycine max* grown with and without molybdenum. Symbiosomes absorbed more molybdenum when plants were grown without molybdenum.

A field site was established to look at the molybdenum profiles within petioles against yield responses over a 3-year period. Molybdenum application did not increase the yield amongst vines despite all vines initially being deficient in molybdenum. There were no cumulative effects of molybdenum application over the trial, however, molybdenum did have limited translocation ability within the vine system.

## Declaration

---

The research presented in this thesis is my own work unless otherwise stated. The project was completed at The University of Adelaide, within the School of Agriculture, Food and Wine. This work contains no material which has been accepted for the award of any other degree or diploma in any university or other tertiary institution except where it is related to the scope of this project and, to the best of my knowledge and belief, contains no material previously published or written by another person, except where due reference has been made in the text.

Work on various aspects of the project were analysed by individuals including Mrs. Teresa Fowles and Mr Lyndon Palmer of Waite Analytical Services who were both involved in the ICP-MS analysis. The Bureau of Meteorology also kindly provided the climatic data.

I give consent to this copy of my thesis being made available in the University Library.

I acknowledge that copyright of published works contained within this thesis (as listed within the bibliography) resides with the copyright holder(s) of those works.

Kate L. Fitzpatrick

April, 2008

## Acknowledgments

---

Firstly, I would like to thank my supervisors, Dr Brent Kaiser and Prof. Steve Tyerman. Thankyou to Brent who has continued to support me in my career and provide endless encouragement in an often difficult and challenging project. I appreciate all the time that he has helped me with experiments, advice, feedback and showing me the ropes in the world of molecular biology. I have been very lucky to have such a supportive a supervisor who was always willing to fit in an uptake experiment!

Also thankyou to Steve, who provided me with my initial stepping stone into plant science. Steve and has supported me throughout my Honours and now my PhD. I appreciate all of his feedback, ideas and encouragement through out my career. I look forward to collaborating with both Brent and Steve in the future.

The CRC for Viticulture and the McLaren Vale Vine Improvement Society have funded my PhD research and I am grateful for the support and continual interest in my work from both organizations and the opportunities that have arisen.

Thankyou to all the people that have helped me in this journey...there are so many! I would like to thank the fabulous lab in which I have spent the last 4 years working in, those include Megan Shelden, Patrick Louglin, Scott Cater, Dr. Sunita Ramesh and Rebecca Vandeleur. Thanks to Meg who taught me so much about molecular biology and always was willing to answer my many, many questions (especially when things didn't work!). Special thanks should be given to Pat and Scotty for helping me with what seemed like endless uptakes, lifting cumbersome hydroponic equipment and lead. Both Pat and Scott have been great to work with in the lab. I also appreciate all the times that Sunita helped me, she was never too busy to offer advice and assistance. You are all not only colleagues, but also life long friends.

Thankyou to all the techies that have helped me along the way, especially Wendy Sullivan who I first met while on work experience in Year 10 at Flinders University. I must have liked it to stick around for so long! Thankyou to all the lab techs that have been with Team Kaiser over the years including Steve Choimes, Jess Parker, Jana Koleski and Nenah MacKenzie. Your help was always appreciated.

Thankyou to my parents and grandparents who have always supported me. They were always interested in my work and listed to me ramble on, often I am sure, not knowing what I was talking about! I appreciate all the times that I practiced my seminars in front of Mum who always nodded approvingly and though I always asked her to stop me if she didn't understand anything, she never did!

My friends, Felicity and Anthony Cox, Kimberley and Matthew Whittle and Pete and Claire Wirth have also been a great support and a stress relief during this time. Thanks for putting up with me during this time and I am sorry for my standard response of my thesis being finished in a month!

Lastly, thankyou to my fiancé, Matthew Fitzpatrick. Thankyou so much for supporting me, loving me, helping me, and giving me the occasional, but not un-due, reality check! I don't think I would have made it through without your encouragement.

## Publications

---

Kaiser, B. N., **Gridley, K.L.**, Ngairé Brady, J., Phillips, T, Tyerman, S. D. (2006) The role of molybdenum in agricultural plant production. *Annals of Botany (London)*. 96(5) 745 – 754.

**Fitzpatrick, Kate L.**, Tyerman, Stephen D., Kaiser, Brent N. (2008) Molybdate transport through the plant sulfate transporter SHST1. *FEBS Letters*, in press.

## Abbreviations

---

Å	Angstrom
AMP	Ampicillin
AO	Aldehyde oxidase
BLAST	Basic local alignment search tool
BNF	Biological nitrogen fixation
Bp	Base pairs
BSA	Bovine serum albumin
cDNA	Complementary deoxyribonucleic acid
DNA	Deoxyribonucleic acid
DTT	Dithiothreitol, threo-2-,3-dihydroxy-1,4-dithiolbutane
dH <sub>2</sub> O	Distilled water
EDTA	Ethylene diamine tetracetic acid
EGTA	Ethylene glycerol tetraacetic acid
EMS	Ethyl methane sulfonate
Gal	Galactose
Glu	Glucose
Kb	Kilobase
kD	Kilo Daltons
K <sub>m</sub>	Michaelis constant
LB	Luria-Bertani media
Low Mo	Low molybdenum media
Low S	Low sulfate media
MSD	Membrane spanning domain
MES	2-(N-Morpholino)ethanesulfonic acid
Moco	Molybdenum cofactor
MPT	Molybdopterin
MSD	Membrane spanning domain
mRNA	Messenger ribonucleic acid
NCBI	National Centre for Biotechnology Information
NRA	Nitrate reductase activity
NR	Nitrate reductase
OD	Optical density
PBM	Peribacteroid membrane

PBS	Peribacteroid space
PCR	Polymerase chain reaction
PVP	Polyvinypolyprrolidone
RNA	Ribonucleic acid
Rnase	Ribonuclease
SBP	Sulfur binding protein
SC	Synthetic complete media
SDS	sodium dodecyl sulfate
SHST1	<i>Stylosanthes hamata</i> sulfate transporter 1
SOX	Sulfite oxidase
STAS	Sulfate transporters and antisigma-factor antagonists
TCA	Trichloroacetic acid
TMD	Transmembrane domain
v/v	volume/volume
$V_{\max}$	maximum velocity of reaction
w/v	weight/volume
XDH	Xanthine dehydrogenase
XO	Xanthine oxidase
YEM	Yeast extract mannitol media
YPAD	Yeast extract peptone dextrose medium with adenine
YSD1	Yeast sulfate deletion mutant 1
2xTL	2 x Homocysteine thiolactone media

# Chapter 1

## Literature review

---

### 1. 1 Introduction

Molybdenum (Mo) is an essential micronutrient required by plants. Within most plants, molybdenum is a trace element found at very low concentrations. Although molybdenum is only required in small amounts in plants, it plays a large role within the plant system. Generally, molybdenum in the soil solution occurs as the molybdate oxyanion ( $\text{MoO}_4^{2-}$ ). Once molybdate is taken up by the plant roots it remains biologically inactive until it is complexed by a unique pterin compound named the molybdenum cofactor (Moco). Moco binds to diverse apoproteins used in both reductive and oxidative reactions (Mendel and Hansch, 2002) including nitrate reductase (NR), aldehyde oxidase (AO), xanthine oxidase/dehydrogenase (XO/XDH) (Marschner, 1995) and sulfite oxidase (SOX) (Hille, 2003).

In *Vitis vinifera* cv. Merlot, molybdenum deficiency is a common occurrence in vines grown in acidic soils on own roots. Molybdenum deficient vines exhibit a bunch phenotype at harvest known as ‘millerandage’. This phenotype results in both reduced



profits for growers and poor bunch quality for winemakers. Jarrett (2002) demonstrated that growing Merlot on rootstocks such as Schwarzmann or 140 Ruggeri reduced the incidence of ‘millerandage’ and possibly the occurrence of molybdenum deficiencies. In a subsequent study, Gridley (2003) found that applying foliar molybdenum to molybdenum deficient vines increased yields by up to 170% among vines grown on own roots, while identical vines grafted to rootstocks did not display the ‘millerandage’ phenotype. This result was interpreted that Merlot grown on own roots may have reduced capacity for molybdenum uptake from the soil or a disruption in molybdenum utilisation once within the plant (Gridley, 2003).

The transport mechanism for molybdenum in plant cells has only recently been discovered (Tejada-Jimenez et. al., 2007; Tomatsu et. al., 2007; Baxter et. al., 2008). In contrast, molybdate transport systems are found in various prokaryotes including *Escherichia coli* (Maupin-Furlow et. al., 1995; Rech et. al., 1996; Imperial et. al., 1998; Grunden et. al., 1999; Self et. al., 1999; Self et. al., 2001; Anderson et. al., 2002; Self, 2002), *Anabaena variabilis* (Thiel et. al., 2002), *Penicillium* spp. (Tweedi and Segel, 1970), *Chlamydomonas reinhardtii* (Llamas et. al., 2000), *Staphylococcus carnosus* (Neubauer et. al., 1999), *Azobacter vinelandii* (Mouncey et. al., 1995), *Clostridium pasteurianum* (Elliot and Mortenson, 1975; Elliot and Mortenson, 1976), in addition to *Rhodobacter capsulatus* (Wang et. al., 1993) and are well characterised.

In plants, it has been suggested that co-transport of molybdenum may occur through various mechanisms including a phosphate uptake system (Heuwinkel et. al., 1992), P-type ATPases, heavy metal transporters (Palmgren and Harper, 1999), non-specific anion transporters (Mendel and Hansch, 2002) in addition to sulfate transporters (Tweedi and Segel, 1970). Sulfate transporters have been implicated in the transport of molybdate in prokaryotes, however this has not been demonstrated in eukaryotes.

## **1.2 Molybdenum nutrition in plants**

### **1.2.1 Soil factors affecting molybdenum uptake by plants**

Molybdenum is a rare element within the soil, with a crustal abundance of 1.2 mg/kg (Smith et. al., 1997). The molybdate ion ( $\text{MoO}_4^{2-}$ ) also has similar electron configurations to tungstate ( $\text{WO}_4^{2-}$ ), vanadate ( $\text{VO}_4^{2-}$ ), sulfate ( $\text{SO}_4^{2-}$ ) and phosphate ( $\text{PO}_4^{2-}$ ).

In most soils, molybdenum is not found in its native state but instead bound with other compounds (Smith et. al., 1997). Molybdenum is found within 4 major fractions: 1) dissolved molybdenum in soil solution (water soluble); 2) molybdenum occluded with oxides (e.g. Fe, Al and Mn oxides); 3) solid phases e.g. molybdenite ( $\text{MoS}_2$ ), powellite ( $\text{CaMo}_4$ ), ferrimolybdate ( $\text{Fe}(\text{MoO}_4)_3$ ) wulfenite ( $\text{PbMoO}_4$ ); and 4) molybdenum associated with organic compounds (Reddy et. al., 1997).

The availability of molybdenum to plants within the soil decreases with increasing soil acidity (Gupta, 1997). In soil solutions above pH 4.23, the soluble oxyanion  $\text{MoO}_4^{2-}$  is the predominate form of plant available molybdenum. Below pH 4.23 other molybdenum species are found in decreasing order of pH namely  $\text{MoO}_4^- > \text{HMoO}_4^- > \text{H}_2\text{MoO}_4^0 > \text{MoO}_2(\text{OH})^+ > \text{MoO}_2^{2+}$  (Smith et. al., 1997). Molybdenum availability in many South Australian soils is often low due to high pH and the presence of iron oxides. However, in sandy, well drained, and weathered soils, molybdenum deficiency can also be observed. As a result, molybdenum deficiencies in plants grown in these areas are most often treated with foliar molybdenum applications. In contrast, higher levels of molybdenum can be found in alkaline soils, soils rich in organic matter, and under wet conditions (Smith et. al., 1997).

### **1.2.2 Molybdenum deficiency symptoms in plants**

Plants require trace amounts of molybdenum for growth however, despite this, molybdenum deficiencies are often reported in many plant species (Gupta, 1997). The first report on molybdenum deficiency was demonstrated by Arnon and Stout (1939) using hydroponically grown tomatoes. Growing plants in solution containing no molybdenum produced mottling lesions on the leaves. Altered leaf morphology known as whiptail, was also observed caused by necrosis of the tissue and insufficient differentiation of vascular bundles at early stages of leaf development (Marschner, 1995). Generally, molybdenum deficient plants show symptoms of nitrogen deficiency. This is assumed to be caused by the lack of nitrate reductase (NR) catalysing the initial step in nitrate reduction (Hewitt and Gundry, 1970). Visual symptoms of molybdenum deficiency in plants correlate well with nitrogen deficiency and include stunted growth, a reduction in leaf size and general chlorosis, cupping of older leaves, and necrosis of leaf tips.

It is hypothesized that molybdenum is readily translocated within the plant system (Gupta, 1997) and is considered both phloem and xylem mobile (Marschner, 1995). However, few

studies have been conducted on molybdenum absorption and transport in plants. Using rice (*Oryza sativa*) and bean (*Phaseolus vulgaris*) Kannan and Ramani (1978) studied molybdenum absorption and transport using  $^{99}\text{Mo}$  and  $^{86}\text{Rb}$  for comparison. Molybdenum absorption by roots of *P. vulgaris* revealed greatest transport to the trifoliate leaf, with less being transported to the stem and primary leaves. Foliar application to a primary leaf resulted in equal distribution of molybdenum between the applied and opposite leaf, with most transport occurring towards the stem and the roots. The authors also reported biphasic absorption with a second phase of absorption occurring approximately 6 hours after initial uptake. The absorption of molybdenum was also influenced by the nutrient media that the plants received. When *O. sativa* plants were placed in 3 different nutrient solutions (0.1mM  $\text{CaSO}_4$ , half or full strength Hoaglands) the absorption of molybdenum by roots was lowest for plants in the presence of  $\text{CaSO}_4$  and higher for plants grown in Hoaglands with little difference between half and full strength Hoaglands. Interestingly, in the presence of  $100\ \mu\text{M}\ \text{FeSO}_4^-$ , molybdenum uptake was greatly enhanced in excised rice roots (Kannan and Ramani, 1978).

In an earlier study by Stout and Meagher (1948) on tomato plants using  $^{99}\text{Mo}$  and  $^{93}\text{Mo}$ , observed that roots accumulated  $^{99}\text{Mo}$  quickly from the nutrient solution, with rapid subsequent translocation from roots to shoots. The amount of molybdenum translocated was strongly influenced by the concentration of phosphate. Radiographs of leaves demonstrated an accumulation of molybdenum in the interveinal areas of the leaf, with the most accumulation occurring in areas with the greatest amount of stomatal openings. Little molybdenum was found in the stem. Molybdenum was also not rapidly accumulated by actively metabolising plant cells adjacent to the vascular tissue in the upper parts of the plant.

### **1.2.3 Effect of molybdenum deficiency amongst plant species**

Research has linked increased yield responses in many crops with the application of molybdenum to suspected molybdenum deficient soils. One of the first reports of yield responses to molybdenum application was reported by Gartrell (1966) in cereals. The yield of Ballidu Oats increased with molybdenum application and harvest maturity was enhanced by 10 days. Chipmann et. al. (1970) observed increased yields in cauliflower (*Brassica oleraea*) with molybdenum application and demonstrated that cv. Snowball 84 was able to take up molybdenum more readily than cv. Pioneer, especially at low levels of supply. However, this increased capacity for molybdenum uptake did not make the cultivar

more resistant to molybdenum deficient soils. Yu (2002) also showed that in wheat, different cultivars had different molybdenum uptake properties. Yields increased by 90% in a molybdenum efficient winter wheat cv. 97003 supplied with 0.13 mg molybdenum per kg of soil, compared with only a 50% yield increase in the molybdenum inefficient cv. 97014.

It has been demonstrated that pollen development can be affected by molybdenum deficiency. Agarwala et. al. (1979) has demonstrated that in maize (*Zea mays*) grown under deficient molybdenum levels, a reduction in the size of tassels, male flowers, and a suppression of anthesis occurred. Anthers contained fewer and smaller pollen grains, which appeared, shrivelled and had poor viability. This result may be due to a decrease in sucrose-utilizing capacity due to low invertase activity in molybdenum deficient pollen (Agarwala et. al., 1979). In winter wheat, Chatterjee and Nautiyal (2001) established that molybdenum deficiency resulted in the production of lightweight, immature seeds, which were poor in vigour and germination potential.

#### **1.2.4 Molybdenum deficiency in *Vitis vinifera* cv. Merlot**

In *Vitis vinifera*, symptoms of molybdenum deficiency are commonly found in Merlot particularly amongst vines grown on own roots and in acidic soil. The exact biological cause of this phenomenon is still unknown but is considered to be further propagated by poor molybdenum availability due to soil cation absorption. This phenotype has become a particular problem in South Australia due to the high incidence of acid soils in grape growing regions such as the Adelaide Hills and McLaren Vale areas. General symptoms include small, chlorotic, downward pointing leaves with necrotic papery edges (Figure 1.1A and 1.1B) and shoots exhibiting a ‘zigzag’ phenotype (Robinson and Burne, 2000). Robinson and Burne (2000) have also reported grapevine shoots displaying a dark inky epidermis. Similar observations were also made by Hale et. al. (2001) in *Brassica* species fed with molybdenum where an accumulation of water-soluble blue crystals was found in the vacuoles of the epidermal cells and was identified as a molybdenum-anthocyanin complex by energy dispersive X-ray analysis. However, an anthocyanin-less mutant of *Brassica* was compared with varieties containing normal or high levels of anthocyanin (Hale et. al., 2001) and did not show any differences in the accumulation of molybdenum.

One of the largest problems associated with molybdenum deficiency in Merlot is a reduction in yield caused through a bunch phenotype known as ‘millerandage’ (Figure

1.2A and 1.2B). In this bunch phenotype there is a large proportion of small berries unsuitable for winemaking and a small proportion of large berries. This results in significant reductions in vine yield therefore decreased profits for growers. However, a foliar application of 300 g/ha of molybdenum (as  $\text{Na}_2\text{MoO}_4 \cdot 2\text{H}_2\text{O}$ ) increased yield by 170% in Merlot vines grown on own roots, and 25% and 14% yield increased amongst vines grafted onto Schwarzmann and 140 Ruggeri rootstocks respectively (Gridley, 2003). Yield increases of up to 750% in Merlot vines grown on own roots have been demonstrated by Williams et. al. (2004) after foliar applications of molybdenum. In Gridley's (2003) study, the highest yields were obtained in vines grown on own roots which had the lowest petiole molybdenum content. Vines grown on rootstocks had improved yield increases, however molybdenum levels within petioles were still found to be low and the response was less than that of vines grown on own roots.

### **1.3 Biochemical and physiological roles of molybdenum in plants**

#### **1.3.1 The molybdenum cofactor (Moco)**

Molybdenum itself is catalytically inactive in biological systems until it is complexed by a unique pterin compound named molybdenum cofactor (Moco) (Figure 1.3). Moco binds to diverse apoproteins (Mendel and Hansch, 2002) and is found in all kingdoms. In certain bacteria containing the nitrogen fixing enzyme nitrogenase, molybdenum is not associated with Moco but rather part of a Fe-Mo cluster. Of the 40, mostly bacterial molybdenum containing enzymes, only 4 similar proteins exist in plants (Mendel and Hansch, 2002).

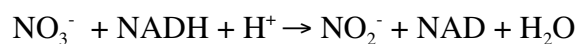
Biosynthesis of Moco occurs in 3 stages. In the first stage a guanosine-X-phosphate derivative is transformed through an unknown mechanism into a sulfur-free pterin compound which contains the typical four carbon Moco side chain by the intermediate named precursor Z. In the second stage, sulfur is transferred to precursor Z that is then converted to molybdopterin (MPT). Lastly, molybdenum is transferred into the MPT to form Moco (Mendel, 1997). Pateman et. al. (1964) was first to identify nitrate reductase (NR) and xanthine dehydrogenase (XDH) deficient mutants in *Aspergillus nidulans* and suggested both enzymes shared a common cofactor. Moco mutants were later discovered in plants that showed a pleiotropic loss of all Mo-enzyme activities including NR, XDH and aldehyde oxidase (AO). These mutant plants can be kept alive on media containing reduced nitrogen as N-source however, plants die when grown on media contained nitrate as the sole N source (Mendel, 1997). Moco deficient plant mutants have also been isolated

as NR-deficient mutants by selection for growth on toxic concentrations of chlorate. In these experiments chlorate toxicity requires Moco dependent NR activity which reduces chlorate to chlorite (Mendel, 1997).

## 1.4 Molybdenum containing enzymes

### 1.4.1 Nitrate reductase (NR)

Nitrate is a main source of inorganic nitrogen used by higher plants (Marschner, 1995). The first reduction step,



is catalysed by the molybdoenzyme nitrate reductase (NR) (Campbell, 1999). NR activity is considered a rate limiting process in the acquisition of reduced nitrogen in most plant systems (Campbell, 1999). NR consists of 3 functional domains: the N-terminal domain associated with Moco, the central haem domain and the C terminal FAD domain (Figure 1.4). These domains are connected via a protease sensitive hinge regions forming 3 redox centres which catalyse the transfer of electrons from the reductant NAD(P)H via FAD, haem and Moco to nitrate (Mendel and Hansch, 2002). Control of NR activity can be achieved by altering the activity levels of the enzyme in the tissue through increasing the concentration of the inducer of NR gene expression or by altering the level of the enzyme Moco (Crawford, 1995).

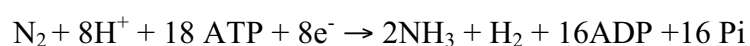
Early studies by Heimer et. al. (1969) showed that tungstate ( $\text{WO}_4^{2-}$ ) was a competitive inhibitor of molybdate, capable of displacing molybdenum from Moco leading to lower NR activity and increases in  $\text{NO}_3^-$  levels in tobacco cells. Deng et. al. (1989) later showed that the substitution of W in NR leads to an over expression of the NR structural gene. More recently Antipov et. al. (1998) found in *Pseudomonas isachenkovii* that 2 catalytically distinct NR enzymes exist, a membrane bound and soluble periplasmic form, in which the later contains vanadium (V) instead of molybdate. Moco was not found in either of the two NR isoforms. Shaked and Bar-Akiva (1967) demonstrated that a simple, rapid and convenient NR assay could be used to measure molybdenum to as low as 0.03 ppm in dry citrus tree material as NR is a Mo-dependent enzyme. To compare the effectiveness of the assay, 2 other methods were used for comparison of molybdenum with

plant tissue that included chemical analysis with dithiol and a bioassay with *Aspergillus niger*.

In molybdenum deficient plants, NR activity is often reduced resulting in the accumulation of high concentrations of  $\text{NO}_3^-$  in the plant (Srivastava, 1997). Molybdenum deficient plants have been shown to grow better on  $\text{NH}_4^+$  or  $\text{NO}_2^-$  as a source of N (Heimer et. al., 1969). Gridley (2003) found high  $\text{NO}_3^-$  levels in petioles of molybdenum deficient (between 0.05-0.09 mg/kg dw<sup>-1</sup>) Merlot vines grown on own roots and on rootstocks. Surprisingly, the accumulation of  $\text{NO}_3^-$  was unaffected by foliar molybdenum sprays. Villora et. al. (2002a) studied the interaction between P supply on molybdenum,  $\text{NO}_3^-$  and *in vivo* NRA (nitrate reductase activity) in eggplant (*Solanum melongena*). High P supply (4mM) induced the highest  $\text{NO}_3^-$  accumulation in the leaf blades, lowered  $\text{NO}_3^-$  transport to the roots and increased molybdenum concentrations in the fruit. Lower P supply (1 and 2 mM) led to increased  $\text{NO}_3^-$  concentrations in the fruit and increased molybdenum in the leaves. In another study Villora et. al. (2002b) looked at varying N amounts (1, 2, and 4 mM  $\text{NH}_4\text{NO}_3$ ) to determine its influence of molybdenum activity and internal  $\text{NO}_3^-$  tissue levels. Increased N application lowered the molybdenum content within the leaves and petioles. The highest levels of molybdenum were found in plants grown on the lowest amount of N whilst producing the highest NRA.

#### 1.4.2 Nitrogenase

Molybdenum is required for biological nitrogen fixation (BNF). BNF occurs in legume root nodules catalysed by the symbiotic bacteria of the *Rhizobiaceae* family and in asymbiotic bacteria such as *Azobacter*, *Rhodospirulum*, *Klebsiella*, and blue-green algae (Srivastava, 1997). Nitrogenase is responsible for the reduction of dinitrogen to ammonium through the following reaction,



The nitrogenase molecule consists of 2 oxygen sensitive metalloproteins, the larger being a Mo-Fe protein known as molybdoferredoxin, and a smaller Fe protein known as azoferredoxin. Nitrogenases have 2 types of centres, the Fe-Mo cofactor (M centre) and a Fe-S cluster (P cluster) and have been suggested in one model to form a dimer linked by 2 sulfides and a third bridging ligand or in an opposing model linked via a common hexa-coordinate S atom (Srivastava, 1997). Four classes of nitrogenase have been characterized,

with 3 classes sharing many similarities, differing only in the heterometal atom contained in the active metal cluster site, either molybdenum, vanadium or iron. The fourth class is distinct from the others isolated from *Streptomyces thermotrophicus*, and is superoxide-dependent rather than Mo-dependant (Christiansen et. al., 2001).

As molybdenum is essential for N<sub>2</sub>-fixing activity, the absence of molybdenum results in poor growth and activity of root nodules in leguminous plants (Srivastava, 1997). Consequently, leguminous plants must have a mechanism for molybdenum transport across the peribacteroid membrane (PBM) into the peribacteroid space (PBS) followed by uptake by the bacteroid (Figure 1.5). Maier and Graham (1988) studied molybdenum transport in bacteroid suspensions of *Bradyrhizodium japonicum* USDA 136 isolated from soybean nodules grown under molybdenum deficient conditions. Using <sup>99</sup>Mo, molybdenum uptake was nearly constant for 1 minute and then began to level off. It was hypothesized by the authors that molybdate was internalised. A K<sub>m</sub> of 0.1 μM and V<sub>max</sub> of 5 pmol/min per mg (dry weight) of bacteroid was reported, however the K<sub>m</sub> for molybdate has shown to vary with the type of *Bradyrhizobium* strain (Graham and Maier, 1987). Bacteroids that were isolated under anaerobic conditions accumulated more molybdenum after 10 minutes of uptake, and after 1 hour of uptake had accumulated twice the amount of molybdenum when compared to bacteroids that were isolated aerobically. The difference in molybdenum uptake between the 2 types of bacteroids was not significant before 10 minutes. Molybdenum uptake also was pH dependant and inhibitor studies suggested a transmembrane proton gradient is required. Generally, uptake increased with a decrease in pH (Graham and Maier, 1987). Rapid pH shift experiments demonstrated a ΔpH of 3.5 causing a 10-fold increase in molybdenum uptake in 10 seconds compared with no pH change. This demonstrated that molybdenum uptake depends on transmembrane proton gradients and is therefore probably transported electroneutrally as H<sub>2</sub>MoO<sub>4</sub> (Maier and Graham, 1988). Competition experiments revealed tungstate to be a competitive inhibitor of molybdate uptake whilst vanadate inhibited uptake only slightly.

### 1.4.3 Other molybdenum containing enzymes

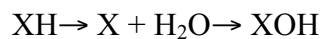
The molybdenum containing aldehyde oxidase (AO) enzyme (Figure 1.4) is widely distributed among eukaryotes and bacteria and catalyses the reaction,





This enzyme has also been shown to be involved with indole acetic acid (IAA) and abscisic acid (ABA) biosynthesis. ABA is essential for seed development, germination, and stomatal aperture whilst IAA is involved in root growth apical dominance and the regulation of phototropic and gravitropic behaviour (Mendel and Schwarz, 1999).

Xanthine oxidase (XO) and xanthine dehydrogenase (XDH) also contain molybdenum within the enzyme structure (Figure 1.4). XO is found within animals while XDH is found in plants. XDH catalyses the reaction,



This enzyme is involved in ureide synthesis and purine catabolism and senescence. No XDH mutants exist in higher plants and in Moco mutants which have pleiotropic loss of all molybdenum enzymes, no symptoms could be found which could be traced back to XDH loss (Mendel and Schwarz, 1999).

Knowledge of SOX (sulfite oxidase) in animals has been known for some time, recently however, SOX has been discovered in plants (Hille, 2003). The structure of plant SOX is very different to animal SOX with a heme domain missing and the enzyme being localized within the peroxisome instead of the mitochondria (Figure 1.4). The molybdenum centre of the enzyme is also quite different to that of animal SOX demonstrating molybdenum is in the oxidized form rather than the reduced form. The enzyme is responsible for catalysing the reaction where it oxidises sulfite into sulfate and is an important step in the oxidative degradation of cysteine, methionine and membrane components such as sulfatides (Eilers et. al., 2001) through the following reaction,



### **1.5 Molybdenum transport in the model organism, *Escherichia coli***

The mechanisms responsible for molybdenum transport in *E. coli* have been well studied (Rech et. al., 1996; Imperial et. al., 1998; Self et. al., 1999; Self et. al., 2001; Anderson et. al., 2002; McNicholas and Gunsalus, 2002). In *E. coli*, molybdate can be transported into the cell via 3 pathways all with varying affinities for molybdate (Self et. al., 2001). The first is by an ABC-type, high affinity transporter ( $K_m = 25\text{-}50$  nM at pH 7.0) system encoded by the *modABC* operon comprising of 3 proteins (Figure 1.6). A mutation in any

one of these 3 genes results in molybdenum being transported via a ABC-type sulfate transport system (Rosentel et. al., 1995), depending on the presence of sulfate (Rosentel et. al., 1995), or through a non specific anion transporter which is less efficient and requires molybdate at higher concentrations (Rosentel et. al., 1995).

Expression of molybdate transport genes in *E.coli* is very low which is consistent with the low rates of molybdenum transport observed (Self et. al., 2001). In most cases, molybdate starvation is required to de-repress the native molybdate ABC transport system (Self et. al., 2001). A molybdate sensor, which also can act as an aporepressor of the *mod* operon, binds molybdenum and regulates transcription of the *mod* operon.

### 1.5.1 The *Escherichia coli* ABC-MoO<sub>4</sub><sup>2-</sup> transport system (*modABCD* operon)

*modA* (774 bp) encodes a 257 amino acid periplasmic binding protein (Figure 1.6). Rech et. al. (1996) demonstrated that ModA exhibited a high specificity for molybdenum and its analogue tungstate with a K<sub>M</sub> of approximately 5 μM. *modA* is essential for the transport of molybdenum. A mutation within *modA* results in decreased cell growth due to low levels of molybdate uptake, even other ModBC and D proteins are present (Rech et. al. 1996). This growth defect can be overcome when cells are transformed with *modA*<sup>+</sup>. ModA consists of 2 well-separated globular domains that are connected via a hinge region. When the ligand binds the protein the domains come together, creating a deep cleft allowing the ligand to bridge the 2 domains. This is similar to how other periplasmic binding proteins react to ligands, including the sulfate binding protein (SBP). However, other oxyanions, sulfate and phosphate do not appear to bind, despite the ligand form of ModA being very similar to the SBP (Self et. al., 2001).

The second gene, *modB* (690 bp) encodes a protein containing 229 amino acids and constitutes the integral membrane channel protein (Figure 1.6). This protein is highly hydrophobic and has five distinct hydrophobic transmembrane spanning regions (Maupin-Furrow et. al., 1995) with the inner membrane containing the ABC transporter motif (Self et. al., 2001). This protein is also similar to the CysT and CysW proteins of *E.coli* that constitute membrane components of the sulfate-thiosulfate transport system with 10 out of 14 amino acids being similar.

*ModC*, the third gene (1059 bp) encodes a protein of 352 amino acids and contains a nucleoside triphosphate-binding domain. The presence of this protein motif suggests that

ATPase activity may be required for the molybdenum transport system (Maupin-Furlow et. al., 1995) (Figure 1. 6).

Adjacent to the *ModC* gene, is the *ModD* gene, encoding a 231 amino acid protein. Its function remains unknown. Downstream from this operon is another operon that encodes *ModE* and *ModF*. *ModE* consists of 262 amino acids and regulates the expression of *modABC* by binding to the operator region of the *modABC* operon (Self et. al., 2001). Downstream of the *modE* gene is an additional ORF (*modF*) encoding a 490 amino acid protein. This protein may play a role in molybdate export out of the cell, but its exact function is unknown. The deletion of this gene results in no metabolic change of molybdate within *E.coli*.

## **1.6 Mechanisms for molybdenum uptake in plants**

Due to the chemical similarity with other divalent anions it has been hypothesised that molybdenum can be transported via other non-specific anion transporters (Mendel and Hansch, 2002) or phosphate transport systems (Heuwinkel et. al., 1992) via P-type ATPases (Palmgren and Harper, 1999) or sulfate transporters (Tweedi and Segel, 1970; Kaiser et. al., 2005). Recently what was thought to be Group 5 of the sulfate transporter super family contained identified as a putative molybdate transporter (MOT1) which was previously assigned the name of AtSultr5;2 in *A. thaliana*. (Tejada-Jimenez et. al., 2007; Tomatsu et. al., 2007; Baxter et. al., 2008). This project has focused on the potential for molybdenum to be transported through sulfate transporters. However, other potential mechanisms of molybdenum transport will now be discussed with emphasis on plant sulfate transporters.

### **1.6.1 Plant phosphate transporters**

Plants take up inorganic phosphate via the Pht1 family of transporters (Smith et. al., 2003). Pht1 transport systems are approximately 58 kD, 520-550 amino acids in length and have 12 membrane spanning domains each composed of 17-25 amino acids with predicted C and N-terminal ends orientated towards the inner surface of the membrane (Smith et. al., 2000). Compared to plant sulfate transporters, little is known about the functional activity of plant phosphate transporters due to their previous poor form when heterologously expressed in yeast phosphate mutants such as PHO84 (Smith, 2002). A yeast double mutant PAM2 has recently become available which may improve the functional analysis of plant phosphate transporters (Smith, 2002; Smith et. al., 2003). Pht1 transporters have been

found in tomato (LePT1), Arabidopsis (Pht1;1, Pht2;1) potato, *Medicago* (Smith et. al., 2000; Smith et. al., 2003) and barley (HORvu;Pht;1 and HORvu;Pht6) (Rae et. al., 2003).

Experiments performed by Heuwinkel et. al. (1992) with tomato demonstrated molybdenum uptake is enhanced by phosphorous deficiency. The uptake of molybdenum increased by 300% when phosphorous was removed from the nutrient solution with the greatest uptake occurring 4-7 days after removal. Approximately 10 times greater molybdenum was found within the roots and 5 times greater molybdenum was found within the shoots when compared to phosphorous sufficient plants. In <sup>99</sup>Mo experiments the rates of molybdenum uptake after 1 hour of phosphorous starvation were 5 times higher and 9 to 12 times higher after a 4-hour starvation period. The authors speculate that as molybdate and phosphate anions have similar physiochemical properties, in the absence of phosphate, molybdate uptake is enhanced. It is therefore possible that the uptake of molybdate across the plasma membrane of root cells may occur via a phosphate transport system.

### **1.6.2 Plant P-type APTases**

P-type ATPases are ATP-fuelled pumps sharing a common enzymatic mechanism involving a phosphorylated reaction cycle (Palmgren and Harper, 1999). P-type ATPases are hydrophobic membrane proteins with 10 transmembrane spanning helices) where both the N and C-terminus face into the cytoplasm. P-type ATPases have been shown to transport a multitude of different ions including protons, calcium, manganese, copper, phospholipids and possibly molybdenum. P-type ATPases have been shown to function as high affinity uptake or efflux transporters. Palmgren and Harper (1999) suggested that the potential functions of these pumps may include the uptake of essential heavy metals from the apoplasts, efflux of toxic metals from the cytoplasm or the compartmentalization of essential metals for special biochemical pathways. As molybdenum is required in trace amounts, even modest levels may prove toxic to the cell (Palmgren and Harper, 1999). However, no experiments have been conducted to confirm this hypothesis. As a result of this, uptake and compartmentalization can be expected to be highly regulated. Unpublished results by Wang and Harper (see Palmgren and Harper, 1999) suggest that molybdenum may be accumulated via a P-type ATPase pump (AMA1) from Arabidopsis. Using a AMA1 T-DNA knockout the uptake of molybdenum showed a 5-fold reduction in accumulation compared to wild-type controls.

## 1.7 Plant sulfate transporters

### 1.7.1 Sulfur assimilation, reduction and metabolism

Transport of sulfate into cells in plants is via plasma membrane-localized  $H^+/SO_4^{2-}$  co-transporters. Transport is driven via an electrochemical gradient of  $H^+$  established by the plasma membrane proton ATPase (Leustek et. al., 2000). Sulfur, like molybdenum, is an essential nutrient for plant growth and is absorbed by the plant predominantly as inorganic sulfate ( $SO_4^{2-}$ ) from soil. Plants are the primary producers of organic sulfur compounds such as the amino acids cysteine and methionine, oligopeptides (gluathionine, phytochelatins, vitamins (biotin and thiamine) cofactors (CoA and S-adenosyl-Met) and a variety of secondary products (Saito, 2004).

Once within the plant, sulfate can be stored in the vacuole or activated to adenosine-5'-phosphosulfate (5'adenylylsulfate [APS]) for further conversion. The activated sulfate (APS) can then serve as a substrate for the synthesis of sulfate esters or sulfate reduction. The major assimilatory pathway is the reduction of APS to sulfite ( $SO_3^{2-}$ ) which is then further reduced to sulfide ( $S^{2-}$ ) (Marschner, 1995).  $S^{2-}$  then reacts with *O*-acetylserine (OAS) to form cysteine catalysed by serine acetyltransferase and OAS thiol-lyase (Leustek et. al., 2000).

### 1.7.2 Phylogenetic analysis of plant sulfate transporters

Sulfate transporters are encoded by a large gene family in plants due to the variety of sulfur needs within the plant system. Alignment and phylogenetic analysis identifies 4 closely related groups with a fifth more divergent group (Buchner et. al., 2004) (Figure 1.7). Transport activity has only been demonstrated in Group 1 and 2, but due to high homology between groups it is reasonable to expect that most are involved in transport of sulfate (Buchner et. al., 2004).

Group 1 contains those transporters that are involved in high affinity root transport with a  $K_m$  for sulfate between 1.5 – 10  $\mu M$ . It is suggested that these proteins found in roots have the capacity for high affinity sulfate influx across the plasma membrane into the symplast (Buchner et. al., 2004). Group 2 encodes low affinity root transporters with a  $K_m$  between 99  $\mu M$  – 1.2 mM (Smith et. al., 1995a; Takahashi et. al., 2000; Buchner et. al., 2004). Group 3 are thought to contain transporters isolated from leaves and Group 4 contains those from plastids. The more divergent group, Group 5 was thought to contain sulfate

influx transporters on the tonoplast, though none have been identified and their involvement has yet to be verified. Recently this class of sulfate transporters has been implicated in molybdate transport in *Arabidopsis* resulting in *AtSult5;2* now named *Mot1* (Molybdenum transporter 1) (Tomatsu et. al., 2007) (see section 1.8).

### **1.7.3 Topology of plant sulfate transporters**

Generally, sulfate transporters are thought to contain 12 membrane spanning domains (MSD), with both the C and N-termini predicted to be on the inside of the membrane and range from 69 kD to 75 kD or 635 to 685 amino acids in length (Smith et. al., 2000). Amino acid comparisons between the C-terminal cytoplasmic domains of sulfate transporters and bacterial antisigma-factor antagonists (ASA) from *Bacillus subtilis* have identified a putative STAS domain (sulfate transporters and antisigma-factor antagonists) (Aravind and Koonin, 2000; Markovich et. al., 2005). The STAS domain is conserved amongst sulfate transporters in Groups 1 to 4. While its exact function remains unknown, it has been suggested to be involved in facilitating localization of the transporter to the plasma membrane, and may also influence the kinetic properties of the catalytic domain of the transporter (Shibagaki and Grossman, 2004) in addition to providing biosynthesis and stability (Shibagaki and Grossman, 2006).

Site directed mutagenesis of charged amino acids in the legume sulfate transporter, SHST1 demonstrated proline-144 is essential for sulfate transport while mutations in either proline-133 or proline-160 resulted in significantly reduced sulfate transport (Shelden et. al., 2001; Shelden et. al., 2003). Western blotting also suggested that SHST1 underwent a post translational change in the endoplasmic reticulum that increased the molecular mass and was also required for trafficking to the plasma membrane. This is possibly due to a formation of a SDS-stable dimer of 2 SHST1 molecules (Shelden et. al., 2001). Transmembrane helices 1, 2 and 3 are of functional importance for SHST1 as well as the charge interaction between residues in helices 3 (E175), 6 (E270) and 8 (R354) which may be involved in transport (Shelden et. al., 2003).

### **1.7.4 Regulation of sulfate transporters**

The regulation of sulfate transport is a complex and poorly understood process. Transporters must be controlled at the level of gene expression as well as at the post translational level (protein turnover or modification of activities etc.) for the optimised uptake and assimilation of sulfate (Maruyana-Nakahita et. al., 2004). However the

signalling events involved in plant sulfate perception, particularly those when external sulfate is limited are currently unknown (Buchner et. al., 2004). Plants respond differently to various sulfate conditions. When plants are grown under limiting sulfate, its uptake, the level of cysteine synthesis and activity of key enzymes in the sulfate assimilatory pathway are activated for survival (Maruyana-Nakahita et. al., 2004). At high concentrations, cysteine and glutathione repress sulfate assimilation and uptake activities (Buchner et. al., 2004). There is also complex expression and regulation pattern for genes within the sulfate transport family. Group 3 transporters with tissue and organ specificity have no regulation by sulfate nutrition. In cell-specific expression studies, some members of groups 1, 2, and 4 transporters under adequate sulfate nutrition are up-regulated by inadequate S nutrition while other sulfate transporters in Groups 1 and 2 that are both cell and tissue specific under sulfate deficiency are repressed (Buchner et. al., 2004).

During S limitation, plants are able to activate the expression of Group 1 sulfate transporters to facilitate uptake by the roots (Maruyana-Nakahita et. al., 2004). Matuyana-Nakahita et. al. (2004) showed the importance of *Arabidopsis thaliana* root sulfate transporters SULTR1;1 and SULTR1;2 as they were induced by sulfate limitation at the mRNA level and were predominantly located in roots hairs, epidermis and cortical cells. The expression of Sultr1;1 and Sultr1;2 was primarily regulated by sulfate in a promoter-dependent manner and the induction of both was also dependent on C and N supply to the plant.

### **1.8 Sulfate transporters-the new molybdenum transport system?**

Sulfate transport systems may also be able to transport molybdate. This is not a new hypothesis, where in prokaryotes alternative systems including sulfate transporters have been shown to transport molybdate. Until recently, the role of sulfate transporters in molybdate transport has yet to be shown despite the similarity in net charge, geometry and hydrogen bonding properties (Dudev and Lim, 2004). Sulfate transport systems are likely candidates for the high affinity transport of molybdate as molybdate uptake is competitively inhibited by large amounts of sulfate (Marschner, 1995).

Recently a specific molybdate transporter, previously assigned a putative sulfate transport role as AtSultr5;2 has been identified as MOT1 in *Arabidopsis* (Tomatsu et. al., 2007). MOT1 was expressed in both roots and shoots and localised to both the plasma membrane and vesicles and classed as a high affinity transported with a  $K_m$  of 21 nM.

Complementation studies performed in the sulfate transport mutant CP154-7B demonstrated that MOT1 did not complement the mutation when grown on media containing minus methionine suggesting that MOT1 specifically transported molybdate and does not transport sulfate.

Concurrently, a molybdate transporter was also identified in *C. reinhardtii* with homology to sulfate transporters and also named MOT1 (Tejada-Jimenez et. al., 2007). Again this was a high affinity transporter with homology to sulfate transporters but with a much lower  $K_2$  of 6 nM when expressed in yeast mutant 31019b and was inhibited by sulfate and partially inhibited by tungstate.

The MOT1 ortholog was also isolated by Baxter et. al. (2008) through studying the natural molybdenum variations within the Arabidopsis population. GUS localization demonstrated that *MOT1* was expressed in the roots and contained a mitochondrial targeting sequence. However the MOT1 was tagged with GFP in protoplasts, this protein was localized to the mitochondrial in contrast to Tomatsu et. al. (2007). Again MOT1 was expressed in wild type yeast BY4742 and accumulated 5 times more molybdenum than empty vector controls.

Before these studies examined above identified molybdate transporters with homology to known sulfate transporters, there was overwhelming evidence within the literature which examined the possibility of sulfate transport proteins having the capability to also transport molybdate. However, at this time, it was not thought that sulfate transporters of belonging to group 5 would specifically transport molybdate. In *E.coli* Self et. al. (2001) suggested that molybdate can be transported via an ABC-type  $\text{SO}_4^{2-}$  transporter or a non-specific anion transporter when a mutation in either *mod A*, *mod B* or *mod C* occurred. Although the ABC-type  $\text{SO}_4^{2-}$  transport system has been implicated in molybdate transport in *E.coli* based on both genetic and physiological studies, direct transport studies have yet to be performed (Self et. al., 2001). Rech et. al., (1996) have shown sulfate does not readily enter the cell via the ModABC transport system even when supplied at high concentrations (2mM). ModA proteins have low affinity for sulfate, while the sulfate binding protein (SBP) proteins have low affinity for molybdate (Rech et. al., 1996; Imperial et. al., 1998; Self et. al., 2001). This may be due to average metal-oxygen distances for molybdate (1.77 Å) and sulfate (1.47 Å) as the larger molybdate oxyanion may not be able to bind effectively to the sulfate binding site in the SBP (Self et. al., 2001). If this is the case, this



raises questions about molybdate transport via a sulfate transporter in *E. coli* when the molybdate concentration is less than 1  $\mu\text{M}$  (Self et. al., 2001). Other *in vivo* studies have shown that the SBP could not replace ModA.

In *Penicillium notatum*, Tweedi and Segel (1970) demonstrated that under sulfate starvation the rate of transport increased 40-fold suggesting a common transport pathway for  $\text{MoO}_4^{2-}$ , as well as  $\text{SeO}_4^{2-}$  and  $\text{S}_2\text{O}_3^{2-}$ . Above pH 5.0 small amounts  $\text{MoO}_4^{2-}$  could be transported by the  $\text{SO}_4^{2-}$  transport system using radioactive  $^{99}\text{MoO}_4^{2-}$  and  $^{35}\text{SO}_4^{2-}$  (Tweedi and Segel, 1970). Transport below pH 5 was not observed leading the authors to speculate that the fungi may have another way of accumulating  $\text{MoO}_4^{2-}$  under acidic conditions and suggest the presence of a molybdate specific permease.

Using excised rice roots, sulfate, copper and chloride were shown to be active inhibitors of  $^{99}\text{Mo}$  uptake (Kannan and Ramani, 1978). Interestingly low  $\text{FeSO}_4$  concentrations (0.01mM) enhanced molybdenum uptake that was not observed when alternative iron was supplied (e.g. FeEDDHA). Llamas et. al. (2000) investigated molybdate transport using a *Chlamydomonas reinhardtii* mutant (12gr) which is defective in the *Nit5* gene involved in the biosynthesis of Moco. When cells were grown with ammonium molybdate, uptake was assumed to involve a sulfate transport system where at low sulfate concentrations (0.3 mM) molybdate uptake was blocked.

In animal systems molybdate transport has recently been shown to involve the placental specific  $\text{Na}^+$  coupled sulfate transporter NaS2 (Dawson et. al., 2005; Markovich et. al., 2005; Miyauchi et. al., 2006). Dawson et al., (2005) cloned NaS2 from rat (rNaS2) while Markovich et al., (2005) cloned NaS2 from humans (hNaS2). In both studies rNaS2 and hNaS2 when expressed in *Xenopus* oocytes accumulated  $^{35}\text{SO}_4^{2-}$ . Substrate specificity experiments also revealed hNaS2 could also transport selenate, thiosulfate, tungstate, phosphate and molybdate while rNaS2 could also transport similar oxyanions in addition to oxalate. When Miyauchi et. al., (2006) also expressed rNaS2 in oocytes, selenium, chromium, arsenic, phosphate and molybdate were transported readily by the proteins.

### **1.8.1 Identification of sulfate transporters in *Saccharomyces cerevisiae***

Identification of the first sulfate transport protein, SUL1 in *S. cerevisiae* was achieved via functional yeast complementation by Smith et. al. (1995). A yeast mutant, CRS149, was created through ethyl methane sulphonate (EMS) mutagenesis of the wild type yeast

Invsc1 using the resistance to selenate and chromate which is sulfates toxic analogues. A clone that complemented this mutation was isolated from a *S. cerevisiae* cDNA library and named SUL1. This cDNA, *SUL1*, was 2775 bp in length and contained a single open reading frame that encoded a 859 amino acid polypeptide with a molecular mass of 96 kD. Expression of SUL1 revealed a high-affinity transport protein with a  $K_m=7.5 \pm 0.6 \mu\text{M}$  for  $\text{SO}_4^{2-}$ . A plasmid harbouring SUL1 was constructed and expressed in CRS149 resulting in sulfate uptake through functional yeast complementation. The cloned gene was then used to construct a mutant of *S. cerevisiae* in which a 1096 bp was deleted from the genomic sequence of *SUL1*, with the remaining sequence cloned into a an integrating plasmid which was used to replace SUL1 in Invsc1 through homologous recombination and subsequently named YSD1 (Yeast sulfate deletion mutant 1). YSD1 was unable to grow on media containing less than 5 mM sulfate unless it was complemented by a plasmid containing the SUL1 insert.

Earlier work by Breton and Surdin-Kerjan (1977) revealed the presence of a high affinity sulfate permease I and a low affinity sulfate permease II. Cherest et. al., (1997) later identified not only *SUL1* as Smith et. al. (1994) did, but also 2 additional genes, another high affinity sulfate permease *SUL2*, and *SUL3*, which is thought to be involved in the transcriptional regulation of *SUL2*. The existence of a yet unknown low-affinity sulfate transport system remains unknown, however yeast strains with both *SUL1* and *SUL2* genes disrupted are still able to grow on 30 mM sulfate.

### **1.8.2 Identification of *Stylosanthes hamata* sulfate transporters**

The first plant sulfate transporters were cloned using functional yeast complementation of YSD1 using a cDNA library constructed of *Stylosanthes hamata* root tissue starved of sulfate for 72 hours by Smith et. al. (1995). This method isolated 3 sulfate transporter cDNAs, *SHST1*, *SHST2* and *SHST3* (Figure 1.8). *SHST1* (667 amino acids) and *SHST2* (662 amino acids) are both high affinity  $\text{H}^+$ /sulfate cotransporters with  $K_m$  of  $10.0 \pm 0.6$  and  $11.2 \pm 0.5 \mu\text{M}$   $\text{SO}_4^{2-}$  respectively. Both genes are highly homologous being 97% similar and 95.3% identical. Southern blots of genomic DNA from *S. hamata* and *S. hamata*'s progenitor species *Stylosanthes humilis* provided preliminary evidence that *SHST1* and *SHST2* may represent homologous genes from the 2 different progenitor genomes with *SHST1* originating from *S. humilis* and *SHST2* originating from *S. hamata* (Smith et. al. 1995a). Expression of *shst1* and *shst2* was root specific and moderate in the root supplied adequately with sulfate. Expression increased after 72 hours with sulfate

starvation and returned to normal levels upon sulfate resupply. SHST3 (644 amino acids) is a low affinity H<sup>+</sup>/sulfate cotransporter with K<sub>m</sub> of 99.2 ± 4.8 μM SO<sub>4</sub><sup>2-</sup> sharing less homology with SHST1 and SHST2 with 74% similarity and 52% identity. Expression levels of *shst3* were much lower than *shst1* and *shst2* and only slightly increased expression of *shst3* was observed after 72 hours of sulfate starvation.

### **1.8.3 Identification of putative sulfate transporters on the symbiotic membrane of nodules**

Nutrients are imported into the nodule to support symbiotic bacterial nitrogen fixation. Movement of nutrients to the nitrogen fixing bacteroids requires transport systems to traverse the peribacteroid membrane (PBM) which encircles the bacteroids (Day and Udvardi, 1997) (Figure 1.5). Recently, a map-based cloning approach was used to verify the functional identity of the mutation in two *Lotus japonicus* mutants incapable of symbiotic nitrogen fixation (Krusell et. al., 2005). In two separate mutants, *sst1-1* and *sst1-2*, two similar alleles were identified encoding a putative sulfate transporter *Sst1* (symbiotic sulfate transporter 1). Previous proteomic data indicated that LjSST1 (645 amino acids) may be located on the symbiosome membrane (Weinkoop and Saalbach, 2003) and was predicted to contain 12 transmembrane domains and the STAS domain in the C-terminus similar to other plant sulfate transporters (Krusell et. al., 2005). This transporter is assumed to be involved in transporting sulfate from the plant cytosol to the bacteroids with sequence analysis suggesting LjSST1 belonged within Group 3. Functional analysis was performed using a yeast double mutant CP154-7A, which has 2 defective sulfate transporters (SUL1 and SUL2) allowed for complementation of the cDNA of SST1, making this the first protein in Group 3 to be confirmed as a sulfate transporter (Krusell et. al., 2005), however direct sulfate transport assays were not presented.

### **1.9 General aims of thesis**

The primary aim of this project was to identify transport proteins from plants that were capable of transporting molybdenum via a functional yeast complementation approach. Only recently have molybdate transporters been identified in higher plants. Identification of plant proteins allowing for molybdenum transport will allow for greater understanding of molybdenum metabolism and acquisition within the plant system. More importantly, this work may also lead to increased understanding of molybdenum nutrition in *V. vinifera* cv. Merlot and why Merlot suffers from molybdenum deficiencies. It appears that sulfate

transporters may be primary candidates for molybdate transport in plants. Plant sulfate transport proteins were tested for their ability to transport molybdenum.



**Figure 1.1 Molybdenum deficiency responses in grapevines.**

**A.** Merlot cultivar D3V14 exhibiting 'zig-zag' shoots, downward curled leaves and **B.** necrotic leaf edges and general chlorosis due to molybdenum deficiency. Vines were grown in the glasshouse.

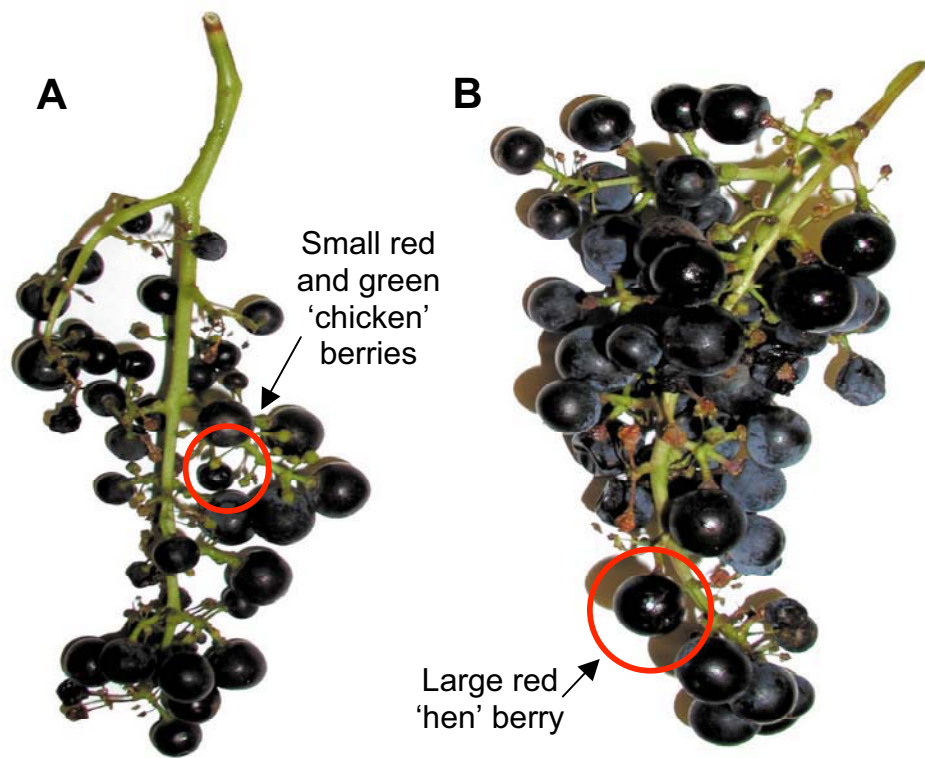


**Figure 1.2 Molybdenum deficiency phenotypes in *V. vinifera* cv. Merlot.**

**A.** Bunch of Merlot berries grown on own roots exhibiting the 'millerandage' phenotype showing a high incidence of small red and green 'chicken berries' and low incidence of large red 'hen berries' indicated by red circles. **B.** Bunch of Merlot berries grown on own roots after a foliar application of molybdenum.

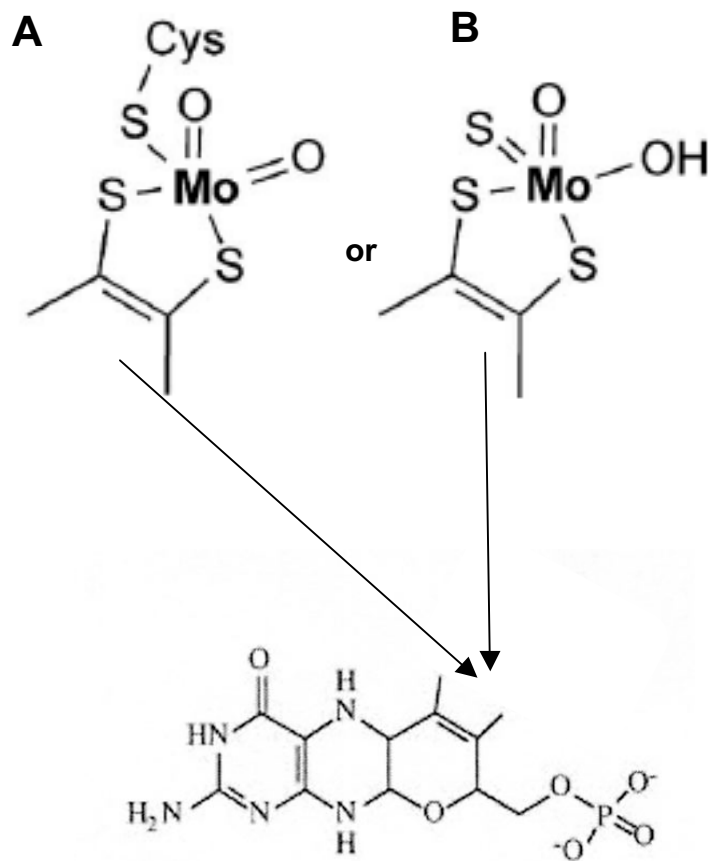


**Figure 1.3 The chemical structure of the molybdenum cofactor (Moco).**

Showing the position of either **A.** the dioxo molybdenum centre in the enzymes of SO/NR or **B.** the molybdenum centre of XDH/AO (Modified from (Mendel and Hansch, 2002; Mendel and Bittner, 2006).

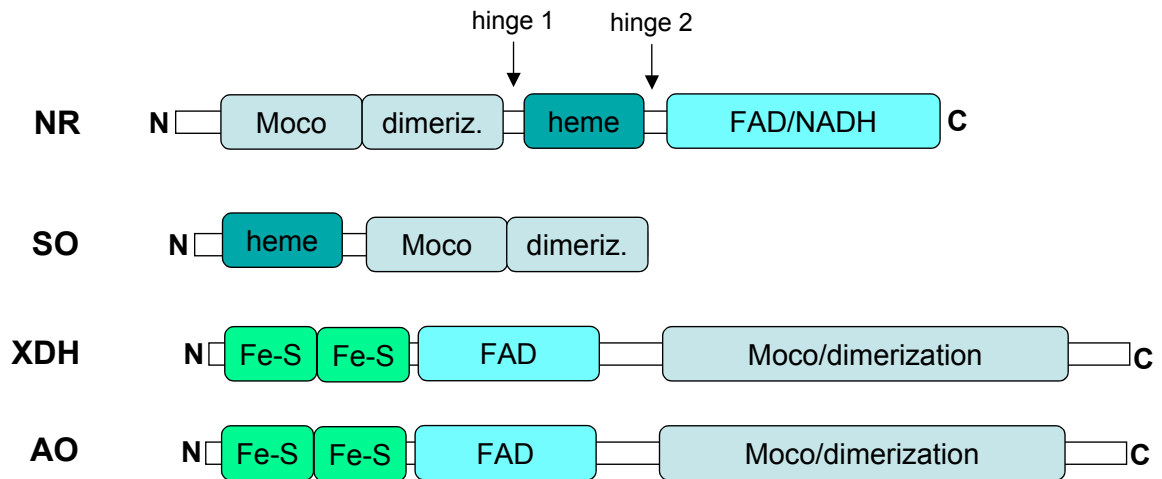


**Figure 1.4 The position in which Moco is found within the 4 plant enzymes (modified from Mendel and Hansch, 2002; Mendel and Bittner, 2006).**

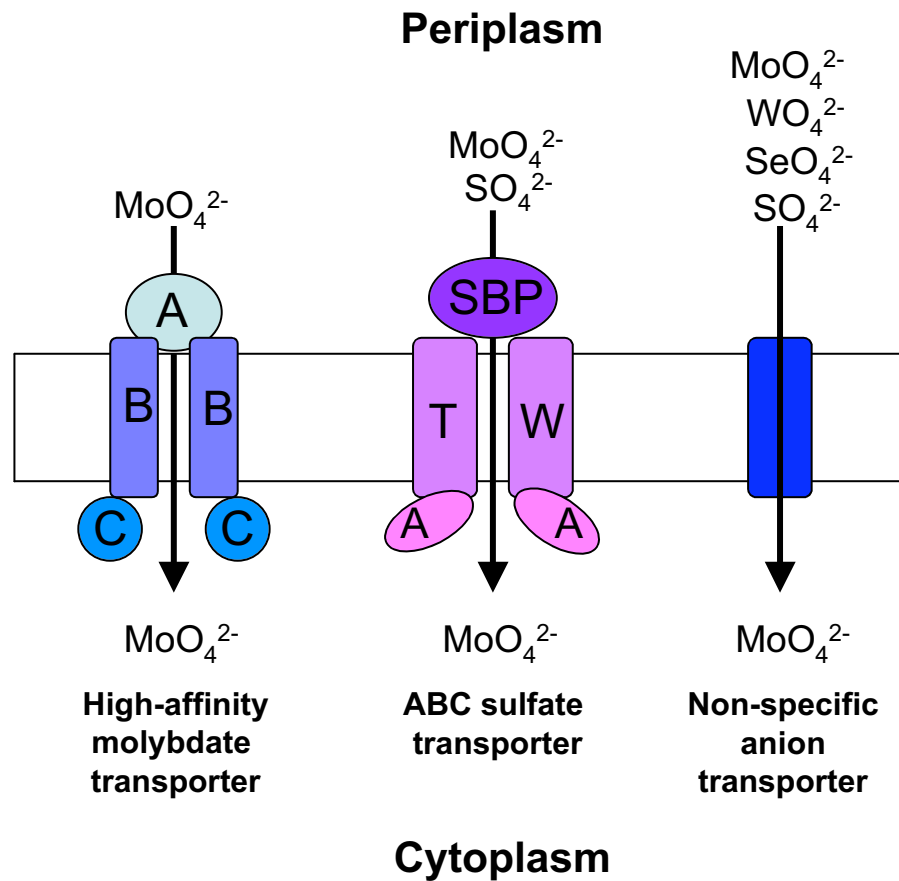
All domains are joined in white. Though Mo-enzymes in plants are homodimeric, the above picture represents the monomer forms. C or N represents the C or N terminus. Dimeriz = dimerization. The electron transport chain is made up of different prosthetic groups FAD, heme, Fe-S and Moco which catalyse the transfer of an oxygen atom (Mendel and Schwarz, 1999).



NOTE: This figure is included on page 48 of the print copy of the thesis held in the University of Adelaide Library.

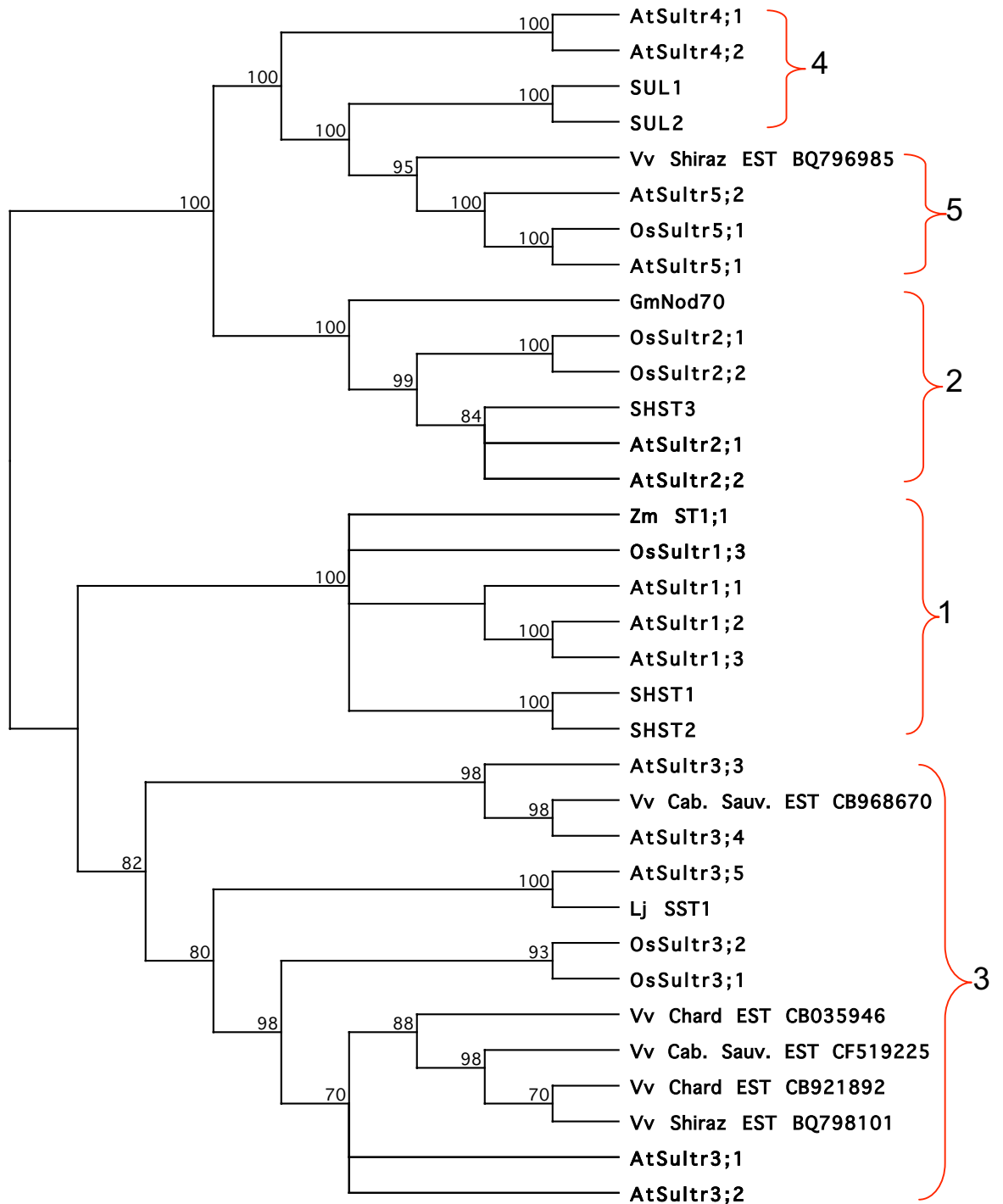
**Figure 1.5 Transmission electron micrograph showing a symbiosome isolated from a soybean root nodule infected cell. The bacterioids are contained within the peribacteriod space (PBS), which is enclosed by the peribacteriod membrane (PBM).**

Photo courtesy of Dean Price, Australian National University, Canberra.



**Figure 1.6 Molybdate transport in *E.coli*.**

The high-affinity molybdate transporter is represented by A, B, and C (ModABC proteins). An ABC sulfate and a non-specific anion transporter also contribute to molybdate transport (modified from Self et. al., 2001).



**Figure 1.7 Phylogenetic analysis of plant sulfate transporters from *Arabidopsis thaliana* (At), *Vitis vinifera* EST's (Vv), *Oryza sativa* (Os) and *Stylosanthes hamata* (Sh), *Glycine max* (Gm) *Lotus japonicus* (Lj) and *Zea mays* (Zm).**

Phylogenetic analysis of sulfate transporters using full-length amino acid sequences aligned using ClustalW using MacVector. Neighbour joining tree with bootstrap values obtained from 100 replicates, uncorrected p and gaps distributed proportionally. Smaller

numbers represent similarity between genes. Larger numbers represent gene assignments into putative sulfate transport groups 1-5. AtSultr4;1 Q9FY46, AtSultr4;2 Q8GYH8, SUL1 P38359, SUL2 Q12325, AtSultr5;2 NP\_180139, OsSultr5;1 BAC05530, AtSultr5;1 BAB03554, OsSultr2; 1AAN59769, OsSultr2;2 AAN59770, SHST3 X82454, AtSultr2;1 O04722, AtSultr2;2 P92946, ZmSt1;1 AAK35215, OsSultr1;3 BAC98594, AtSultr1;1 Q9SAY1, AtSultr1;2 Q9MAX3, AtSultr1;3 BAB16410, SHST1 X82255, SHST2 X82256, AtSultr3;3 Q9SXS2, AtSultr3;4 Q9LW86, AtSultr3;5 AB061739, Lj SST1 BAA02723, OsSultr3;2 AAN06871, OsSultr3;1 NP\_921514, AtSultr3;1 Q9SV13, AtSultr3;2 O04289.

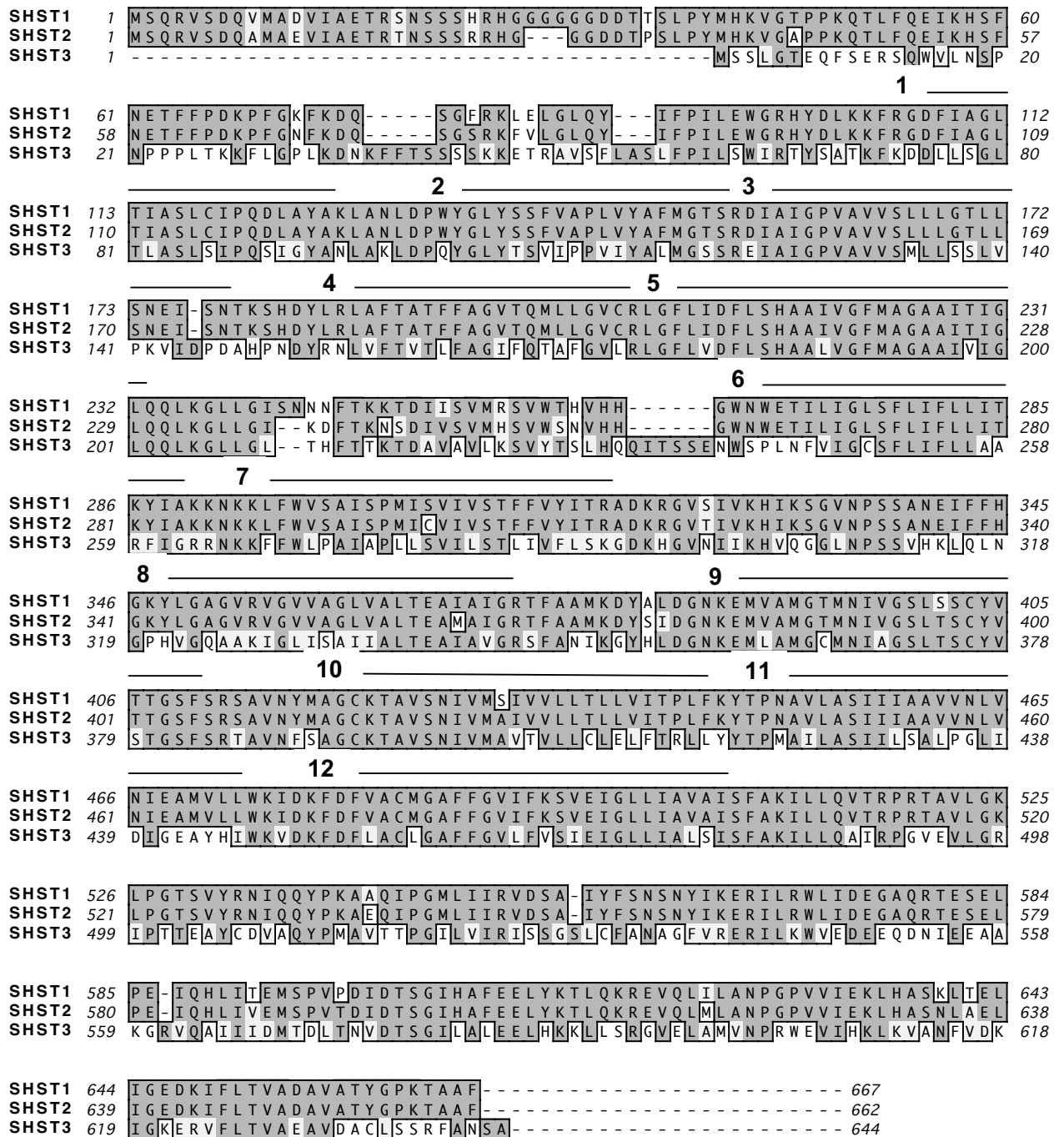


**Figure 1.8** Alignment of amino acid sequences of SHST1, SHST2 and SHST3.

Alignment was performed using ClustalW in MacVector. Identical residues are shaded in dark grey, and conserved residues are shaded in light grey. Putative transmembrane domains are indicated by the numbered horizontal bars.

## Chapter 2

# Identification of $\text{MoO}_4^{2-}$ transport proteins by functional yeast complementation

---

### 2.1 Introduction

Only recently have molybdate transporters been identified in plants (Tejada-Jimenez et. al., 2007; Tomatsu et. al., 2007; Baxter et. al., 2008) and still required further characterisation. In contrast, the molybdate transport system have been well characterised in a number of prokaryotic systems including *Escherichia coli* (Maupin-Furlow et. al., 1995; Rech et. al., 1996; McNicholas et. al., 1998; Grunden et. al., 1999), *Azobacter vinelandii* (Mouncey et. al., 1995), *Anabaena variabilis* (Zahalak et. al., 2004), *Staphylococcus carnosus* (Neubauer et. al., 1999), *Rhodobacter capsulatus* (Wang et. al., 1993) and *Clostridium pasteurianum* (Elliot and Mortenson, 1975).

In prokaryotes, molybdate transport involves the *ModABCD* system. This system involves genes encoding a periplasmic binding (*ModA*), a membrane channel protein (*ModB*), an energizer ATPase (*ModC*) and a protein of unknown function (*ModD*) (Maupin-Furlow et. al., 1995). Downstream of the *ModABCD* operon is another operon consisting of the gene responsible for the expression of the *ModABCD* operon (*ModE*) and another gene of unknown function (*ModF*) which may be involved in molybdate export from the cell (Self

et. al., 2001). Surprisingly, similar protein orthologs of the *ModABCD* system are absent in eukaryotes, which suggests that different systems are involved in molybdate transport in plants. It has been hypothesized that the transport of molybdenum in plants may occur through a variety of transport proteins including phosphate transporters (Heuwinkel et. al., 1992), P-type ATPases (Palmgren and Harper, 1999) and sulfate transporters (Marschner, 1995; Mendel and Schwarz, 1999; Llamas et. al., 2000). Although no conclusive study has shown these systems to be involved, there are examples for instance where physiological responses to sulfate starvation can enhance molybdate uptake (Alhendawi et. al., 2005).

Functional complementation using heterologous organisms such as *Saccharomyces cerevisiae*, has allowed the isolation, expression and functional analysis of many unknown plant transport proteins (Frommer and Ninnemann, 1995). This method has proved invaluable for the identification of protein functions where no plant mutants or screening protocols exist (Frommer and Ninnemann, 1995). One of the first transporters isolated via this method was KAT1, a K<sup>+</sup> channel from an *A. thaliana* cDNA library, using the yeast strain CY162 (Anderson et. al., 1992). The first plant sulfate transporter, SHST1 (*Stylosanthes hamata* sulfate transporter 1), was isolated via functional yeast complementation of the mutant YSD1 by an *S. hamata* cDNA library (Smith et. al., 1995a).

In this work, a number of experimental approaches were tested to identify putative molybdenum transport proteins in plants. The first approach involved developing a yeast mutant from the wild-type yeast, Invsc1, using the chemical mutagen ethyl methane sulphonate (EMS). This approach was based around developing a negative molybdenum screen where a mutant resistant to high external concentrations of molybdate could be used to identify plant proteins that restored the toxicity phenotype in the mutant background. Identified transport proteins were assumed to have an ability to remove toxic levels of molybdenum from the cell or act in accumulating it in the vacuole.

In the last approach, an attempt was made to identify novel molybdenum and sulfate transport proteins using a functional yeast complementation screen of a root cDNA library from *V. vinifera* cv. Pinot noir cDNAs transformed into YSD1 were selected for based on their ability to rescue cell growth on either low sulfate (Low S) or low molybdenum (Low Mo) media.

Unfortunately the both of the above approaches failed in their attempts to firstly create and develop a molybdenum yeast mutant and secondly identify putative molybdate and sulfate transport cDNA's from a *V. vinifera* cDNA library. This was a high risk approach at identifying a putative molybdenum transporter.



## 2.2 Methods

### 2.2.1 Mutant generation

#### 2.2.1.1 Toxicity determination

Three strains of yeast including wild type *Invsc1* (*MAT $\alpha$  his3- $\Delta$ 1 leu2 trp1-289 ura3-52*),  $\Sigma$ 1278b ( $\alpha$  wild-type *MPR1 MPR1 AZC<sup>r</sup>*), and S288C (*MAT $\alpha$  SUC2 gal2 mal mel flo1 flo8-1 hap1*) were examined for the ability to grow on high concentrations of molybdenum. Cells were obtained from glycerol stocks and plated on to YPAD media [1% (w/v) yeast extract; 2% (w/v) peptone; 2% (w/v) glucose; 0.004% (w/v) adenine sulfate; 2% (w/v) agar] and incubated at 28°C for 2-3 days. Cells were then plated onto YPAD media containing varying concentrations (100  $\mu$ M – 20 mM) of molybdenum added to the media as  $\text{Na}_2\text{MoO}_4 \cdot 2\text{H}_2\text{O}$  and incubated for 2-3 days at 28°C to determine the amount at which molybdenum becomes toxic to the cell (approximately 20 mM).

#### 2.2.1.2 EMS mutagenesis of wild type yeast *Invsc1*

Wild type *Invsc1* (*MAT $\alpha$  his3- $\Delta$ 1 leu2 trp1-289 ura3-52*) was mutagenised as per Lawrence (1991). 10 mL of liquid YPAD [1% (w/v) yeast extract; 2% (w/v) peptone; 2% (w/v) glucose; and 0.004% (w/v) adenine sulfate] was inoculated with *Invsc1* to give approximately  $1 \times 10^6$  cells/mL. Cells were incubated at 28°C overnight with vigorous shaking. When cells reached approximately  $2 \times 10^8$  cells/mL, cells were washed twice in 50 mM potassium phosphate buffer (pH 7) and resuspended in 10 mL of the same buffer to give a final concentration of  $5 \times 10^7$  cells/mL according to the protocol of Lawrence (1991) and put into a sterile glass screw cap tube. 300  $\mu$ L of EMS was added to the cells to produce transitions at G-C sites, cells vortexed and incubated at 28°C for 30 mins. Mutagenesis was stopped with the addition of an equal volume of freshly made 10% (w/v) filter sterilized  $\text{Na}_2\text{S}_2\text{O}_3 \cdot 5\text{H}_2\text{O}$ .  $5 \times 10^7$  cells/mL were mixed well and washed twice in sterile water.  $5 \times 10^7$  cells/mL of the cells plated onto 10, 200 mm diameter petri dish plates containing YPAD media supplemented 20 mM  $\text{Na}_2\text{MoO}_4 \cdot 2\text{H}_2\text{O}$ . Kill rate as a result of the mutagenesis was not determined. Plates were incubated at 28 °C until colonies grew. Colonies that appeared white/cream in colour were picked of and subsequently plated onto normal YPAD media or YPAD media supplemented with 20 mM  $\text{Na}_2\text{MoO}_4 \cdot 2\text{H}_2\text{O}$  for further screening.

## **2.2.2 Targeted gene approach to identify molybdenum transport proteins using the Low Mo assay**

### **2.2.2.1 Molybdenum removal from media and glassware**

Ultra pure chemicals were used for all media mixtures to ensure molybdenum free status. Trace amounts of molybdenum were removed from water using a modified version of Schneiders et. al. (1991) protocol. Activated charcoal (Sigma-Aldrich) was used to absorb trace amounts of molybdenum by adding 50 g of charcoal to 1L of deionised water purified from a Millipore Filter purification unit and stirred for 2 days at room temperature. This mixture was degassed by boiling for 10 minutes and cooled. 50 mL aliquots of the charcoal and water mixture were filtered through a paper Millipore filter (125 mm) with a medium pore size and collected water discarded. This resulted in a layer of carbon through which acted as a filter to remove molybdenum from water. To this filter, 200 mL of deionised water purified from a Millipore Filter purification unit was added to the filter and suctioned through the filter. The resulting water was classed as molybdenum free water. Molybdenum free water was used in all *S. cerevisiae* experiments where growth medium was required to be molybdenum free. Where molybdenum was required, molybdate as  $\text{Na}_2\text{MoO}_4 \cdot 2\text{H}_2\text{O}$  was added back into the molybdenum free media. All water, media and nutrient solutions were stored in glass wear free of molybdenum. Subsequent ICP-MS analysis of the water for molybdenum revealed that molybdenum levels were below that of detection.

Molybdenum free glass ware was prepared using a similar protocol described in Zahalak (2004). All glassware was soaked for a minimum of 24 hours in 1% (v/v) Decon90 (Perkin-Elmer) with 10 mM EDTA and rinsed with molybdenum free water. Where glassware was not used, disposable sterile plastic laboratory consumables were used.

## **2.2.3 Identification of putative $\text{MoO}_4^{2-}$ and $\text{SO}_4^{2-}$ transport proteins using functional yeast complementation**

### **2.2.3.1 *Vitis vinifera* culture**

One year-old *Vitis vinifera* cv. Pinot noir (clone 123-3) grafted to rootstock 101-14 rootlings were purchased from Loxton Vine and Citrus Nursery. Vines were planted in UC soil (University of California soil mix) and grown in a controlled temperature glasshouse at 24 °C / 19 °C day/night with an artificial light supplement for 1 hour at 12 am to prevent

dormancy. Vines were fertilised weekly with 1/2 strength Hoaglands solution (Hoagland and Arnon, 1938). Mature leaves from these plants were picked and the end of the petiole submerged in 0.1% (w/v) indole-butyric-acid in 50% (v/v) ethanol for 30 seconds. Leaves were planted in 50:50% (w/w) perlite/vermiculite mix in a misting bed. After the formation of callus, and subsequent roots, leaves were transferred into 50 L tanks with an air supply containing 1/2 strength Hoaglands solution (Hoagland and Arnon, 1938).

### **2.2.3.2 Total and Poly (A)<sup>+</sup> RNA isolation**

*V. vinifera* cv. Pinot noir hydroponically grown leaves were grown in 1/2 strength Hoaglands solution for 3 weeks. Molybdenum starvation was induced by transferring plants into a Hoaglands solution that did not contain Na<sub>2</sub>MoO<sub>4</sub>·2H<sub>2</sub>O for 10 days. Total RNA was isolated from roots that were collected at midday and frozen immediately in liquid N<sub>2</sub> and stored at -80 °C. Roots (450 – 800 mg) were ground in liquid nitrogen in a mortar and pestle. 1 mL of extraction buffer [5 M NaClO<sub>4</sub>; 0.2 M Tris pH 8.3; 8.5% (w/v) insoluble polyvinylpyrrolidone; 5% (w/v) sodium dodecyl sulfate; 1% (v/v) β-mercapoethanol] was added and ground with the root tissue. More extraction buffer was added to larger samples to produce a viscous solution. Samples were left at room temperature for 30 minutes and vortexed several times during the incubation time. The extract was poured into a Rneasy Mini Kit Qias shredder (Qiagen) and centrifuged for 2 minutes at maximum speed. The column flow through was collected and 450 μL of solution 1 [5 M NaClO<sub>4</sub>; 0.2 M Tris pH 8.3; 1% (v/v) β-mercapoethanol] was added to the Qias shredder and spun again. Both column flow throughs were combined and equal volumes of 100% (v/v) ethanol were added. Samples were spun for 15 minutes at full speed resulting RNA pellet that was then resuspended in 100 μL of Rnase-free H<sub>2</sub>O with 350 μL of RLT buffer (Qiagen Rneasy Mini Kit) containing 1% (v/v) β-mercapoethanol and vortexed until resuspended. To the RNA lysate, 250 μL of 100% (v/v) ethanol was added and mixed well by pipetting then added to a Rneasy spin column sitting in a collection tube and spun at 10 000 rpm for 15 seconds. The flow through was discarded. The column was then washed with 700 μL of buffer RW1, spun at 10 000 rpm for 15 seconds and the flow through discarded. The column was transferred to a new collection tube and washed twice with 500 μL of buffer RPE and spun at 10 000 rpm for 15 seconds discarding the flow through each time. The column was spun again at 10 000 rpm for 2 minutes to dry the membrane and placed in a new collection tube. The RNA was eluted from the membrane with 2 washes of 30 μL of RNase-free H<sub>2</sub>O and spun at 10 000 rpm for 1 minute between the additions of Rnase-free H<sub>2</sub>O. The RNA was then stored at -80 °C.

Poly (A)<sup>+</sup> RNA was isolated from 652  $\mu\text{g}$  of total RNA using oligo (dT)-cellulose columns (Amersham Biosciences) following the manufactures protocol.

### **2.2.3.3 cDNA library construction**

Poly (A)<sup>+</sup> RNA (3.5  $\mu\text{g}$ ) of molybdenum starved root tissue was used to synthesise a cDNA library using the CloneMiner<sup>TM</sup> cDNA Library Construction Kit (Invitrogen) (Figure 2.4). Single strand mRNA was converted into double stranded cDNA by SuperScript<sup>TM</sup> II RT with the 3' end flanked with the *aatB2* adapter. The *aatB1* adapter was then ligated to the 5' end of the double stranded cDNA (Figure 2.4A). Size fractionation was performed by column chromatography to optimise the presence of large cDNA inserts. With the use of site-specific recombination, the *aatB* flanked cDNA was cloned directly into an *aatP1/aatP2* containing donor vector, pDONR222 (Figure 2.5) to produce a cDNA library with an approximate total of  $6.94 \times 10^6$  transformants.

### **2.2.3.4 Ligation into pYES3 via Gateway® Technology**

cDNA's in pDONR222 (Figure 2.5) were cloned into the yeast/*E. coli* shuttle vector pYES3-DEST (Figure 2.6). This vector originated from pYES3 and was made into a Gateway® destination vector by ligating the Gateway Conversion reading frame cassette A into the *Bam* H1 sites (M. Shelden, pers. comm.). The pYES3-DEST vector contains the yeast *GAL1* promoter that regulates gene transcription of the 2 $\mu$  origin of replication, and the *URA3* gene to complement *URA3*- minus strains. The AMP gene is used for selection in *E.coli*. The presence of *aatR2* and *aatR1* sites allows cDNA inserts to be switched between other Gateway® ready vectors (Figure 2.4B). Upon recombination, the *ccdB* gene is replaced by the cDNA insert. A LR reaction using LR Clonase<sup>TM</sup> (Invitrogen) was used to facilitate the recombination of an *aatL* entry library in pDONR222 (Figure 2.5) to create an *attB*-containing expression library in pYES3-DEST (Figure 2.6).

### **2.2.3.5 cDNA library amplification**

An aliquot (3  $\mu\text{L}$ ) of the LR Clonase reaction was transformed into 20  $\mu\text{L}$  of *E. coli* DH10B Electromax cell by electrophoration. Cells were then grown for 1 hour at 37 °C in SOC media [2% (w/v) tryptone; 0.5% (w/v) yeast extract; 0.05% (w/v) NaCl; 2% (w/v) glucose; 10 mM MgCl<sub>2</sub>; 10 mM MgSO<sub>4</sub>] and 100  $\mu\text{L}$  plated onto LB plates [2% (w/v) NaCl; 2% (w/v) Bactotryptone (Difco); 1% (w/v) yeast extract (Difco); 2% (w/v) agar] containing 100  $\mu\text{g mL}^{-1}$  ampicillin (LB-AMP) to check for transformation efficiency.

Remaining SOC culture was used to inoculate 25 mL of liquid LB-AMP for library amplification using a Midi Plasmid Kit (Qiagen) according to the manufacturer's protocol.

### 2.2.3.6 Functional complementation of YSD1 with *Vitis vinifera* cDNA

YSD1 (*sull1 his3-Δ1 leu2 trp1-289 ura3-5*) was obtained from Dr. Susan Howitt (Australian National University) and grown in liquid YPAD [1% (w/v) yeast extract; 2% (w/v) peptone; 2% (w/v) glucose; and 0.004% (w/v) adenine sulfate] at 28 °C to an OD<sub>600</sub> 0.5-0.7. Cells were then transformed with 10 μL of the *V. vinifera* cDNA library using the LiAc/PEG method (Smith et. al., 1995b). Transformed cells were plated onto 20 x 200 mm petri dish plates containing 2 different types of media (see below) depending on selection method.

To either encourage SO<sub>4</sub><sup>2-</sup> transport proteins to complement YSD1, cells were transformed with the *V. vinifera* cDNA library, and plated onto the final Low S media as described by Smith et. al. (1995a). In this method cells were first plated onto 2xTL Glu media [1 mL/L 1000 x Trace Elements [50 mg/100 mL H<sub>3</sub>BO<sub>3</sub>; 4 mg/100 mL CuCl<sub>2</sub>·(H<sub>2</sub>O)<sub>2</sub>; 10 mg/100 mL KI; 20 mg/100 mL FeCl<sub>3</sub>; 40 mg/100 mL Mn<sub>2</sub>Cl<sub>4</sub>·4H<sub>2</sub>O; 20 mg/100 mL Na<sub>2</sub>MoO<sub>4</sub><sup>2-</sup>·2H<sub>2</sub>O; 40 mg/100 mL ZnCl<sub>2</sub>]; 4 mL/L 250 x Vitamins [0.5 mg/100 mL biotin; 50 mg/100 mL calcium pantothenate; 0.05 mg/100 mL folic acid; 250 mg/100 mL inositol; 10 mg/100 mL niacin; 5 mg/100 mL p-Aminobenzoic acid; 10 mg/100 mL pyridoxine hydrochloride; 5 mg/100 mL Riboflavin; 10 mg/100 mL thiamine hydrochloride]; 100 mL 10 x Salts [1.25 g/L K<sub>2</sub>HPO<sub>4</sub>; 8.75 g/L KH<sub>2</sub>PO<sub>4</sub>; 20 g/L NH<sub>4</sub>Cl; 1 g/L NaCl; 6.2 g/L MgCl<sub>2</sub>; 1g/L CaCl<sub>2</sub>·2H<sub>2</sub>O; 10mg/L NaFeEDTA]; 0.7 g Amino Acids [minus uracil and methionine]; 2% (w/v) galactose; 76.52 mg/L homocysteine thiolactone; pH 5.6 with NaOH (M.Shelden, pers. comm.)] and left to grow at 29 °C until colonies were visible. Cells were then washed off the plate with the 2xTL Glu media and were grown for 5 hours while shaking at 29 °C. After 5 hours cells were washed in Low S Gal media [1 mL/L 1000 x Trace elements; 4 mL/L x 250 Vitamins; 100 mL/L 10 x Salts; 0.67 g/L Amino Acids [minus uracil and methionine]; 100 μM MgSO<sub>4</sub>; 2% (w/v) galactose; 2.4 % (w/v) Agarose LE; pH 5.6 with NaOH (M. Shelden, pers. comm.)], before being plated onto the same media and left to grow for 72 hours at 29 °C. Colonies that grew faster than the control (empty vector pYES3-DEST) were collected and plasmids isolated. Isolated cDNA's were then transformed back into new YSD1 cells and re-plated onto Low S media containing either galactose or glucose media to regulate gene expression.

To identify putative  $\text{MoO}_4^{2-}$  transport proteins YSD1 cells were transformed with the *V. vinifera* cDNA library and grown on a low molybdenum media (Low Mo Gal) made from molybdenum free water [98.9 mL/L 10 x Salts [7 g/L  $\text{MgSO}_4 \cdot 7\text{H}_2\text{O}$ ; 10 g/L  $\text{KH}_2\text{PO}_4$ ; 4 g/L  $\text{Ca}_2\text{Cl}_2 \cdot 2\text{H}_2\text{O}$ ; 5 g/L NaCl; 10 g/L  $\text{K}_2\text{SO}_4$ ; 105 g/L citric acid. $\text{H}_2\text{O}$ ; 160 mL/L 10M KOH; pH 6.1]; 1 mL/L Micronutrients [10 mg/L  $\text{H}_3\text{BO}_3$ ; 1 mg/L  $\text{CuSO}_4 \cdot 5\text{H}_2\text{O}$ ; 2 mg KI; 14 mg/L  $\text{ZnSO}_4 \cdot 7\text{H}_2\text{O}$ ; 10 g/L citric acid. $\text{H}_2\text{O}$ ; 400 mg/L  $\text{MnSO}_4 \cdot \text{H}_2\text{O}$ ; 5 g/L  $\text{FeCl}_3 \cdot 6\text{H}_2\text{O}$ ]; 10 mL/L Vitamins [250  $\mu\text{g/L}$  D-Biotin; 100 mg/L thiamine.HCl; 1 g/L inositol; 200 mg/L calcium D-pantothenate; 100 mg/L pyridoxine. HCl]; 2 % (w/v) galactose; 2% (w/v) agar; pH 6.5 with KOH]. Colonies which grew faster than the control (empty vector pYES3-DEST) were collected and plasmids isolated. Isolated cDNA's were then transformed back into new YSD1 cells and re-plated onto Low Mo media containing either galactose or glucose media to regulate gene expression.

### **2.2.3.7 Yeast plasmid isolation**

To determine the size and sequence of the cDNA insert that complemented YSD1, plasmid DNA was extracted from a 1.5 mL of pelleted yeast cells grown overnight in SC Glu media [0.67% (w/v) yeast nitrogen base without amino acids with ammonium sulfate (Difco); 0.01% (w/v) tryptophane; 0.01% (w/v) leucine; 0.005% (w/v) histidine; 2% (w/v) glucose; pH 6.5] and resuspended in 200  $\mu\text{L}$  of lysis buffer [300 mM NaCl; 10 mM Tris pH 8.0; 1mM EDTA pH8.0; 0.1% (w/v) sodium dodecyl sulfate] and 300  $\mu\text{L}$  of 0.45 nm acid washed glass beads vortexed vigorously for 1 minute. The aqueous layer containing the plasmid DNA was collected by adding 500  $\mu\text{L}$  of phenol:chloroform:isoamyl alcohol (25:24:1 v/v/v) and vortexing for a further 2 minutes and then centrifuged for 5 minutes at maximum speed. A maximum of 2  $\mu\text{L}$  of aqueous phase was transformed into *E. coli* DH5 $\alpha$  and amplified in LB-AMP. The plasmid was then extracted with a Mini Prep Kit (Qiagen). Plasmid was used to determine the size of the cDNA insert from pYES3-DEST by digestion with BsrG1 restriction enzyme. Digests were run on a 1% (w/v) agarose gel, and plasmids with expected sized cDNA inserts were sequenced and transformed back into YSD1.

### **2.2.3.8 DNA sequencing**

Plasmids were sequenced using BigDye® Terminator v3.1 Cycle Sequencing Kit (Applied Biosystems) according the manufactures protocols. Sequencing products were analysed by the Institute of Medical and Veterinary Science, Adelaide. Sequences were analysed using

MacVector (Eastman Kodak) and compared to those on NCBI gene and protein databases using BLAST programs.

## 2.3 Results

### 2.3.1 Determination of molybdenum toxicity to yeast

Three strains of yeast were tested for their ability to grow on increasing concentrations of  $\text{Na}_2\text{MoO}_4 \cdot 2\text{H}_2\text{O}$  (Figure 2.1, 2.2 and 2.3). The growth of all strains appeared normal at lower concentrations of molybdenum, however growth significantly decreased from 10 mM to 20 mM in all 3 strains. At the higher concentrations of molybdenum, the phenotype of the cells changed significantly and background growth of cells began to turn black. In all cases at higher levels of molybdenum, some cells retained their cream phenotype. From this preliminary screen it was determined that molybdenum became toxic to the cells at concentrations between 18 to 20 mM.

As a result of the toxicity screen, 20 mM molybdenum proved toxic to yeast. Yeast cells that were treated with EMS were plated onto YPAD media supplemented with 20 mM  $\text{Na}_2\text{MoO}_4 \cdot 2\text{H}_2\text{O}$ . Unfortunately, none of the potential white/creamy yeast isolates that were identified through the EMS mutagenesis screen when re-streaked on fresh YPAD media supplemented with 20 mM  $\text{Na}_2\text{MoO}_4 \cdot 2\text{H}_2\text{O}$  would consistently grow on toxic levels of molybdenum. No yeast mutant was able to be created that would successfully grow on toxic levels of molybdenum. As a result, this approach was abandoned for a pre-characterised yeast mutant.

### 2.3.2 Identification of putative $\text{MoO}_4^{2-}$ and $\text{SO}_4^{2-}$ transport proteins using functional yeast complementation

#### 2.3.2.1 cDNA library construction and ligation into pYES3 via Gateway® Technology

cDNA was synthesised using the CloneMiner™ cDNA Library Construction Kit (Invitrogen) (Figure 2.4) from Poly (A)<sup>+</sup> RNA extracted from hydroponically grown *V. vinifera* cv. Pinot noir roots starved of molybdenum for 10 days. cDNA was ligated into pDONR222 (Figure 2.5) to produce a cDNA library with an approximate total of  $6.94 \times 10^6$  transformants with cDNA insert size ranging between 500 bp to 5 Kb (Figure 2.7).

#### 2.3.2.2 Functional complementation of YSD1 with *Vitis vinifera* cv. Pinot noir root cDNA's

YSD1 was transformed with the *V.vinifera* root cDNA library and cells plated onto a final selection media of either Low S Gal (100  $\mu\text{M}$  S) (Appendix 1 Table 1 and Figure 2.8) or



Low Mo Gal (Appendix 1 Table 2). After about 5-6 days, approximately 40 colonies demonstrated growth under sulfate deficient conditions in the presence of galactose. In contrast, cell growth on the Low Mo media took much longer, where after 3-4 weeks of growth approximately only 20 colonies grew. Each colony was picked and plated on to SC Glu media and grown in liquid culture, shaking over night at 28 °C for yeast plasmid isolation.

Plasmid isolation was performed on all colonies for both Low S and Low Mo screens. Plasmid was then digested with BsrG1 to determine the size of the cDNA inserts that complemented the mutation in YSD1. cDNA insert sizes ranged from 250 bp to 2.4 Kb. Plasmids were labelled LSKG (Low S Gal) (Appendix 1 Table 1) or LMKG (Low Mo Gal) (Appendix 1 Table 2). Only plasmids that contained the largest inserts and appeared first on the final selection plates were further investigated and subsequently isolated and retransformed into YSD1.

On the Low S Gal media one of the cDNA's to partially complement the mutation of YSD1 was an amino acid transporter, LHT1 (Accession number NP\_851109). This cDNA was isolated from potentially 8 different colonies, all of which contained the cDNA of various cDNA lengths (based on plasmid digest), with cDNA LS KG5 possibly being the full length clone (Appendix 1 Table 1). A total of 10 metallothionein like proteins (Accession number CAC39481) with homology to those in *Quercus suber* also partially complemented YSD1. RING-type/zinc finger (Accession number ABE82278) with homology to *Medicago truncatula* (LS KG20) and a HRD complex with a RING-finger domain (Accession number NP\_001047138) cDNA's were also isolated on the Low S Gal media (Appendix 1 Table 2). In addition a GTP binding proteins was isolated (LS KG1) with homology to the *Helianthus annuus* GTP binding protein (Appendix 1 Table 1).

Fewer cDNA's partially complemented YSD1 on the Low Mo Gal media. These included a Cyclin-like F-Box (Accession number ABE907081; LMo KG1), a major latex-like protein (Accession number AAK 14060.1; LMo KG 4), a translationally controlled tumor like protein (Accession number AB184255; LMo KG 9) and an osmotin-like protein (Accession number CAA71883.1 LMo KG10) (Appendix 1 Table 2). The only similar cDNA that was isolated on both the Low S Gal and Low Mo Gal was a zinc finger; RING type PHD type with homology to *M. truncatula* (LMo KG7) (Accession number ABE80612) (Appendix 1 Table 2).

Unfortunately upon retransformation of each of the cDNA's into YSD1, none were found to be capable of improving growth on Low Mo or Low S selection media and which were able to be transcriptionally controlled using galactose or glucose.

## 2.4 Discussion

Molybdenum toxicity of yeast was determined by screening 3 strains of yeast on concentrations of up to 20 mM molybdenum. Toxicity symptom phenotypes began to be observed from 10 mM, which included a dramatic reduction in growth and the appearance of black colonies (Figure 2.1, 2.2 and 2.3). From this it was determined that molybdenum became toxic to the cells at concentrations between 18 to 20 mM. There have been no known reports of determining at which levels molybdenum becomes toxic to microorganisms. However, it is assumed that molybdenum transport in plants, and also yeast, is tightly regulated due to the small amounts of molybdenum required in these systems. It is possible that higher amounts of molybdenum (above 18 mM) would eventually saturate any mechanisms capable of effluxing toxic levels of molybdate from the cell resulting in cell death. Although kill rate as a result of EMS mutagenesis was not determined, if future experiments were performed, the kill rate should be determined. This could be used to determine if the mutagenesis was actually successful, as it may be possible that not enough cells survived. However, of the cells that did survive, none would continue to grow on toxic concentrations of molybdenum.

Unfortunately *V. vinifera* membrane transporters capable of either molybdenum or sulfate transport on low concentrations of molybdenum or sulfate respectively could not identify putative cDNA's. It is unknown why retransformation into YSD1 and subsequent transcriptional regulation using the galactose promoter failed. This led to many false positives that only partially complemented YSD1. More rigorous growth assays could be performed, such as the use of dilution spot plates, to further reduce the number of false positives. It is possible that the library did not contain the sulfate or molybdenum cDNAs that encoded functional transporters, despite a sufficient number of cDNA's being transformed. It is somewhat surprising that the cDNA library did not contain any putative sulfate transporter proteins especially since Smith et. al., (1995a) had considerable success in identifying 3 sulfate transporters via this method. One possible explanation may be because the library was not enriched for these proteins through sulfate starvation of plants as Smith et. al. (1995a) had done. However, the library did contain some interesting cDNAs that partially complemented YSD1.

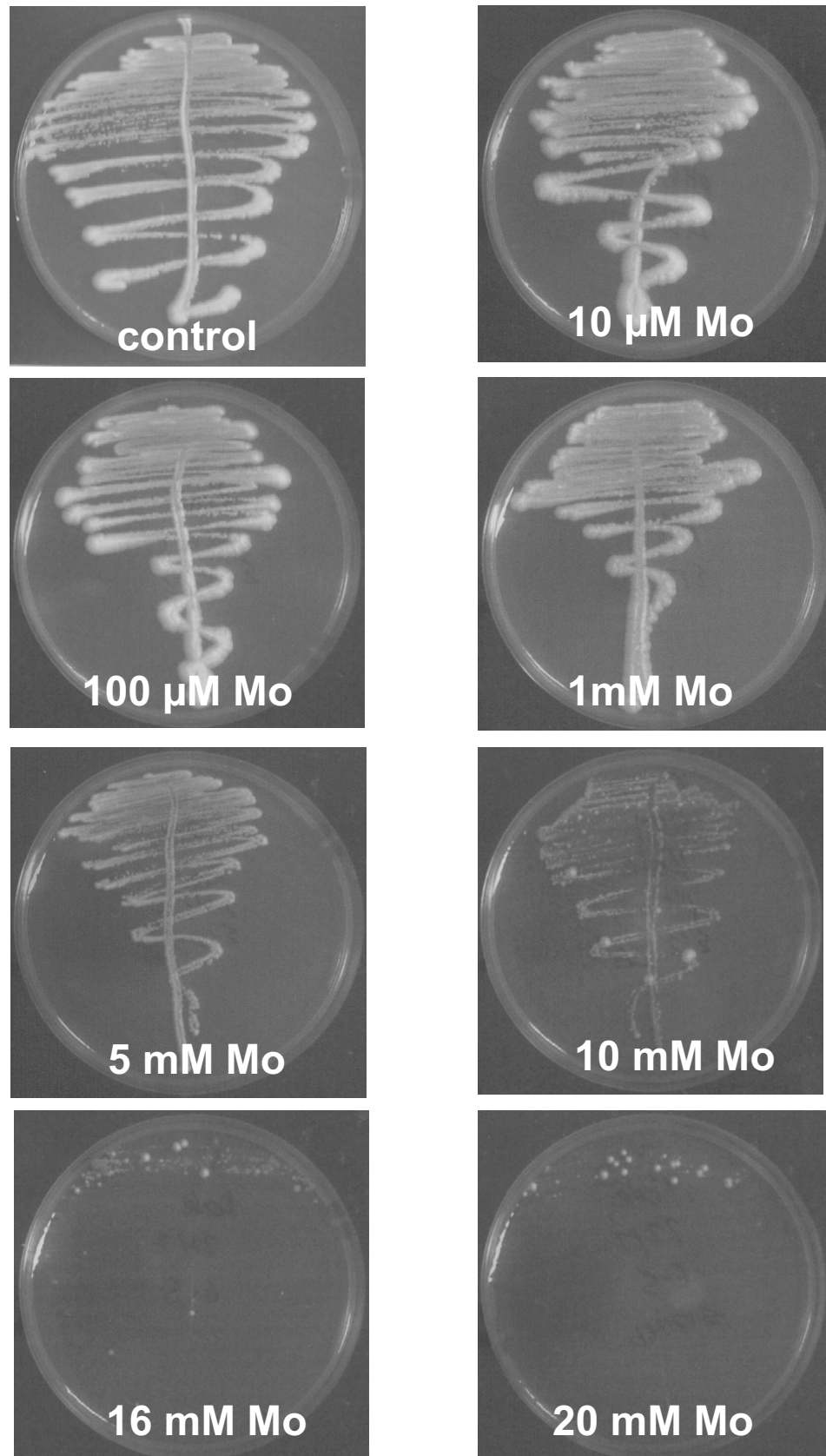


**Figure 2.1** Yeast strain  $\Sigma 1278b$  plated on varying concentrations of molybdenum to determine toxicity levels.

Cells were plated onto YPAD media (pH 6.5) containing 10  $\mu\text{M}$ , 100  $\mu\text{M}$ , 1 mM, 5 mM, 10 mM, 16mM and 20 mM of  $\text{Na}_2\text{MoO}_4 \cdot 2\text{H}_2\text{O}$ . Control plates contain no added molybdenum.

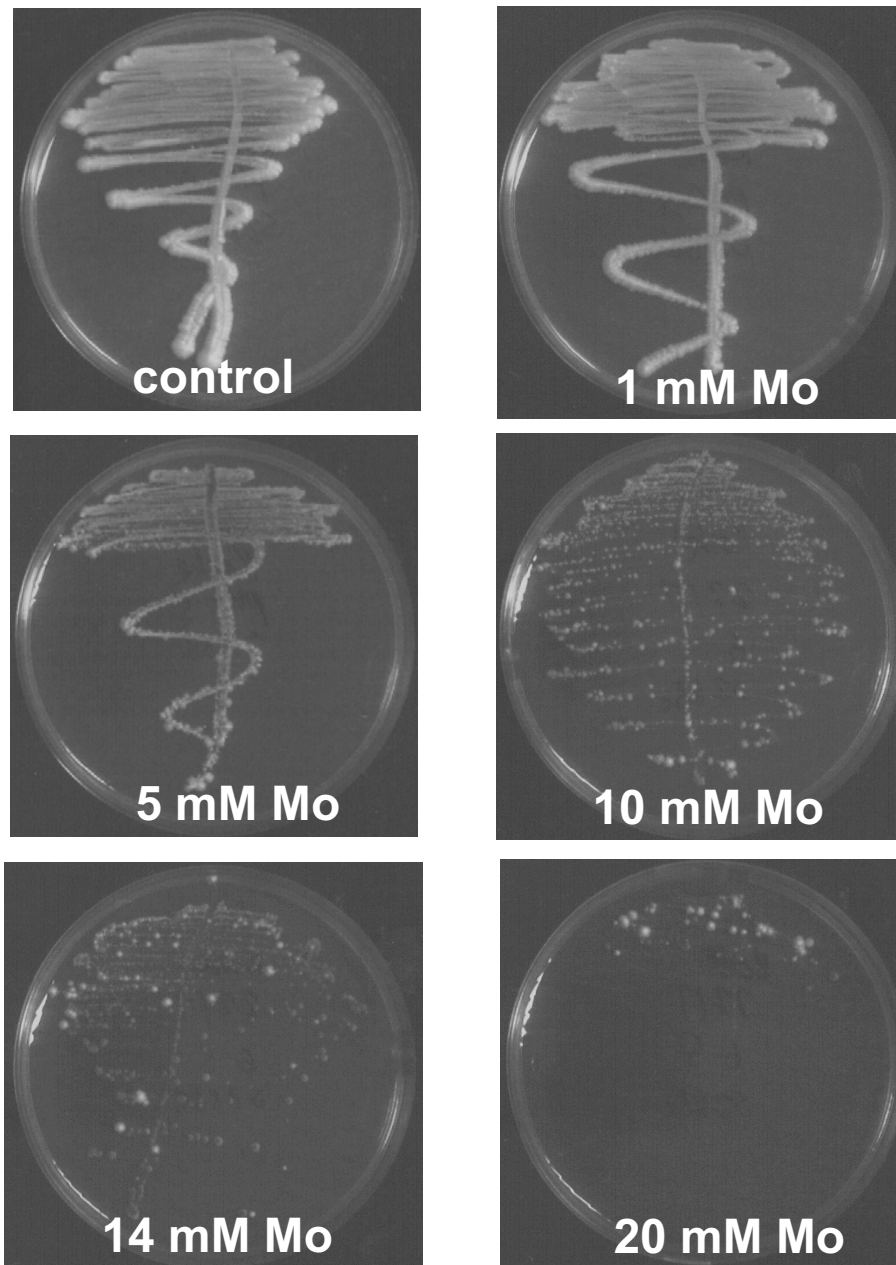


**Figure 2.2 Yeast strain S288c plated on varying concentrations of molybdenum to determine toxicity levels.**

Cells were plated onto YPAD media (pH 6.5) containing 1 mM, 5 mM, 10 mM, 14 mM and 20 mM of  $\text{Na}_2\text{MoO}_4 \cdot 2\text{H}_2\text{O}$ . Control plates contain no added molybdenum.

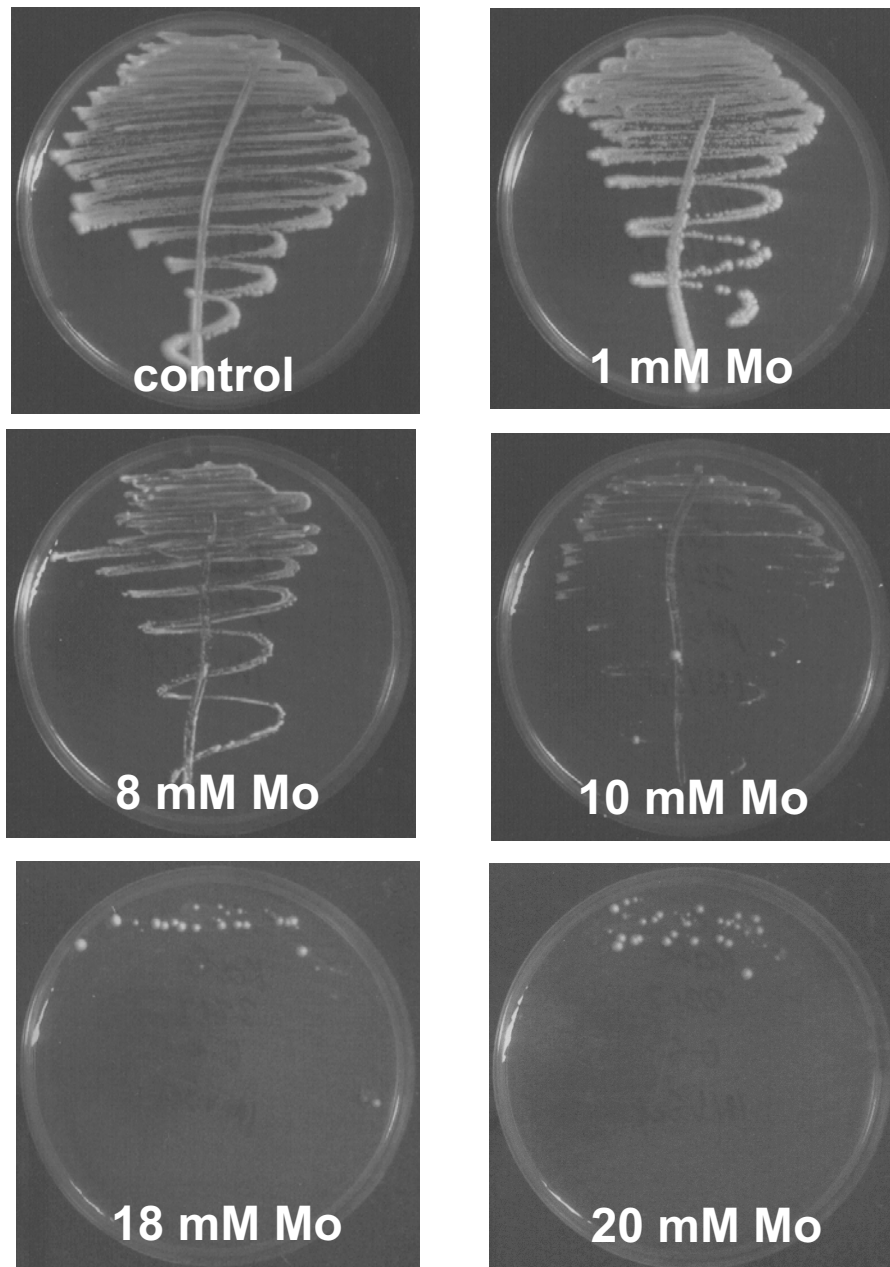


**Figure 2.3 Yeast strain Invscl plated on varying concentrations of molybdenum to determine toxicity levels.**

Cells were plated onto YPAD media (pH 6.5) containing 1 mM, 8 mM, 10 mM, 18 mM and 20 mM of  $\text{Na}_2\text{MoO}_4 \cdot 2\text{H}_2\text{O}$ . Control plates contain no added molybdenum.

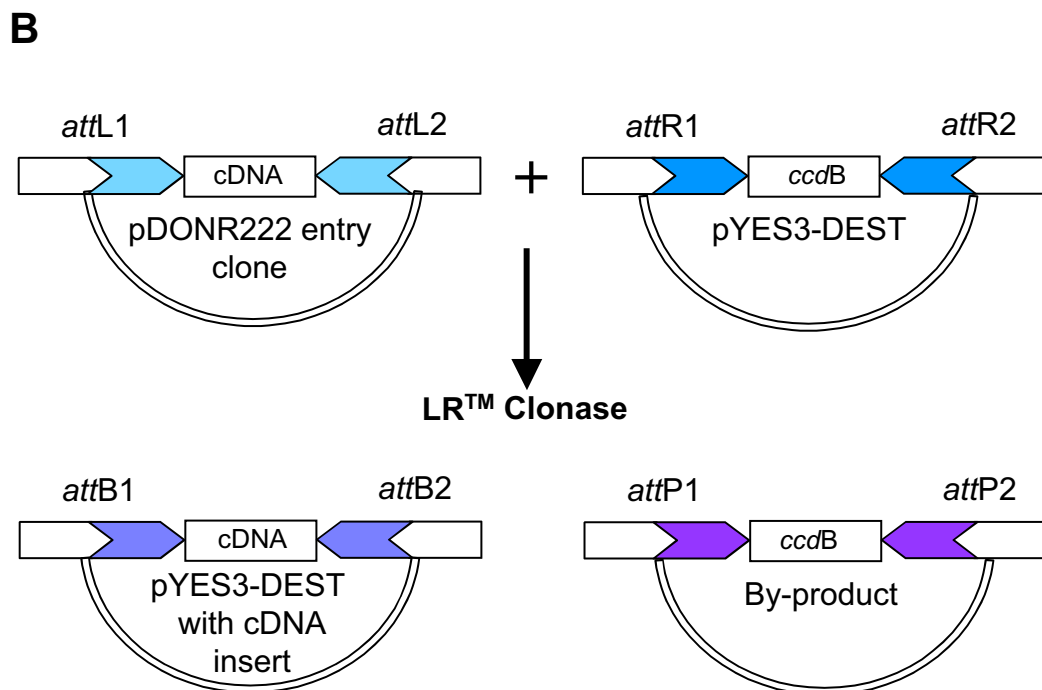
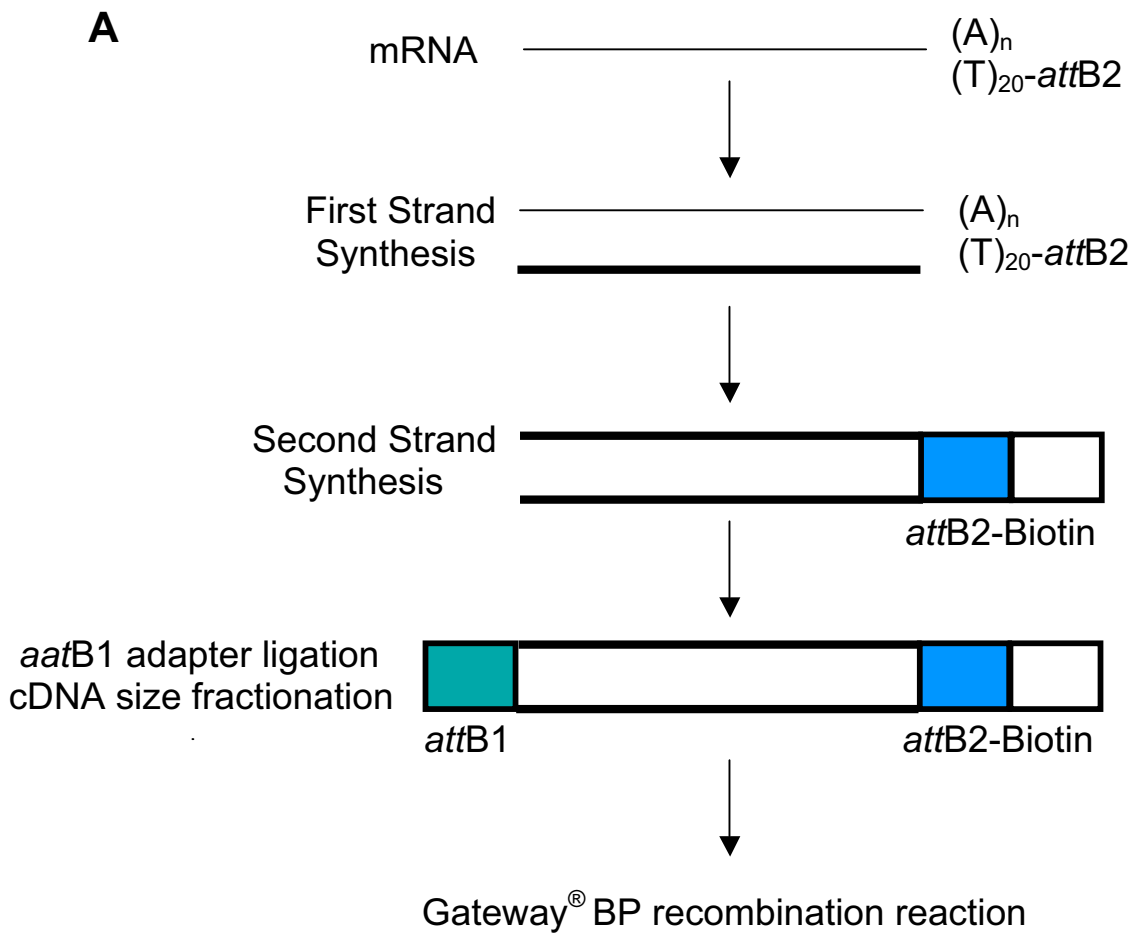


**Figure 2.4** A schematic diagram of Gateway® cDNA library construction and Gateway® recombination reactions used in the Gateway cDNA library construction manual.

**A.** Summary of the steps involved in the cDNA synthesis process. mRNA was extracted from *V.vinifera* and Poly(A)<sup>+</sup> mRNA isolated. The Biotin-*aatB2*-Oligo(dT) primer hybridises to the mRNA Poly(A)<sup>+</sup>. SuperScript™ II Reverse Transcriptase synthesises the first strand of cDNA using the mRNA as a template. *E.coli* Polymerase I synthesises the second strand of cDNA using the first strand of cDNA as a template. Finally, the *aatB1* adapter is ligated to the 5' end of the cDNA with the Biotin preventing ligation to the *aatB1* adapter to the 3' end of the cDNA (Invitrogen, 2003). **B.** Summary of the recombination steps of moving cloned cDNA from the entry vector into the destination vector via a LR™ Clonase reaction. The LR™ Clonase reaction facilitates recombination of the *aatL*-flanked cDNA with an *aatR* substrate (pYES3-DEST) to create an *aatB* containing expression library (Invitrogen, 2003).



NOTE: This figure is included on page 72 of the print copy of the thesis held in the University of Adelaide Library.

**Figure 2.5 Vector map of pDONR<sup>TM</sup>222 (Invitrogen, 2006).**

Vector pDONR222 was used in the construction of the *V. vinifera* cv. Pinot noir root cDNA library. Upon recombination, the *ccdB* gene between attP1 and attP2 is replaced by the cDNA insert into the attP1/attP2 sites.

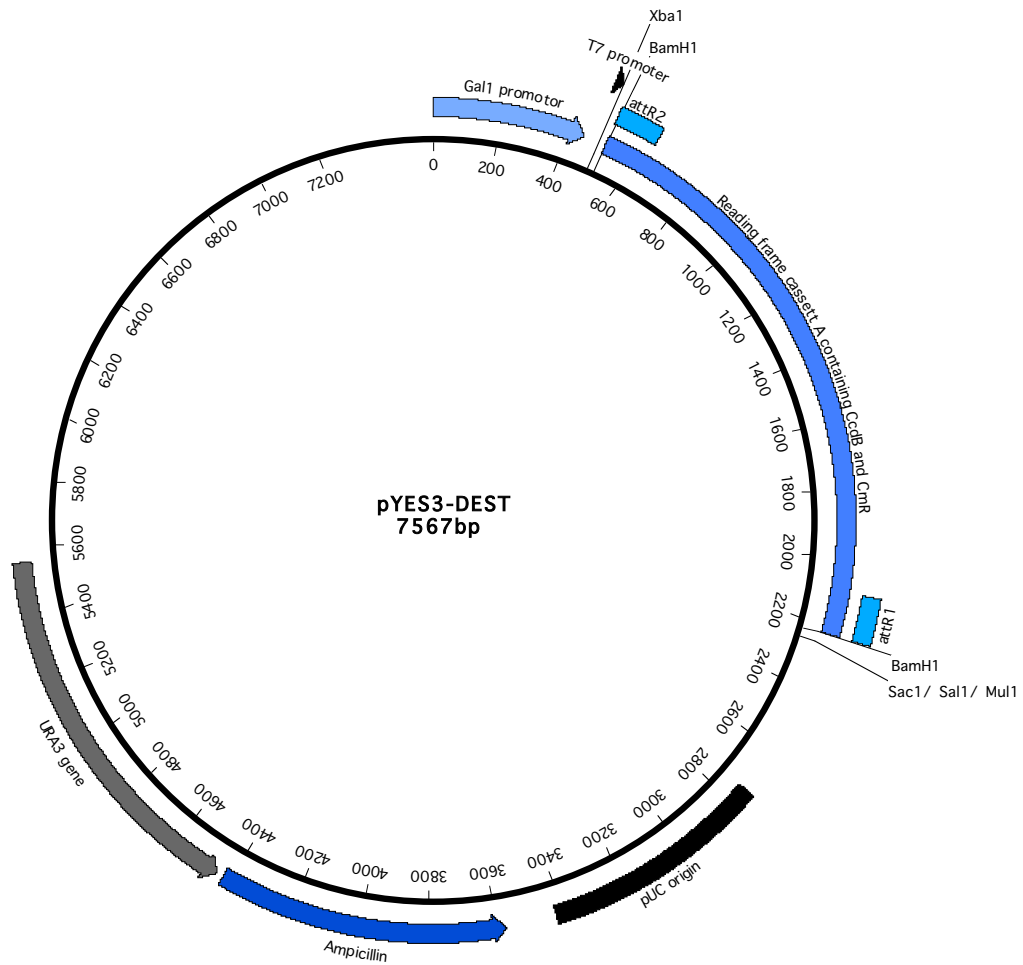


**Figure 2.6 Vector map of pYES3-DEST.**

Vector pYES3-DEST (M. Sheldon) was used as a destination vector for the *V. vinifera* cv. Pinot noir root cDNA library. A pYES3 vector was converted into a Gateway® destination vector by ligating the reading frame cassette A containing the *ccdB* (death gene) and the chloramphenicol resistance into the *BamHI* site. Upon recombination, the Reading Frame Cassette A between attR2 and attR2 was replaced by the cDNA insert.

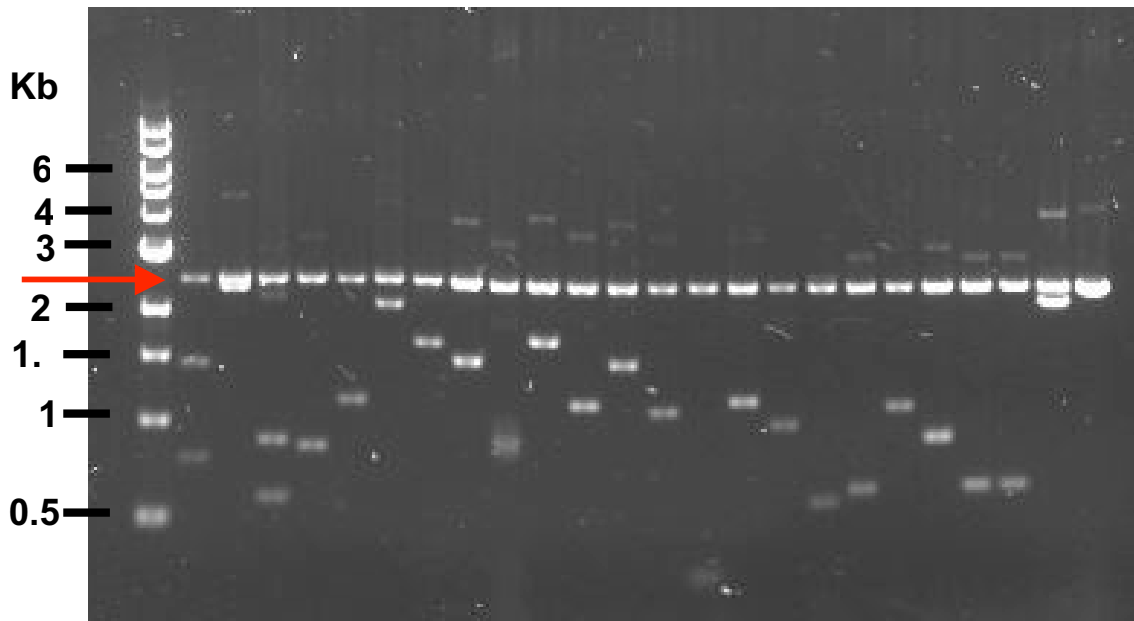
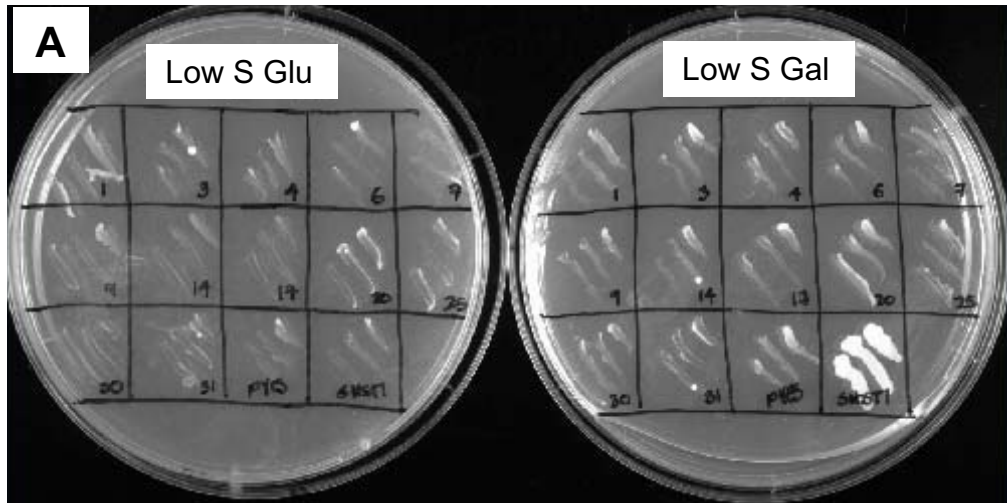


**Figure 2.7 Digest of inserts contained within *V.vinifera* cv. Pinot noir cDNA library.** cDNA inserts contained within pDONR222 were digested with *Bsr*G1 to liberate inserts from the vector. Red arrow indicates pDONR222 vector backbone that runs as a 2.5 Kb band. Digests were run on a 1% (w/v) agarose gel and the size of fragments determined with a 1 Kb ladder and stained with ethidium bromide.



**B**

GTP binding protein	Abnormal suppressor SUS2	Metallothionein like protein	Ubiq. ligase ER membrane RING finger	Metallothionein like protein
Amino acid permease LHT1	Cellulose synthase like protein Cs1G	Metallothionein like protein	RING-type/ zinc finger	Preprotein translocase SedY
Protein kinase Ck2 regulatory subunit 2	Sinapyl alcohol dehydrogenase like protein	pYES3	SHST1	

**Figure 2.8 Low S (100  $\mu$ M) Glu and Low S (100  $\mu$ M) Gal plates containing putative sulfate transport proteins in YSD1.**

**A.** *V. vinifera* cDNAs that initially rescued growth of YSD1 on low sulfate were further investigated by plating onto Low S media containing either glucose or galactose to induce or repress expression. YSD1/SHST1 and YSD1/pYES were used as a control to determine levels of yeast growth. **B.** Diagram of plate containing cDNA's identified.

## Chapter 3

# Functional complementation and characterisation of *Stylosanthes hamata* root cDNA SHST1 and *Glycine max* nodule cDNA GmNod70

---

### 3.1 Introduction

There is strong correlative evidence to suggest the uptake of molybdenum by plants is linked to sulfate transport mechanisms (Marschner, 1995; Mendel and Schwarz, 1999; Llamas et. al., 2000). MOT1 has recently been identified in Arabidopsis which was previously assigned as a putative sulfate transporter (Tejada-Jimenez et. al., 2007; Tomatsu et. al., 2007; Baxter et. al., 2008).

Direct measurements of molybdenum uptake into plants and the identification of the transport systems responsible for this uptake (molybdenum specific, sulfate or other anion transport systems) has been limited due to the difficulty in working with extreme low levels of molybdenum required by most plants is often below the level of detection of most analytical methods with the exception of ICP-MS. Radioactive isotopes are available for molybdenum transport studies, however their use has been limited due to the necessity of excessive lead shielding for the strong  $\beta$  and  $\lambda$  emissions released during its decay and the difficulty in measuring low quantities of accumulated molybdenum by most organisms.

SHST1 (Accession number X82255) is a previously characterised plant sulfate transporter expressed in the roots of the tropical legume *Stylosanthes hamata* upon sulfate starvation (Smith et. al., 1995a). When expressed in the sulfate transport deficient yeast strain YSD1, SHST1 accumulated sulfate and is capable of rescuing cell growth when sulfate concentrations in the yeast media were low and when no other source of sulfur is present (Smith et. al., 1995a). Previous work by Smith et. al. (1995a) has demonstrated that SHST1 is a high affinity  $H^+/SO_4^{2-}$  cotransporter with a  $K_m$  of 10  $\mu M$ . Within *S. hamata*, another two sulfate transporters have also been identified and characterised, another high affinity transporter, SHST2 (Accession number X82256) and a low affinity transporter, SHST3 (Accession number X824554) (Smith et. al., 1995a).

GmNod70 (Accession number D13505 and previously known as GmN#70 in Kouchi and Shingo (1993)), was originally identified through a library screen aimed at characterising novel nodulins involved in nodule formation and functional symbiosis from *Glycine max* (Kouchi and Shingo, 1993). GmNod70 was characterised as an intermediate nodulin as transcripts appeared well before the onset of nitrogen fixation but were not detected in 4 day old infected root segments (Kouchi and Shingo, 1993). Subsequent BLAST searches have demonstrated homology with plant sulfate transporters, however sequence analysis performed by Kouchi and Shingo (1993) revealed 10 hydrophobic domains, unlike to the classical 12 trans membrane domains (TMD). The intercellular location of this putative sulfate transporter is currently unknown in nodules, however the PBM is often considered a likely location.

In this chapter, the interaction between sulfate and molybdenum transport was explored further as a possible tool to help characterise and identify novel molybdenum/sulfate transport proteins. Using the yeast sulfate transport mutant YSD1 (yeast sulfate transport deletion mutant 1) (Smith et. al., (1995b)), a modified media was prepared where molybdenum levels were reduced to a level which restricted cell growth (Low Mo media). Using a restricting molybdenum concentration range, the Low Mo assay was then used to test targeted sulfate transport genes including SHST1 for the ability to rescue cell growth. Previous work has suggested, molybdenum transport may involve known sulfate transport systems in plants (Marschner, 1995; Mendel and Schwarz, 1999; Llamas et. al., 2000). SHST1 seemed a likely candidate gene to test this hypothesis due to similarities of both molybdate and sulfate in chemical geometry, hydrogen bonding properties and net charge

and importantly its expression in roots is enhanced under sulfate deprivation (Dudev and Lim, 2004).

In this study, the capacity for molybdenum and sulfate transport by SHST1 in the YSD1 yeast strain when challenged with low external molybdenum concentrations has been explored. Functional transport activity was measured using radioactive isotopes for sulfate ( $^{35}\text{SO}_4^{2-}$ ) and molybdate ( $^{99}\text{MoO}_4^{2-}$ ). In parallel, a second putative sulfate transporter, GmNod70, was also tested for its ability to transport sulfate.

## 3.2 Methods

### 3.2.1 Gene constructs of SHST1 and GmNod70

SHST1 was obtained from Dr. Susan Howitt (Australian National University, Canberra). SHST1 is cloned into the Sal1/Not1 sites of the yeast/*E. coli* shuttle vector pYES3 directly downstream of the yeast GAL1 promoter (Smith et. al., 1995a).

A cDNA of GmNod70 was amplified from a *Glycine max* nodule cDNA library (Kaiser et. al., 1998) by J.L. Parker (unpublished results). The PCR utilised a proofreading enzyme (PFU Stratagene) to minimise misread of the cDNA template during amplification. PCR primers designed against GmNod70 (forward 5'-TAACTCAGAGGGTGGTTGCTTCA-3' and reverse 5'-TGAATAGCCAATATTTGTCAG-3') amplified a 2.1 Kb cDNA which was then cloned into the pGEM T Easy vector (Promega USA) and transformed into *E. coli*. An individual colony containing a cDNA of the expected size was sequenced from both the 5' and 3' ends to verify sequence integrity against the deposited clone (Accession # D13505) found on NCBI. The full-length sequence verified cDNA was then sub cloned into the EcoR1 restriction sites of pYES3.

### 3.2.2 Transformation of YSD1 with SHST1 and GmNod70

GmNod70 and SHST1 were transformed into YSD1 as described previously in section 2.2.3.6. Cells were first plated onto SC Glu [0.67% (w/v) synthetically defined media without amino acids with ammonium sulfate (Difco), 2% (w/v) glucose, 0.1% (w/v) leucine, 0.1% (w/v) tryptophan, and 0.05% (w/v) histidine and 2% (w/v) agar]. Once cell growth was observed (3-4 days) individual colonies were streaked separately onto modified sulfate media containing various concentrations of sulfate or molybdenum media (see section 2.2.3.6).

### 3.2.3 Functional complementation of YSD1 with GmNod70

GmNod70 and transformed with empty vector controls (pYES3) into YSD1 (*sul1 his3-Δ1 leu2 trp1-289 ura3-5*) as above in section 3.2.2. Transformed GmNod70 cells were plated onto Low S media described in section 2.2.3.6. Additional sulfate as Na<sub>2</sub>SO<sub>4</sub><sup>2-</sup> was added back to this media at selected concentrations (Low S (100 μM) 1 mM, 2 mM and 5 mM) and growth phenotypes observed.



### **3.2.4 Functional complementation of YSD1 with SHST1 on the Low Mo Gal media assay**

SHST1 and transformed with empty vector controls (pYES3) into YSD1 (*sul1 his3-Δ1 leu2 trp1-289 ura3-5*) as above in section 3.2.2. Transformed SHST1 cells were plated onto Low Mo gal media described in section 2.2.3.6. Additional molybdenum as  $\text{Na}_2\text{MoO}_4 \cdot 2\text{H}_2\text{O}$  was added back to this media at selected concentrations (Low Mo, 80 nM and 800 nM) and growth phenotypes observed.

### **3.2.5 Functional expression of SHST1 and GmNod70 in YSD1**

#### **3.2.5.1 Yeast cell growth and harvest**

For both the  $^{35}\text{SO}_4^{2-}$  and  $^{99}\text{MoO}_4^{2-}$  uptake experiments, YSD1 cells were transformed with either the empty vector control pYES3, SHST1 or GmNod70. For each experiment, starter yeast cultures in SC Glu (see section 2.2.3.7) were grown at 28°C in flasks shaken at 200 rpm. After 2-3 days of growth and/or when the cells approached an  $\text{OD}_{600\text{nm}}$  of 1.0, cultures were harvested by centrifugation at 4000 rpm for 2 mins. Collected cells were washed twice in either sterile  $\text{dH}_2\text{O}$  for  $^{35}\text{SO}_4^{2-}$  uptakes or with sterile Mo-scrubbed  $\text{H}_2\text{O}$  for the  $^{99}\text{MoO}_4^{2-}$  uptake experiments. Cells were then spiked into various media described below.

For the  $^{35}\text{SO}_4^{2-}$  uptake experiments, cells were spiked into 2xTL Gal media modified from Smith et. al., (1995b) (see section 2.2.3.6) at  $\text{OD}_{600\text{nm}}$  of 0.15 and left to grow to mid-log phase for approximately 18 hours. In contrast, for the  $^{99}\text{MoO}_4^{2-}$  uptake experiments, cells were spiked into Low Mo Gal media (see section 2.8.8) to an  $\text{OD}_{600\text{nm}}$  of 0.15 and left to grow to mid-log phase for approximately 43 hours. Cells grown in either 2xTL Gal or Low Mo Gal were harvested by centrifugation at 4000 rpm for 2 mins and washed twice in sterile  $\text{dH}_2\text{O}$  or sterile  $\text{MoO}_4^{2-}$  scrubbed  $\text{H}_2\text{O}$  respectively, before finally being resuspended to an  $\text{OD}_{600\text{nm}}$  of 5 in 20 mM  $\text{KPO}_4$  buffer containing 2% (w/v) galactose; pH 5.6 for 2xTL Gal or pH 6.5 for Low Mo Gal. For all  $^{35}\text{SO}_4^{2-}$  uptake experiments, all buffers were made with  $\text{dH}_2\text{O}$  while in each of the  $^{99}\text{MoO}_4^{2-}$  uptake experiments  $\text{MoO}_4^{2-}$  scrubbed  $\text{H}_2\text{O}$  was specifically used.

#### **3.2.5.2 $^{35}\text{SO}_4^{2-}$ and $^{99}\text{MoO}_4^{2-}$ uptake in yeast**

Yeast uptake assays consisted of taking 50-100  $\mu\text{L}$  of cells ( $\text{OD}_{600\text{nm}}$  of 5) and shaking in a 2 mL microfuge tube (round bottom) with equal amounts of labelled and unlabelled  $^{99}\text{MoO}_4^{2-}$  (as  $\text{Na}_2^{99}\text{MoO}_4$ , ANSTO-ARI, Lucas Heights) or  $^{35}\text{SO}_4^{2-}$  (as  $\text{Na}^{35}\text{SO}_4^{2-}$  GE

Healthcare) in 20 mM  $\text{KPO}_4$  buffer with pH modifications and added anion competitors as required. At determined time points, 50-100  $\mu\text{L}$  of the cell/buffer mix were harvested and placed in 5 mL ice cold buffer  $\text{KPO}_4$  and quickly filtered by vacuum onto a 0.45  $\mu\text{M}$  nitrocellulose filter (Millipore, USA). Cells collected on the membranes were washed with a further 10 mL of ice-cold potassium phosphate buffer before being placed into 4 mL of aqueous scintillant (StarScint-Perkin-Elmer) and radioactivity measured in a scintillation counter (Tri-Carb 2100, Beckmann). Protein determinations for each assay were performed by TCA precipitation of yeast cells by the method described by Peterson (1977).

### 3.3 Results

#### 3.3.1 GmNod70 analysis

Identification of putative GmN#70 homologues through BLAST searches revealed approximately 50% homology between GmN#70 and members of the plant sulfate transporter family, namely those within the *Brassica* spp. (Table 3.1). Hydrophilicity analysis using the Kyte/Doolittle algorithm revealed GmNod70 to be membrane bound protein containing 10-12 putative TMD's (Figure 3.1). Subsequent cloning of GmN#70 and sequencing revealed that GmN#70 contained an extended open reading frame encoding a C-terminal containing the STAS domain (Figure 3. 2) and since has been named GmNod70 by J. Parker (pers. comm.). A phylogenetic analysis of GmNod70 with other known sulfate transporters and homologues placed GmNod70 between Groups 4 and 2 (Figure 3.3). Based on these results, GmNod70 was putatively assigned as a plant sulfate transporter.

#### 3.3.2 Functional complementation of YSD1/GmNod70

Expression of GmNod70 failed to complement growth of the sulfate transport mutant YSD1 on Low S (100  $\mu$ M) media (Figure 3.4A and B). In contrast, SHST1 readily rescued YSD1 cells growth under similar conditions (Figure 3.4A and B). Empty vector (pYES3) transformed YSD1 controls, were unable to grow at this low sulfate (100  $\mu$ M) concentration, however the wild type control, *Invsc1* exhibited good growth (Figure 3.4 A and B). At higher levels of  $\text{SO}_4^{2-}$  (1mM) both SHST1 expressed in YSD1 and wild type cells (*Invsc1*) cells grew well (Figure 3.1 C and D). However, growth of both GmNod70 expressed in YSD1 and the empty vector control in YSD1 continued to remain slow (Figure 3.4 C and D). At even higher  $\text{SO}_4^{2-}$  concentrations, (2 and 5 mM) all cell lines were able to grow (Figure 3.4 E, F. G and H).

#### 3.3.3 $^{35}\text{SO}_4^{2-}$ accumulation by YSD1 cells containing GmNod70 or pYES3

The expression of GmNod70 in YSD1 resulted in no  $^{35}\text{SO}_4^{2-}$  accumulation over time (Figure 3.5).  $^{35}\text{SO}_4^{2-}$  transport was similar to that of the control pYES3 cells. This result indicates that GmNod70 is not functional when expressed in yeast or alternatively is not a sulfate transporter *per se* despite extensive sequence homology (Figure 3.2) and a similar hydropathy profile (Figure 3.1).

### **3.3.4 Identification of pre-characterised sulfate transporter SHST1 through a targeted gene approach and functional yeast complementation using the Low Mo Gal media assay**

To explore the possibility that sulfate transporters were also capable of transporting molybdenum, a yeast screen was developed which limited cell growth on low concentrations of molybdenum (Low Mo Gal assay). Using the yeast sulfate transport mutant YSD1, it was possible to reduce cell growth when the media was specifically prepared to remove trace amounts of molybdenum from a complete yeast media recipe. YSD1 cells transformed with an empty vector control (pYES3) grew poorly on this Low Mo Gal media (Figure 3.6A), while wild-type (*Invsc1*) cells transformed with the empty vectors control (pYES3) with active sulfate transporters continued to grow (Figure 2.4A, 3.6B and 3.6C). Raising the molybdenum levels above 80 nM did allow pYES3 transformed YSD1 to eventually grow. When YSD1 was transformed with the sulfate transporter SHST1, and plated onto Low Mo media containing 2% (w/v) galactose to induce the GAL1 promoter of pYES3, YSD1 expressing SHST1 grew better than the pYES3 control on media containing less than 80 nM Mo (Figure 3.6A). Although capable of rescuing cell growth on Low Mo Gal media, the extent of the complementation of YSD1 by SHST1 was not dramatic, however the phenotype could be routinely repeated when SHST1 was re-transformed into YSD1 cells.

### **3.3.5 $^{35}\text{SO}_4^{2-}$ accumulation by YSD1 cells containing SHST1 or pYES3**

The expression of SHST1 in YSD1 increased the accumulation of  $^{35}\text{SO}_4^{2-}$  compared to the pYES3 control when cells were grown with either 2xTL Gal (Figure 3.7) or Low Mo Gal (Figure 3.8). Over a 20-minute time course,  $^{35}\text{SO}_4^{2-}$  accumulation by SHST1 significantly increased linearly when cells were grown in 2xTL Gal media compared to that of the control. A similar trend was also observed when cells were grown in the Low Mo Gal media, where cells containing SHST1 accumulated significantly more than that of the control pYES3. Interestingly, YSD1 cells containing pYES3 displayed different background levels of  $^{35}\text{SO}_4^{2-}$  uptake, where uptake increased when cells were grown on Low Mo Gal over that of cells grown on 2xTL Gal media (Figure 3.7 and 3.8).

The capacity of SHST1 to transport other divalent and monovalent anions other than  $\text{SO}_4^{2-}$  was determined through yeast competition assays. In the presence of a competitor at equimolar concentrations the rate of  $^{35}\text{SO}_4^{2-}$  uptake was measured in YSD1 cells containing SHST1 or pYES3. With cells grown on 2xTL Gal, equimolar concentrations (25  $\mu\text{M}$ ) of

$\text{Na}_2\text{MoO}_4^{2-}$  significantly reduced  $^{35}\text{SO}_4^{2-}$  uptake by 50% (Figure 3.9).  $^{35}\text{SO}_4^{2-}$  in the presence of  $\text{Na}_2\text{WO}_4^{2-}$  uptake was also reduced by 10%, but this was not statistically significant (Figure 3.9). In the presence of equal concentrations of either  $\text{NaCl}$  or  $\text{NO}_3^-$  there was no statistically significant change in  $^{35}\text{SO}_4^{2-}$  uptake (Figure 3.9).

In cells previously grown in Low Mo Gal media, equal molar concentrations of  $\text{Na}_2\text{MoO}_4^{2-}$  and  $\text{Na}_2\text{WO}_4^{2-}$  anions significantly reduced  $^{35}\text{SO}_4^{2-}$  uptake by approximately 30% and 10% respectively (Figure 3.10). As observed previously, neither  $\text{NaCl}$  nor  $\text{NO}_3^-$  significantly reduced the capacity of SHST1 to accumulate  $^{35}\text{SO}_4^{2-}$  uptake. These studies demonstrate that SHST1 is primarily a sulfate transport protein but may transport to much lesser extent other anions including  $\text{MoO}_4^{2-}$  and  $\text{WO}_4^{2-}$ .

Competition of  $^{35}\text{SO}_4^{2-}$  uptake by  $\text{MoO}_4^{2-}$  was explored further by increasing the relative concentrations of both anions in solution (Figure 3.11A). As external  $\text{MoO}_4^{2-}$  concentrations increased from 80 nM – 40  $\mu\text{M}$ , the rate of  $^{35}\text{SO}_4^{2-}$  uptake decreased however there was little change in the measured  $K_M$  values for  $^{35}\text{SO}_4^{2-}$ . Concentration curves demonstrated a reduction in uptake of  $^{35}\text{SO}_4^{2-}$  when cells were incubated with 40  $\mu\text{M}$   $\text{MoO}_4^{2-}$  when compared to 0.08  $\mu\text{M}$  and 0.8  $\mu\text{M}$   $\text{MoO}_4^{2-}$ . (Figure 3.11A).  $V_{\max}$  were generally low with values decreasing with increasing concentrations of  $\text{MoO}_4^{2-}$ . Further analysis using a Lineweaver-Burke plot demonstrated that  $\text{MoO}_4^{2-}$  was a poor competitive inhibitor of  $^{35}\text{SO}_4^{2-}$  uptake with a calculated  $K_i$  of 33.99  $\mu\text{M}$  (Figure 3.11C).

### 3.3.6 $^{99}\text{MoO}_4^{2-}$ accumulation by YSD1 cells containing SHST1 or pYES3

The expression of SHST1 in YSD1 significantly increased the uptake of  $^{99}\text{MoO}_4^{2-}$  over that of the control (pYES3) cells after 10 and 15 minutes in the presence of 10 nM  $\text{MoO}_4^{2-}$  (Figure 3.12) and after 15 and 20 minutes in the presence of 80 nM  $\text{MoO}_4^{2-}$  (Figure 3.13). After a 15-minute uptake period in the presence of 10 nM, YSD1 cells containing SHST1 had a 3-fold increase in  $^{99}\text{MoO}_4^{2-}$  content compared to those cells containing the empty vector control pYES3 (Figure 3.12). YSD1 cells transformed with pYES3 were also able to accumulate  $^{99}\text{MoO}_4^{2-}$ , but at a much-reduced level compared to SHST1. This increase in  $^{99}\text{MoO}_4^{2-}$  uptake was evident at both 10 and 80 nM external  $\text{MoO}_4^{2-}$  concentrations (Figure 3.12 and 3.13).

The rate of  $^{99}\text{MoO}_4^{2-}$  uptake by cells expressing SHST1 significantly increased linearly as external  $\text{Na}_2\text{MoO}_4^{2-}$  was supplied from 0 to 1000 nM (Figure 3.14A and 3.14B). A similar

trend was also demonstrated in cells containing the pYES3 control, however at a much lower rate across all concentrations tested. Interestingly, a similar linear uptake pattern was also observed by SHST1 cells exposed to  $^{35}\text{SO}_4^{2-}$  at lower (nM) concentrations as used in the  $^{99}\text{MoO}_4^{2-}$  experiments (Figure 3.15).

There was no measurable significant competition observed between  $\text{Na}_2\text{MoO}_4^{2-}$  and  $\text{Na}_2\text{SO}_4^{2-}$  at 80 nM external concentrations (Figure 3.16) and any other monovalent or divalent anions at equal external concentrations when SHST1 was expressed in YSD1 (Figure 3.16). This demonstrates that SHST1 is primarily a sulfate transporter with a secondary capacity to transport low concentrations of  $\text{MoO}_4^{2-}$ .

A pH response of  $^{99}\text{MoO}_4^{2-}$  uptake was measured with YSD1 cells containing either SHST1 and pYES3. Uptake of molybdenum decreased with increasing external pH from pH 4 to 7 (Figure 3.17) with all pH levels being significantly different to that of the control. Highest uptake of molybdenum occurred at pH 4, with little difference in uptake at pH 7 and 8. This indicates SHST1 may act as a  $\text{H}^+/\text{MoO}_4^{2-}$  cotransporter as well as a  $\text{H}^+/\text{SO}_4^{2-}$  cotransporter.

### 3.4 Discussion

#### 3.4.1 Molybdenum transport through SHST1

Molybdenum is an essential micronutrient required for plants and effective transport systems are required to take molybdenum from the soil solution into root cortical cells and then distribute it within the plant (Williams and Frausto da Silva, 2002). However, the mechanisms controlling molybdenum transport in plants are poorly understood.

It has been hypothesised that molybdenum anions could be transported through sulfate transport proteins found in both prokaryotic systems (Self et. al., 2001) and in plants (Marschner, 1995; Mendel and Schwarz, 1999). The prokaryotic molybdate transport system in *E.coli* has been intensively studied and shown to consist of three systems including a high affinity molybdate specific permease, a non-specific anion transporter, in addition to an ABC type sulfate transport protein. Recently, the Na<sup>+</sup> coupled sulfate transporter, rNaS2 (Miyachi et. al., 2006) and a human ortholog of the rat gene, hNaS2 (Markovich et. al., 2005) when expressed in *Xenopus* oocytes were both shown to also transport molybdenum.

In *S. cerevisiae* there are two genes primarily responsible for the high affinity transport of sulfate, *SUL1* and *SUL2* (Cherest et. al., 1997). A third gene not involved in transport, *SUL3*, is possibly involved in transcriptional regulation of *SUL2* (Cherest et. al., 1997). The yeast mutant YSD1 contains a disruption of *SUL1* (Smith et. al., 1995b). YSD1 when plated on low concentrations of sulfate grows poorly (Smith et. al., 1995b), but does start to grow on 2 to 5 mM SO<sub>4</sub><sup>2-</sup> (Figure 3. 4). Using this growth phenotype, YSD1 was pivotal in the discovery of plant sulfate transport proteins through functional yeast complementation studies (Smith et. al., 1995a). This mutant has been used to explore how the loss of *SUL1* activity would influence yeast growth on low concentrations of molybdenum and whether it would be useful to characterise plant sulfate transport proteins for molybdenum transport activity. Analysis of SHST1 activity in the sulfate deletion mutant YSD1 provided preliminary evidence that molybdenum transport may occur through sulfate transport proteins (Figure 3.6). SHST1 allowed for slow growth on Low Mo Gal media while YSD1 cells containing the empty vector pYES3 grew poorly (Figure 3.6). Although the plate growth was not robust, this subtle phenotype was consistently observed and highlights that the mutations in YSD1 are most likely impacting on the cells capacity for molybdenum accumulation. It would appear SHST1 is capable of providing

molybdenum into the cell and would suggest it and most likely other sulfate transport proteins are capable of molybdenum transport. However, when glucose was used as the carbon source, the growth of YSD1 improved on the low molybdenum media (data not shown) and on the various concentrations of sulfate media (Figure 3.6). Based on this observation, the reduced growth of YSD1 on the Low Mo Gal media allowed for the molybdenum availability deficiencies in YSD1 to be exploited when better growth conditions existed on the Low Mo Glu media. Though this was a subtle growth phenotype that existed between the 2 carbon sources, the reduced growth rate allowed for the characterisation of plant molybdate transporters. This preliminary result suggested the loss of the *SUL1* activity also reduced the cells ability to scavenge molybdenum from the growth media. The first plant sulfate transport proteins identified using functional complementation of YSD1 were three members of the multigene family SHST (1-3) in the tropical legume *Stylosanthes hamata*. Using SHST1 as model sulfate transport protein, the functional activity was tested in YSD1 under a range of media solutions and exposure to either  $^{35}\text{SO}_4^{2-}$  or  $^{99}\text{MoO}_4^{2-}$  to further explore its specific transport properties and specificities.

Expression of SHST1 in YSD1 increased sulfate uptake (Figure 3.7 and 3.8) as has been previously observed (Smith et. al., 1995a; Shelden et. al., 2001; Shelden et. al., 2003). A comparison of cells grown in either 2xTL Gal (Figure 3.7) or Low Mo Gal media (Figure 3.8) revealed a small difference in background transport activity, where control (empty vector) cells showed higher levels of sulfate uptake in response to molybdenum starvation conditions. Correspondingly, the level of sulfate uptake by SHST1 followed a similar trend accumulating more in the low molybdenum growth media. This result might be explained by the role of another native yeast sulfate transporter anion transporter contributing to the enhanced uptake of sulfate.

Challenging  $^{35}\text{SO}_4^{2-}$  uptake with other external anions demonstrated that  $\text{MoO}_4^{2-}$  equal concentrations were capable of decreasing SHST1  $^{35}\text{SO}_4^{2-}$  transport activity (Figure 3.9 and 3.10). At the same time, neither  $\text{NaCl}^-$  nor  $\text{NO}_3^-$  were found to be effective competitors of  $\text{SO}_4^{2-}$  uptake by SHST1. However, sulfate failed to compete with molybdenum in  $^{99}\text{MoO}_4^{2-}$  influx experiments (Figure 3.16). This is relevant to the potential function of SHST1 as a molybdenum uptake system in plants where sulfate would normally be at higher concentrations than molybdenum. The  $K_i$  of molybdenum inhibition of sulfate uptake in yeast to be approximately 34  $\mu\text{M}$  (Figure 3.11C). This is far in excess to the available



molybdenum levels found in most yeast media, which is approximately 80 nM (Difco), which in essence is a control within this particular experiment. Higher concentrations of molybdenum were not tested, as this was not physiologically relevant and would rarely occur within the environment. Consequently, the relatively high  $K_I$  value suggests that the preferred substrate by SHST1 is  $\text{SO}_4^{2-}$  but that  $\text{MoO}_4^{2-}$  can compete to some extent at higher concentrations as competition reduces uptake.

The capacity of SHST1 to transport  $\text{MoO}_4^{2-}$  in a series of flux experiments involving the radioactive tracer  $^{99}\text{MoO}_4^{2-}$  has been explored. Over time (0-20 minutes), SHST1 accumulated  $^{99}\text{MoO}_4^{2-}$  at a significantly greater level than that observed with control cells containing the empty vector (Fig 3.12 and 3.13). The quantity of uptake appeared to be dependent on the external concentration of molybdenum, where identical measurements using 80 nM (Figure 3.13) rather than 10 nM  $\text{MoO}_4^{2-}$  (Figure 3.12) increased both SHST1 activity and native systems allowing  $^{99}\text{MoO}_4^{2-}$  into the cell. To determine the optimal concentration for  $\text{MoO}_4^{2-}$  transport, a concentration dependence experiment was performed. SHST1 showed a linear increase in molybdenum transport as external concentrations increased from 0 to 1000 nM (Figure 3.14). This concentration range should represent that naturally occurring with most biological systems where plant available  $\text{MoO}_4^{2-}$  concentrations would never exceed such levels (Williams and Frausto da Silva, 2002). This system may eventually saturate; however, since molybdenum transport by SHST1 operates at approximately a 1000-fold lower concentration range than that of sulfate uptake it is highly unlikely this would ever occur under most biological available molybdenum concentrations. At similar concentrations (0 to 1000 nM  $\text{SO}_4^{2-}$ ), the rate of sulfate uptake by SHST1 was also examined. SHST1 acted in a similar manner showing linear uptake of sulfate but at rates approximately 20-fold greater than that of molybdenum, which is to be expected with Michaelis-Menten kinetics (Figure 3.14). Competition experiments proved difficult to obtain accurate replicates of experiments with large variations occurring between experiments (Figure 3.16) and it not clear why this is the case but may be due to system limitations of the functional yeast complementation method for protein analysis due to other native transporters in YSD1. However,  $^{35}\text{SO}_4^{2-}$  experiments demonstrated the preference for sulfate transport, with a capacity to also transport molybdenum. Analysis of the pH response to molybdenum uptake revealed that SHST1 expressed in yeast prefers a more acidic cellular environment (Figure 3.17). As SHST1 was originally identified as a  $\text{H}^+/\text{SO}_4^{2-}$  cotransporter by Smith et. al., (1995) it was not unexpected to find that SHST1 acted in a similar way when exposed to  $^{99}\text{MoO}_4^{2-}$

buffered at varying pH's. It would appear that under these conditions, SHST1 acted as a  $H^+/MoO_4^{2-}$  cotransporter. The YSD1/pYES3 control followed a similar trend to SHST1, which to indicated the presence of native yeast transporter also capable of molybdenum transport across the plasma membrane.

The question that arises from this work is - why does SHST1 have the ability to also transport molybdenum? This may be explained by the similar sizes of the sulfate and molybdate metal-O lengths (S-O = 1.47-1.49 Å and Mo-O=1.75-1.78 Å), net charge, hydrogen bonding properties and tetrahedral geometry (Dudev and Lim, 2004). However, it is not unusual for plant transport proteins to also transport other molecules of similar size. One such example can be found in aquaporins, or water transporters, some of which are also able to transport other small neutral molecules such as glycerol (Weig and Jakob, 2000) and ammonia (Jahn and Moller, 2004).

Within *E.coli*, molybdate can be transported through an ABC-type  $SO_4^{2-}$  transporter when a mutation occurs in one of 3 essential *ModABC* genes in the *E.coli* native molybdate transport system, but direct transport studies are yet to be performed (Self et. al., 2001). Research has examined the sulfate binding protein (SBP) in *Azobacter vinelandii* (Lawson et. al., 1998) and the ModA in *E.coli* (Lawson et. al., 1998; Self et. al., 2001) in terms of both proteins ability to bind molybdate and sulfate. The ModA protein has a very low affinity for sulfate (dissociation constant of >2 mM) while SBP does not readily bind molybdate (Rech et. al., 1996; Lawson et. al., 1998; Self et. al., 2001). This is possibly due to the size of the metal binding site with molybdate being slightly larger than sulfate (Lawson et. al., 1998; Self et. al., 2001). It is still not clear why molybdenum cannot be transported via a sulfate transporter when the molybdenum concentration of the medium is less than 1  $\mu$ M within the prokaryotic system (Self et. al., 2001).

The results obtained here are further supported by the recent discovery of MOT1, a putative molybdate specific transporter. MOT1 was identified in Arabidopsis in an attempt to understand the genetic mechanisms that control molybdenum concentrations in shoots through recombinant inbred lines (Tomatsu et. al., 2007). Genetic analysis of chromosome 2 identified polymorphisms within the region containing AtSult5;2 (Figure 1.7). The authors suspected that AtSult5;2 maybe responsible for molybdenum transport, as subsequent experiments demonstrated molybdenum transport through AtSult5;2, now known as MOT1. The activity of MOT1 is different to SHST1 as MOT1 did not

complement the other yeast sulfate transport mutant CP154-7B suggesting that sulfate could not be transported (Tomatsu et. al., 2007). Tejada-Jimenez et. al. (2007) also demonstrated that MOT1 is a molybdate specific transporter with functional yeast complementation using the yeast mutant 30109b, where molybdate uptake was not inhibited by sulfate. Although it could be assumed that the other member of the Group 5 sulfate transporters, AtSultr5;1 may also function as a molybdate specific transporter, this is not so (Figure 1.7). Analysis of AtSultr5;1 by Baxter et. al. (2008) demonstrated again using functional yeast complementation that AtSultr5;1 does not transport molybdate.

### **3.4.2 GmNod70 properties**

Despite GmNod70s DNA and amino acid homology to other plant sulfate transporters and the presence of the STAS (sulfate transporters and antisigma-factor antagonists) domain in the protein, GmNod70 did not complement the mutant YSD1 or accumulate  $^{35}\text{SO}_4^{2-}$ . The STAS domain is essential for the transport of sulfate and its subsequent deletion results in an abolishment of sulfate transport (Shibagaki and Grossman, 2004). Manipulation of the STAS domain in other Arabidopsis sulfate transporters (AtSultr2;1 and AtSultr3;1) further demonstrated that the STAS domain was essential either directly or indirectly in facilitating the localization of the protein to the plasma membrane (Shibagaki and Grossman, 2004). The STAS domain is found at the C-terminal end of the protein after the 12 TMD's and extends into the cytoplasm of the cell (Shibagaki and Grossman, 2006). This domain is joined to the catalytic domain of the protein by a linking region that can vary in length and which is not as highly conserved relative to the rest of the protein (Shibagaki and Grossman, 2006). Why GmNod70 contains the STAS domain and does not transport sulfate remains unclear. The extended C-terminal tail of GmNod70 compared to other sulfate transport proteins may contribute to the lack of transport ability (Figure 3.1 and 3.2). A study of the STAS domain in *A. thaliana* determined that *AtSultr3;1* was not able to complement the sulfate transport yeast mutant CP145-7B despite high amounts of polypeptide in the plasma membrane. This suggested to the authors that *AtSultr3;1* was not active (Shibagaki and Grossman, 2004). Although polypeptide amounts of GmNod70 protein were not measured in this study, similar problems with association to the plasma membrane may have occurred with GmNod70. Shibagaki and Grossman (2004) suggest *AtSultr3;1* may require post-translational modification to elicit high levels of activity. Future experiments may include polypeptide measurements of GmNod70 associated with the plasma membrane to determine if similar problems exist. This protein could also be expressed in *Xenopus laevis* oocytes. The other reason that GmNod70 may not have

transported sulfate may be due to the extended C-terminal tail as other sulfate transporters have a considerably shorter tail. This may result in protein misfolding that may cause a non-functional protein. The STAS domain is also found in LjSST1 and has been shown to transport sulfate when transformed into the yeast strain CP154-7A (Krusell et. al., 2005). Loss of LjSST1 resulted in a disruption of plant nitrogen fixation, indicating that this gene is crucial for this process. As sulfate, as well as molybdenum is required for nitrogenase activity, it is plausible that LjSST1 may also function as a molybdate transporter, in a similar manner to SHST1.

Results from this chapter have demonstrated through kinetic analysis that SHST1 is capable of enhancing the uptake of molybdenum at nM concentrations when expressed in yeast. Though uptake was not inhibited by sulfate, sulfate transport via SHST1 was reduced with molybdenum.

**Table 3.1 Initial identification of GmN#70 (D13505) homologues through BLAST searches of the public protein databases.**

Sequence comparisons were performed using protein public databases. Highest results are presented. Query: GmNod70 (D13505), Sbjct: subject

**1. AAZ67533 *Brassica rapa* subsp. Pekinensis Sulfate transporter family.**

Score = 495 bits (1275), Expect = 2e-138, Method: Composition-based stats.  
Identities = 262/473 (55%), Positives = 340/473 (71%), Gaps = 10/473 (2%)

Query	4	QWVLNAPEPPSMLRQVVDNVKETLLPHNPNTFSYLRNQPFKRAFALLQNLFPILASLQ	63
		+W+L+ PEPPS +++ VKE+ L F LR QP KR +LQ +FPI +	
Sbjct	50	KWLLDCPEPPSPWQELKTQVKESYLT--KAKKFKSLRKQPLPKRILFILQAVFPIFGWCR	107
Query	64	NYNAQKCLKCDLMAGLTLAIFAIPQCMGNATLARLSPEYGLYTGIVPPLIYAMLASSREIV	123
		NY K DLMAGLTLA IPQ +G ATLA+L P+YGLYT +VPPLIYA++ +SREI	
Sbjct	108	NYKLTMFKNLDMAGLTLASLCIPQSIGYATLAKLDPQYGLYTSVVPPLIYALMGTSREIA	167
Query	124	IGPGSVDSLLLSSMIQTLKVIHDSSTYIQLVFTVTFAGIFQVAFGLFRFGFLVEHLSQ	183
		IGP +V SLL+SSM+Q L P D Y +LV T TFFAGIFQ +FG+FR GFLV+ LS	
Sbjct	168	IGPVAVSVLLVSSMLQKLIDPETDPLGYKLVLTTFAGIFQASFGIFRLGFLVDFLSH	227
Query	184	ATIVGFLAAAAGVIGLQQLKGLFGIDNFNNKTDLFSVVKSLWTSFKNQSAWHYPYLIIGF	243
		A IVGF+ AA+ IGLQQLKGL GI NF TD+ SV+++W S Q W P+ I+G	
Sbjct	228	AAIVGFMGGAAIVIGLQQLKGLLGITNFTNTDIVSVLRAVWRSCHQQ--WSPHTFILGC	285
Query	244	SFLCFILFTRFLGKRNNKLMWLSHVAPLLSVIGSSAIYKINFNELQVKDYKVAVLGPIK	303
		SFL FIL TRF+GK+NKKL WL +APL+SV+ S+ + + +E VK K IK	
Sbjct	286	SFLSFILITRFIGKKNKFLWLPAPLISVAVVSTLMVFLTKADEHGVKTVK-----HIK	340
Query	304	GGSLNPSSLHQLTFDSQVVGHLIRIGLTIATISLGTGSIYAVGRSFASLKGHSIDPNREVV	363
		GG LNP S++ L F++ +GH+ +IGL +AI++LT +IAVGRSFA +KG+ +D N+E+V+	
Sbjct	341	GG-LNPISINDLEFNTPHLGHIAKIGLVAIVALTEAIAVGRSFAGIKGYRLDGNKEMVA	399
Query	364	LGIMNIVGSLTSCYIASGSLRTAVNYNAGSETMVSIIVMALTVLMSLKFLTGLLYFTPK	423
		+G MN++GS TSCY A+GS SRTAVN+ AG ET +S IVMA+TV ++L+ LT LLY+TP	
Sbjct	400	IGFMNVIGSFTSCYAATGSFRTAVNFAAGCETAMSNIVMAVTVFVALECLTRLLYYTPI	459
Query	424	AILAAIILSAVPLIDLNKAREIWKVDKMDFLACTGAFLGVLFASVEIGLAIG	476
		AILA+IILSA+PGLID+++A IWK+DK+DFLA GAF GVLF SVEIGL +	
Sbjct	460	AILASIIISALPGLIDIDEAIIHWKIDKLDLALIGAFFGVLFGSVEIGLLVA	512

**2. CAG17931 *Brassica oleracea* var. acephala plasma membrane sulfate transporter.**

Score = 492 bits (1267), Expect = 1e-137, Method: Composition-based stats.  
Identities = 260/473 (54%), Positives = 339/473 (71%), Gaps = 10/473 (2%)

Query	4	QWVLNAPEPPSMLRQVVDNVKETLLPHNPNTFSYLRNQPFKRAFALLQNLFPILASLQ	63
		+W+L+ PEPPS ++ VKE+ L F LR QP KR +LQ +FPI +	
Sbjct	50	KWLLDGPEPPSPWHELKTQVKESYLT--KAKKFKSLRKQPLPKRILFILQAVFPIFGWCR	107
Query	64	NYNAQKCLKCDLMAGLTLAIFAIPQCMGNATLARLSPEYGLYTGIVPPLIYAMLASSREIV	123
		NY K DLMAGLTLA IPQ +G ATLA+L P+YGLYT +VPPLIYA++ +SREI	
Sbjct	108	NYKLTMFKNLDMAGLTLASLCIPQSIGYATLAKLDPQYGLYTSVVPPLIYALMGTSREIA	167
Query	124	IGPGSVDSLLLSSMIQTLKVIHDSSTYIQLVFTVTFAGIFQVAFGLFRFGFLVEHLSQ	183
		IGP + SLL+SSM+Q L P D +Y +LV T TFFAGIFQ +FG+FR GFLV+ LS	
Sbjct	168	IGPVAAVSVLLVSSMLQKLIDPETDPLSYKLVLTTFAGIFQASFGIFRLGFLVDFLSH	227
Query	184	ATIVGFLAAAAGVIGLQQLKGLFGIDNFNNKTDLFSVVKSLWTSFKNQSAWHYPYLIIGF	243
		A IVGF+ AA+ IGLQ+LKGL GI NF TD+ SV+++W S Q W P+ I+G	
Sbjct	228	AAIVGFMGGAAIVIGLQRLKGLLGITNFTNTDIVSVLRAVWRSCHQQ--WSPHTFILGC	285
Query	244	SFLCFILFTRFLGKRNNKLMWLSHVAPLLSVIGSSAIYKINFNELQVKDYKVAVLGPIK	303
		SFL FIL TRF+GK+NKKL WL +APL+SV+ S+ + + +E VK K IK	

Sbjct 286 SFLSFILITRFIGKKNKFLWLPAPLISVTVSTLMVFLTKADEHGVKTVK-----HIK 340

Query 304 GGSLNPSSLHQLTFDSQVVGHLIRIGLTIATISLTGSIIVGRSFASLKGHSIDPNREVVS 363  
GG LNP S++ L F++ +GH+ +IGL +AI++LT +IAVGRSFA +KG+ +D N+E+V+

Sbjct 341 GG-LNPISINDLEFNTPHLGHIAGIQLVIAIVALTEAIAVGRSFAGIKGYRLDGNKEMVA 399

Query 364 LGIMNIVGSLTSCYIASGSLSRRTAVNYNAGSETMVSIIVMALTVLMSLKFLTGLLYFTPK 423  
+G MN++GS TSCY A+GS SRTAVN+ AG ET +S IVMA+TV ++L+ LT LLY+TP

Sbjct 400 IGFMNVIGSFTSCYAATGSSSRTAVNFAAGCETAMSNIVMAVTVFIALECLTRLLYYTPI 459

Query 424 AILAAIILSAVPLIDLNKAREIWKVDKMDFLACTGAFLGVLFASVEIGLAIG 476  
AILA+IILSA+PGLID+++A IWK+DK+DFLA GAF GVLF SVEIGL +

Sbjct 460 AILASIILSALPGLIDIDEAIIHWKIDKLDLFLALIGAFFGVLFASVEIGLLVA 512

### 3. NP\_196580 *Arabidopsis thaliana* sulfate transporter

Score = 486 bits (1251), Expect = 1e-135, Method: Composition-based stats.  
Identities = 260/473 (54%), Positives = 338/473 (71%), Gaps = 10/473 (2%)

Query 4 QWVLNAPEPPSMLRQVVDNVKETLLPHNPNTFSYLRNQPFKRAFALLQNLFPILASLQ 63  
+W+L+ PEPPS ++ VK + L F L+ QPF K+ ++LQ +FPI +

Sbjct 51 KWLDDCEPPSPWHELKRQVKGSLT--KAKKFKSLQKQFPKQILSVLQAIFFIFGWCR 108

Query 64 NYNAQKCLKCDLMAGLTLAIFAIPQCMGNATLARLSPEYGLYTGIVPPLIYAMLASSREIV 123  
NY K DLMAGLTLA IPQ +G ATLA+L P+YGLYT +VPPLIYA++ +SREI

Sbjct 109 NYKLTMFKNLDMAGLTLASLCIPQSIGYATLAKLDPQYGLYTSVVPPLIYALMGTSREIA 168

Query 124 IGPGSVDSLLLSSMIQTLKVPIDHSSTYIQLVFTVTFEFAGIFQVAFGLFRFGFLVEHLSQ 183  
IGP +V SLL+SSM+Q L P D Y +LV T TFFAGIFQ +FGLFR GFLV+ LS

Sbjct 169 IGPVAVVSLLISSMLQKLIDPETDPLGYKLVLTTFEFAGIFQASFGFLRGLVDFLSH 228

Query 184 ATIVGFLAAAAGVIGLQQLKGLFGIDNFNKTDLFSVVKSLWTSFKNQSAWHPYNLIIGF 243  
A IVGF+ AA+ IGLQQLKGL GI NF TD+ SV++++W S + Q W P+ I+G

Sbjct 229 AAIVGFMGGAAIVIGLQQLKGLLGITNFTTNTDIVSVLRAVWRSQQQ--WSPHTFILGC 286

Query 244 SFLCFILFTRFLGKRNNKMLWLSHVAPLLSVIGSSAIYKINFNELQVKDYKVAVLGPIK 303  
SFL FIL TRF+GK+ KKL WL +APL++V+ S+ + + +E VK + IK

Sbjct 287 SFLSFILITRFIGKKYKFLWLPAPLISVTVSTLMVFLTKADEHGVKTVR-----HIK 341

Query 304 GGSLNPSSLHQLTFDSQVVGHLIRIGLTIATISLTGSIIVGRSFASLKGHSIDPNREVVS 363  
GG LNP S+ L F++ +G + +IGL IAI++LT +IAVGRSFA +KG+ +D N+E+V+

Sbjct 342 GG-LNPMSIQDLDFNTPHLQGIAGIQLVIAIVALTEAIAVGRSFAGIKGYRLDGNKEMVA 400

Query 364 LGIMNIVGSLTSCYIASGSLSRRTAVNYNAGSETMVSIIVMALTVLMSLKFLTGLLYFTPK 423  
+G MN++GS TSCY A+GS SRTAVN+ AG ET +S IVMA+TV ++L+ LT LLY+TP

Sbjct 401 IGFMNVIGSFTSCYAATGFSRTAVNFAAGCETAMSNIVMAVTVFVALECLTRLLYYTPI 460

Query 424 AILAAIILSAVPLIDLNKAREIWKVDKMDFLACTGAFLGVLFASVEIGLAIG 476  
AILA+IILSA+PGLI++N+A IWKVDK DFLA GAF GVLFASVEIGL +

Sbjct 461 AILASIILSALPGLININEAIIHWKVDKDFLALIGAFFGVLFASVEIGLLVA 513

### 4. AAZ67600 *Brassica rapa* subsp. *Pekinensis* sulfate transporter

Score = 474 bits (1219), Expect = 6e-132, Method: Composition-based stats.  
Identities = 250/473 (52%), Positives = 331/473 (69%), Gaps = 20/473 (4%)

Query 4 QWVLNAPEPPSMLRQVVDNVKETLLPHNPNTFSYLRNQPFKRAFALLQNLFPILASLQ 63  
+W+L+ PEPPS ++ VKE+ L F L+ QP KR ++LQ +FPI +

Sbjct 23 KWLDDCEPPSPWHELKIQVKESFLT--KAKRFKSLQKQPLPKRILSILQAVFPIFGWCR 80

Query 64 NYNAQKCLKCDLMAGLTLAIFAIPQCMGNATLARLSPEYGLYTGIVPPLIYAMLASSREIV 123  
NY K DLMAGLTLA IPQ +G ATLA+L P+YGLY+ + PPLIYA++ +SREI

Sbjct 81 NYKLTMFKNLDMAGLTLASLCIPQSIGYATLAKLDPQYGLYSSVGPPLIYALMGTSREIA 140

Query 124 IGPGSVDSLLLSSMIQTLKVPIDHSSTYIQLVFTVTFEFAGIFQVAFGLFRFGFLVEHLSQ 183  
IGP +V+ L P D Y +LV T TFFAGIFQ +FG+FR GFLV+ LS

Sbjct 141 IGPVAVE-----LIDPETDPLGYKLVLTTFEFAGIFQASFGIFRGLVDFLSH 190

Query 184 ATIVGFLAAAAGVIGLQQLKGLFGIDNFNKTDLFSVVKSLWTSFKNQSAWHPYNLIIGF 243  
A IVGF+ AA+ IGLQQLKGL GI NF TD+ SV++++W S Q W P+ I+G

Sbjct 191 AAIVGFMGGAAIVIGLQQLKGLLGITNFTTNTDIVSVLRAVWRSCHQQ--WSPHTFILGC 248

Query 244 SFLCFILFTRFLGKRNKLMWLSHVAPLLSVIGSSAIAYKINFNELQVKDYKVAVLGP 303  
SFL FIL RF+GKRNKKL WL +APL+SV+ S+ + + +E VK + I+  
Sbjct 249 SFLSFILIARFIGKRNKKLFWLPAPLISVVVSTLMVFLTKADEHGVTVR-----HIR 303

Query 304 GGSLNPSSLHQLTFDSQVVGHLIRIGLTIAIISLTGSIIVGRSFASLKGHSIDPNREVV 363  
GG LNP S++ L F++ +GH+ +IGL +A+++LT +IAVGRSFA +KG+ +D N+E+V+  
Sbjct 304 GG-LNPISINDLEFNTPHLGHIKIGLIVAVVALTEAIAVGRSFAGIKGYRLDGNKEMVA 362

Query 364 LGIMNIVGSLTSCYIASGSLSRRTAVNYNAGSETMVSIIVMALTVLMSLKFLTGLLYFTP 423  
+G+MN++GS TSCY A+GS SRTAVN+ AG ET +S IVMA+TV ++L+ LT LLY+TP  
Sbjct 363 IGVMNVLGSFTSCYAATGSFSRTAVNFAAGCETAMSNIVMAVTVFIALECLTRLLYTP 422

Query 424 AILAAIILSAVPGGLIDLNKAREIWKVDKMDFLACTGAFLGVLFASVEIGLAIG 476  
AILA+IILSA+PGLID+N+A IWK+DK+DFLA GAF GVLF SVEIGL +  
Sbjct 423 AILASIILSALPGLIDINEAIIHWKIDKLDLFLALIGAFFGVLFSGSVEIGLLVA 475

### 5. AAZ08077 *Brassica napus* putative sulfate transporter

Score = 467 bits (1201), Expect = 8e-130, Method: Composition-based stats.  
Identities = 255/473 (53%), Positives = 334/473 (70%), Gaps = 13/473 (2%)

Query 4 QWVLNAPEPPSMLRQVVDNVKETLLPHPNPNTFSYLRNQPFKRAFALLQNLFPILASLQ 63  
QW++N PEPP+M ++ V ++ +L NQ +S L+++FPIL +  
Sbjct 21 QWLINMPEPPTMWQEFVGYIRTNVLSKKRNMKKKPSNQVYS-----YLSVFPILIWGR 75

Query 64 NYNAQKCLKCDLMAGLTLAIFAIPOCMGNATLARLSPEYGLYTGIVPPLIYAMLASSREIV 123  
Y K DLMAGLTLA IPQ +G A LA L PEYGLYT +VPLIY+M+ SSRE+  
Sbjct 76 QYKLNMFKKDLMAGLTLASLCIPQSIGYANLAGLDPEYGLYTSVVPPLIYSMMGSSRELA 135

Query 124 IGPVAVVSVLLSSMIQTLKVIHDSSTYIQLVFTVTFAGIFQVAFGLFRFGFLVEHLSQ 183  
IGP +V SLLSSM+ L+ P+ D Y ++VFT TFFAG FQ FGLFR GFL++ LS  
Sbjct 136 IGPVAVVSVLLSSMVSVDLQDPVTDPIAYRKIVFTATFFAGAFQAI FGLFRLGFLMDFLSH 195

Query 184 ATIVGFLAAAAVGIGLQQLKGLFGIDNFNKTDLFSVVKSLWTSFKNQSAWHPYNIIGF 243  
A +VGF+A AA+ IGLQQLKGLFG+ +F +KTD+ SV+ S++ S + W P N +IG  
Sbjct 196 AALVGFMAAGAAIVIGLQQLKGLFGLSHFTSKTDVVSVLSSVFHSLHH--PWQPLNFVIGS 253

Query 244 SFLCFILFTRFLGKRNKLMWLSHVAPLLSVIGSSAIAYKINFNELQVKDYKVAVLGP 303  
SFL FIL RFLGKRNKKL W+ +APL+SVI ++ I Y N VK ++ IK  
Sbjct 254 SFLIFILLARFLGKRNKKLFWIPAMAPLISVILATLIVYLTNAETRGVK-----IVKNIK 308

Query 304 GGSLNPSSLHQLTFDSQVVGHLIRIGLTIAIISLTGSIIVGRSFASLKGHSIDPNREVV 363  
G N S++QL F+ +G + +IG+ AII+LT +IAVGRSFA++KG+ +D N+E+++  
Sbjct 309 PG-FNRPSVNQLEFNGPHLGQVAKIGIICAIIALTEAIAVGRSFATIKGYRLDGNKEMMA 367

Query 364 LGIMNIVGSLTSCYIASGSLSRRTAVNYNAGSETMVSIIVMALTVLMSLKFLTGLLYFTP 423  
+G NI GSLTSCY+A+GS SRTAVN++AG ET+VS IVMA+TV++SL+ LT LYFTP  
Sbjct 368 MGSNIAGSLTSCYVATGSFSRTAVNFSAGCETVVSNIIVMAITVMVSLEVLTRFLYFTP 427

Query 424 AILAAIILSAVPGGLIDLNKAREIWKVDKMDFLACTGAFLGVLFASVEIGLAIG 476  
AILA+IILSA+PGLID++ A IWK+DK+DFL AFLGVLFASVEIGL +  
Sbjct 428 AILASIILSALPGLIDISGALHIWKLDKLDLFLILVAAFLGVLFASVEIGLLLA 480

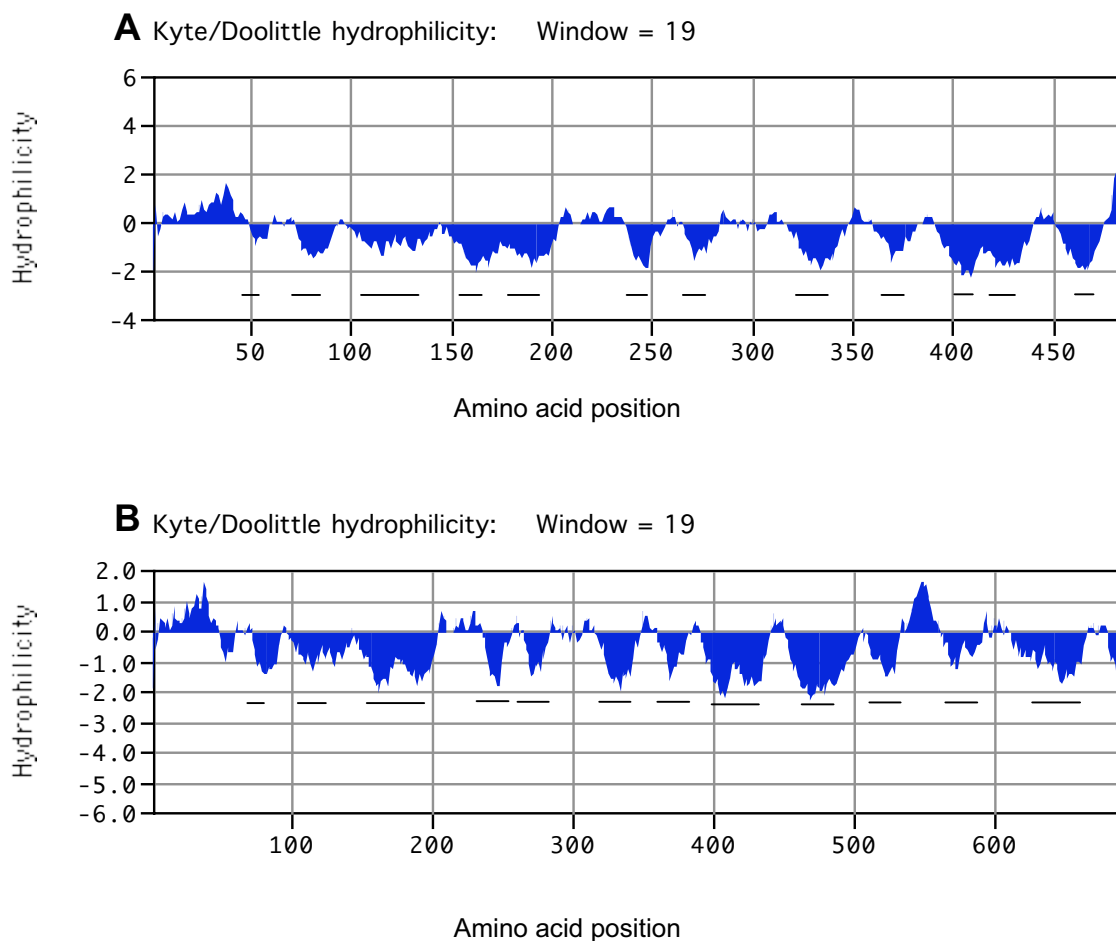


**Figure 3.1 Kyte/Doolittle hydrophilicity analysis of GmN#70 and GmNod70.**

**A.** GmN#70 (D13505) cloned by Kouchi and Shingo (1993) and **B.** GmNod70 cloned from a *Glycine max* nodule cDNA library. Hydrophilicity plot of Gm#70 and GmNod70 using the Kyte/Doolittle algorithm with a window size of 19. Regions with positive values are hydrophilic and the regions with negative values are hydrophobic. Horizontal bars indicate putative transmembrane spanning regions.





**Figure 3.2 Multiple sequence alignment of amino acid sequences of LjSST1, AtSultr1;2, AtSultr1;2, SHST1, GmN#70 and GmNod70.**

Alignment was performed using ClustalW in MacVector. Identical and conserved residues are shaded in grey. Red boxes highlight putative STAS domain as assigned from Rouached et. al., (2005).

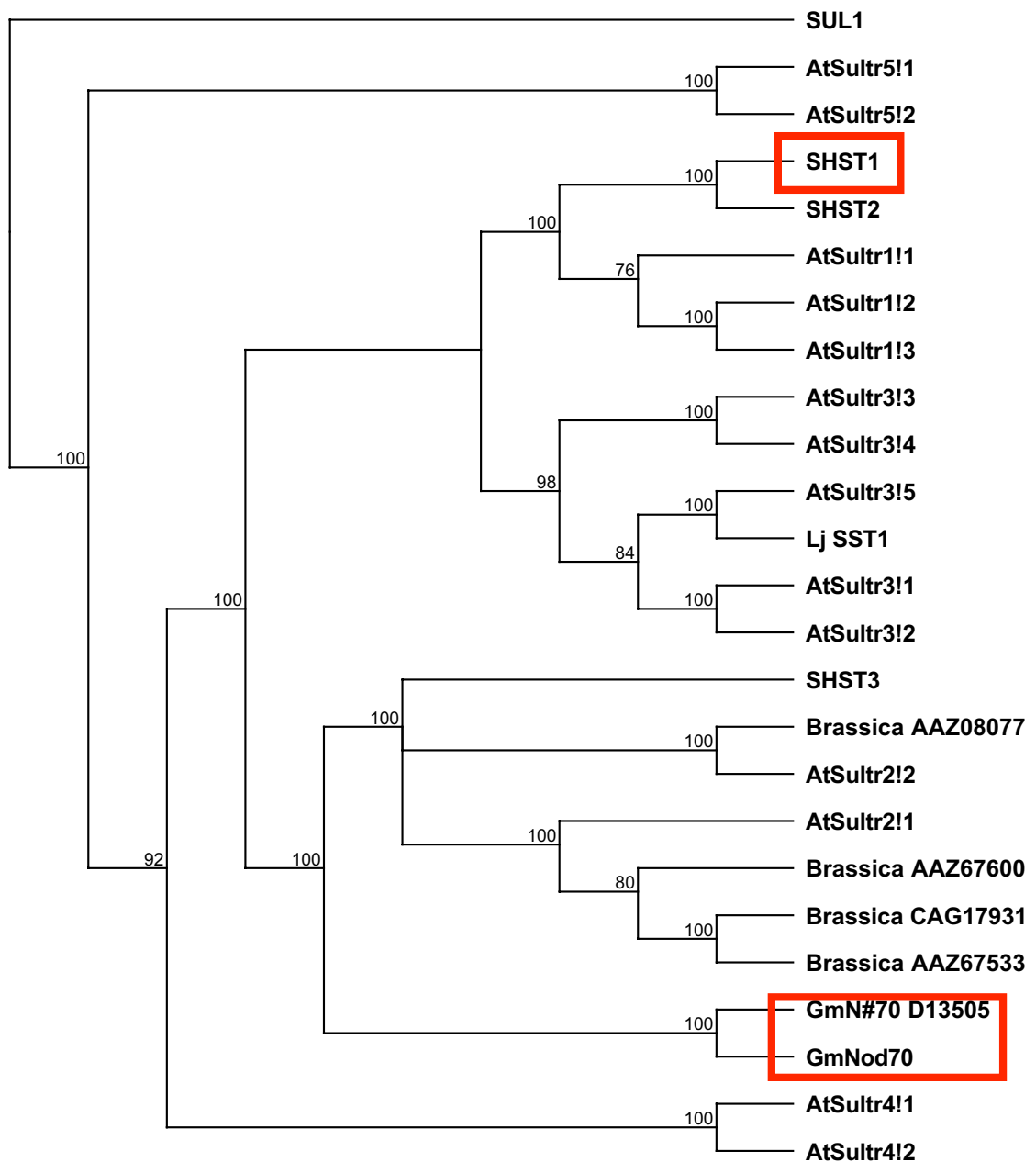


**Figure 3.3 Phylogenetic tree of sulfate transporters from *Arabidopsis thaliana*, *S. cerevisiae*, *Lotus japonicus*, *Stylosanthes hamata*, *Glycine max* and *Brassica* spp. with homology to GmNod70 cloned from this study in addition to GmN#70 identified by Kouchi and Shingo (1993).**

Phylogenetic analysis of sulfate transporters using full-length amino acid sequences aligned using ClustalW using MacVector. Neighbour joining tree with bootstrap values obtained from 100 replicates, uncorrected p and gaps distributed proportionally.

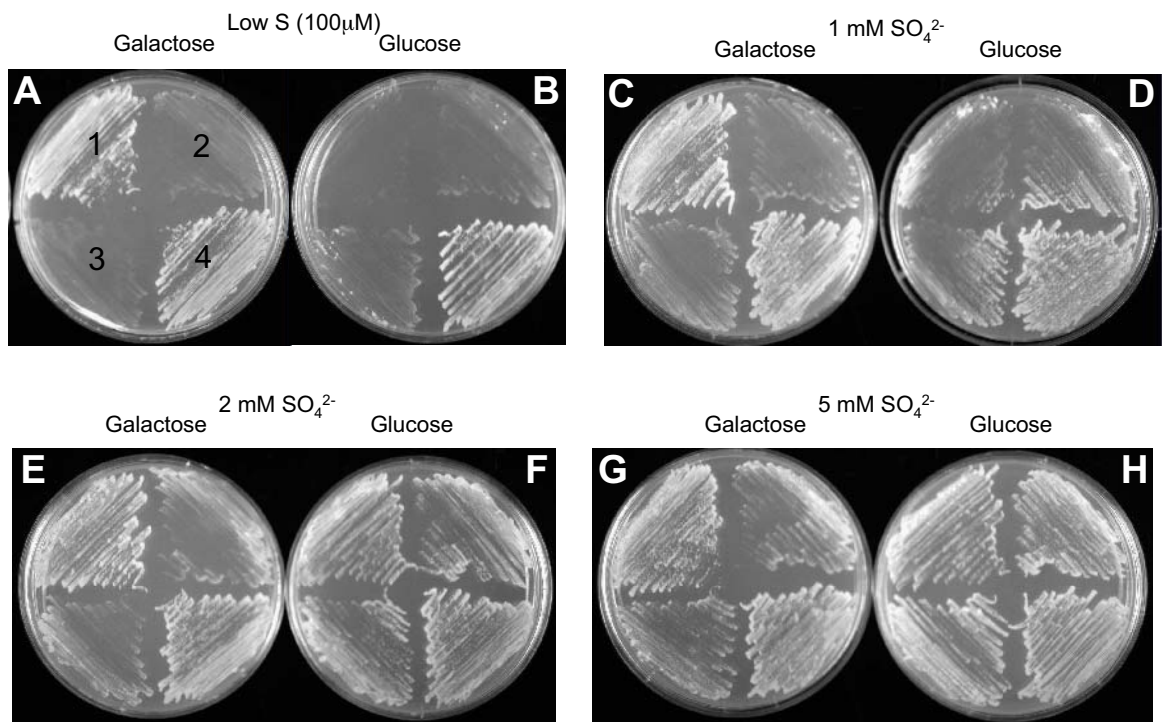


**Figure 3.4 Growth of YSD1 and Invsc1 cells transformed with either the empty pYES3 vector, or pYES3 vectors containing either SHST1 or GmNOD70. 1=SHST1/pYES3 expressed in YSD1, 2=GmNod70/pYES3 expressed in YSD1, 3=pYES3 expressed in YSD1 4=pYES3 expressed in Invsc1.**

Transformed cells were plated onto media containing increasing concentrations of  $\text{SO}_4^{2-}$  (100  $\mu\text{M}$ , 1 mM, 2 mM, 5 mM) with either 2% (w/v) galactose or 2% (w/v) glucose to induce or repress expression respectively. A, B, C, D, E, F, G and H refer to each individual plate.

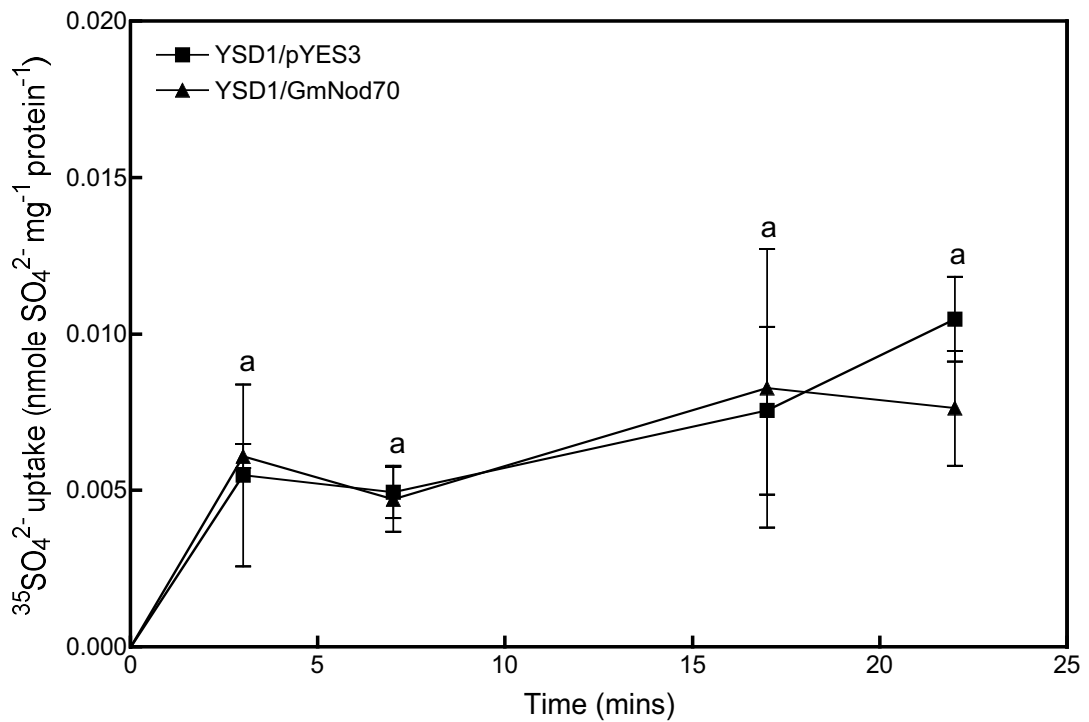


**Figure 3.5. Accumulation of  $^{35}\text{SO}_4^{2-}$  by YSD1 cells containing GmNod70 or pYES3.**

$^{35}\text{SO}_4^{2-}$  uptake was measured in YSD1 cells transformed with either GmNod70 or the empty cloning vector pYES3 as described in section 2.2.3.6 and section 3.2.2. Cells were grown in SC Glu and transferred 2xTL Gal to induce gene expression. Cells were harvested and washed in dH<sub>2</sub>O and incubated with 25  $\mu\text{M}$   $^{35}\text{SO}_4^{2-}$  between 3 and 22 mins to estimate  $^{35}\text{SO}_4^{2-}$  uptake. Data points with the same letter are not significantly different ( $p > 0.05$ ). Values are means  $\pm$  SEM (n=5).

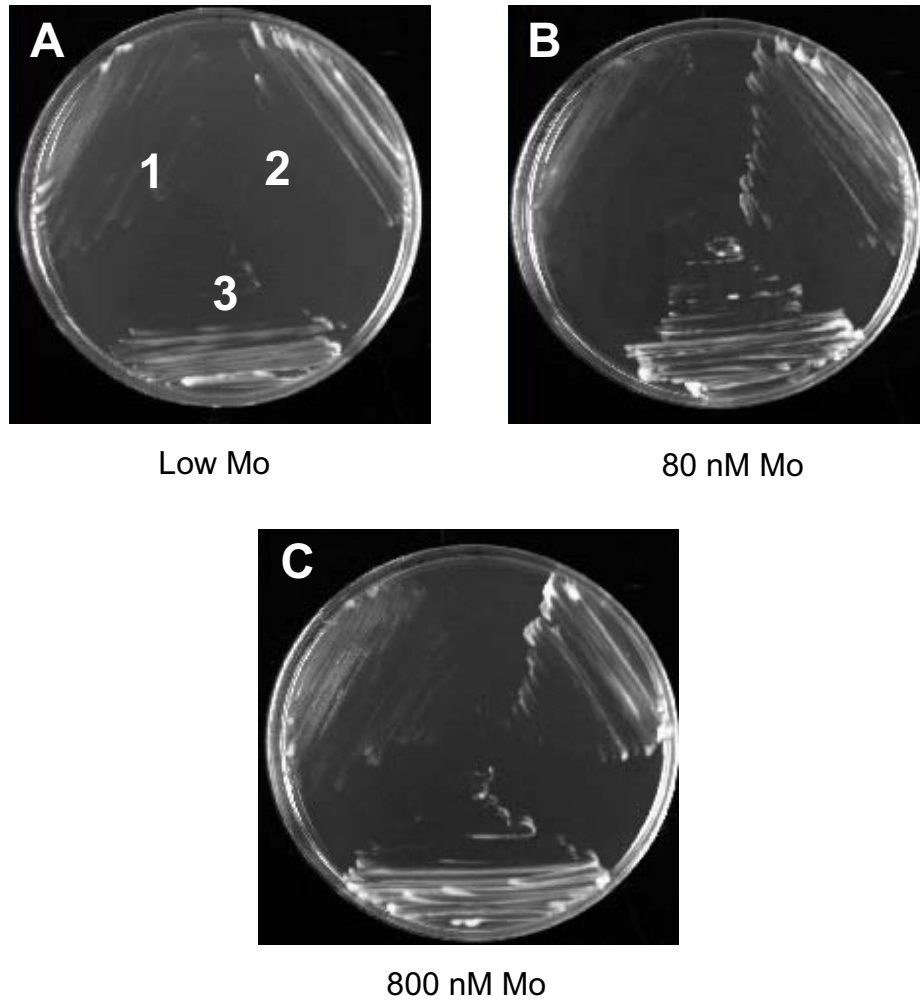


**Figure 3.6 Growth of YSD1 and Invsc1 cells transformed with either the empty pYES3 vector or the pYES3 vector containing SHST1 on various concentrations of molybdenum.**

1=pYES3 expressed in YSD1 2=SHST1/pYES3 expressed in YSD1 and 3=pYES3 expressed in Invsc1. Transformed cells were plated onto media containing increasing concentrations of  $\text{MoO}_4^{2-}$  (Low Mo, 80 nM, or 800 nM) with 2% (w/v) galactose and grown for 5-6 days at 28 °C.

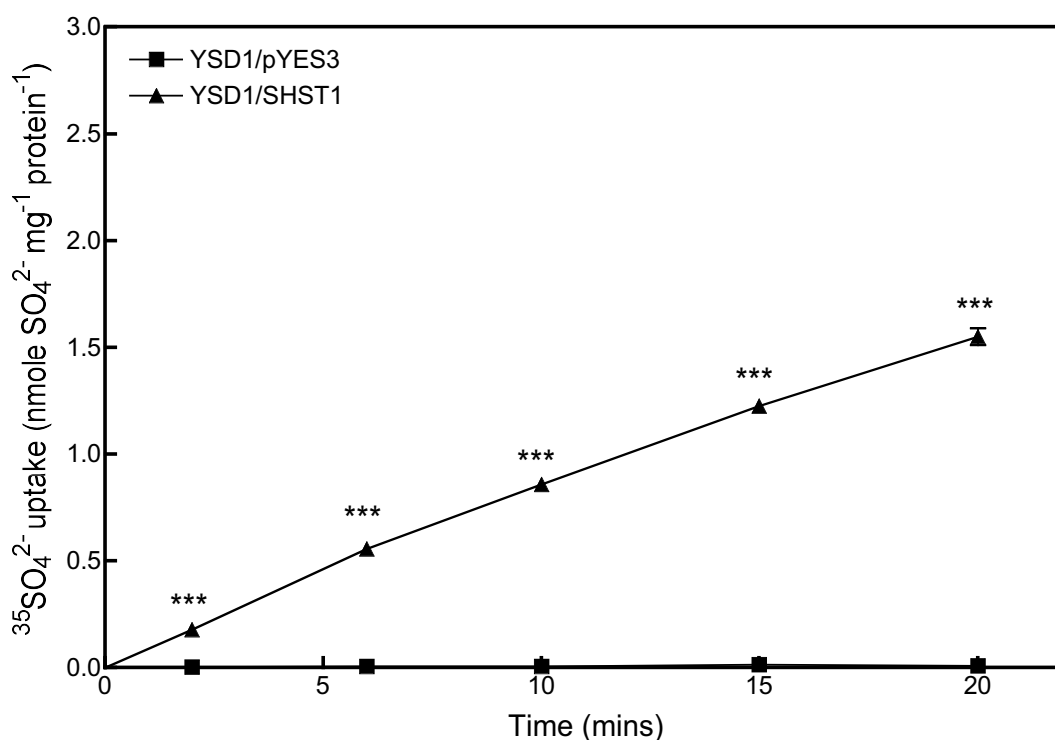


**Figure 3.7. Accumulation of  $^{35}\text{SO}_4^{2-}$  YSD1 cells containing SHST1 or pYES3 grown in 2xTL Gal media.**

$^{35}\text{SO}_4^{2-}$  uptake was measured in YSD1 cells transformed with either SHST1/pYES3 or the empty vector pYES3 as described in section 2.2.3.6 and section 3.2.2. Cells were grown in SC Glu, and then transferred 2xTL Gal to induce gene expression. Cells were harvested and washed in dH<sub>2</sub>O and incubated with 25  $\mu\text{M}$   $^{35}\text{SO}_4^{2-}$  for increasing periods of time. Data points with \*\*\* are significantly different from controls at  $p < 0.001$ . Data presented consists of the mean SE  $\pm$  (n=4) and is representative of 2 independent experiments.

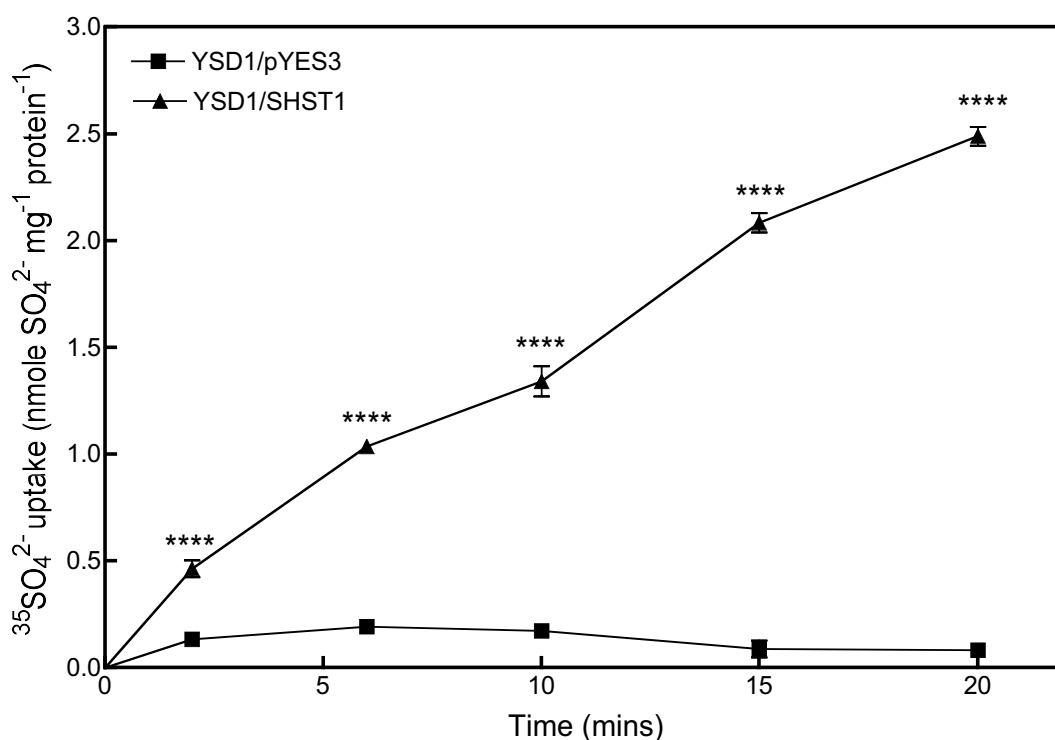


**Figure 3.8 Accumulation of  $^{35}\text{SO}_4^{2-}$  by YSD1 cells containing SHST1 or pYES3 grown in Low Mo Gal media.**

$^{35}\text{SO}_4^{2-}$  uptake was measured in YSD1 cells transformed with either SHST1/pYES3 or the empty vector pYES3 as described in section 2.2.3.6 and section 3.2.2. Cells were grown in SC Glu and transferred into Low Mo Gal media to induce expression. Cells were harvested and washed in dH<sub>2</sub>O and incubated with 25  $\mu\text{M}$   $^{35}\text{SO}_4^{2-}$  for increasing periods of time. Data points with \*\*\*\* are significantly different from controls at  $p < 0.0001$ . Data presented consists of the mean  $\pm$  SE (n=4) and is representative of 2 independent experiments.



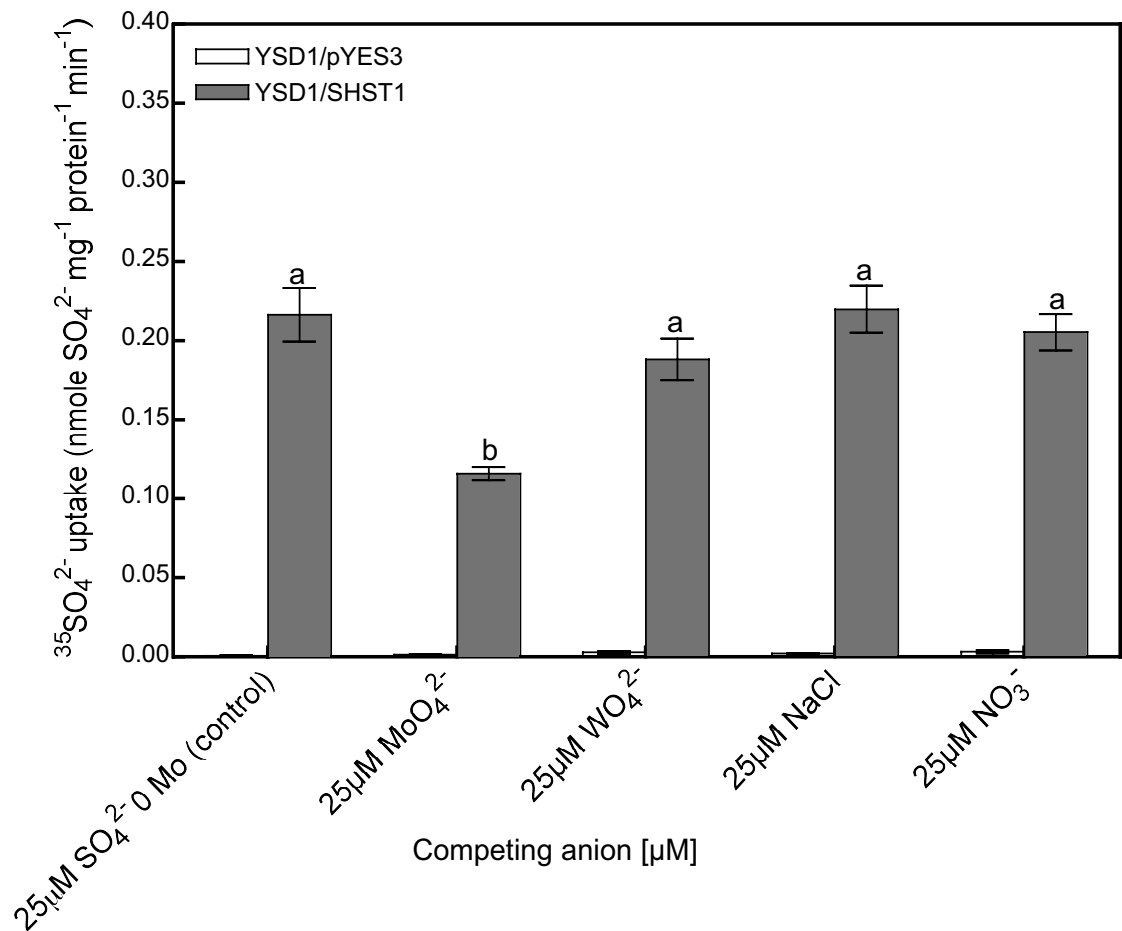


**Figure 3.9 Competition of  $^{35}\text{SO}_4^{2-}$  uptake in YSD1 cells containing SHST1 or pYES3 grown in 2xTL Gal.**

$^{35}\text{SO}_4^{2-}$  uptake was measured in YSD1 cells transformed with either SHST1/pYES3 or the empty vector pYES3 as described in section 2.2.3.6 and section 3.2.2. Cells were grown in SC Glu and transferred into 2xTL Gal media to induce gene expression. Cells were harvested and washed in dH<sub>2</sub>O scrubbed of Mo and incubated with 25 µM  $^{35}\text{SO}_4^{2-}$  with equal concentrations of the competing ion for 4 minutes. Data points with the same letter are not significantly different ( $p > 0.05$ ). Values are means  $\pm$  SEM (n=4).

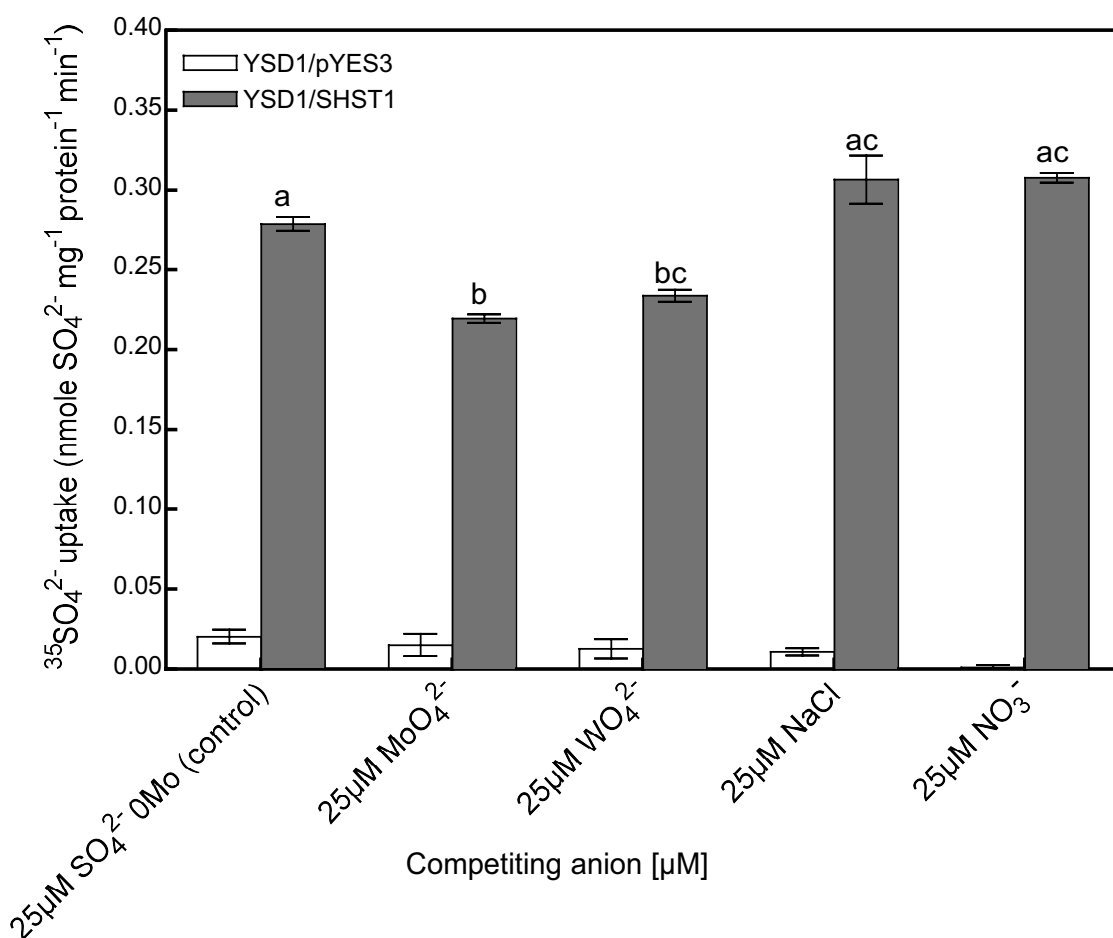
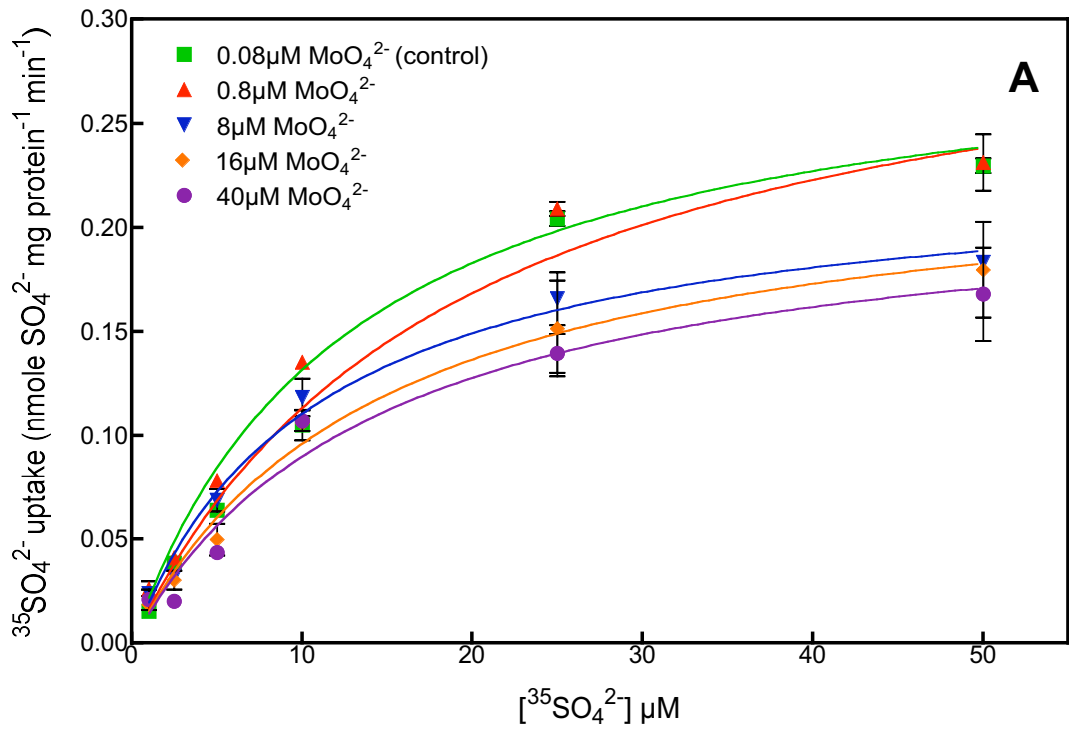


**Figure 3.10 Competition of  $^{35}\text{SO}_4^{2-}$  uptake in YSD1 cells containing SHST1 or pYES3 grown in Low Mo Gal.**

$^{35}\text{SO}_4^{2-}$  uptake was estimated in YSD1 cells transformed with either SHST1/pYES3 or the empty vector pYES3 as described in section 2.2.3.6 and section 3.2.2. Cells were grown in SC Glu and transferred into Low Mo Gal media to induce gene expression. Cells were harvested and washed in dH<sub>2</sub>O scrubbed of Mo and incubated with 25 µM  $^{35}\text{NaSO}_4^{2-}$  with equal amounts of the competing anion. After 4 minutes,  $^{35}\text{SO}_4^{2-}$  uptake was measured. Data points with the same letter are not significantly different ( $p > 0.05$ ). Values are means  $\pm$  SEM (n=4).



	0.08 μM (control)	0.8 μM	8 μM	16 μM	40 μM
<b>VMAX</b>	0.3291	0.2995	0.2294	0.2358	0.2206
<b>KM</b>	19.07	12.74	10.76	14.54	14.54
<b>Std. Error</b>					
<b>VMAX</b>	0.02866	0.01632	0.01398	0.01654	0.02711
<b>KM</b>	3.844	1.818	1.801	2.568	4.497

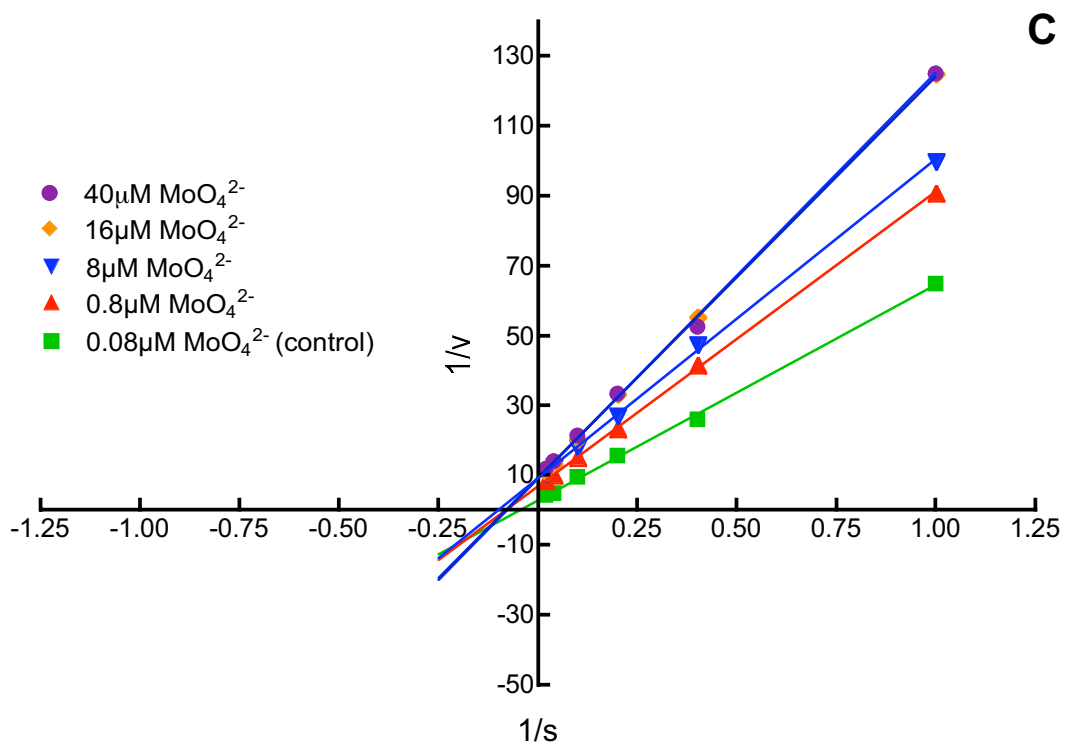


**Figure 3.11 Competitive inhibition of  $^{35}\text{SO}_4^{2-}$  uptake by YSD1 cells containing SHST1 grown in 2xTL Gal.**

**A.**  $^{35}\text{SO}_4^{2-}$  uptake was measured in YSD1 cells transformed with either SHST1/pYES3 or the empty vector pYES3. Cells were grown in SC Glu and transferred into 2xTL Gal media to induce gene expression. Cells were harvested and washed in sterile  $\text{dH}_2\text{O}$  and incubated for 10 minutes with increasing concentrations from 1 to 50  $\mu\text{M}$   $^{35}\text{SO}_4^{2-}$  and with increasing concentrations from 0.08  $\mu\text{M}$  (control), 0.8  $\mu\text{M}$ , 8  $\mu\text{M}$ , 16  $\mu\text{M}$  and 40 $\mu\text{M}$  of  $\text{Na}_2\text{MoO}_4^{2-}$ . Values are means  $\pm$  SEM (n=4). **B.** Characteristics of SHST1 when expressed in YSD1 and incubated with varying levels of sulfate as  $^{35}\text{SO}_4^{2-}$  and  $\text{Na}_2\text{MoO}_4^{2-}$ .  $K_m$  ( $\mu\text{M}$ ) and  $V_{\text{max}}$  (nmole  $\text{SO}_4^{2-}$  mg protein protein $^{-1}$  min $^{-1}$ ) values were determined by fitting the kinetic equation  $y = V_m \cdot x / (K_m + x)$  to sulfate uptakes rates measured after transferring cells in media containing  $^{35}\text{SO}_4^{2-}$ . **C.** Lineweaver-Burke plot of  $^{35}\text{SO}_4^{2-}$  uptake in the presence of increasing  $\text{Na}_2\text{MoO}_4^{2-}$  concentrations.  $^{35}\text{SO}_4^{2-}$  uptake was measured in YSD1 cells transformed with either SHST1/pYES3 or the empty vector pYES3. Cells were grown in SC Glu and transferred into 2xTL Gal media to induce gene expression. Cells were harvested and washed in sterile  $\text{dH}_2\text{O}$  and incubated for 10 minutes with increasing concentrations from 1 to 50  $\mu\text{M}$   $^{35}\text{SO}_4^{2-}$  and with increasing concentrations from 0.08 $\mu\text{M}$  (control), 0.8 $\mu\text{M}$ , 8 $\mu\text{M}$ , 16 $\mu\text{M}$  and 40 $\mu\text{M}$  of  $\text{Na}_2\text{MoO}_4^{2-}$ . Values are means  $\pm$  SEM (n=4). Regression analysis of each  $^{35}\text{SO}_4^{2-}$  concentration gave a line of best fit with  $R^2$  values of 0.998, 0.999, 0.999, 0.999, and 0.999 for 0.08 $\mu\text{M}$ , 0.8 $\mu\text{M}$ , 8 $\mu\text{M}$ , 16 $\mu\text{M}$  and 40 $\mu\text{M}$  of  $\text{Na}_2\text{MoO}_4^{2-}$  respectively. Values are means  $\pm$  SEM (n=4).

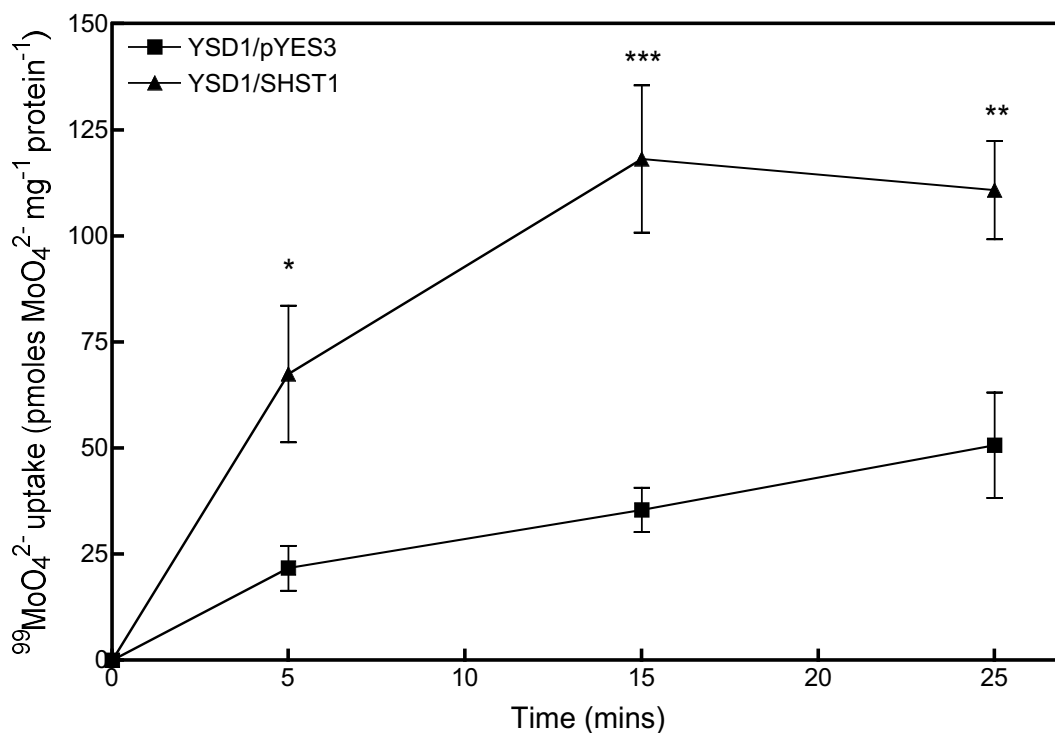


**Figure 3.12 Accumulation of  $^{99}\text{MoO}_4^{2-}$  in YSD1 cells containing SHST1 or pYES3 grown in Low Mo Gal (10 nM  $\text{MoO}_4^{2-}$ ).**

$^{99}\text{MoO}_4^{2-}$  uptake was measured in YSD1 cells transformed with either SHST1 or the empty vector pYES3 as described in section 2.2.3.6 and section 3.2.2. Cells were grown in SC Glu and transferred into Low Mo Gal media to induce expression. Cells were harvested and washed in Mo scrubbed  $\text{dH}_2\text{O}$  and incubated with  $^{99}\text{MoO}_4^{2-}$  for up to 26 mins. Data points with \*, \*\* and \*\*\* are significantly different from controls at  $p > 0.05$ ,  $< 0.05$  and 0.001 respectively. Values are means  $\pm$  SEM (n=4) and is representative of 2 independent experiments.

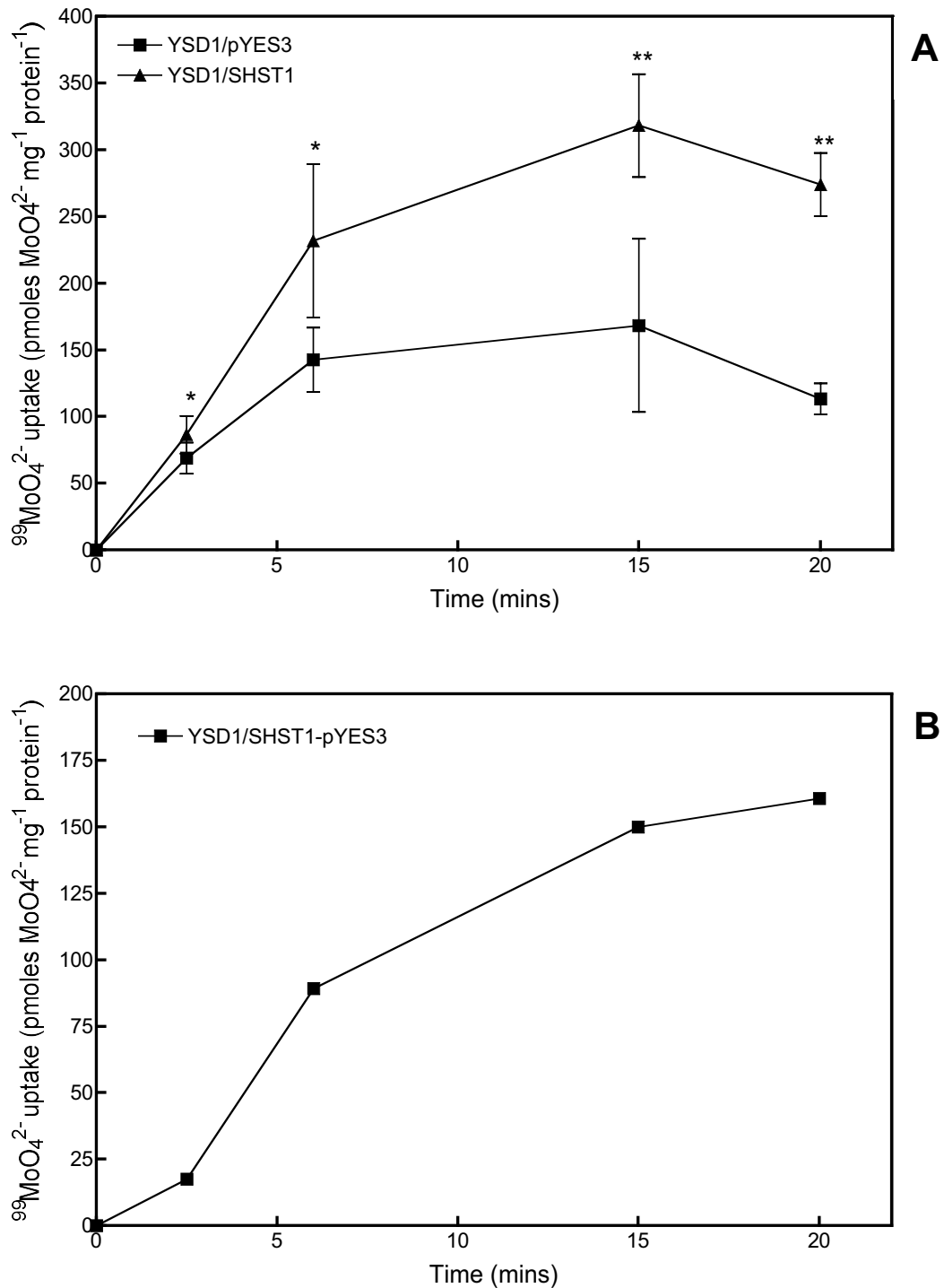


**Figure 3.13 Accumulation of  $^{99}\text{MoO}_4^{2-}$  in YSD1 cells containing SHST1 or pYES3 grown in Low Mo Gal (80 nM  $\text{MoO}_4^{2-}$ ).**

**A.**  $^{99}\text{MoO}_4^{2-}$  uptake was estimated in YSD1 cells transformed with either SHST1 or the empty vector pYES3 as described in section 2.2.3.6 and section 3.2.2. Cells were grown in SC Glu and transferred into Low Mo Gal media to induce expression. Cells were harvested and washed in Mo scrubbed  $\text{dH}_2\text{O}$  and incubated with  $^{99}\text{MoO}_4^{2-}$  for up to 26 mins. Data points with \* and \*\* are significantly different from controls at  $p > 0.05$  and  $< 0.05$ . Values

are means  $\pm$  SEM (n=4) and is representative of 2 independent experiments. **B.** Control pYES3 values subtracted from SHST1 demonstrate net influx.

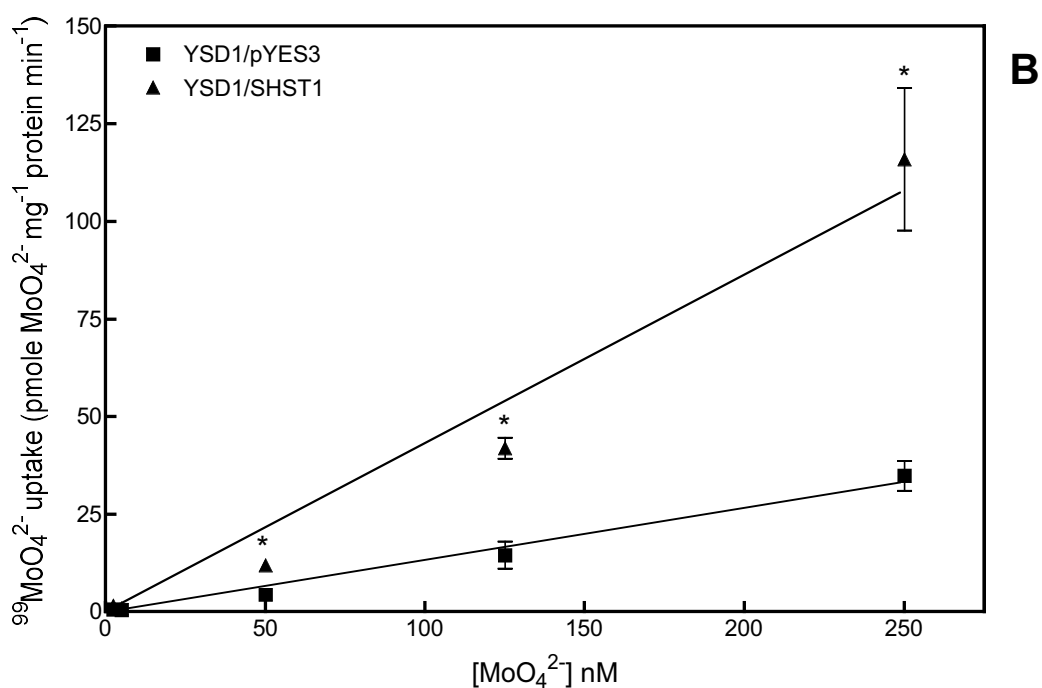
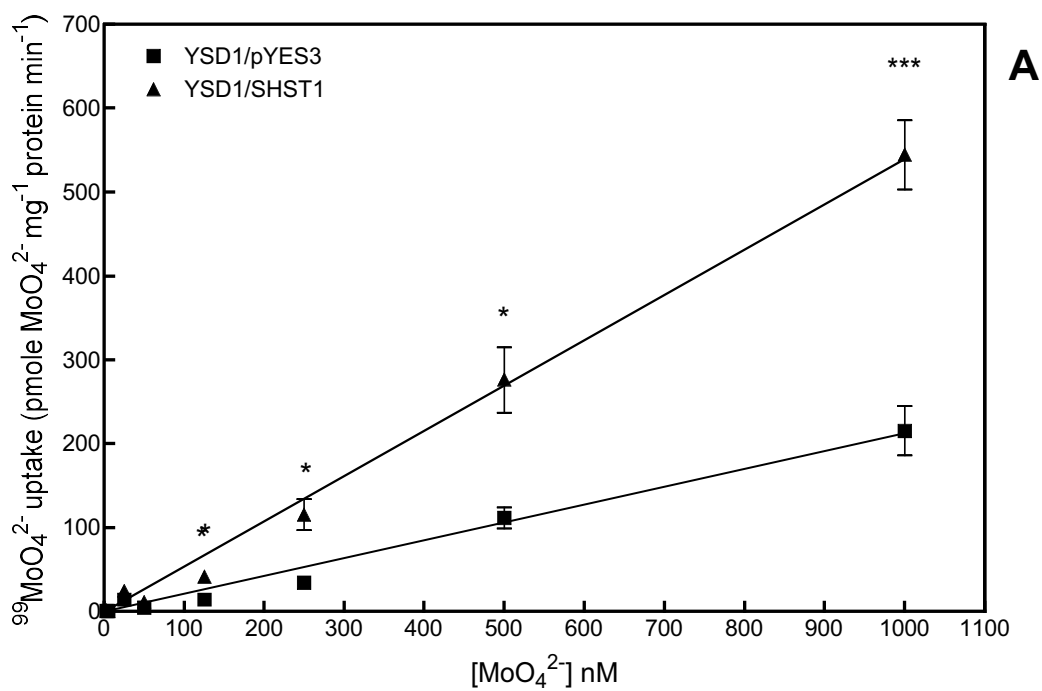


**Figure 3.14 Concentration dependent accumulation of  $^{99}\text{MoO}_4^{2-}$  in YSD1 cells containing SHST1 or pYES3 grown in Low Mo Gal.**

$^{99}\text{MoO}_4^{2-}$  uptake was measured in YSD1 cells transformed with either SHST1/pYES3 or the empty vector pYES3 as described in section 2.2.3.6 and section 3.2.2. Cells were grown in SC Glu and transferred into Low Mo Gal media to induce expression. Cells were harvested and washed in Mo scrubbed dH<sub>2</sub>O and then incubated with  $^{99}\text{MoO}_4^{2-}$  for 10 mins. **A.** Concentration of Mo from 0 to 1000 nM external molybdate concentrations. **B.** Inset of



same data as shown in A, from 0 to 250 nM Mo. Data points with \* and \*\*\* are significantly different from controls at  $p > 0.05$  and 0.001. Values are means  $\pm$  SEM (n=4) and representative of 3 independent experiments.

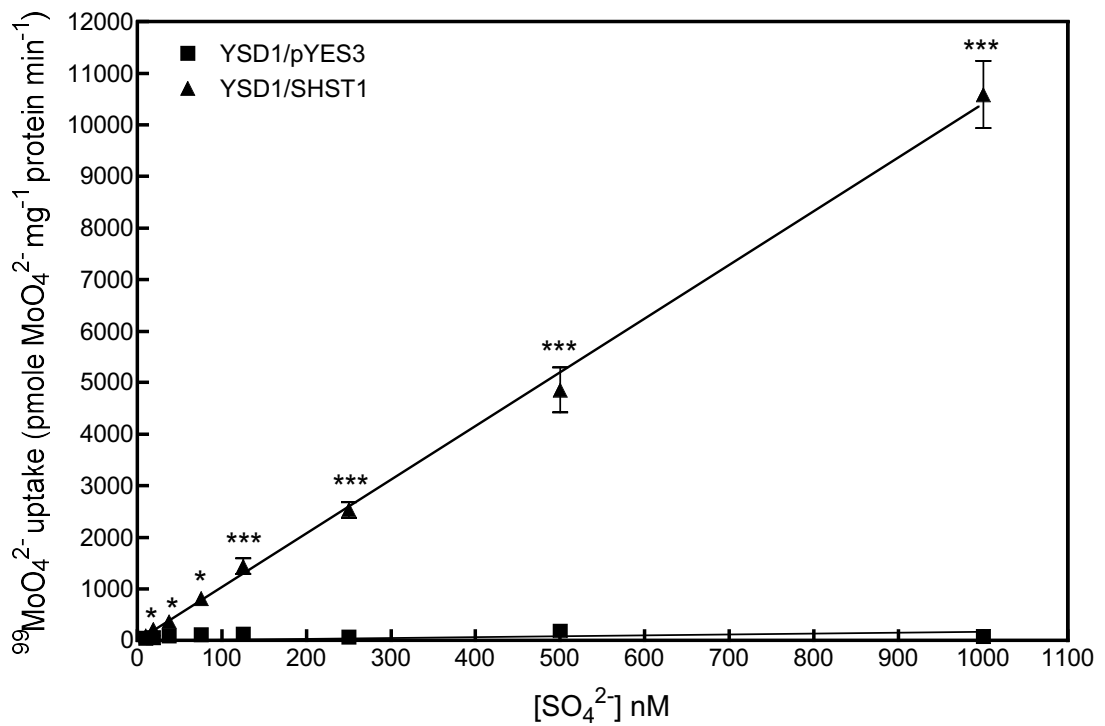


**Figure 3.15 Concentration dependent accumulation of <sup>35</sup>SO<sub>4</sub><sup>2-</sup> in YSD1 cells containing SHST1 or pYES3 grown in 2xTL.**

<sup>35</sup>SO<sub>4</sub><sup>2-</sup> uptake was measured in YSD1 cells transformed with either SHST1/pYES3 or the empty vector pYES3 as described in section 2.2.3.6 and section 3.2.2. Cells were grown in SC Glu and transferred into 2xTL Gal media to induce gene expression. Cells were harvested and washed in sterile dH<sub>2</sub>O and incubated with increasing concentrations of <sup>35</sup>SO<sub>4</sub><sup>2-</sup> for 10 minutes. Data points with \* and \*\*\* are significantly different from controls at p>0.05 and 0.001. Values are means ± SEM (n=4) and a representative of 2 independent experiments.

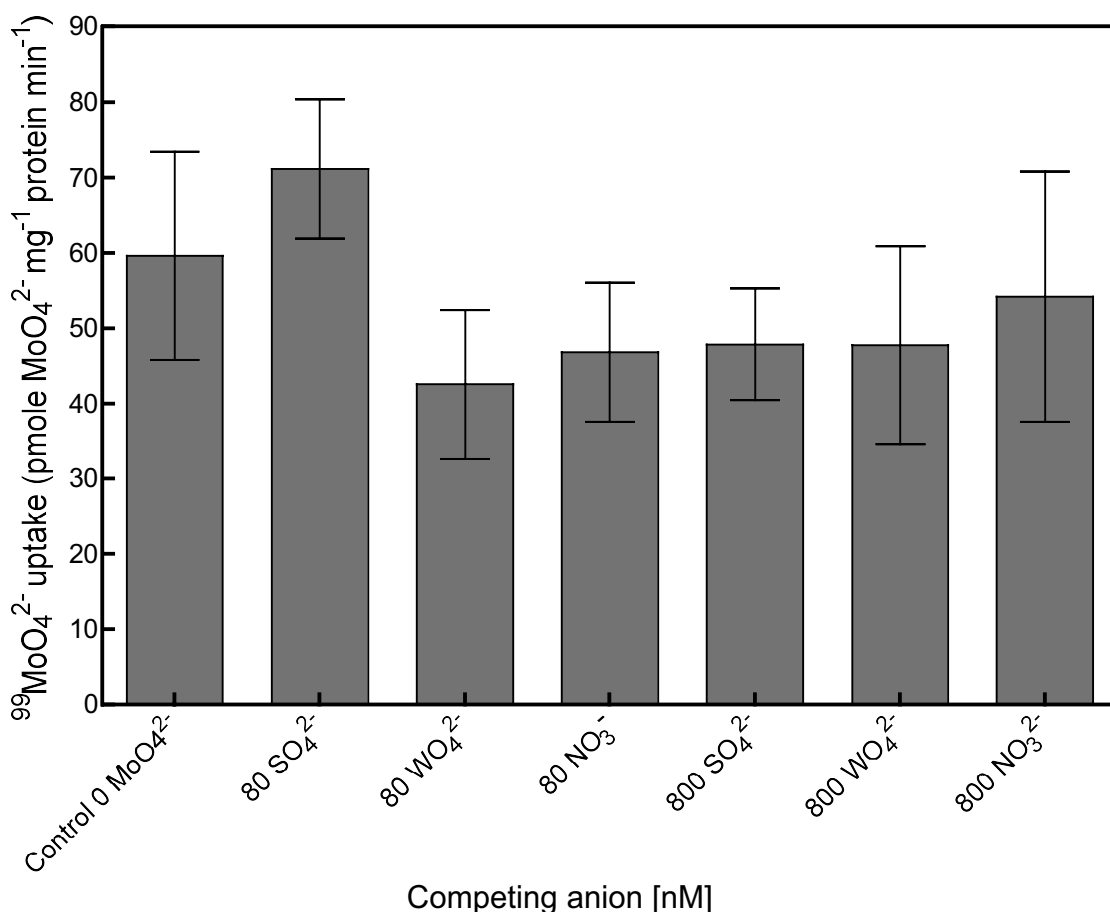


**Figure 3.16 Substrate competition of <sup>99</sup>MoO<sub>4</sub><sup>2-</sup> uptake in YSD1 cells containing SHST1 or pYES3 grown in Low Mo Gal.**

<sup>99</sup>MoO<sub>4</sub><sup>2-</sup> uptake was estimated in YSD1 cells transformed with either SHST1 or pYES3 as described in section 2.2.3.6 and section 3.2.2. Cells were grown in SC Glu and transferred into Low Mo Gal media to induce gene expression. Cells were harvested and washed in dH<sub>2</sub>O scrubbed of Mo and then incubated with 80 nM <sup>99</sup>MoO<sub>4</sub><sup>2-</sup> without (control) or with or 80 or 800 nM of a competing anion. After 10 minutes, cells were harvested and the quantity of <sup>99</sup>MoO<sub>4</sub><sup>2-</sup> measured. Bars indicate pYES3 subtracted from SHST1. Values are means 2 representative combined experiments.

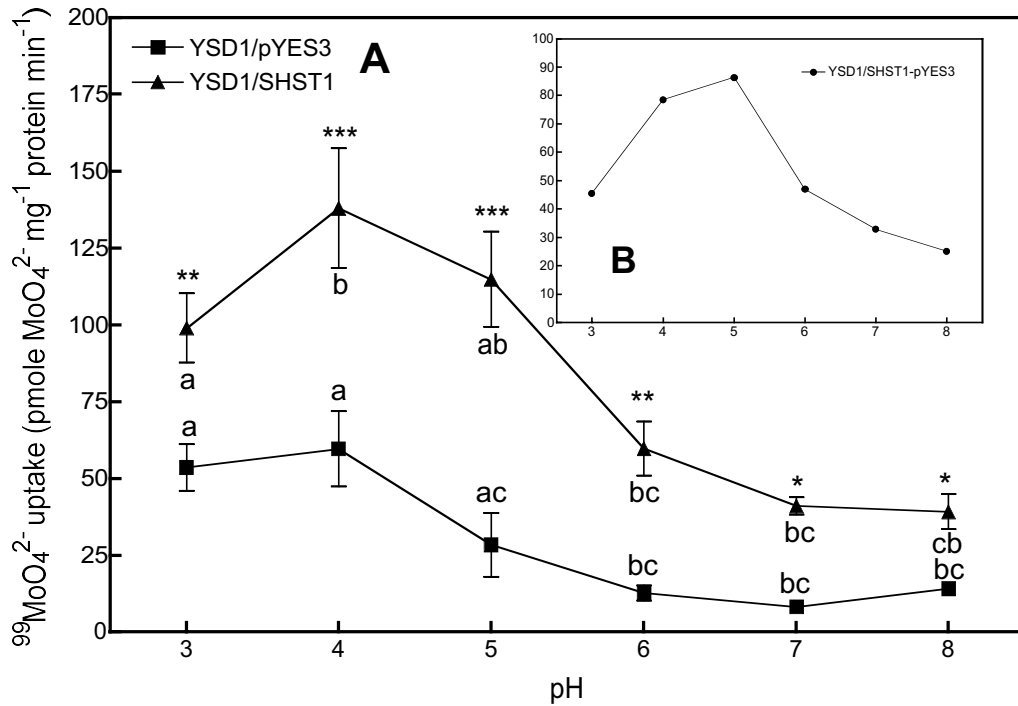


**Figure 3.17 Influence of external pH on the uptake of <sup>99</sup>MoO<sub>4</sub><sup>2-</sup> YSD1 cells containing SHST1 or pYES3.**

**A.** Cells were grown in SC Glu and transferred into Low Mo Gal media to induce expression. Cells were harvested and washed in dH<sub>2</sub>O scrubbed of molybdenum and incubated with 80 nM <sup>99</sup>MoO<sub>4</sub><sup>2-</sup> diluted in potassium phosphate buffer (pH 3-8). After 10 mins cells were washed with potassium phosphate buffer and <sup>99</sup>MoO<sub>4</sub><sup>2-</sup> uptake was measured. Data points with \*, \*\* and \*\*\* are significantly different from controls at p<0.05, 0.01 and 0.001 respectively. Data points with the same letters are not significantly different at p,0.05. Values are means ± SEM (n=4). **B.** Inset of control pYES values subtracted from SHST1.

## Chapter 4

### **$^{99}\text{MoO}_4^{2-}$ uptake in *Vitis vinifera* L. rootlings and *Glycine max* symbiosomes**

---

#### **4.1 Introduction**

It is poorly understood how molybdenum is transported into plant roots and subsequently translocated into shoots. However, it is thought that long distance transport of molybdenum in plants is both via the xylem and phloem (Kannan and Ramani, 1978) and that it is readily translocated within the plant system (Gupta, 1997).

#### **4.1.1 Molybdenum uptake in *Vitis vinifera***

Molybdenum deficiency is common in *Vitis vinifera* cv. Merlot grown on own roots in acidic soils (Williams et. al., 2004). Phenotypes of molybdenum deficiency in vines range from necrosis of the leaf edge, leaf chlorosis, stunted and ‘zig-zag’ cane growth, and cupped leaves (Figure 1.1A and 1.1B). Grape bunches are the most affected by this nutrient deficiency and display a phenotype known as ‘millerandage’ or more commonly known in Australia as ‘hen and chicken’. With severe cases of ‘millerandage’, bunches display a high incidence of small green and low amounts of large red berries suitable for winemaking purposes (Figure 1.2A). This results in low yields and reduced profits for growers. The emergence of this phenotype across many regions in Australia was a major

concern for many growers who were considering removing Merlot vines for more profitable varieties not subject to the phenotype (G. Oakley pers. comm.). However, recent research has demonstrated that simple foliar applications of molybdenum and or grafting Merlot scions onto rootstocks can remedy this problem and restore yields (Gridley, 2003; Williams et. al., 2004).

Gridley (2003) found that Merlot vines displaying ‘millerandage’ were deficient in molybdenum according to the levels defined by Williams et. al. (2004). However, vines grafted to rootstocks where millerandage phenotypes were absent were still found to be technically classed as molybdenum deficient. Upon application of molybdenum, the molybdenum content and yield responses of vines grown on both own roots and on rootstocks increased accordingly. This resulted in an increase in petiolar molybdenum content as well as an increase in bunch weight (Gridley, 2003). From Gridley’s (2003) study it was hypothesised that Merlot grown on own roots may have a reduced capacity absorb molybdenum from the soil compared to other varieties such as Chardonnay do not suffer from molybdenum deficiency and related phenotypes. A reduced capacity to uptake molybdenum in Merlot may explain the high incidence of molybdenum deficiency and associated phenotypes.

Most studies have focused on shoot molybdenum transport, where foliar applications of  $^{99}\text{MoO}_4^{2-}$  is tracked as it moves from the site of application (Stout and Meagher, 1948; Kannan and Ramani, 1978). Kannan and Ramani (1978) demonstrated that molybdenum is both xylem and phloem mobile through experiments involving the application of  $^{99}\text{MoO}_4^{2-}$  to roots and or shoots where the  $^{99}\text{MoO}_4^{2-}$  label ended up in either the shoots, stem or roots, respectively.

In this study, differences in molybdenum uptake were compared between Merlot, a variety known for molybdenum deficiency, and Chardonnay, which does not appear to suffer from molybdenum deficiency. The radioactive isotope  $^{99}\text{MoO}_4^{2-}$  was used to trace molybdenum uptake on rooted cuttings.

#### **4.1.2 Molybdenum uptake in *Glycine max* symbiosomes**

Molybdenum is required in the symbiotic bacterial enzyme complex, nitrogenase, which catalyses the reduction of di-nitrogen ( $\text{N}_2$ ) to ammonia ( $\text{NH}_3$ ). In legumes, nitrogen fixation takes place in the root nodule where symbiotic *Rhizobium* bacteria (bacteroids) are

housed. Bacteroids are located within modified cortical cells of the nodule and separated from the cell cytosol by the plant derived peribacteroid membrane (PBM). For nitrogen fixation to occur the essential micronutrient, molybdenum, must be supplied by the plant. This necessitates the presence of a molybdenum transporter across the PBM in order to deliver sufficient molybdenum into the peribacteroid space and eventually onto the bacteroid. Many nutrient transporters on the PMB have already been isolated and characterised (Day and Udvardi, 1997). However, the mechanism controlling molybdenum transport across the PBM has yet to be fully examined. The likely presence of a PBM molybdenum transporter can be inferred by a number of studies that have identified and characterised molybdenum transport into isolated bacteroids using the ModABC system (Graham and Maier, 1987; Maier et. al., 1987; Maier and Graham, 1988).

The transport of molybdenum across the PBM was examined using  $^{99}\text{MoO}_4^{2-}$  and isolated intact symbiosomes isolated from soybean nodules. These experiments were designed to determine if a transport mechanism exists on the PBM to facilitate transport of molybdenum into the peribacteroid space and where it would be available to the nitrogen fixing bacteroids.

## 4.2 Methods

### 4.2.1 *Vitis vinifera* uptake assay

#### 4.2.1.1 *Vitis vinifera* cv. Merlot and Chardonnay culture

Cuttings of *Vitis vinifera* cv. Merlot (clone D3V14) and cv. Chardonnay (clone I10V) were collected during bud dormancy from the Waite vineyard. Cuttings were divided into smaller, 1 bud cuttings, and the ends soaked in 0.1% (w/v) indole-butyric acid dissolved in 50% (v/v) ethanol and water for 30 seconds and then placed in Oasis foam media. Cuttings were placed in a misting chamber until callus and subsequent roots developed. Rootlings were placed in hydroponic media [0.5 mM MgSO<sub>4</sub>, 0.5 mM KH<sub>2</sub>PO<sub>4</sub>, 0.1 mM Fe-EDTA, 0.1 mM FeEDDTA, 1.25mM Ca(NO<sub>3</sub>)<sub>2</sub>.4H<sub>2</sub>O, 2.5 mM KNO<sub>3</sub>, 0.05 mM KCl, 0.025 mM H<sub>3</sub>BO<sub>3</sub>, 0.002 mM ZnSO<sub>4</sub>.7H<sub>2</sub>O, 0.002 mM CuSO<sub>4</sub>.5H<sub>2</sub>O and 200 mg/L CaCO<sub>3</sub>] containing either media supplemented with or without 0.8 μM Na<sub>2</sub>MoO<sub>4</sub>.2H<sub>2</sub>O with an air supply and grown under controlled glasshouse conditions 24 °C/ 19 °C day/night. Hydroponic solutions were changed every 10 days. Plants were grown under these conditions until the development of a single shoot and well developed root system.

#### 4.2.2.2 <sup>99</sup>MoO<sub>4</sub><sup>2-</sup> uptake assay in *Vitis vinifera* cv. Merlot and Chardonnay plants

Plants were transferred from 50 L tanks and placed in 3 L of hydroponic media (section 4.2.1.1) containing media supplemented with or without Na<sub>2</sub>MoO<sub>4</sub>.2H<sub>2</sub>O with air supply and under mercury halide lamps at canopy level (600 μmole m<sup>-2</sup> sec<sup>-1</sup>). Molybdenum, as <sup>99</sup>Na<sub>2</sub>MoO<sub>4</sub> (Lucas Heights, ANSTO-ARI) was added to 2 L of hydroponic media with or without added molybdenum as Na<sub>2</sub>MoO<sub>4</sub>.2H<sub>2</sub>O. Plants were transferred into the media containing <sup>99</sup>MoO<sub>4</sub><sup>2-</sup> media for predetermined times with air supply. Plants were then washed in 3 L of hydroponic media with non-radioactive Na<sub>2</sub>MoO<sub>4</sub>.2H<sub>2</sub>O for 10 mins to desorb apoplastic molybdenum and then washed again for 5 mins in 3L of 2mM CaSO<sub>4</sub>. Roots were patted dry with paper towel, and plants cut to retain 50% of their total root system. The younger bottom half of the root systems were selected, weighted and placed into scintillation vials to be counted in a scintillation counter (Tri-Carb 2100, Beckmann).

### 4.2.2 *Glycine max* symbiosome assay

#### 4.2.2.1 *Glycine max* culture



*Glycine max* cv. Boyer 2000 were grown in a glasshouse with a 28 °C/ 18° C day/night temperature. Seeds were planted directly in Golden Grove sand and at germination, inoculated with cultures of *Bradyrhizobium japonicum* USDA110 previously cultured in YEM medium [10 g/L Mannitol; 0.4 g/L Yeast Extract (Difco); 0.66 g/L K<sub>2</sub>HPO<sub>4</sub>·3H<sub>2</sub>O; 0.2 g/L MgSO<sub>4</sub>·7H<sub>2</sub>O; 0.1 g/L NaCl; pH 7.0] at 28 °C for 7 days. Seedlings were inoculated with *B. japonicum* again 7 days later and watered daily until the emergence of the first trifoliolate leaf. Plants were then watered every second day with a modified Herridge nutrient solution prepared without nitrogen to enhance nodule formation and with or without Na<sub>2</sub>MoO<sub>4</sub>·2H<sub>2</sub>O (Herridge, 1977). After 21-28 days of growth, plants were harvested and nodules collected for symbiosome isolation. At harvest, dissected nodules were pink indicating active nitrogen fixation regardless of molybdenum treatment.

#### **4.2.2.2 Aerobic *Glycine max* symbiosome isolation**

Nodules (10-15 g) were picked from soybean plants and placed on ice. Nodules were squashed in a chilled mortar and pestle, one third at a time in homogenising buffer [350 mM mannitol; 25 mM MES-KOH (pH 7.0); 10 mM EGTA; 10 mM MgSO<sub>4</sub>; 1 % (w/v) BSA (fatty acid free); 1 % PVP-40 (insoluble); 5 mM DTT; 20 mM ascorbic acid; pH 7.0]. The nodule homogenate was filtered through a chilled glass funnel containing 4 layers of miracloth moistened with homogenising buffer. The filtrate was evenly and slowly layered over chilled 3-step percoll gradients (1.5 mL 80% (v/v) percoll, 2.5 mL 60% (v/v) percoll; 2 mL 30% (v/v) percoll) in 15 mL cortex tubes with a broken pasture pipette. Tubes were centrifuged in a swing out rotor at 4000 g for 15 mins at 4 °C with the brake off. The upper layers were siphoned off to remove bacteroids and broken symbiosomes, leaving the remaining layer at the 60/80 % percoll interface containing the symbiosomes. This layer was transferred using a broken pasture pipette into a Sovrall SS34 polycarbonate tube. Symbiosomes were resuspended in 30 mL of ice-cold wash buffer [350 mM mannitol; 25 mM MES-KOH (pH 7.0); 3 mM MgSO<sub>4</sub>; pH 7.0 with KOH], and covered with a parafilm lid. The tube was gently inverted to mix the solutions. A 4 mL cushion of 80% (v/v) percoll was added to the bottom of the tube and centrifuged in a swing out rotor for 15 sec at 4000g, at 4 °C with the brake off. The supernatant was siphoned off again, and symbiosomes resuspended in 15 mL ice-cold wash buffer and kept on ice until use.

#### **4.2.2.3 <sup>99</sup>MoO<sub>4</sub><sup>2-</sup> uptake assay and protocol for *Glycine max* symbiosomes**

Uptake assays were similar to those described in section 3.2.5.2 which consisted of taking 50-100 µL of symbiosomes with cut 0-200 µL pipette tips and gently incubating with equal

amounts of labelled and unlabelled  $^{99}\text{MoO}_4^{2-}$  (as  $\text{Na}_2\text{MoO}_4$  ANSTO-ARI, Lucas Heights) either at 4 °C or 30 °C. At determined time points, 50-100  $\mu\text{L}$  of the symbiosome/reaction buffer were harvested by vacuum filtration onto 0.45  $\mu\text{M}$  nitrocellulose filter (Millipore) and washed with 10 mL of ice cold wash buffer. Membranes were added to 4 mL of StarScint scintillant (Perkin-Elmer) and counted in a scintillation counter (Tri-Carb 2100, Beckmann). Protein determinations were performed by TCA precipitation by the method described by Peterson (1977).

## 4.3 Results

### 4.3.1 $^{99}\text{MoO}_4^{2-}$ accumulation in *Vitis vinifera* cv. Merlot and Chardonnay plants

Grapevines were capable of accumulating molybdenum into their root tissues over time (Figure 4.1). In Merlot, molybdenum uptake was approximately two-thirds higher than that of Chardonnay after a 10-minute exposure, however this was not statistically significant. By 30 minutes, Chardonnay increased its level of  $^{99}\text{MoO}_4^{2-}$  uptake by at least one-third compared to Merlot, which remained unchanged from the 10-minute exposure period, again this was not statistically significant (Figure 4.1).

However, with plants grown in the presence of molybdenum, Chardonnay accumulated approximately 50% more molybdenum than Merlot in the first 10 minutes of exposure (Figure 4.2), but this was not statically significant. After 30 minutes this trend changed and Merlot accumulated approximately 1/3 more compared to cv. Chardonnay (Figure 4.2) and not statistically significant.

Overall, there was no general trend of Merlot having reduced capacity for molybdenum uptake when compared to Chardonnay.

### 4.3.2 Uptake of $^{99}\text{MoO}_4^{2-}$ by *Glycine max* symbiosomes

The molybdenum transport properties of the soybean PBM were tested by measuring the uptake of  $^{99}\text{MoO}_4^{2-}$  into purified symbiosomes. Soybean plants were grown in the presence or absence of external molybdenum and nodules harvested and the symbiosomes isolated approximately 30 days after planting.

In plants grown without molybdenum,  $^{99}\text{MoO}_4^{2-}$  uptake into symbiosomes increased with higher external  $\text{MoO}_4^{2-}$  concentrations from 1 to 4000 nM at 30 °C (Figure 4.3). In contrast, the uptake of  $^{99}\text{MoO}_4^{2-}$  was repressed when the incubation temperature was maintained at 4 °C (Figure 4.3). Plants grown with a complete nutrient solution (plus molybdenum) had much lower rates of symbiosome  $^{99}\text{MoO}_4^{2-}$  uptake which was reduced by approximately 40% compared to symbiosomes extracted from plants grown without  $\text{MoO}_4^{2-}$  (Figure 4.3). Only a small increase in uptake was measured with increasing external  $\text{MoO}_4^{2-}$  supply, and little difference between experiments performed at 4 °C and 30 °C, respectively (Figure 4.3) (Table 4.1).

In plants grown with and without molybdenum,  $^{99}\text{MoO}_4^{2-}$  uptake also increased with increasing external  $\text{MoO}_4^{2-}$  supply from 1-100  $\mu\text{M}$  (Figure 4.4A and 4.4D) and again uptake was significantly decreased when incubation temperature was reduced to 4 °C. Similar trends were also observed when plants grown with molybdenum had a 50% reduced rate of  $^{99}\text{MoO}_4^{2-}$  uptake compared to those in the molybdenum-starved tissues (Figure 4D).

## 4.4 Discussion

### 4.4.1 $^{99}\text{MoO}_4^{2-}$ accumulation of *Vitis vinifera* cv. Merlot and Chardonnay plants

Robinson and Burne (2000) demonstrated that poor growth in Merlot may be linked with molybdenum deficiency. Later Gridley (2003) and Williams et. al. (2004) linked poor growth in Merlot grown on own roots with molybdenum deficiency, however this could be remedied by foliar applications of molybdenum or by planting Merlot on rootstocks. Based on these results, it was hypothesised that Merlot may have a decreased uptake capacity for molybdenum compared to other varieties of *V. vinifera*.

Few studies have focused on the transport of molybdenum in whole plant systems possibly due to the minute quantities of molybdenum required and found within plants. Low molybdenum levels in plant tissues create a technical barrier for both its detection and manipulation of plant material with varied levels of internal molybdenum. Tracking molybdenum transport into and within a plant is also limited by the method of detection. ICP-MS can resolve total molybdenum levels within a plant tissue, however the level of resolution makes it difficult to measure differences in transport rate in short term experiments. The use of radioactive tracers offers the possibility to study molybdenum transport, as readily available  $^{99}\text{MoO}_4^{2-}$  is a commonly used isotope for medical imaging worldwide. Unfortunately,  $^{99}\text{MoO}_4^{2-}$  is a very strong Beta (1.21 Energy MeV) and Gamma (0.74 Energy MeV) emitter that requires extreme lead and Perspex shielding. Consequently, the initial set-up to begin using  $^{99}\text{MoO}_4^{2-}$ , as a safe tracer for the movement of molybdenum through a whole plant system is a strong deterrent to research in the field. Working with grapevines, this system was found to be quite difficult due to the size of plants and the woody canes that act as a potential sink for residual molybdenum or restrict the rapid transport of nutrients to the leaves due to the density of the tissue. In this study, it was found that in whole plant uptake experiments there was no overall decrease in molybdenum uptake in Merlot when compared to Chardonnay vines.

Unfortunately, the experiments conducted looking at molybdenum uptake over time did not provide enough evidence that Merlot had a decreased capacity to uptake molybdenum. This observation does not rule out a transport problem in Merlot *per se* as molybdenum may be taken up by the root system and stored within the root or plants may have difficulties in translocating molybdenum into the shoot and other developing organs. If this is the case, this may explain why planting Merlot on rootstock may alleviate the

molybdenum deficiency. Alternatively, downstream vascular movement of molybdenum to the other parts of the plant may be limited such as loading into the phloem. Phillips (2004) investigated translocation of foliar applied molybdenum using Merlot grown in sand culture and ICP-MS to measure molybdenum amounts within plant tissue. The pools of molybdenum were found within the old wood and new roots. However, more molybdenum was measured in the old wood amongst Merlot grown on own roots compared to 2 rootstocks Schwarzmann and 99 Richter. In this study, experiments were performed to examine the movement of molybdenum into the shoots, however after a 90 min uptake period, no measurable amount of uptake was observed in leaf tissue, possibly due to the restriction of movement through the cane (data not shown).

It is also possible that Merlot may have a Moco deficiency, such as a mutational block in the cells ability to synthesis MPT (molybdopterin), the organic component of Moco, or bind molybdenum to MPT (Mendel and Schwarz, 1999). However, for this to be the case, Moco deficient plants show the pleiotropic loss of all Moco related enzymes, NR, SOX, XDH and AO and death of the plant would result (Mendel and Schwarz, 1999). Plants can be kept alive, as *in vitro* plants, on media containing reduced nitrogen, but die on media containing nitrate (Mendel and Schwarz, 1999). For a Moco mutation to exist in Merlot, vines in essence would behave like one of the many Moco deficient Arabidopsis mutants and would most likely die (Mendel and Schwarz, 1999) or be extremely unhealthy. Brady (2004) examined the mobility of molybdenum and the inducibility of NR by painting leaves with or without  $\text{Na}_2\text{MoO}_4 \cdot 2\text{H}_2\text{O}$ . It was shown that molybdenum was phloem mobile and was able to be incorporated into Moco as increased levels of nitrate reductase activity were found in leaves opposite those receiving the molybdenum treatment.

#### **4.4.2 Uptake of $^{99}\text{MoO}_4^{2-}$ by *Glycine max* symbiosomes**

Molybdenum uptake has been studied in bacteroids (Graham and Maier, 1987; Maier and Graham, 1988) which have a ModABC transport system for to enable nitrogen fixation to be catalysed by nitrogenase. However, there are no published reports of molybdenum transport measurements across the PBM. Maier and Graham (1988) measured molybdenum accumulation into bacteroids using  $^{99}\text{MoO}_4^{2-}$  in strain USDA 136. Time course experiments revealed constant uptake for 1 minute before levelling off. Concentration dependence experiments predicted a  $K_M$  of 0.1  $\mu\text{M}$ , however the authors report variation within  $K_m$  values, which range from 0.05 to 0.12  $\mu\text{M}$ . Lower  $K_m$  values are reported for *E.coli* which has a  $K_m$  for molybdate uptake between 25-50 nM (Self et. al.,

2001). However,  $K_m$  for molybdenum transport in *C. pasteurianum* is much higher at 48  $\mu\text{M}$  ( $4.8 \times 10^{-5} \text{ M}$ ).

Due to the low concentrations of  $\text{MoO}_4^{2-}$  found naturally, molybdenum uptake systems are expected to be high affinity. In this study, molybdenum transport was evident across the PMB (Figure 4.3 and 4.4) where molybdenum uptake into symbiosomes followed typical Michaelis-Menten saturation kinetics with a predicted  $K_M$  of 910.2 and 3404 nM with a  $V_{\text{max}}$  of 81.54 and 81.78 pmole  $\mu\text{g protein}^{-1} \text{ min}^{-1}$  for minus and plus molybdenum symbiosomes at 30 °C respectively (Figure 4.3). The  $K_M$  calculated in this study appear to be higher than those previously reported in *E. coli* (Self et. al., 2001) and bacteroids (Maier and Graham, 1988). At higher concentrations (Figure 4.4A and 4.4D) uptake was linear with no saturation even at 100  $\mu\text{M}$  which is well above the 50 nM levels predicted to occur in soil by Lawson et. al. (1998).

Approximately 40-50% more uptake was measured in symbiosomes from plants grown without molybdenum (Figure 4.3, 4.4A). A reduction in external molybdenum supply during plant growth may have led to an increased demand for molybdenum by the bacteroids resulting in increased molybdenum uptake across the PBM. Plants grown with molybdenum therefore had a reduced requirement for molybdenum, as levels were already sufficient within the bacteroid (Figure 4.3 and 4.4D). Although the lack of molybdenum can cause a reduction in plant growth and also nitrogen fixation activity, the minus molybdenum grown plants appeared healthy and nodules did not visually appear any different to plants and nodules grown with molybdenum.

The molecular mechanism responsible for molybdenum transport across the PBM is unknown. Sulfate transporters are possible candidates and may include sulfate transporters similar to LjSST1 from *L. japonicus* root nodules. Krusell et. al., (2005) recently employed a map bases cloning strategy to identify the genes involved in symbiotic (sym) nitrogen fixation. Analysis of 2 sym mutants (*sst1-1* and *sst1-2*) revealed the underlining mutation was a lesion (9 bp) in a putative sulfate transporter (*LjSst1*). LjSST1 was first identified from a proteomic screen of the PBM (Weinkoop and Saalbach, 2003). The LjSST1 cDNA complemented the yeast sulfate transporter mutant CP154-7A when plated on 0.5 mM  $\text{MgSO}_4$ . As molybdenum can be transported via a sulfate transporter such as SHST1, it may also be plausible that LjSST1 may also transport molybdenum into the PBS. However, it is unclear whether this is the case as LjSST1 may not behave as a  $\text{H}^+/\text{SO}_4^{2-}$

transporter similar to SHST1, but rather a proton exchanger like the mammalian sulfate transport systems, as the proton motive force is directed out of the symbiosome towards the cytoplasm and accumulation of anions in symbiosomes is favoured by positive membrane potential on the inside of the PM (Krusell et. al., 2005). Sulfate uptake assays were not performed on the symbiosomes isolated from the plants grown with and without molybdenum; there have been no reports of direct sulfate transport measurements into symbiosomes (Benedito et. al., 2006). Future work may involve performing sulfate transport experiments in symbiosomes. This may demonstrate the ability of sulfate to be transported across the PBM providing further evidence of molybdenum transport through sulfate transport proteins. Additional future experiments may involve determining if molybdenum can be transported through a Group 3 sulfate transport system, specifically LjSST1, in addition to SHST1 from Group 1 when expressed in yeast cells.



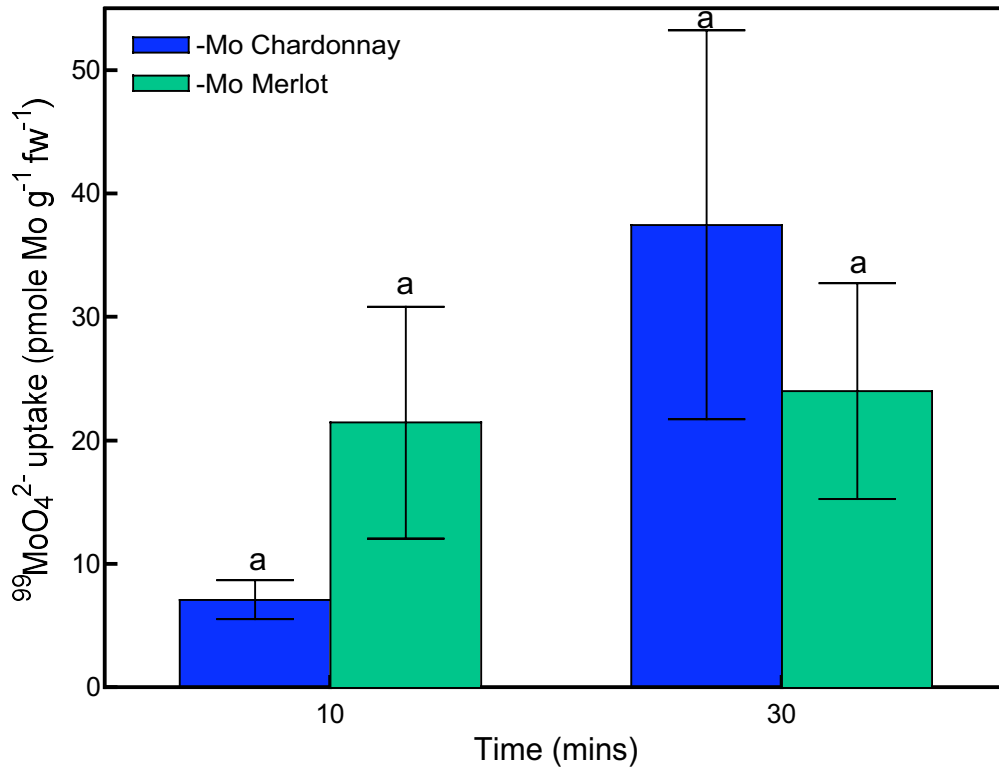


**Figure 4.1 Accumulation of  $^{99}\text{MoO}_4^{2-}$  over time in root tissue of Merlot and Chardonnay rootlings grown without molybdenum.**

$^{99}\text{MoO}_4^{2-}$  uptake was measured in root tissue of either Merlot or Chardonnay from plants grown without molybdenum and incubated with 500 nM  $^{99}\text{MoO}_4^{2-}$ . Data point with \* are not statistically significant at  $p > 0.05$ . Values are means  $\pm$  SEM (n=4) and representative of 2 independent experiments.

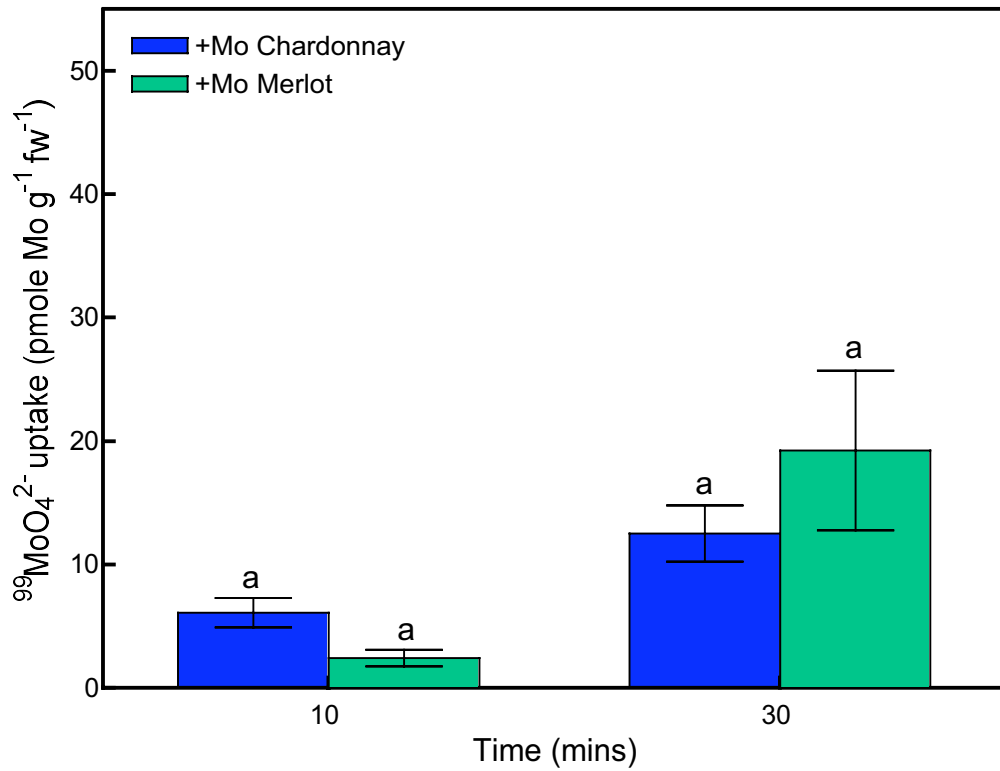
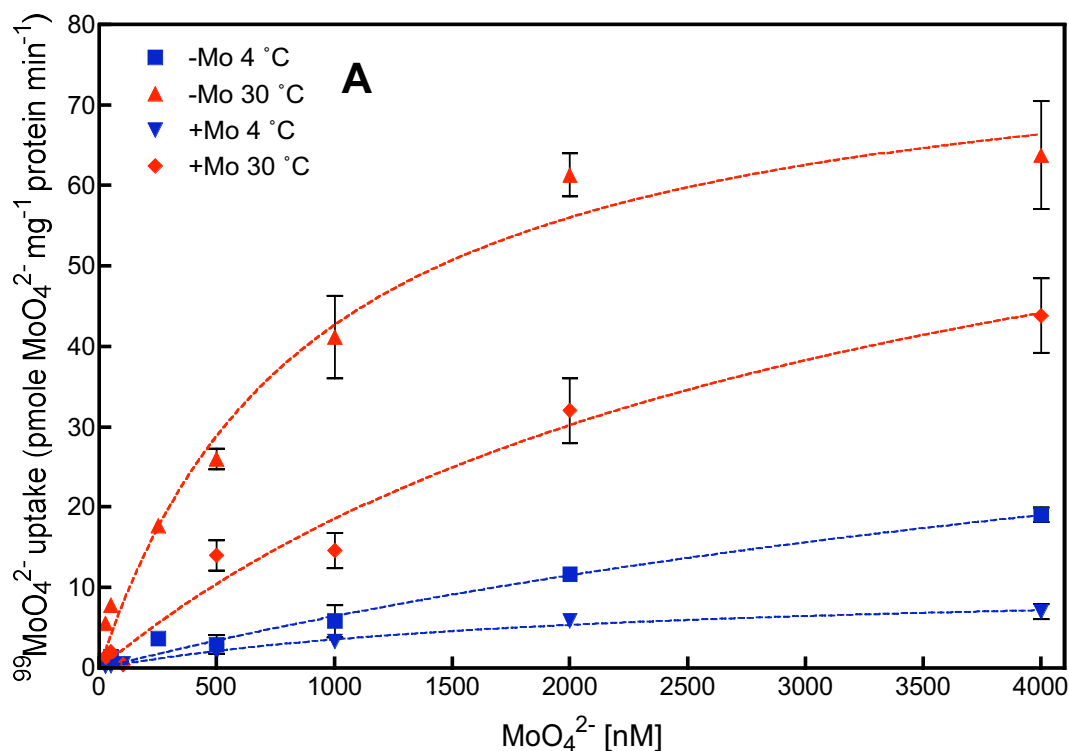


**Figure 4.2 Accumulation of  $^{99}\text{MoO}_4^{2-}$  over time in root tissue of Merlot and Chardonnay rootlings grown with molybdenum.**

$^{99}\text{MoO}_4^{2-}$  uptake was measured in root tissue of either Merlot or Chardonnay from plants grown with molybdenum and incubated with 500 nM  $^{99}\text{MoO}_4^{2-}$ . Data point with \* are not statistically significant at  $p > 0.05$ . Values are means  $\pm$  SEM (n=4) and representative of 2 independent experiments.



**B**

	-Mo 30 °C	+Mo 30 °C
<b>Best-fit values</b>		
<b>VMAX</b>	81.54	81.78
<b>KM</b>	910.2	3404
<b>Std. Error</b>		
<b>VMAX</b>	6.616	17.46
<b>KM</b>	200.4	1281

**Figure 4.3 Concentration dependent accumulation of  $^{99}\text{MoO}_4^{2-}$  in soybean symbiosomes from plants grown with and without molybdenum.**

**A.**  $^{99}\text{MoO}_4^{2-}$  uptake was measured in soybean symbiosomes isolated from plants grown with or without  $\text{Na}_2\text{MoO}_4 \cdot 2\text{H}_2\text{O}$ . Symbiosomes were incubated at 4 °C or 30 °C with reaction buffer containing  $^{99}\text{MoO}_4^{2-}$  -  $\text{Na}_2\text{MoO}_4 \cdot 2\text{H}_2\text{O}$  at increasing concentrations for 5 mins. Values are means  $\pm$  SEM (n=4) and representative of 2 independent experiments. **B.** Characteristics of soybean symbiosomes isolated from plants grown with and without  $\text{Na}_2\text{MoO}_4 \cdot 2\text{H}_2\text{O}$ .  $K_m$  (nM) and  $V_{\max}$  (pmole  $\text{MoO}_4^{2-}$  mg protein $^{-1}$  min $^{-1}$ ) values were determined by fitting the kinetic equation  $y = V_m \cdot x / (K_m + x)$ .

**Table 4.1 Statistical analyses of the concentrations in concentration dependent accumulation between 0 and 4000 nM of  $^{99}\text{MoO}_4^{2-}$  in soybean symbiosomes isolated from plants grown from plants with and without molybdenum.**

Only statistically significant data is presented.

<b>Treatment</b>	<b>Concentration 1 (nM)</b>	<b>Concentration 2 (nM)</b>	<b>Significance at 5% level</b>
-Mo 30 °C	25	250	P<0.05
+Mo 30 °C			P<0.001
-Mo 30 °C	25	500	P<0.001
+Mo 30 °C			P<0.05
-Mo 30 °C	25	1000	P<0.001
+Mo 30 °C			P<0.01
-Mo 4 °C	25	2000	P<0.05
-Mo 30 °C			P<0.001
+Mo 30 °C			P<0.001
-Mo 4 °C	25	4000	P<0.001
-Mo 30 °C			P<0.001
+Mo 30 °C			P<0.001
+Mo 30 °C	50	250	P<0.001
-Mo 30 °C	50	500	P<0.001
+Mo 30 °C			P<0.05
-Mo 30 °C	50	1000	P<0.001
+Mo 30 °C			P<0.01
-Mo 4 °C	50	2000	P<0.05
-Mo 30 °C			P<0.001
+Mo 30 °C			P<0.001
-Mo 4 °C	50	4000	P<0.001
-Mo 30 °C			P<0.001
+Mo 30 °C			P<0.001
+Mo 30 °C	100	250	P<0.01
-Mo 30 °C			P<0.001
+Mo 30 °C	100	500	P<0.001

-Mo 30 °C			P<0.05
+Mo 30 °C	100	1000	P<0.001
-Mo 30 °C			P<0.05
+Mo 30 °C	100	2000	P<0.001
-Mo 30 °C			P<0.001
-Mo 4 °C	100	4000	P<0.001
+Mo 30 °C			P<0.001
-Mo 30 °C			P<0.001
+Mo 30 °C	250	500	P<0.001
+Mo 30 °C	250	1000	P<0.001
-Mo 30 °C			P<0.001
-Mo 30 °C	250	2000	P<0.001
-Mo 4 °C	250	4000	P<0.001
-Mo 30 °C			P<0.001
+Mo 30 °C			P<0.01
-Mo 30 °C	500	1000	P<0.01
-Mo 30 °C	500	2000	P<0.001
+Mo 30 °C			P<0.001
-Mo 4 °C	500	4000	P<0.001
-Mo 30 °C			P<0.001
+Mo 30 °C			P<0.001
-Mo 30 °C	1000	2000	P<0.001
+Mo 30 °C			P<0.001
-Mo 4 °C	1000	4000	P<0.05
-Mo 30 °C			P<0.001
+Mo 30 °C			P<0.001
+Mo 30 °C	2000	4000	P<0.05

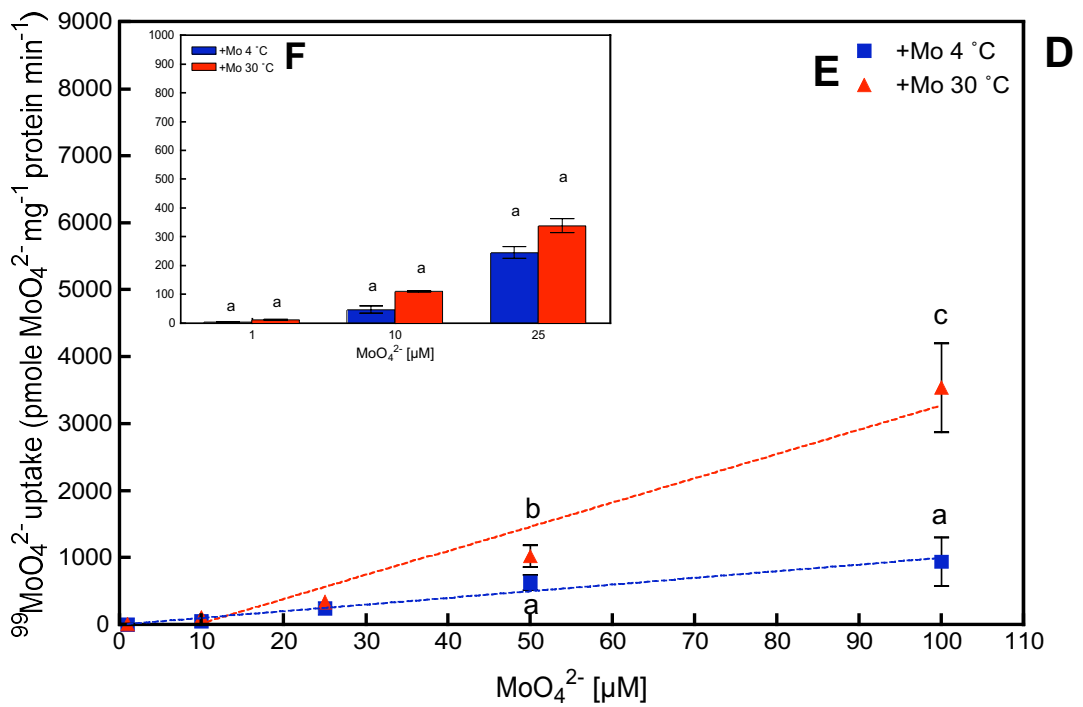
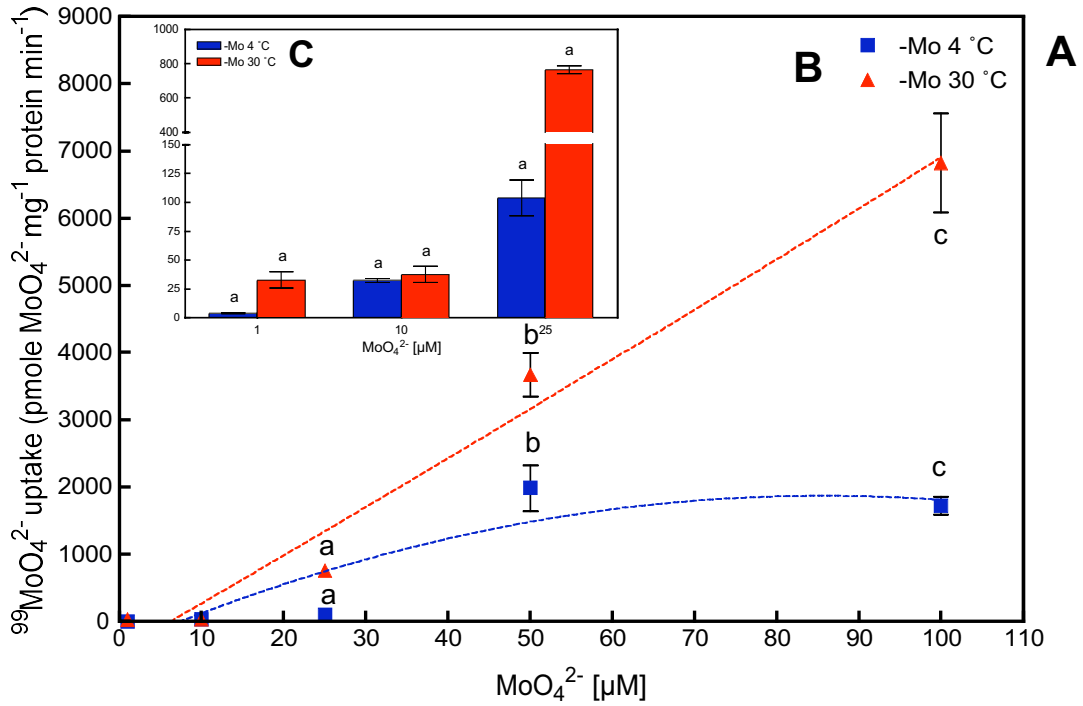


**Figure 4.4 A. Concentration dependent accumulation of  $^{99}\text{MoO}_4^{2-}$  in soybean symbiosomes from plants grown without molybdenum and D. Concentration dependent accumulation of  $^{99}\text{MoO}_4^{2-}$  in soybean symbiosomes from plants grown with molybdenum.**

**B.**  $^{99}\text{MoO}_4^{2-}$  uptake was measured in soybean symbiosomes isolated from plants grown without molybdenum incubated at 4 °C or 30 °C with reaction buffer containing  $^{99}\text{MoO}_4^{2-}$  -

$\text{Na}_2\text{MoO}_4 \cdot 2\text{H}_2\text{O}$  at increasing concentrations for 5 mins. **C.** Inset of the rate of influx between 1-25  $\mu\text{M}$ . Values are means  $\pm$  SEM (n=4). **E.**  $^{99}\text{MoO}_4^{2-}$  uptake was measured in soybean symbiosomes isolated from plants grown with molybdenum incubated at 4 °C or 30 °C with reaction buffer containing  $^{99}\text{MoO}_4^{2-}$  -  $\text{Na}_2\text{MoO}_4 \cdot 2\text{H}_2\text{O}$  at increasing concentrations for 5 mins. **F.** Inset of the rate of influx between 1-25  $\mu\text{M}$ . Values are means  $\pm$  SEM (n=4). Statistical comparisons are only appropriate between either 30 °C or 4 °C with results with the same letter not being statistically different.

## Chapter 5

# Effects of foliar applied molybdate on yield, yield components, quality parameters and petiole nutrient content in *Vitis vinifera* cv. Merlot

---

### 5.1 Introduction

*Vitis vinifera* cv. Merlot is an economically important wine grape variety for South Australia with approximately 4536 hectares planted in 2006. During the 2005/2006 vintage, Merlot was the third most popular variety purchased (based on tonnes harvested), accounting for 7% of South Australia's total wine grape crush (Hathaway, 2006). In McLaren Vale, the 2006 price offered for Merlot by Fosters Wine Estates was between \$700 and \$1200, with most growers receiving between \$700 and \$850 per tonne (F. Cox pers. comm.). Estimated production and demand for this variety has been forecast to increase from 2007 to 2011 (Hathaway, 2006). However, the establishment of Merlot within the wine industry as a profitable variety has been troubled due to what is commonly referred to in the industry as 'the Merlot problem' (Robinson and Burne, 2000) or the 'Merlot disorder' (Smart, 1992). Merlot vines grown on own roots exhibit a variety of symptoms including altered berry development, small downward rolling leaves, general chlorosis and necrosis of the leaf edge, and shoots which exhibit a 'zig-zag' growth phenotype often stunted with extensive lateral shoots (Habibi et. al., 1998; Robinson and



Burne, 2000). One of the most dramatic and economically damaging phenotypes in Merlot is the significant loss in berry yield. 'Millerandage' or 'hen and chicken' is a bunch phenotype disorder where large proportions of small immature green berries develop instead of the large fully matured purple berries suitable for winemaking purposes. Robinson and Burne (2000) linked these symptoms to molybdenum deficiency and reported foliar sprays of molybdenum resulted in a recovery.

In South Australia, particularly within the acidic soils of the Mt Lofty Ranges, molybdenum deficiency is common in Merlot vines grown on own roots as the availability of molybdate decreases with decreasing soil pH. Other soil factors including the presence of Fe oxides, can also bind plant available molybdate (Smith et. al., 1997). Though soil pH modification through liming is a potential remedy to liberate plant available molybdenum, this is both costly and time consuming.

For many viticulturalists, the simple application of molybdenum sprays has proved to be a successful technique to remedy yield problems and is now a widely used method within the industry. Williams et. al. (2004) reported a 750% yield increase while Gridley (2003) reported yield increases of 170% amongst vines grown on own roots and sprayed with foliar molybdenum. Though the use of molybdenum spray is relatively new to the industry and unfortunately, the long-term effects of foliar molybdenum application on vine biology and yield is unknown. It is important to quantify whether vine health is improved long-term and to develop guidelines with respect to the required frequency of foliar application.

A field trial was established at McLaren Vale with the aim of measuring yield, yield components, quality parameters and both macro and micronutrient profiles in response to foliar application of molybdenum over a 3-year period within a clonal trial row of Merlot. Previous work by Gridley (2003) demonstrated that the vines were deficient of molybdenum (0.05-0.09 mg/kg) according to the deficiency range established by Williams et. al. (2004) in *Vitis*. This fact alone made this particular site ideal to analyse the in yield response to molybdenum sprays as a yield responses are traditionally seen amongst molybdenum deficient vines only (Williams et. al. 2003; Williams et. al. 2004). The application of molybdenum was applied to ensure that vines received either 1, 2 or 3 years of molybdenum sprays. This approach allowed for molybdenum profiles associated with fruiting tissues to be traced from year to year in response to molybdenum application or

not. Yield components were examined at the end of each year of the trial to assess which, if any molybdenum treatment, were responsible for an increase in yield.

How yield components are influenced can be used to assess the potential yield in one season (Tassie and Freeman, 1992). Yield component compensation dictates that as one yield component is changed, the level of one or more other yield components will also change accordingly (Tassie and Freeman, 1992). This relationship can be demonstrated with the following equations,

$$\text{Yield (t/ha)} = \text{vines/ha} \times \text{bunch number per vine} \times \text{mean bunch weight (g)} \times 10^{-6}$$

$$\text{Bunch number/vine} = \text{shoots per vine} \times \text{bunches per shoot}$$

$$\text{Bunch weight (g)} = (\text{berries/bunch} \times \text{mean berry weight (g)}) + \text{rachis weight (g)}$$

$$\text{Berries/bunch} = \text{flowers per bunch} \times \% \text{ fruit set}$$

$$\% \text{ fruit set} = \text{berry number} / \text{flower number}$$

In addition, the quality parameters of berry juice including total soluble solids (°Brix), pH, extractable anthocyanins and total phenolics were also determined to observe what effect molybdate application may have on these important grape quality components. This is important to determine from a winemaking perspective, as it is undesirable to change berry quality that may ultimately affect wine quality.

## 5.2 Methods

### 5.2.1 McLaren Vale Visitor Centre cv. Merlot trial

This trial was conducted over 3 growing seasons (2003/2004, 2004/2005 and 2005/2006) at the McLaren Vale Visitor Centre Merlot clonal trial. This trial consisted of 4 commercial clones of Merlot and included D3V14, 6R, 8R and Q45-14 all grown on own roots. The row contained 186 vines spaced 1.5m apart with a row width of 3m and orientated in an east-west direction. All vines were drip irrigated with *V. vinifera* cv. Shiraz vines growing on either side of this trial row. Each panel contained 4 vines, each representing a different clone and planted in a randomised design. For the purpose of this study, the trial site was randomly divided into 4 treatments resulting in 3-4 replicates containing the spray regimes consisting of a control, and foliar sprays of  $\text{Na}_2\text{MoO}_4 \cdot 2\text{H}_2\text{O}$ , which occurred once, twice, or three times over the 3 year trial period (see Table 5.1 and 5.2). At least 4 buffer vines were at the end of the panel to eliminate any edge effects. The pruning system consisted of 2 node spurs on both the upper unilateral and lower bilateral cordons.

**Table 5.1 Molybdenum foliar spray regime for growing seasons 2003/2004 to 2005/2006.**

Molybdenum was applied as a foliar spray over 3 years. Vines received 1 of 4 treatments, either a control (water) spray, or spraying of molybdenum for 1, 2 or 3 years.

	Year 1	Year2	Year3	Molybdenum treatments
	2003/2004	2004/2005	2005/2006	
<b>Treatment 1 (T1 + + +)</b>	Spray Mo	Spray Mo	Spray Mo	3
<b>Treatment 2 (T2 + - -)</b>	Spray Mo	No Spray	No spray	1
<b>Treatment 3 (T3 - + +)</b>	No spray	Spray Mo	Spray Mo	2
<b>Control (C)</b>	H <sub>2</sub> O spray	H <sub>2</sub> O spray	H <sub>2</sub> O spray	0

### 5.2.2 Molybdenum application

$\text{MoO}_4^{2-}$ , as  $\text{Na}_2\text{MoO}_4 \cdot 2\text{H}_2\text{O}$ , was applied to the vines as a foliar spray in accordance with the trial design (Table 5.1 and 5.2). Foliar application was performed at E-L Stage 12 (Appendix 2) at a rate of 300 g  $\text{Na}_2\text{MoO}_4 \cdot 2\text{H}_2\text{O}$  per hectare (1.54 mM) dissolved in RO

H<sub>2</sub>O. Red food colouring (Queen) was added to the foliar spray (50 mL to 20 L of RO H<sub>2</sub>O and 7.5 g of Na<sub>2</sub>MoO<sub>4</sub>·2H<sub>2</sub>O), enabling the spray to be seen on the vines to ensure even spraying. Control panels received a foliar spray of RO H<sub>2</sub>O and red food colouring (50 mL to 20 L of RO H<sub>2</sub>O). A second foliar application was performed again 7-10 days later depending on vine growth and weather conditions.

### **5.2.3 Petiole collection and analysis**

Petioles were collected between E-L stages 23-25 (Appendix 2) for all treatments using clean secateurs and gloved hands to prevent contamination from grease and sunscreen. Petioles were collected from the positions opposite basal inflorescences 1, 2 and 3 (Figure 5.1). From each vine in each treatment, 30-40 petioles were collected (15-20 each side on the vine) to ensure that 2 g of dried mass could later be obtained. Petioles were collected in the morning to eliminate potential diurnal fluctuations (Nagarajah, 1999). After collection, petioles were placed on ice for transport, and later rinsed in RO H<sub>2</sub>O and towel dried before being placed into an 80°C oven until dry.

After oven drying, petioles were ground into a fine powder using a grinding mill (IKA) with titanium chamber to prevent molybdenum contamination. Nutrients were analysed by Waite Analytical Services, The University of Adelaide, Waite Campus. Molybdenum analysis was performed using ICPMS (Inductively Coupled Plasma Mass Spectrometry). Nitrogen analysis was performed using a combustion technique and analysed using an Elementar Instrument. Remaining nutrients including P (Appendix 3), K, Na (Appendix 3), Mg (Appendix 3), Mn (Appendix 3), Cu, B, Ca (Appendix 3), Al, S, B, Zn and Fe (Appendix 3), were analysed using ICPAES (Radial CIROS Inductively Coupled Plasma Atomic Emission Spectrometry).

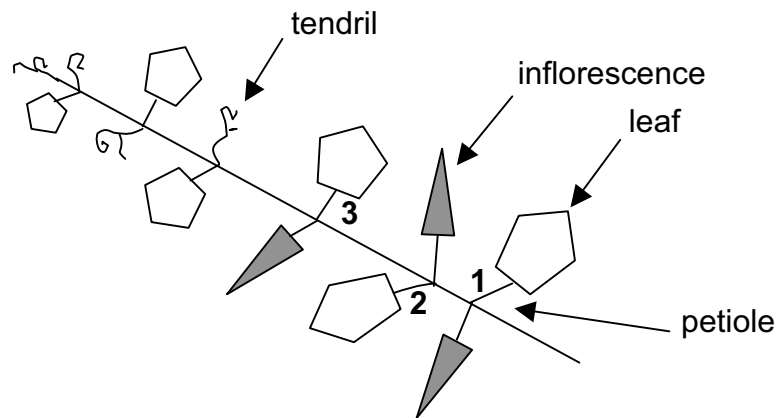


**Figure 5.1 Diagram showing grapevine shoot structure.**

At flowering, petioles were collected from positions 1, 2 or 3 opposite inflorescences for nutrient analysis.

#### **5.2.4 Fruit set analysis**

At E-L stages 23-25 (Appendix 2) inflorescences of various sizes were randomly collected from vines. The rachis and wing lengths of the inflorescence were recorded and the number of flowers on each counted. The total number of flowers and the length of the rachis and wing were combined and analysed using regression analysis (Prism, Version 4.0). Graphs were constructed (Figure 5.3) to enable the number of flowers to be determined if the combined length of the rachis and wing were known (Gridley, 2003).

At E-L stages 23-25, 2 inflorescences were randomly chosen and labelled per vine for all treatments and lengths of the rachis and wing recorded. Using the graphs constructed, the total number of flowers per inflorescence was determined. At harvest, labelled bunches were collected and coloured berries counted. The % fruit set was determined using the following equation,

$$\% \text{ fruit set} = \frac{\text{number of coloured berries/bunch}}{\text{number of flowers/bunch}} \times 100$$

#### **5.2.5 Bunch and berry sampling and analysis**

At harvest, for each treatment, all bunches on vines were counted and from which 8 were randomly selected from each vine in the panel. Bunches were stored in zip-locked bags,

placed in cooled eskies for transportation, and then finally stored at -20°C for further analysis.

### **5.2.6 Grape berry juice extraction**

From each of the 8 bunches collected at harvest, 50 berries were randomly collected from the top, bottom and middle of the bunch and their weight recorded. Berries were placed in a hand held juice extractor and crushed ensuring that seeds were not broken. The resulting grape juice was then transferred to 10 mL Falcon tubes and centrifuged for 5 mins at 3500 rpm. Tubes were stored upright at 4 °C and the supernatant was then used to perform total soluble solids and pH measurements.

### **5.2.7 Total soluble solids (°Brix) determination**

Juice samples were allowed to adjust to room temperature (approximately 20 °C) before measurements were taken. A digital refractometer (Atago PR-101) with built-in temperature compensation was used to determine total soluble solids (°Brix) on approximately 500 µL of juice. Milli Q H<sub>2</sub>O was used to blank the refractometer between sample readings.

### **5.2.8 pH determination**

The same sample used for total soluble solids (°Brix) was also used to determine pH. pH was measured using a hand held pH meter (Cyberscan 310 series) after calibration with pH 4 and pH 7 solutions.

### **5.2.9 Anthocyanin and total phenolics determination of grape berries**

From each of the 8 bunches collected at harvest, another 50 berries were randomly collected from the top, bottom and the middle of the bunches and the weight recorded. Berries were placed in 125 mL plastic containers and macerated 30 seconds using a Poly-Tron homogeniser at 2400 rpm. The samples were mixed and macerated again for 30 seconds at 2400 rpm or until an homogenous mixture was produced which did not contain any large pieces of berry, skin or seeds (Iland et. al., 2000).

The major anthocyanin, malvidin-3-glucose, and total phenolics of the grape berries were determined as described in Iland et. al. (2000). Approximately 1 g of the homogenised grape berries was transferred to a 10 mL Falcon tube and the weight recorded. 10 mL of 50% (v/v) ethanol pH 2 was added to the Falcon tube containing the macerate and inverted

every 10 mins for an hour. After this incubation period, tubes were centrifuged at 3500 rpm for 5 mins. 500  $\mu$ L of the supernatant was added to 10 mL of 1M HCl and incubated at room temperature for 3 hours. The remaining supernatant was measured in a measuring cylinder and the volume recorded. ‘Final extract volume’ was determined by adding together the supernatant measured in the measuring cylinder plus the 500  $\mu$ L added to the 1M HCl. After the 3-hour incubation period, the absorbance of the HCl extract was measured at 280 and 520 nm. The following equations were used to determine anthocyanins and phenolics in the grape berries,

Colour per berry (mg anthocyanin per berry) =

$$\frac{\text{Abs (520)} \times \text{dilution factor} \times \text{final extract volume (mL)} \times \text{weight of 50 berries (g)} \times 1000}{500 \quad \quad \quad 100 \quad \quad \quad \text{weight of homogenate taken for extraction (g)} \quad \quad 50}$$

Colour per g berry weight (mg anthocyanin per gram berry weight) =

$$\frac{\text{Abs (520)} \times \text{dilution factor} \times \text{final extract volume (mL)} \times \text{weight of 50 berries (g)} \times 1000}{500 \quad \quad \quad 100 \quad \quad \quad \text{weight of homogenate taken for extraction (g)} \quad \quad \text{weight of 50 berries (g)}}$$

Total phenolics per berry (absorbance units per berry) =

$$\frac{\text{Abs (280)} \times \text{dilution factor} \times \text{final extract volume (mL)} \times \text{weight of 50 berries (g)} \times 1}{100 \quad \quad \quad \text{weight of homogenate taken for extraction (g)} \quad \quad 50}$$

Total phenolics per gram berry weight (absorbance units per gram berry weight) =

$$\frac{\text{Abs (280)} \times \text{dilution factor} \times \text{final extract volume (mL)} \times \text{weight of 50 berries (g)} \times 1}{100 \quad \quad \quad \text{weight of homogenate taken for extraction (g)} \quad \quad \text{weight of 50 berries (g)}}$$

### 5.2.10 Climatic data

Climate data was obtained from the Bureau of Meteorology. Data was sourced from the closest station to McLaren Vale, which is Kuinto Forest Weather Station, approximately 11 km SE of McLaren Vale.

### **5.2.11 Statistical analysis**

Field site data was analysed using SPSS 11.0. Data was tested for normality and variability. When this was achieved, General Analysis of Variance (ANOVA) was used to determine significant differences at the 5% level. When the assumptions of normality and variability were not met, data was transformed appropriately. Where significance was determined, post hoc tests Bonferroni or Tukey for analysing the yield components or LSD for analysing the petiole nutrients were performed to determine where significance lay within the data. Statistical comparisons are only appropriate within each graph. Additional information related to differences associated with both treatments and clones are provided within the text of the results section for the yield components or within tables for the petiole nutrients.



## **5.3 Results**

### **5.3.1 Fruit set**

#### **5.3.1.1 Regression analysis of flower number and inflorescence length**

Regression analysis revealed a high correlation between the number of flowers on an inflorescence against the combined length of the wing and main rachis inflorescence with an  $R^2$  value of 0.865, 0.907 and 0.918 for the growing seasons 2003/2004, 2004/2005 and 2005/2006 respectively (Figure 5.2). There was no significant difference between the slopes of the regression lines ( $p=0.71$ ) indicating that it was possible to calculate one slope for all the data. This data showed that only one year of data collection was required to calculate rate of fruit set using this method.

#### **5.3.1.2 Fruit set over 3 years**

In year 1, there were no significant differences in % fruit set between the control and treatment 1 for D3V14, Q45-14 and 8R (Figure 5.3). Clone 6R was the exception showing a significant increase in % fruit set ( $p=0.033$ ) with molybdenum application. In year 2, clone 6R continued to show a trend towards higher % fruit set with molybdenum treatments, but this was not found to be a statistically significant difference from the controls. There was a significant difference in % fruit set in year 2 for D3V14 ( $p=0.042$ ) between the control and treatment 1 and also between the control and treatment 2. The other clones Q45-14 and 8R in year 2 did not increase % fruit set significantly regardless of treatment. Analysis of % fruit set in year 3 revealed no significant changes in % fruit set between any of the clones or treatments (Figure 5.3).

### **5.3.2 Yield components**

#### **5.3.2.1 Mean yield per vine**

In year 1, D3V14 was the only clone to show a response to molybdenum application where yield increased by approximately 50% compared to the control (Figure 5.4). There was a significant difference between the yields of D3V14 and 8R in treatment 1 ( $p=0.014$ ) while the yields of both 8R and 6R actually decreased by approximately 25% compared to the control, but this was not statistically significant.

In year 2 there were no changes in yield. The yield in both D3V14 and Q45-14 decreased in treatment 1, however this was not statistically significant. In year 3 8R was the only cultivar with a significant increase in yield ( $p=0.014$ ) between the control and treatment 1. However, over the 3-year trial, the yield on a per vine basis decreased regardless of clone and treatment (Figure 5. 4).

#### **5.3.2.2 Mean bunches per vine**

There were no significant changes in bunch number per vine within any of the clones and treatments for year 1 and year 3 of the trial (Figure 5.5). In year 2 however, there was a significant decrease in bunch number between the control and treatment 1 ( $p=0.032$ ) and the control and treatment 2 ( $p=0.045$ ) for Q45 and 8R. Bunch number per vine stayed at similar levels over the 3 years of the trial period, though year 3 generally had the lowest number of bunches per vine.

#### **5.3.2.3 Mean bunch weight**

In year 1 there was a small increase in bunch weight between the control and treatment 1 for 8R, Q45-14 and 6R, however this was not statistically significant (Figure 5.6). D3V14 in year 1 had a increase in bunch weight ( $p=0.041$ ) which may be partially responsible for the increase in yield associated with this clone. There was a significant difference between clones with treatment 1 year 1 ( $p=0.001$ ) with a significant difference between Q45-14 and 6R. Clone 6R generally produced the heaviest bunches, regardless of the treatment. In year 2, the only significant increase in bunch weight was measured in 6R, where heavier bunches were produced in response to molybdate treatment. In year 3, there was a significant increase in bunch weight in Q45-14 relative to the control and treatment 2 which also received molybdate in that year. There were no other bunch weight increases in any of the other clones regardless of treatment.

#### **5.3.2.4 Mean berries per bunch**

In year 1, there was a small increase in the number of berries per bunch between the control and treatment 1, however this was not statistically significant (Figure 5.7). Clone 8R in year 2 had a significant increase in berries per bunch ( $p=0.005$ ) in treatments 1 and 2, while in year 3, Q45-14, had a larger number of berries per bunch ( $p=0.024$ ) after the third molybdenum application (treatment 1) but not after the second (treatment 3).

### **5.3.2.5 Mean berry weight**

Overall, there were no statistically significant increases in berry weight in year 1 and 3 of the trial (Figure 5.8). A small increase in berry weight was measured in year 1 in clones D3V14, Q45-14 and 6R, but this was not significant. In year 2, berry weight increased in D3V14 ( $p=0.035$ ) with treatment 1, and decreased in treatment 2. This response was also evident in clones Q45-14 and 6R but was not statistically significant.

### **5.3.2.6 Mean rachis weight**

There was no increase in rachis weight in year 1 or year 3 regardless of the clone or treatment. The only increase in rachis weight was recorded in 8R year 2 ( $p=0.012$ ) where there was an increase between the control and treatment 1 (Figure 5.9).

### **5.3.3 Climate data**

Reduced levels of rainfall were recorded in 2006 compared to the previous years (Figure 5.10). This may explain why no increases in yields were measured due to significantly decreased rainfall compared to other years as a result of the drought.

### **5.3.4 Berry quality**

#### **5.3.4.1 Total soluble solids and pH measurements of grape berry juice from Year 3 (2005/2006)**

There were no interactions between the spray regimes and clones for total soluble solids ( $^{\circ}$ Brix) ( $p=0.855$ ) and pH ( $p=0.853$ ) in the last season of the trial (2005/2006) (Figure 5.11). In general, Q45-14 had the lowest total soluble solids in all treatments with the exception of treatment 1. This data demonstrates that there are no effects of the application of molybdenum over a 3-year period nor is there a superior clone in 2005/2006 that produced greater amounts of sugars.

There were significant differences between treatments ( $p=0.045$ ) for juice pH (Figure 5.12). There was a significant increase in pH in treatment 2 ( $p=0.045$ ) relative to the control. Between clones, 6R generally had the lowest pH while clones D3V14 and Q45-14 generally displayed higher pH. This data indicated that in treatment 2, an initial application of molybdenum may influence subsequent juice pH.

#### **5.3.4.2 Anthocyanin and total phenolics determination of grape berry juice from the 2005/2006 growing season**

There were no interactions between spray regimes and clones for berry colour (Figure 5.13A,  $p=0.651$ ), colour per gram berry weight (Figure 5.13B,  $p=0.699$ ), total phenolics per berry (Figure 5.14A,  $p=0.496$ ) or total phenolics per gram berry weight (Figure 5.14B,  $p=0.692$ ). This data indicates that there are no effects of the application of molybdenum over a 3 year period to either the quality parameters of colour or total phenolics. This data also indicates that there is no one superior clone in terms of colour and phenolic properties.

#### **5.3.5 Petiole nutrients**

##### **5.3.5.1 Molybdenum petiole concentration**

Trends of molybdenum concentration in regards to the treatment and the year emerged throughout the data (Figure 5.15 and 5.16). All control vines were deficient in molybdenum and there were no significant differences in the molybdenum levels over the 3-year trial period. Generally, in treatment 1, levels of molybdenum increased slightly in year 2, but decreased in year 3, despite another application of molybdenum in the last year. In treatment 2, initial application increased the levels of molybdenum within the vine within the first year, but when no molybdenum was applied in the second and third years, molybdenum deficiency returned. Treatment 3 also had a significant difference between the years of molybdenum application, with all clones starting in year 1 of the trial with deficiency, which was then removed with a spray of molybdenum in year 2. By year 3 the levels of molybdenum had decreased compared to year 2, despite another foliar spray. This resulted in significant differences between treatments ( $p=0.000$ ) (Table 5.3). There were also differences between control clones ( $p=0.004$ ) (Table 5.4). In year 1 and year 3 within treatment 1, clone 8R generally had higher molybdenum content in petiole.

##### **5.3.5.2 Sulfur petiole concentrations**

Generally in Year 1 in the beginning of the trial sulfur levels were highest, which then decreased at year 2, and then increased slightly in year 3 (Figure 5.17 and 5.18). There were no significant differences between treatments ( $p=0.384$ ). There was significant difference between clones ( $p=0.000$ ) (Table 5.5) and generally, clone 8R had higher sulfur levels in Year 1.

### **5.3.5.3 Total nitrogen petiole concentrations**

The trends established for sulfate petiole concentrations were also similar to those seen for total N (Figure 5.19 and 5.20). Generally, total N amounts were highest in year 1, decreased in year 2, before increasing again in year 3. All vines had less than adequate total N, with lowest amounts occurring in year 2. There was a significant difference between the treatments of molybdenum application and the total N ( $p=0.003$ ) (Table 5.6). There were no difference in year 1, but in year 2 there were difference between the control and treatment 2 for all clones except 6R and differences between treatment 2 and 3 for Q45-14 and 8R. There was also a significant difference between and the clones with Q45-14 having higher total N levels in year 1, treatment 1 and 2 and again in year 3 treatment 1 ( $p=0.004$ ) (Table 5.7)

### **5.3.5.4 Copper petiole concentrations**

Distinct levels of fluctuation in the petiolar levels of copper occurred over the 3-year trial period in all clones and treatments (Figure 5.21 and 5.22). Again, levels were highest in year 1 before dropping in year 2 and increasing in year 3 for all cases. There was no significant difference between the copper levels between clones ( $p=0.816$ ), however there was a significant difference between treatments ( $p=0.013$ ) (Table 5.8). There were significant differences in year 1 and 2 between the control and treatment 1 and 2 for all clones except Q45-14 in year 1, Q45-14, and 8R in year 2.

### **5.3.5.5 Potassium petiole concentrations**

Regardless of treatment or clone, all concentrations of potassium within the petioles followed a similar pattern over the 3 years of the trial (Figure 5.23 and 5.24). Highest potassium levels were measured in year 1 of the trial. This increased slightly in year 2, but was not statistically significant. Levels significantly decreased in year 3. In both year 1 and 2, potassium petiole concentrations were high, though still adequate according to Reuter and Robinson (1997). By year 3 of the trial levels had decreased to levels that were between the adequate levels 1.8 – 3%. There was a significant effect of the treatment of molybdenum sprays on potassium levels ( $p=0.006$ ) in certain cases however there was no general trend (Table 5. 9). There was also a clonal difference ( $p=0.000$ ) in certain instances (Table 5. 10).

### **5.3.5.6 Boron petiole concentrations**

No clear pattern of boron petiole levels emerged over the trial period (Figure 5.25 and 5.26). Generally, within each clone or the control treatment, boron increased in year 2 before decreasing in year 3. In treatment 1, boron levels generally decreased over the 3 year whereas for vines in treatment 2, boron levels decreased in year 2 before increasing in year 3. Treatment 3 had no general trends occurring within the treatments. There was a significant effect of the molybdenum spray treatments on the boron petiole content ( $p=0.003$ ) (Table 5. 11) that only occurred after year 2 of the trial. For D3V14, 8R and 6R there were significant differences between the control and treatment 2 for all clones except Q45-14 in year 2 and D3V14 in year 3. There were also differences in clones ( $p=0.000$ ) with 8R and 6R generally having higher levels of boron (Table 5. 12).

### **5.3.5.7 Zinc petiole concentrations**

The levels of zinc within the petiole also fluctuated over the years of the trial with the control, treatment 1 and 2 experiencing a decrease after year 2 compared to the control and then increasing again in year 3 (Figure 5.27 and 5.28). The zinc levels within the varying molybdenum treatments appeared to be more stable with less fluctuation in zinc levels between the years of the trial. This resulted in no significant effects of molybdenum treatments on zinc levels ( $p=0.054$ ) and no clonal effect ( $p=0.828$ ).

## 5.4 Discussion

### 5.4.1 Molybdenum transport and translocation within *Vitis* sp.

Foliar application of molybdenum is a well accepted method of remedying molybdenum deficiencies in many plant species including grapevine (Robinson and Burne, 2000; Gridley, 2003; Williams et. al., 2003; Phillips, 2004; Williams et. al., 2004), Poinsettia (Cox, 1992b; Cox, 1992a), and common bean (Vieira et. al., 1998a; Vieira et. al., 1998b). However, little is known about the transport, translocation and potential cumulative effects of molybdenum treatments in woody perennial species like grapevines. In this study, a field trial was conducted using *V. vinifera* cv. Merlot to observe the effects of yearly molybdenum application on fruit-set, berry quality parameters and final yield. The trial also allowed for an investigation of molybdenum transport and redistribution over successive seasons.

A site was chosen in McLaren Vale, SA, which consisted of 11 year old Merlot vines, containing four different Merlot clones. Grapevines grown on this site have previously been shown to have molybdenum deficiencies and there has been no corrective molybdenum treatments applied to these plants (Gridley, 2003) (Figure 5.15 and 5.16). Vines received 1 of 4 potential treatments, either a control (H<sub>2</sub>O spray) or combinations of molybdenum sprays for 1, 2 or 3 years (see Table 5.1). Prior to and during the experiment control vines were shown to be deficient in molybdenum as described by Williams et. al. (2004) with deficiency occurring between 0.05-0.09 mg/kg. In fact, on occasion, the molybdenum levels measured within the vines was below this described deficiency level (Figure 5.15 and 5.16). The consistently low molybdenum levels indicated that no new pools of plant available molybdenum were being accessed through continuing root growth and penetration of the soil profile.

As molybdenum is required in trace amounts by plants, the excessive foliar application to vines over successive years was of some concern due to possible toxicity, or alternatively, changes in vine and fruit quality may occur due to cumulative application over many years. Initial work on molybdenum nutrition in grapevine by Gridley (2003) indicated that toxic amounts of molybdenum may have occurred amongst vines grown on rootstocks. This was deemed plausible due to the reduced yield response amongst treated vines grown on rootstocks with adequate molybdenum levels when compared to vines grown on own roots. There are limited reports of molybdenum toxicity occurring in plants. Lyon and Beeson

(1948) demonstrated that tomatoes grown with molybdenum at 100 mg/L showed a reduction in both plant fresh and dry weights and an overall reduction in fruit size. Defining molybdenum toxicity is difficult as the mechanism of action, if any, is unknown. It has been shown that excess molybdenum when applied to plants will result in its accumulation in specific plant parts possibly to toxic levels or quantities that initiate other responses in the plant including changes to N nutrition and ABA synthesis (Pasricha et. al., 1977). Although this current study did not involve the use of rootstocks where yield responses were previously shown to be subdued (Gridley, 2003), it was shown that there was no cumulative negative effect on yield with successive molybdenum sprays (treatment 1). This is an important finding as many viticulturists use molybdenum sprays over successive seasons that may result in accumulation of molybdenum within the plant. Molybdenum levels in petioles measured at the 50 – 80 % flowering stage showed higher levels of molybdenum relative to the water sprayed plants. Interestingly, suspension of molybdenum application in the second year of treatment 2 returned petiole molybdenum levels to those of the molybdenum deficient or control sprayed plants (Fig 5.15 and 5.16). This suggests the supply of molybdenum in a current season will remain localised in the canopy and possibly not retranslocate and accumulate elsewhere in the plant (root system, trunk, cordon). Unfortunately due to the commercial nature of the trial site, I was unable to physically destroy the plants to quantify molybdenum levels in the woody (trunk and cordon) and root tissues. Alternatively, if accumulation did occur in the mature tissues, retranslocation of molybdenum back to developing canes may not be possible in Merlot.

Evidence of molybdenum retranslocation in plants is limited. Previous work by Phillips (2004) investigated the translocation of foliar applied molybdenum on the leaves of pot grown vines within a greenhouse. It was shown that the largest pools of accumulated molybdenum were found in the old wood, while the highest concentration of molybdenum was in the new roots of Merlot grown on own roots. This indicated that Merlot translocated foliar applied molybdenum basipetally over a single growing season. Similar experiments were also conducted on Merlot grown on 2 rootstocks which also accumulated molybdenum in the old wood and new roots, but in substantially different proportions when compared to Merlot grown on own roots. Translocation patterns differed somewhat compared to vines grown on own roots with translocation of molybdenum occurring acropetally (Phillips, 2004). In *Vigna mungo*, molybdenum translocation appears to respond to molybdenum nutrition levels, where when sufficient, molybdenum moves to growing regions of the plant but remains localised under molybdenum deficiency



Jongruaysup et. al. (1994). The authors concluded that molybdenum had varying levels of phloem mobility that was based on the molybdenum nutritional status of the plant.

#### **5.4.2 Petiole nutrient profiles**

Petiole sulfate levels was of particular interest in this study due to previous work implicating sulfate in suppressing molybdate absorption (Stout et. al., 1951; Pasricha et. al., 1977). However, statistical analysis revealed no interaction between the effects of molybdenum treatment and sulfate content (Figure 5.17 and 5.18).

Total N levels are low within petiole tissue and a distinct pattern of fluctuation was measured over the years with levels decreasing in year 2 before increasing slightly in year 3 (Figure 5.19 and 5.20). Similar fluctuation was also measured in various other nutrients including, copper (Figure 5.21 and 5.22), iron, magnesium, phosphorous, and sodium (Appendix 3). Although nitrate-N was not measured, previous studies at this site revealed high levels within petioles (Gridley, 2003). Accumulation of nitrate pools has been shown to occur in other plant species that are deficient in molybdenum including bean (Vieira et. al., 1998a; Vieira et. al., 1998b) and wheat (Yu et. al., 1999). Molybdenum treatments did not consistently increase total-N content of petioles where as other studies have measured an increase in total N with the application of molybdenum (Adams et. al., 1990).

Boron and zinc are important requirements for fruit set and both have been implicated with variability in berry size and shot berry formation (Sharma et. al., 1995). It is possible that previous observations of molybdenum deficiency phenotypes may have been improperly diagnosed for zinc and boron deficiency due to the similarities in bunch phenotype. This was further compounded due to the difficulties in detecting molybdenum in plant tissues. In this study, the levels of both boron and zinc were found to be adequate even though levels did decline in year two however the decline was not found to be significant (Figure 5.25, 5.26, 5.27 and 5.28). Boron as a foliar spray has been investigated for its ability to increase fruit set in Hazelnut, however it was found that boron did not increase fruit set but only increased nut and kernel mass (Silva et. al., 2003).

Differences in the nutrient content between clones were found for molybdenum (Table 5.4), sulfate (Table 5.5), total nitrogen (Table 5.7), potassium (Table 5.10) boron (Table 5.12), sodium (Appendix 3), calcium (Appendix 3), and phosphorous (Appendix 3). Previous research by Gridley (2003) also demonstrated difference between the clones of

Merlot at this site. Similar trends were seen between this study and Gridley's (2003) study in terms of certain clones having higher levels of certain nutrients than others. However, within this study different trends occurred in terms of clone superiority and it is difficult to determine one superior clone in terms of its ability to acquire nutrients.

#### **5.4.3 Yield and yield component responses in relation to foliar application of molybdenum**

Though control vines were deficient in molybdenum (Figure 5.15 and 5.16) foliar application of molybdenum did not result in yield increases in Merlot despite the results of previous studies (Gridley, 2003; Williams et. al., 2004; Kaiser et. al., 2005). However it was observed that there was a small incidence of 'hen and chicken' within the vineyard. Unfortunately other tests that may have assisted in confirmed actual molybdenum deficiency such as nitrate reductase assays were not performed. However, future work should include this analysis to provide further evidence of molybdenum deficiency. The only effect of molybdenum stimulating yield was in year 1 with D3V14. Though it appears that molybdenum increased yield, the yield of the D3V14 control is actually lower than all other clones, which suggests that a yield increase may not have occurred. There are other corresponding increases in any of the other yield components to suggest that molybdenum did in fact increase yield in this clone. The only other yield increase in the trial was in year 3 clone Q45-14 (treatment 1) where there was approximately a 50% increase in yield compared to the control. This was the result of an increase in bunch weight (Figure 5.6) berries per bunch (Figure 5.7), and rachis weight (Figure 5.9). Despite the lack of yield response in year 1 the trial was not modified for a number of reasons. Firstly, this was a commercial site where the grapes are sold to winery's for wine production. Changing the trial, such as increasing the dosage or frequency of sprayings may have affected the yield or grape quality adversely, as it is not known how grapevines respond to large doses of molybdenum. Increasing the quantities of micronutrients may be dangerous to the plant health and lead to toxicity effects. Secondly, the trial was designed to represent the molybdenum spraying regimes of viticulturists, thus allowing measurements of the cumulative affects of molybdenum sprays. The fruit set in Q45-14 was also slightly elevated, through this was not significant (Figure 5.3). Other reports have implicated an increase the number of 5-15 mm coloured berries by increasing the percent of berries with functional seeds (Williams et. al., 2004) and suggest that molybdenum application affected pollination/fertilization and therefore berry development. Previously fruit set has been implicated in increasing yields in Williams et. al. (2003) however this was not shown to be

the cause of yield increase in Gridley's (2003) study. Overall, there was a net drop in yields over the 3-year trial period irrespective of treatment. This may be due to a reduction in rainfall over this time (Figure 5.10).

This study has highlighted the importance to growers, that molybdenum sprays may not be as effective as previously thought under certain growing conditions. The incidence of drought is likely to have limited yield increases in this study (Figure 5.10). Previously it has been demonstrated that vines must be deficient in molybdenum in order for increases in yield to be achieved. Clearly, at this site this is not the case, as these vines were deficient and no consistent increase in yield was measured. However important parameters such as climate, soil structure, soil temperature and soil pH should also be considered when deciding to apply molybdenum as a foliar spray in a vineyard. This field site had higher soil pH, and potentially higher temperatures compared to other field sites that similar experiments are conducted. The soil type at this site is very different to other studies that have associated yield increases in molybdenum deficient Merlot. The soil at this site is a Black Vertosol (cracking clay) with a pH of 6.5-7 (Appendix 4) in contrast to the fine sandy loam soils that exist at both sites where Gridley (2003) and Williams et. al., (2004) conducted their trials. Traditional sites that are used for these studies are cooler eg cool wet springs and have more acidic soils (Gridley, 2003; Williams et. al., 2003; Williams et. al., 2004). Therefore, molybdenum levels within petioles may not be as a robust predictor and the only predictor of the potential for yield increase in Merlot as previously indicated. Molybdenum sprays may not be the answer to achieving yield increases in certain instances and each site should be examined closely before this method is used.

#### **5.4.4 Berry quality parameters**

As many winemakers will grade fruit on the levels of total soluble solids, pH or anthocyanins and phenolics it was imperative to determine if the application of molybdenum within the vineyard adversely affected these parameters (Figure 5.11, 5.12, 5.13 and 5.14). Adverse effects of spray may not only affect eventual wine quality, but also price for growers. Molybdenum application appears to have no effect on the quality parameters associated with grape berry juice. Again, there was little difference between the clones as previously reported by Gridley (2003) and it is difficult to determine a superior clone in terms of colour, sugar and pH.

**Table 5.2 Table of vineyard trial site and spray regime imposed.**

Vines received either a foliar application of molybdate or a control (water) spray. Within each panel, there are 4 vines planted in randomised design and include D3V14, 6R, 8R and Q45-14. NT=no treatment, C=control, T1=Treatment 1, T2=Treatment 2, and T3=Treatment 3.

Panel Number	Treatment	Year		
		Year 1 2003/2004	Year 2 2004/2005	Year3 2005/2006
1	NT			
2	NT			
3	NT			
4	T3	No spray	Spray Mo	Spray Mo
5	T3	No spray	Spray Mo	Spray Mo
6	C	H <sub>2</sub> O spray	H <sub>2</sub> O spray	H <sub>2</sub> O spray
7	C	H <sub>2</sub> O spray	H <sub>2</sub> O spray	H <sub>2</sub> O spray
8	T1	Spray Mo	Spray Mo	Spray Mo
9	NT			
10	NT			
11	T3	No spray	Spray Mo	Spray Mo
12	C	H <sub>2</sub> O spray	H <sub>2</sub> O spray	H <sub>2</sub> O spray
13	NT			
14	NT			
15	NT			
16	C	H <sub>2</sub> O spray	H <sub>2</sub> O spray	H <sub>2</sub> O spray
17	NT			
18	T1	Spray Mo	Spray Mo	Spray Mo
19	T2	Spray Mo	No Spray	No spray
20	NT			
21	T1	Spray Mo	Spray Mo	Spray Mo
22	NT			
23	C	H <sub>2</sub> O spray	H <sub>2</sub> O spray	H <sub>2</sub> O spray
24	T3	No spray	Spray Mo	Spray Mo
25	T2	Spray Mo	No Spray	No spray
26	NT			
27	NT			
28	C	H <sub>2</sub> O spray	H <sub>2</sub> O spray	H <sub>2</sub> O spray
29	T1	Spray Mo	Spray Mo	Spray Mo
30	NT			
31	T2	Spray Mo	No Spray	No spray
32	T2	Spray Mo	No Spray	No spray
33	T1	Spray Mo	Spray Mo	Spray Mo
34	T1	Spray Mo	Spray Mo	Spray Mo
35	T3	No spray	Spray Mo	Spray Mo
36	T2	Spray Mo	No Spray	No spray
37	NT			
38	T2	Spray Mo	No Spray	No spray

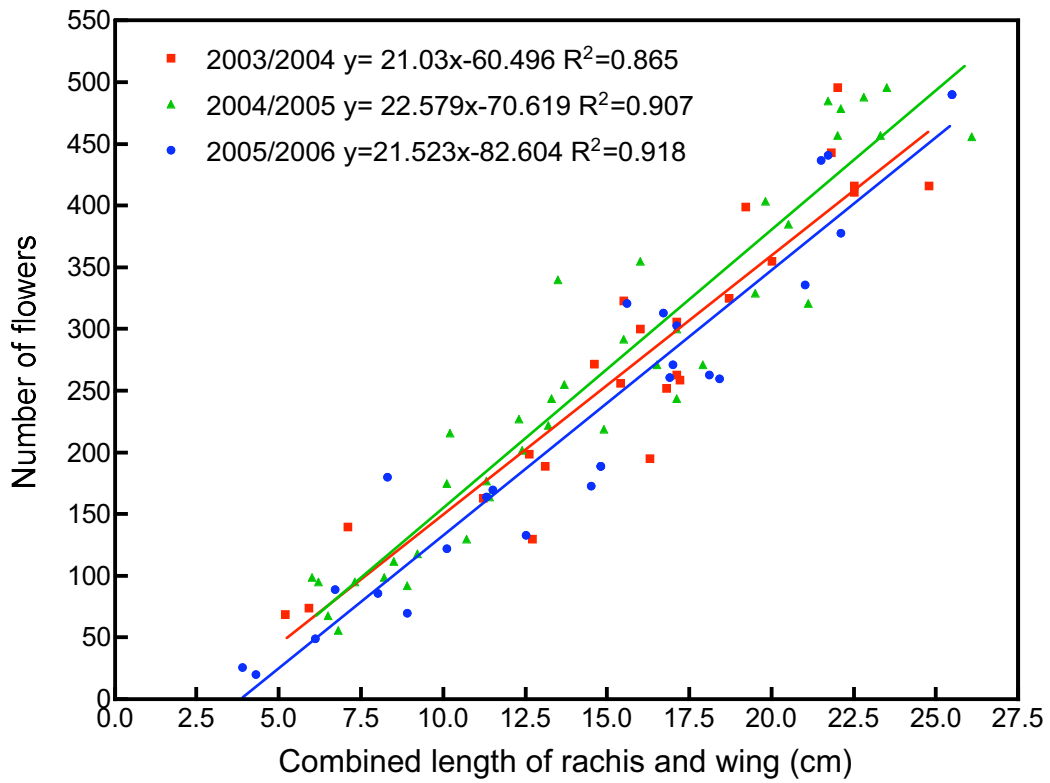


**Figure 5.2. Regression analysis to determine number of flowers per inflorescence.**

Regression analysis of each year gave a line of best fit with  $R^2$  values of 0.865, 0.907 and 0.918 for 2003/2004, 2004/2005 and 2005/2006 respectively.

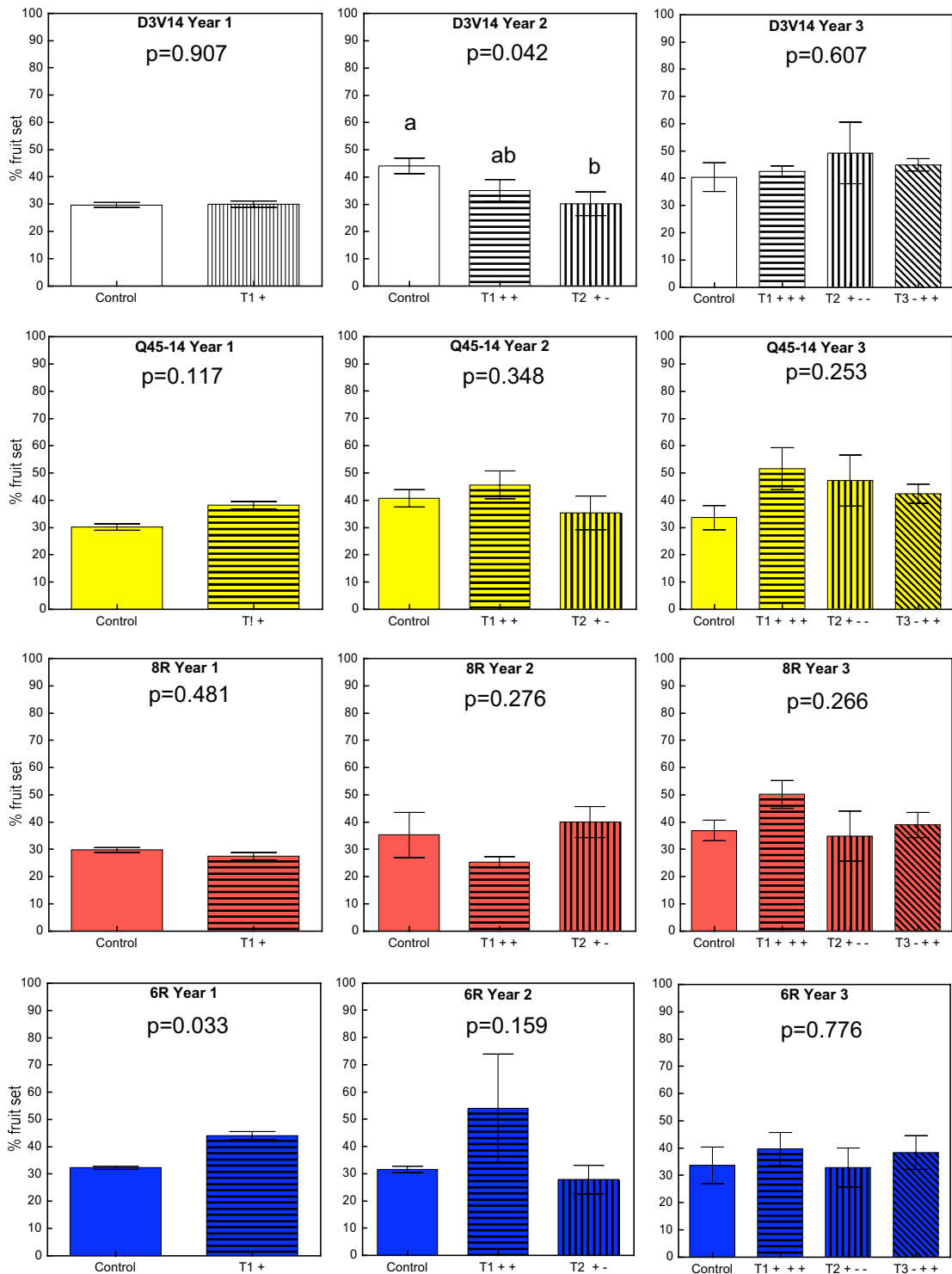


**Figure 5.3 Mean % fruit set over the 3 year trial period for the 4 clones.**

Mean % fruit set was calculated by determining the number of flowers per inflorescence using regression analysis at flowering and counting the number of berries per bunch at harvest. See section 5.2.1 or table 5.1 for detailed information about the treatments. Statistical comparisons are only appropriate for each clone within each year Results with the same letter are not significantly different. Values are mean  $\pm$  SEM (n=3 vines).

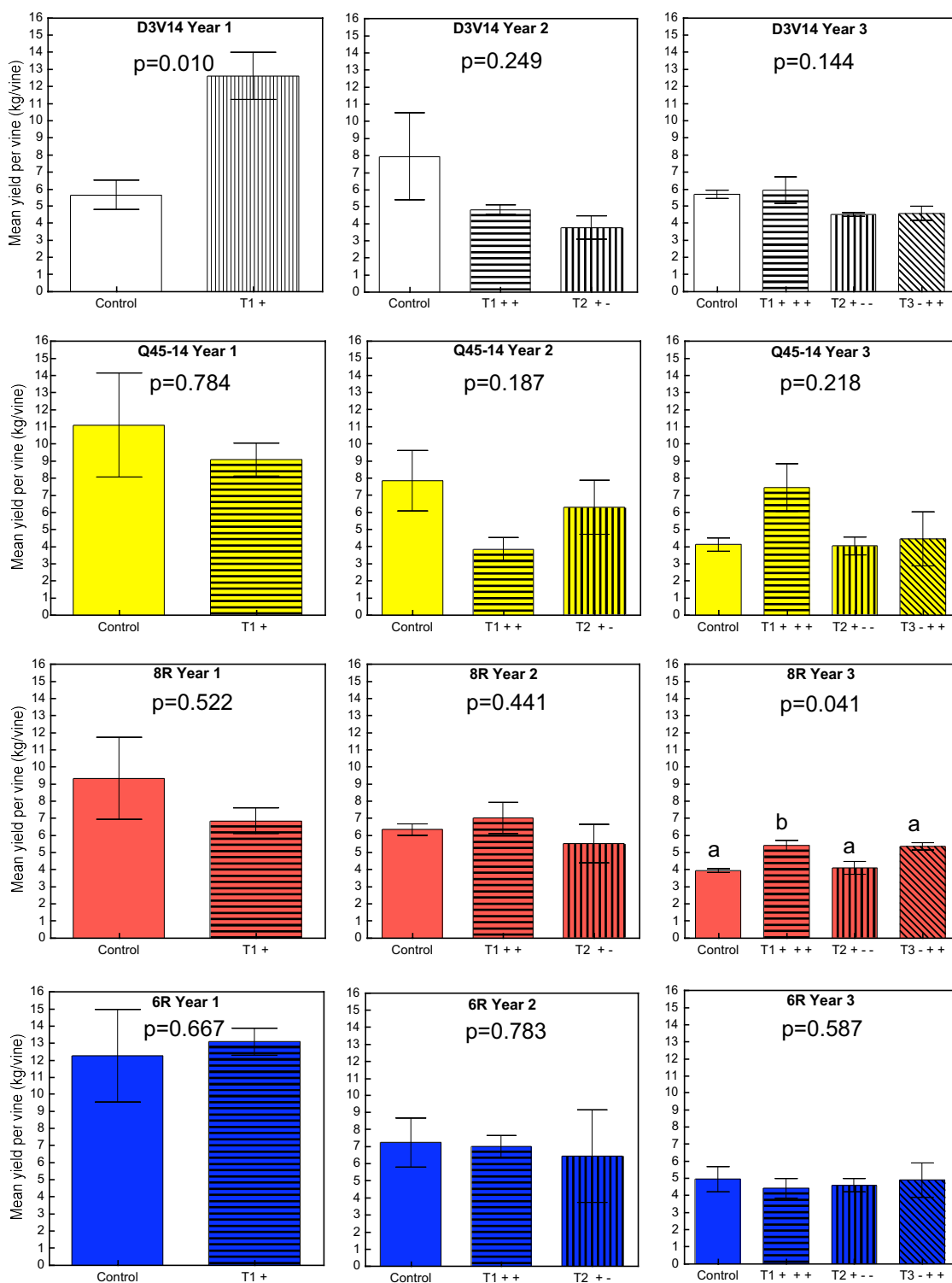


**Figure 5.4 Mean yield per vine (kg/vine) over the 3 year trial period for the 4 clones.**

Yield was calculated on a per vine basis by counting the number of bunches per vine and multiplying by the mean bunch weight. See section 5.2.1 or Table 5.1 for detailed information about the treatments. Statistical comparisons are only appropriate for each clone within each year. Results with the same letter are not significantly different. Values are mean  $\pm$  SEM (n=3 vines).

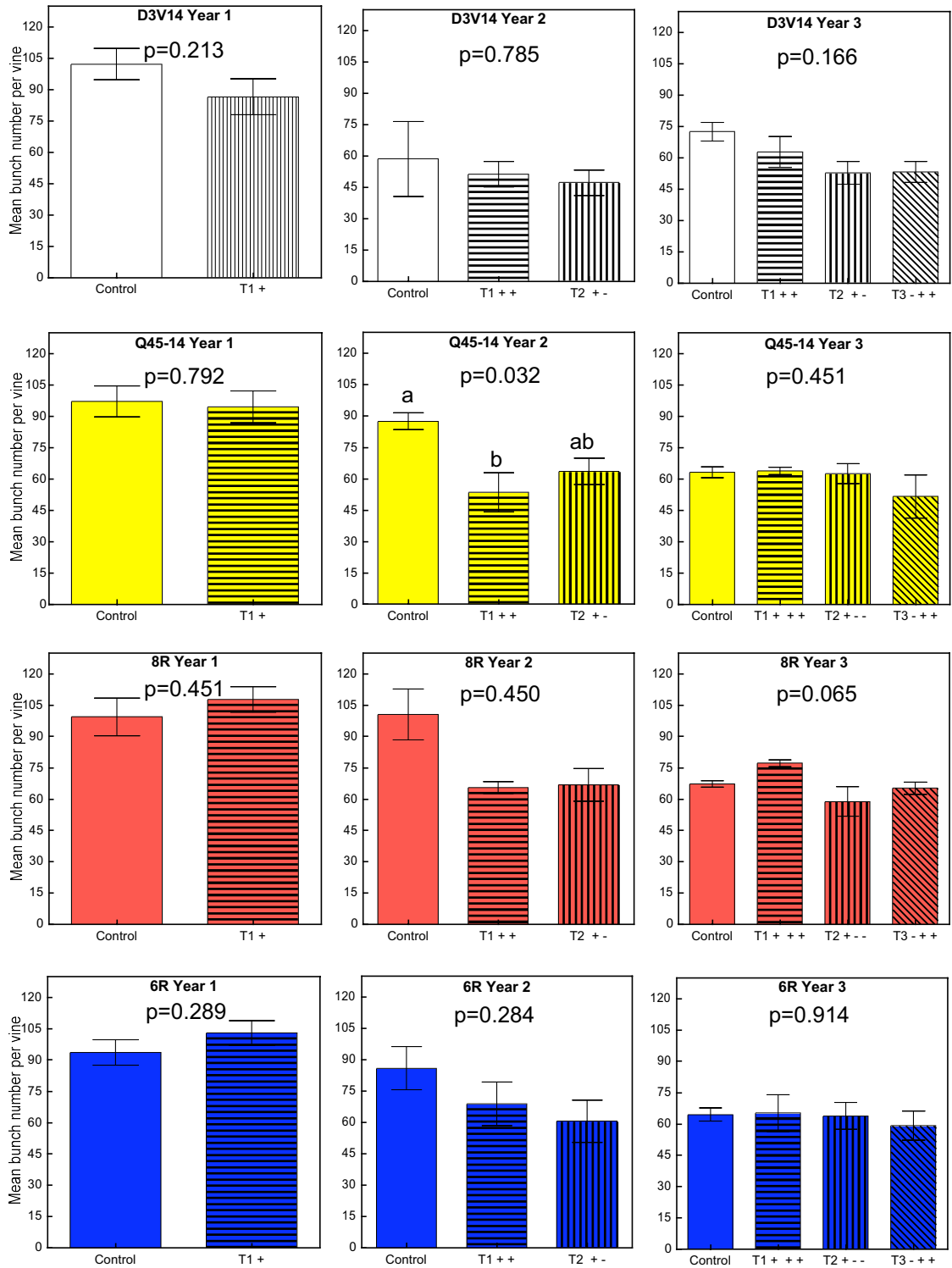


**Figure 5.5 Mean bunch number per vine over the 3 year trial period for the 4 clones.** The total number of bunches were counted on each vine at harvest. Vines in year 1 T1 +Mo received a foliar application or a control H<sub>2</sub>O spray. See section 5.2.1 or Table 5.1 for detailed information about the treatments. Statistical comparisons are only appropriate for each clone within each year. Results with the same letter are not significantly different. Values are mean ± SEM (n=3 vines).



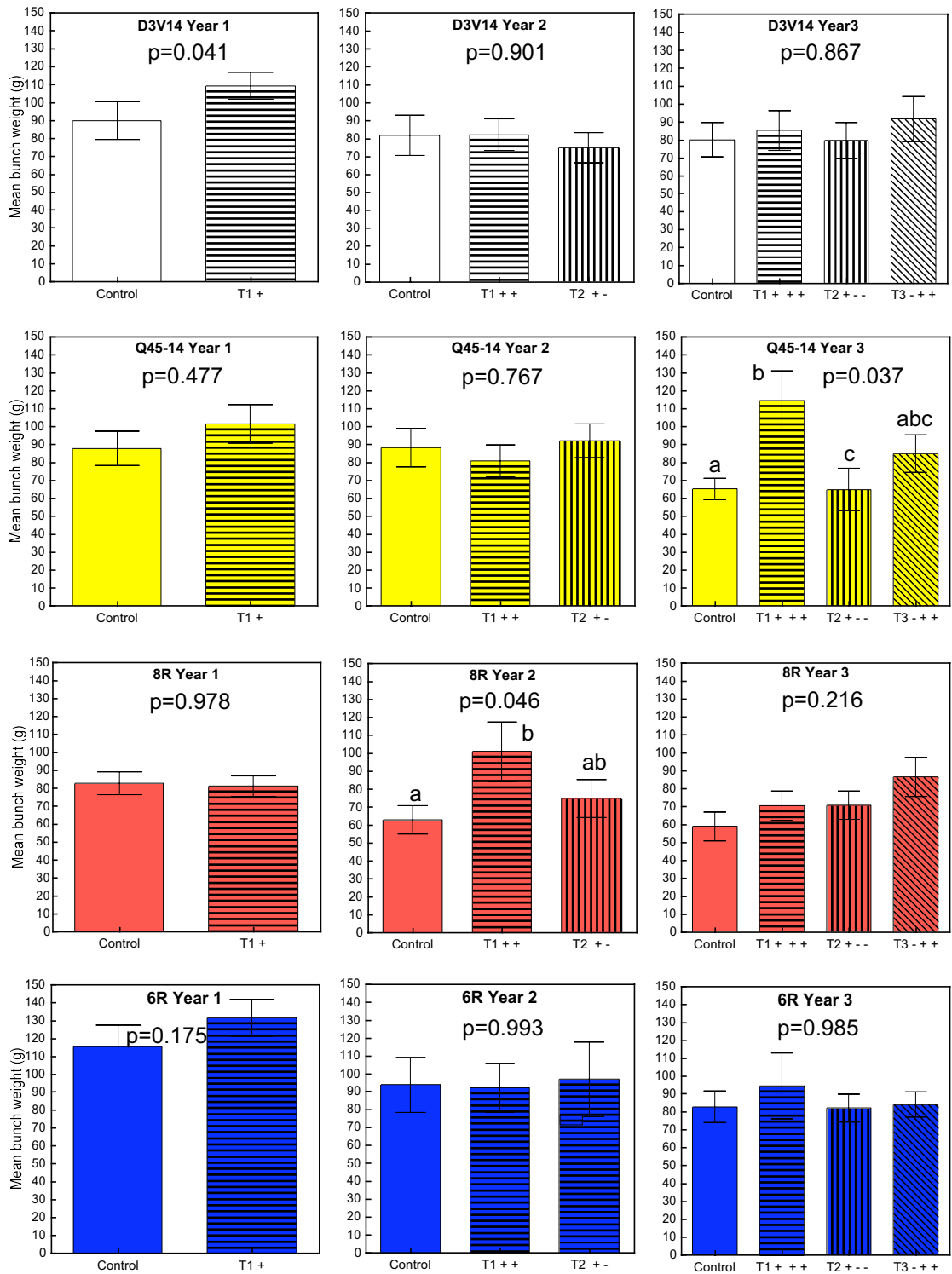


**Figure 5.6 Mean bunch weight (g) over the 3 year trial period for the 4 clones.**

A random samples of bunches were collected at harvest and weighed. See section 5.2.1 or Table 5.1 for detailed information about the treatments. Statistical comparisons are only appropriate for each clone within each year. Results with the same letter are not significantly different. Values are mean  $\pm$  SEM (n=12-27 bunches).

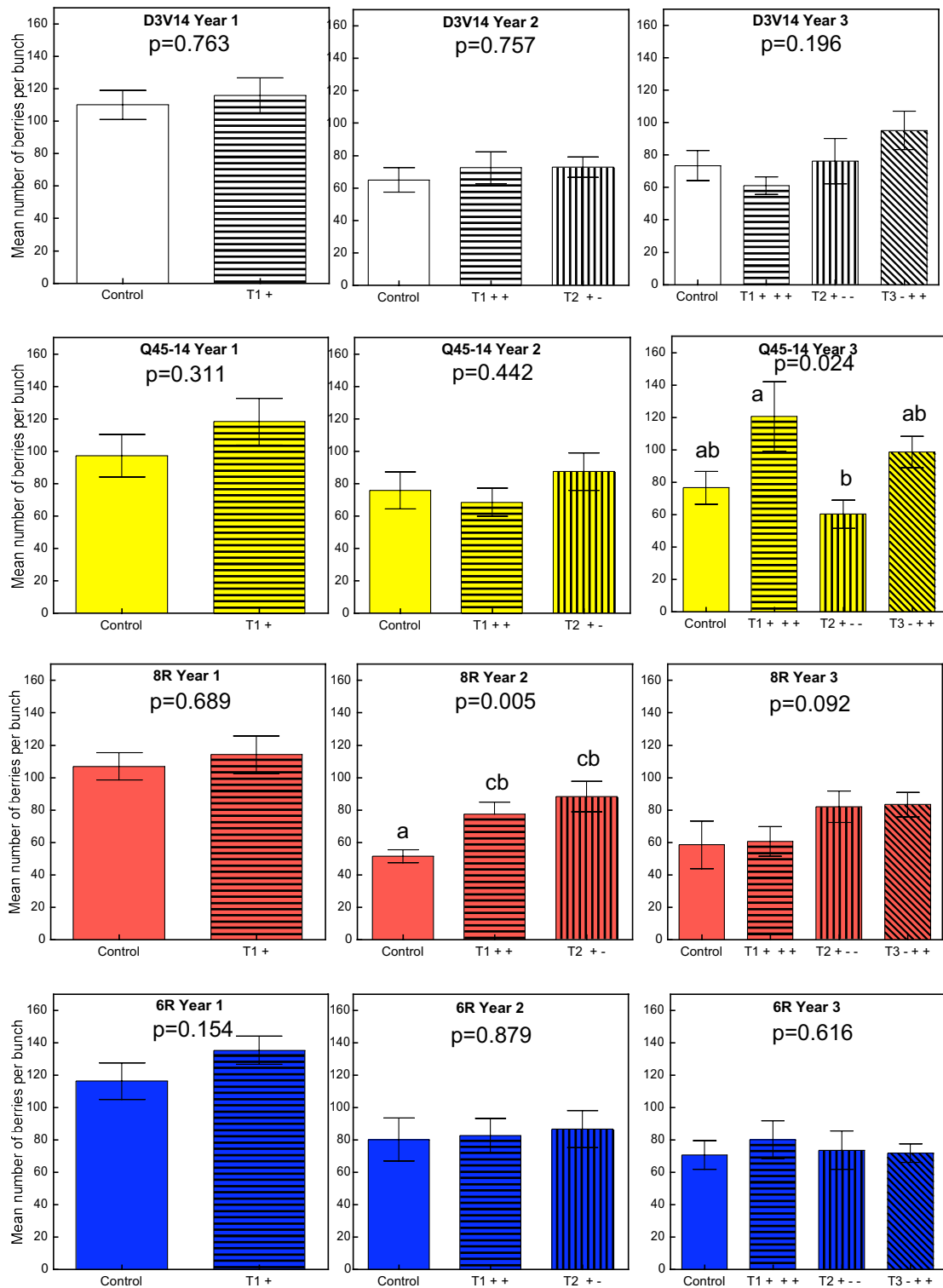


**Figure 5.7 Mean berry number per bunch over the 3 year trial period for the 4 clones.**

Berries were counted on randomly selected bunches at harvest. See section 5.2.1 or Table 5.1 for detailed information about the treatments. Statistical comparisons are only appropriate for each clone within each year. Results with the same letter are not significantly different. Values are mean  $\pm$  SEM (n=9-12 bunches).

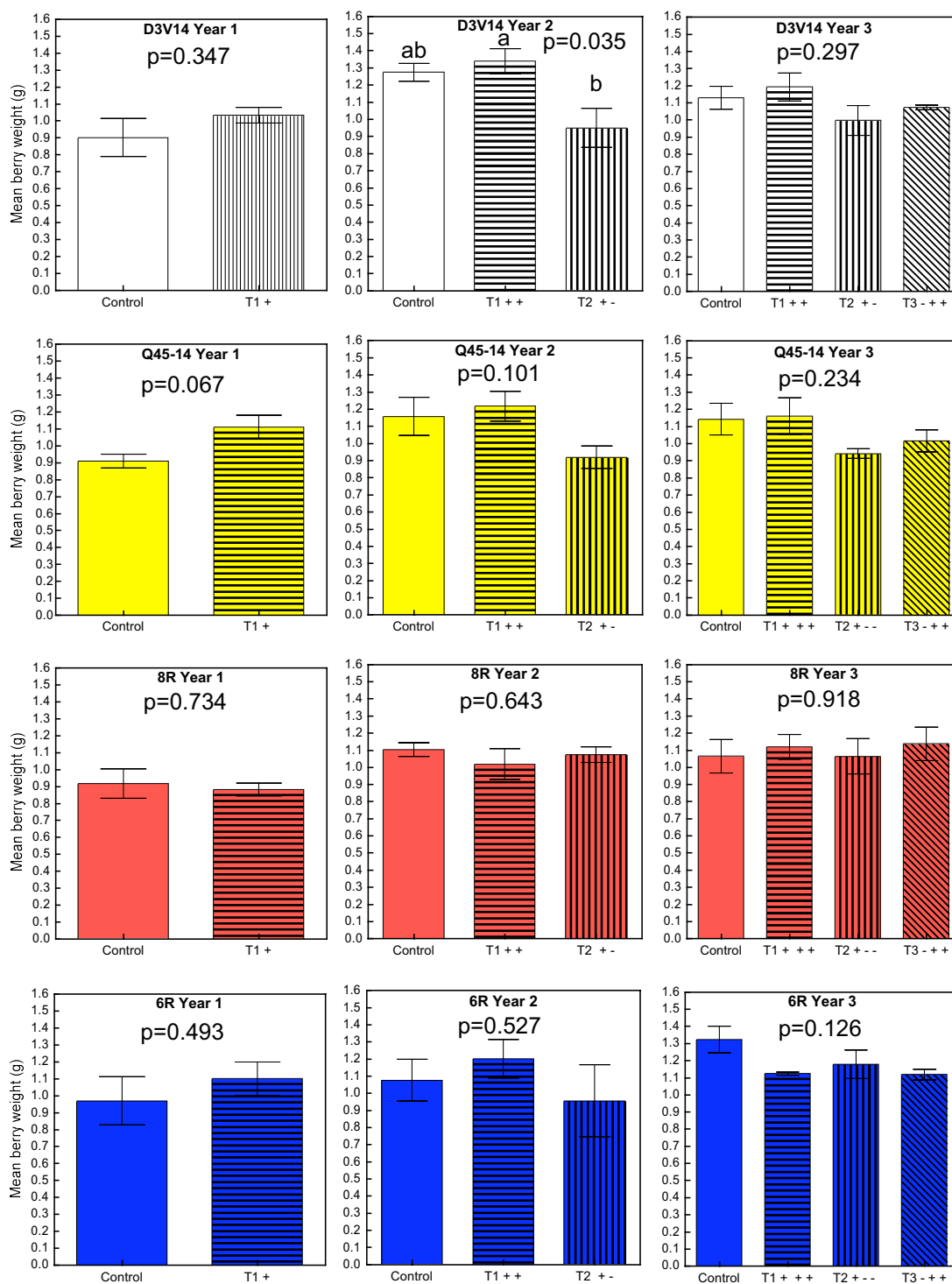


**Figure 5.8 Mean berry weight (g) over the 3 year trial period for the 4 clones.**

Berries were weighed at harvest. See section 5.2.1 or Table 5.1 for detailed information about the treatments. Statistical comparisons are only appropriate for each clone within each year. Results with the same letter are not significantly different. Values are mean  $\pm$  SEM (n=100-150 berries).

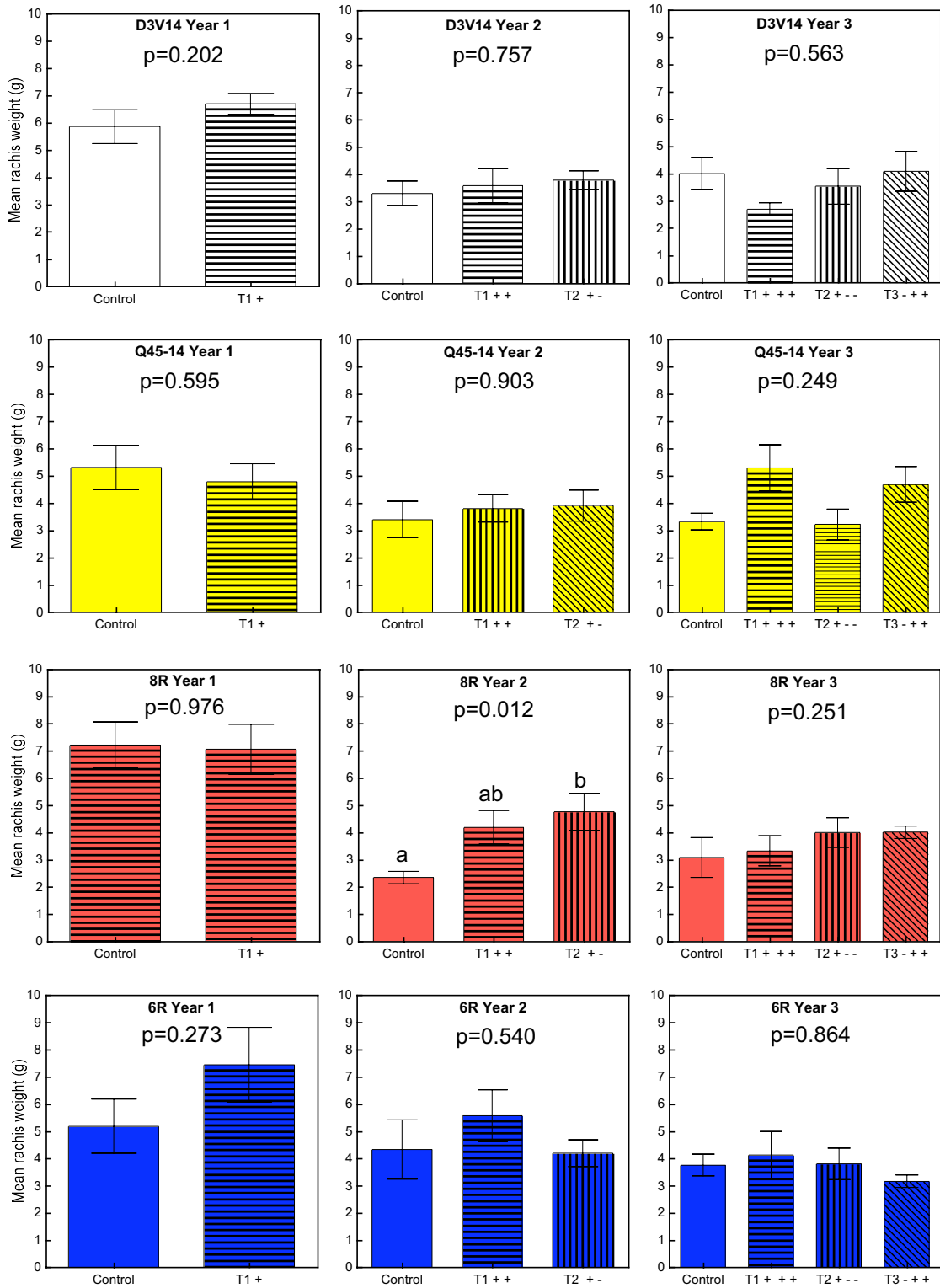


**Figure 5.9 Mean rachis weight (g) over the 3 year trial period for the 4 clones.**

Rachis's were weighed at harvest. See section 5.2.1 or Table 5.1 for detailed information about the treatments. Statistical comparisons are only appropriate for each clone within each year. Results with the same letter are not significantly different. Values are mean  $\pm$  SEM (n=9-12 rachis).

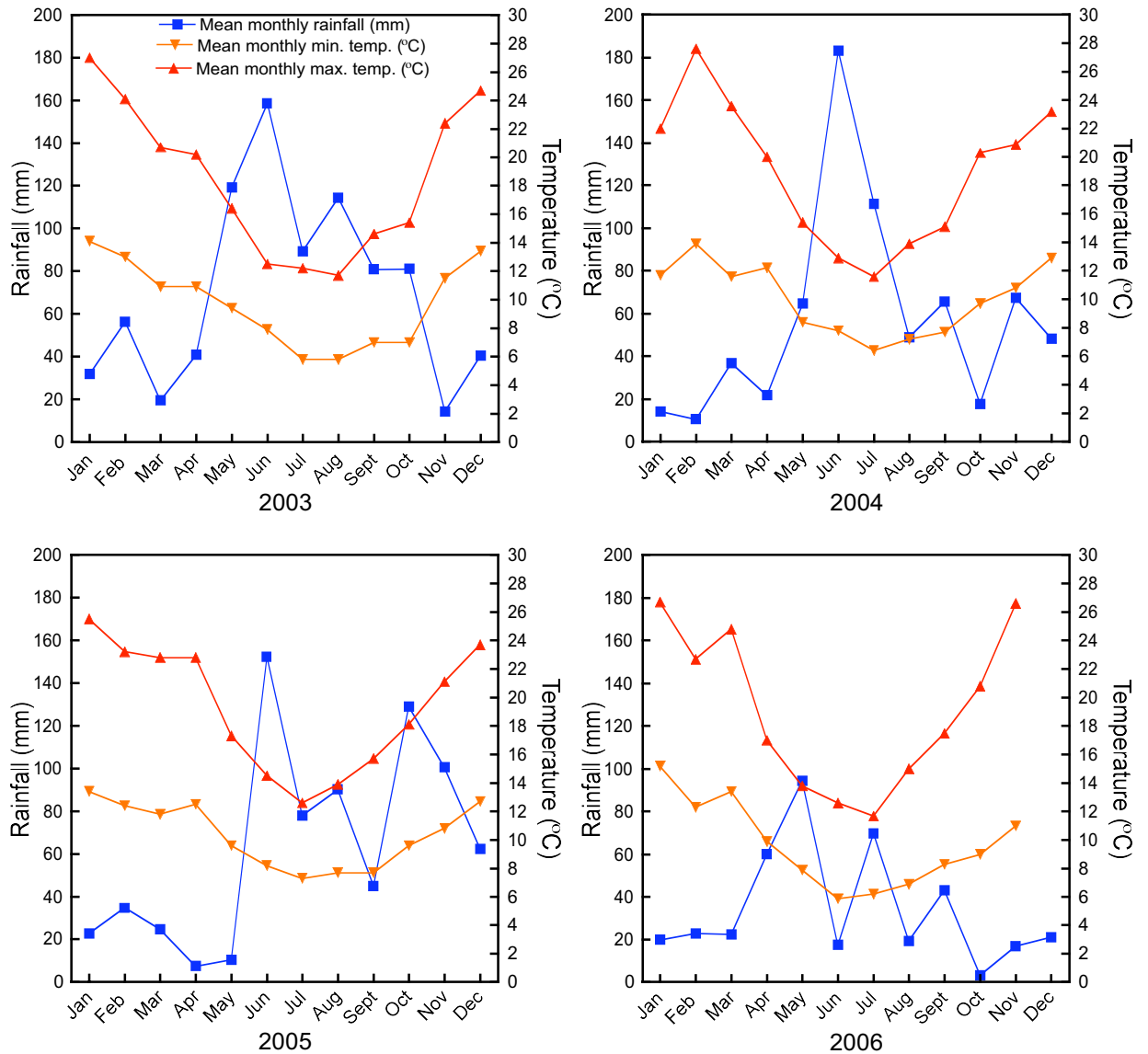


**Figure 5.10 Mean monthly minimum, maximum and rainfall for years 2003 to 2006.**

Data was obtained from the Bureau of Meteorology and from the closest weather station to McLaren Vale.

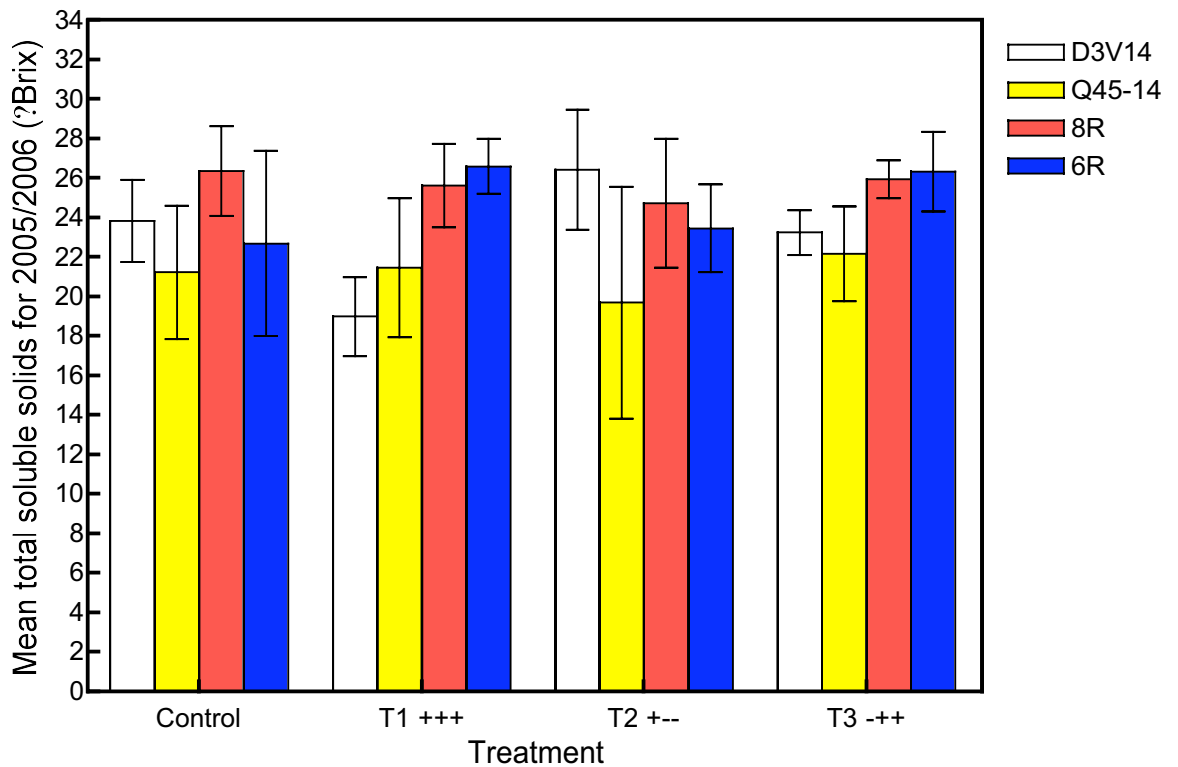


**Figure 5.11 Mean harvest total soluble solids (°Brix) from the 2005/2006 growing season.**

Fifty berries were collected at harvest from the varying clones and treatments and total soluble solids measured. See section 5.2.1 or table 5.1 for detailed information about the treatments. Values are mean  $\pm$  SEM (n=3 x 50 random samples of berries).

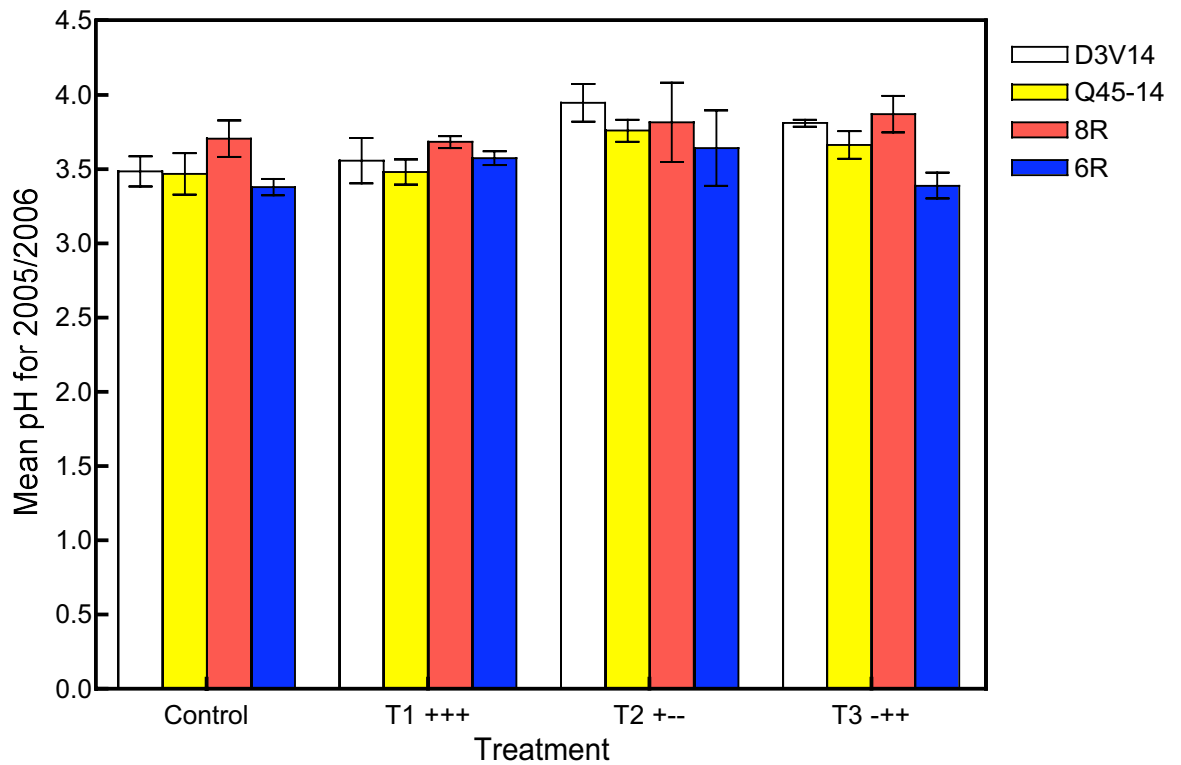


**Figure 5.12 Mean harvest pH from the 2005/2006 growing season.**

Fifty berries were collected at harvest from the varying clones and treatments and pH measured. See section 5.2.1 or table 5.1 for detailed information about the treatments. Values are mean  $\pm$  SEM (n=3 x 50 random samples of berries).

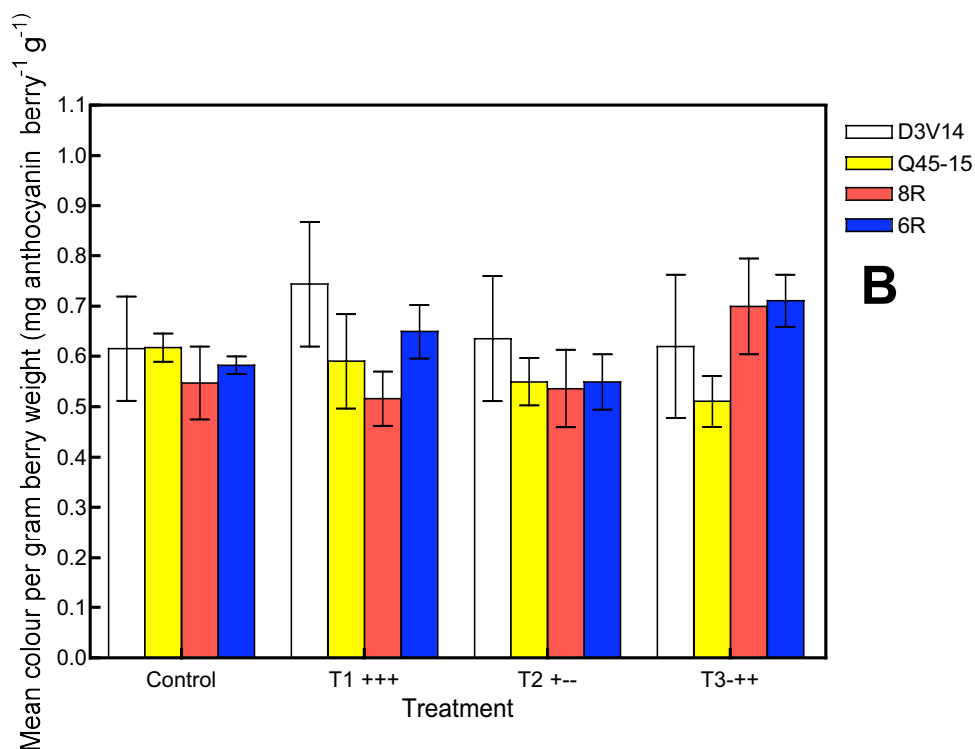
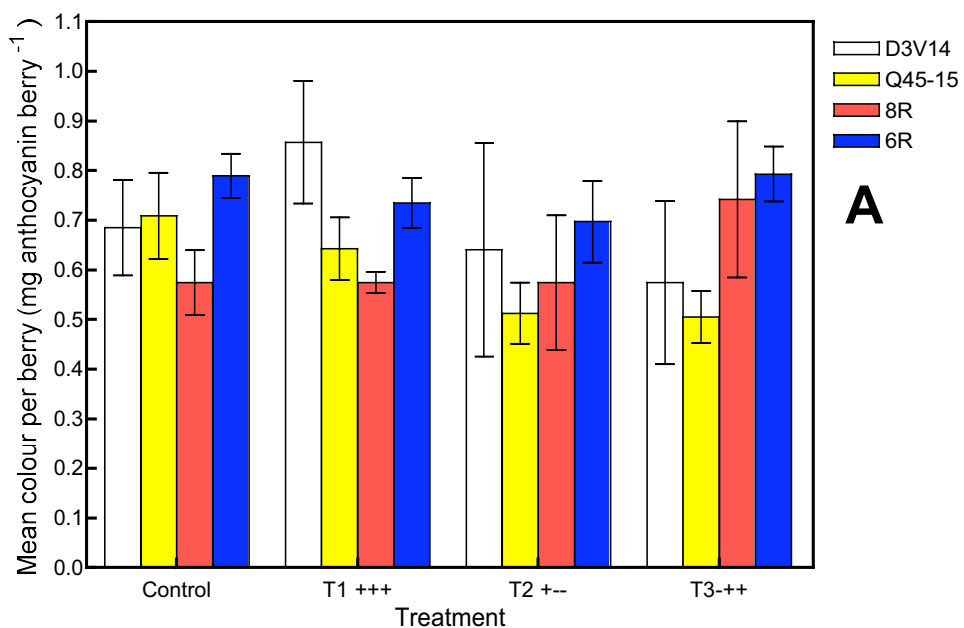


**Figure 5.13 Colour or anthocyanin (malvidin-3-glucose) of berries at harvest in 2005/2006 after 3 years of different molybdenum treatments.**

**A.** Colour per berry (mg anthocyanin berry<sup>-1</sup>) after 3 years various molybdenum sprays. **B.** Colour per gram berry weight (mg anthocyanin berry<sup>-1</sup> g<sup>-1</sup>) after 3 years of various molybdenum sprays. See section 5.2.1 or table 5.1 for detailed information about the treatments. Values are mean  $\pm$  SEM (n=3 x 50 random samples of berries).



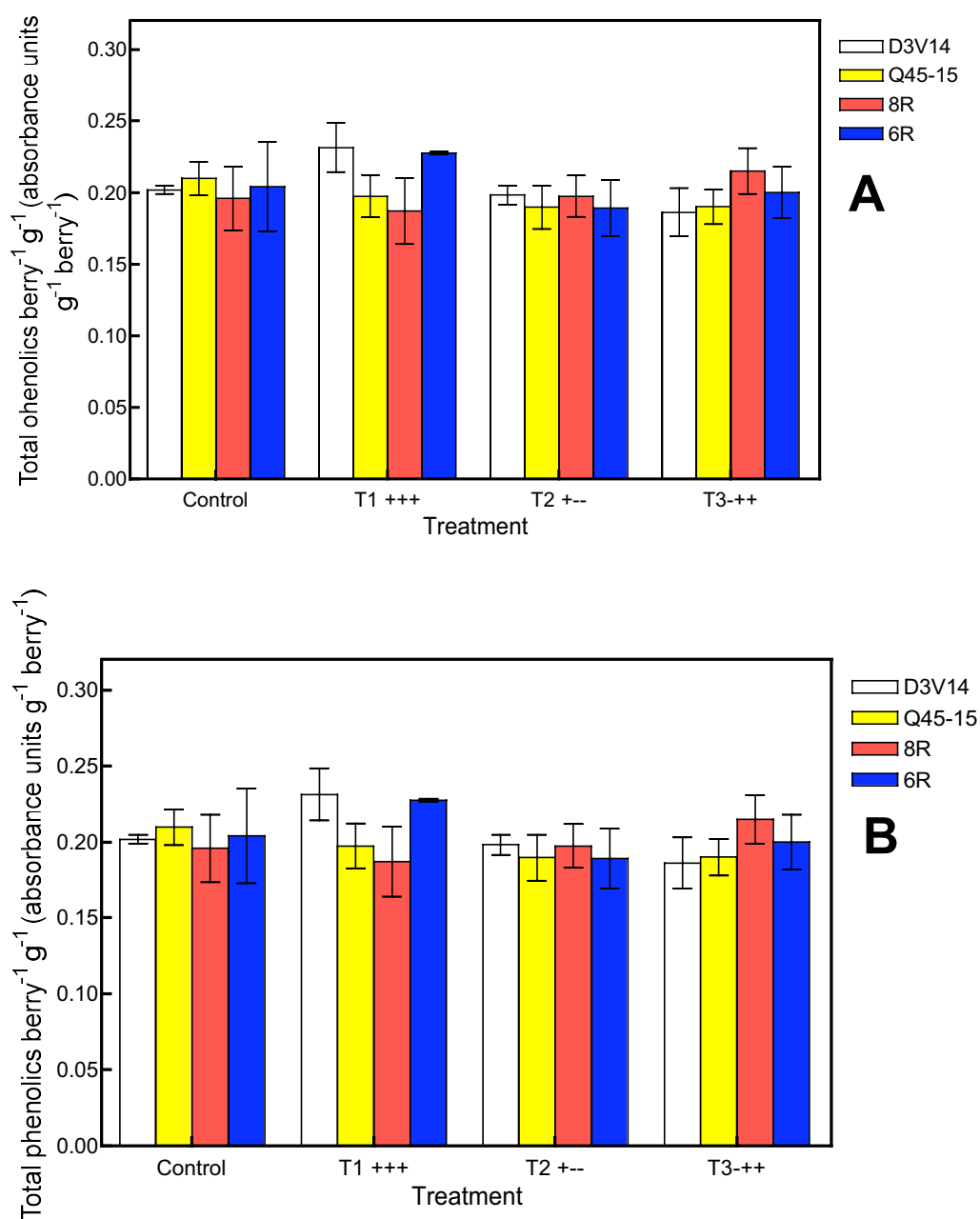


**Figure 5.14 Total phenolics of berries at harvest in 2005/2006 after 3 years of different molybdenum treatments.**

**A.** Total phenolics per berry (absorbance units berry<sup>-1</sup>) after 3 years various molybdenum sprays. **B.** Total phenolics per gram berry weight (absorbance units g<sup>-1</sup> berry<sup>-1</sup>) after 3 years of various molybdenum sprays. See section 5.2.1 or table 5.1 for detailed information about the treatments. Values are mean ± SEM (n=3 x 50 random samples of berries).

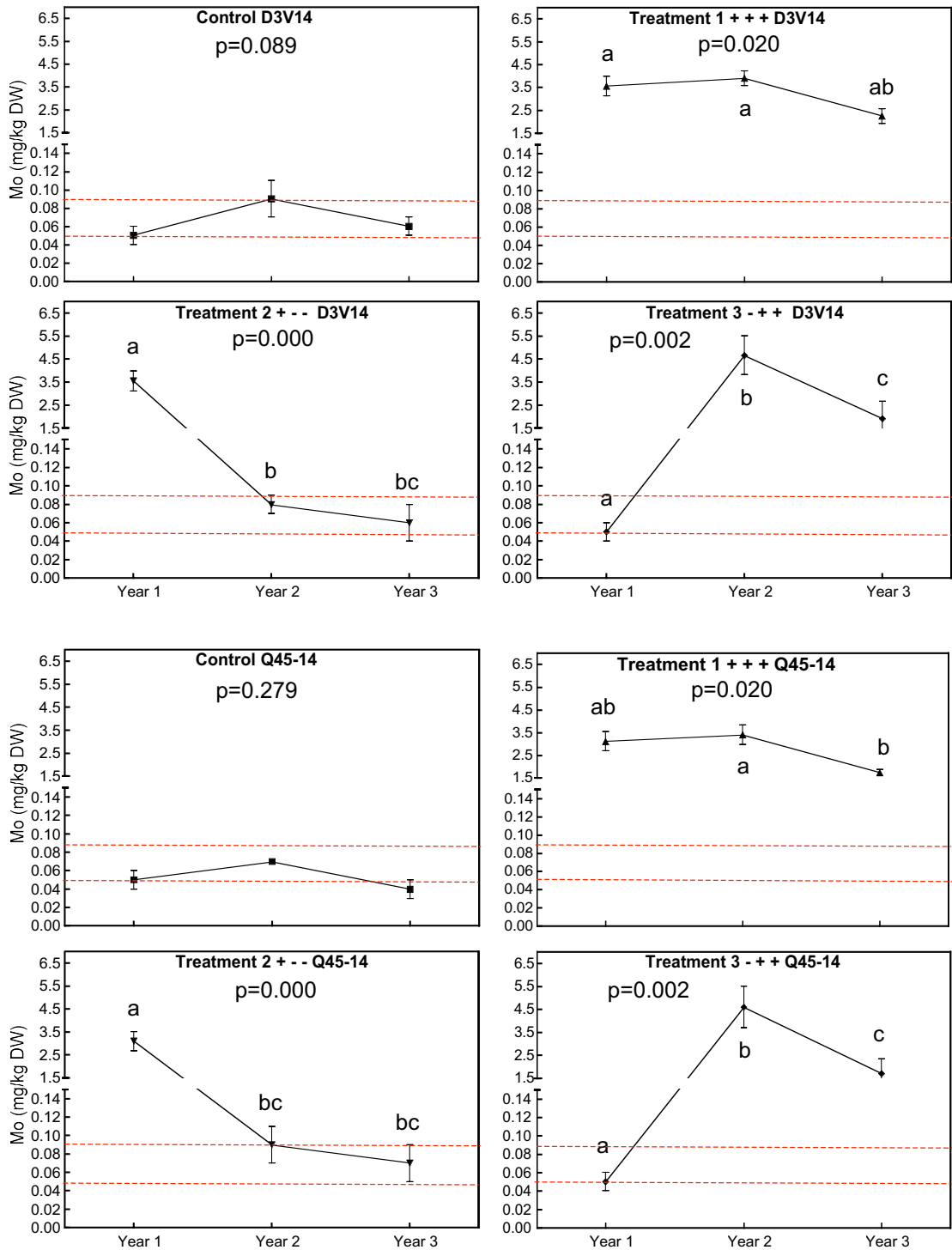


**Figure 5.15 Mean Mo (mg/kg) concentration in petioles at 50 – 80% flowering for clones D3V14 and Q45-14 over the 3 years of the trial. Suggested deficiency concentrations for molybdenum may occur between 0.05 – 0.09 mg/kg DW (Williams et. al., 2004).**

Values are mean ± SEM (n=3). Results with the same letter are not significantly different.

Dashed lines indicated where deficiency is thought to occur (Williams et. al., 2004).

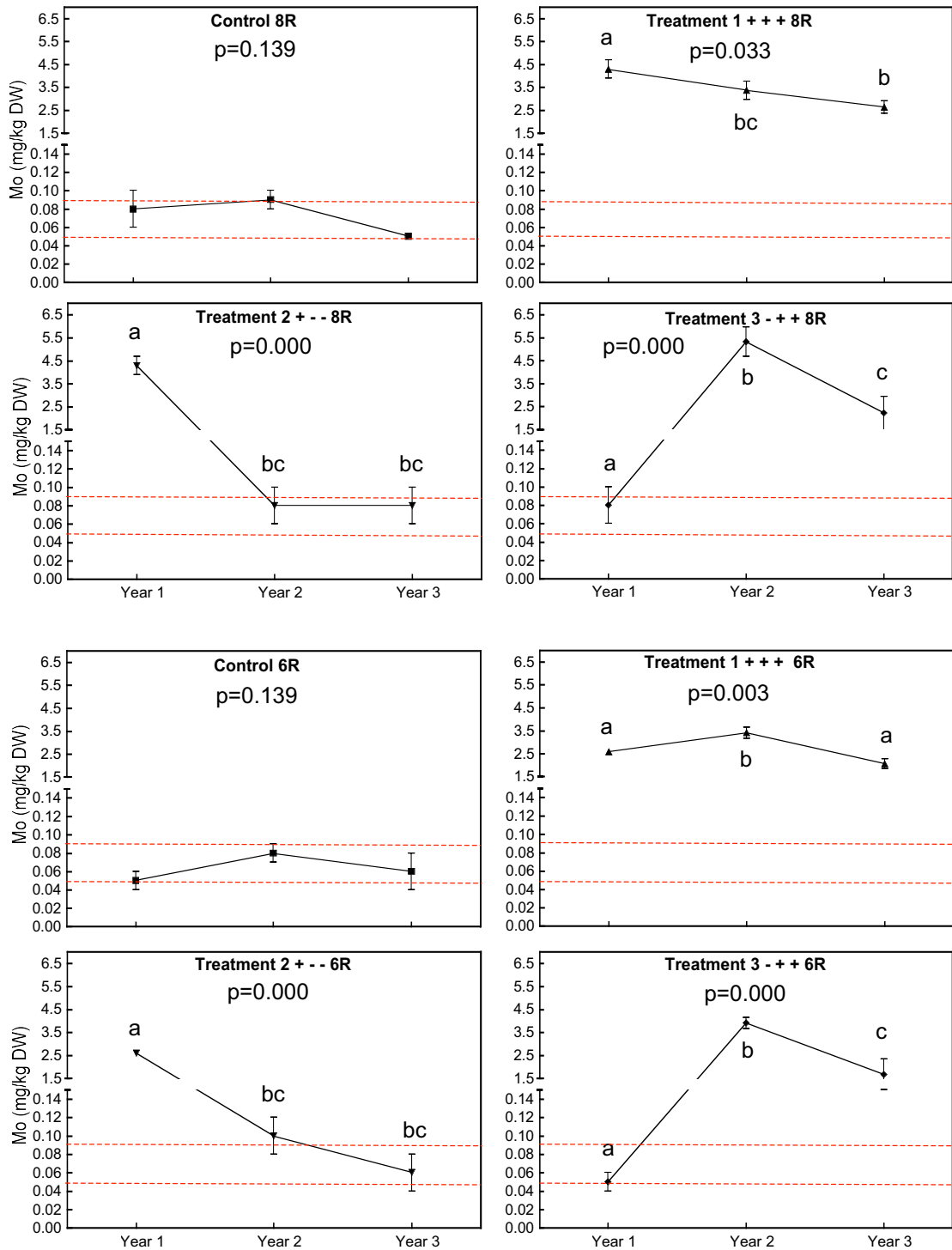


**Figure 5.16 Mean Mo (mg/kg) concentration in petioles at 50 – 80% flowering for clones 8R and 6R over the 3 years of the trial. Suggested deficiency concentrations for molybdenum may occur between 0.05 – 0.09 mg/kg DW (Williams et. al., 2004).**

Values are mean  $\pm$  SEM (n=3-4). Results with the same letter are not significantly different. Dashed lines indicated where deficiency levels are reached (Williams et. al., 2004).

**Table 5.3 Treatment differences between the treatments for molybdenum petiole concentrations in years 1, 2 and 3 of the trial.**

For example in year 1 for clone D3V14 there was a significant difference between the control and treatment 1 ( $p=0.0000$ ). Differences are at the 5% level and only significant data is presented.

<b>Year</b>	<b>Clone</b>	<b>Treatment X is significantly different to treatment Y</b>	<b>Treatment Y is significantly different to treatment X</b>	<b>P value (0.05 level)</b>	
<b>Year 1</b>	D3V14	Control	Treatment 1	0.000	
			Treatment 2	0.000	
		Treatment 1	Treatment 3	0.000	
		Treatment 2	Treatment 3	0.000	
		Q45-14	Control	Treatment 1	0.000
				Treatment 2	0.000
	Treatment 1		Treatment 3	0.000	
	8R	Control	Treatment 1	0.000	
			Treatment 2	0.000	
		Treatment 1	Treatment 3	0.000	
	6R	Control	Treatment 1	0.000	
			Treatment 2	0.000	
		Treatment 1	Treatment 3	0.000	
		Treatment 2	Treatment 3	0.000	
	<b>Year 2</b>	D3V14	Control	Treatment 1	0.000
Treatment 3				0.000	
Treatment 1			Treatment 2	0.000	
Treatment 2			Treatment 3	0.000	
Q45-14		Control	Treatment 1	0.002	
			Treatment 3	0.000	
		Treatment 1	Treatment 2	0.001	
		Treatment 2	Treatment 3	0.000	
8R		Control	Treatment 1	0.000	
			Treatment 3	0.000	
		Treatment 1	Treatment 2	0.000	
		Treatment 3	0.005		
6R		Control	Treatment 1	0.000	
			Treatment 3	0.000	
		Treatment 1	Treatment 2	0.000	
Treatment 2	Treatment 3	0.000			
<b>Year 3</b>	D3V14	Control	Treatment 1	0.003	
			Treatment 3	0.007	
		Treatment 1	Treatment 2	0.003	
		Treatment 2	Treatment 3	0.007	
	Q45-14	Control	Treatment 1	0.003	

			Treatment 3	0.003
		Treatment 1	Treatment 2	0.003
		Treatment 2	Treatment 3	0.004
	8R	Control	Treatment 1	0.001
			Treatment 3	0.002
		Treatment 1	Treatment 2	0.001
		Treatment 2	Treatment 3	0.002
	6R	Control	Treatment 1	0.002
			Treatment 3	0.008
		Treatment 1	Treatment 2	0.002
		Treatment 2	Treatment 3	0.008

**Table 5.4 Clonal differences between the treatments for molybdenum petiole concentrations in years 1 and 3 of the trial.**

Differences are at the 5% level and only significant data is presented.

<b>Year</b>	<b>Treatment</b>	<b>Clone X is significantly different to clone Y</b>	<b>Clone Y is significantly different to clone X</b>	<b>P value (0.05 level)</b>
<b>Year 1</b>	Treatment 1	Q45-14	8R	0.035
		6R	8R	0.006
	Treatment 2	Q45-14	8R	0.035
		6R	8R	0.006
<b>Year 3</b>	Treatment 1	Q45-14	8R	0.026

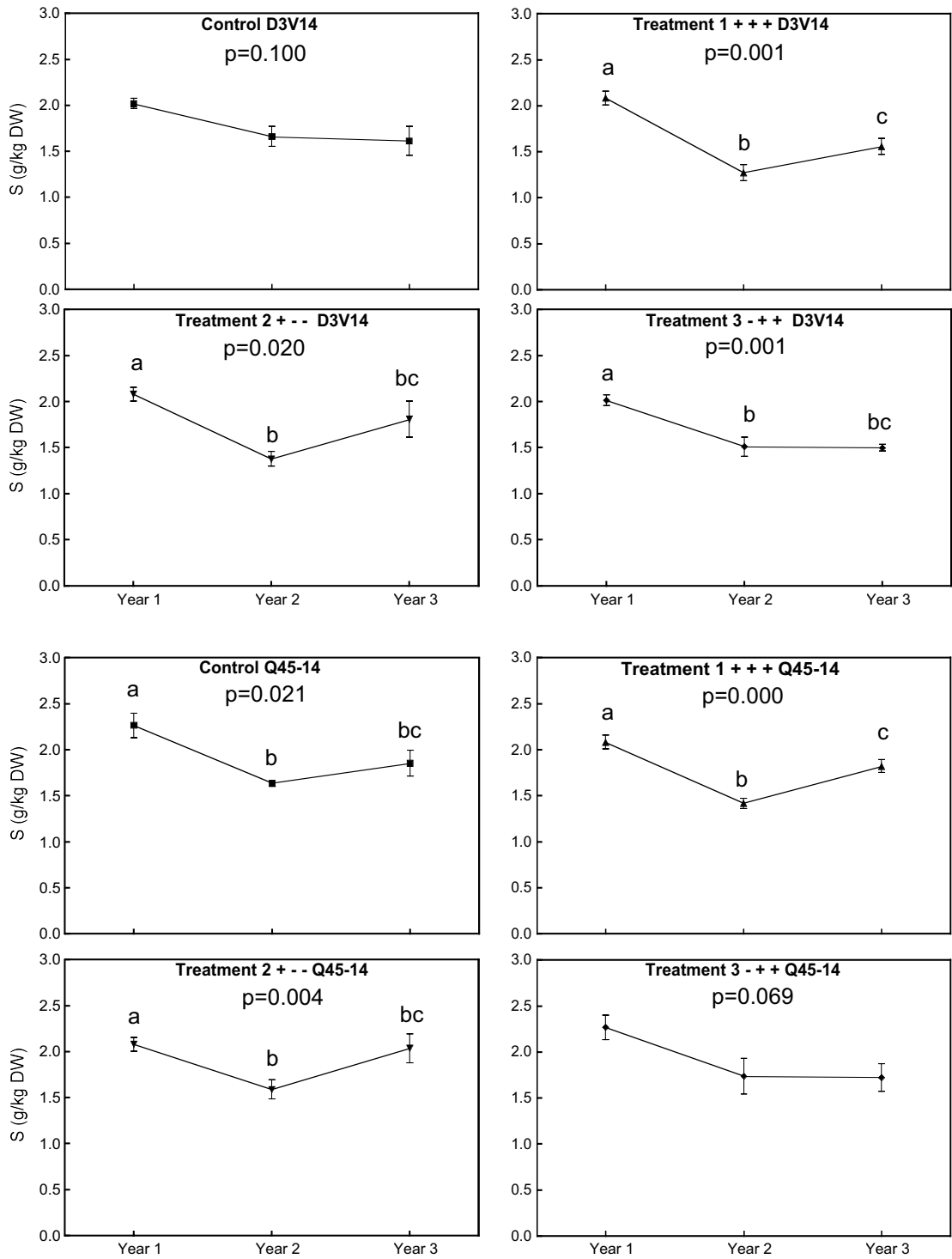


**Figure 5.17 Mean S (g/kg DW) concentration in petioles at 50 – 80% flowering for clones D3V14 and Q45-14 over the 3 years of the trial.**

Values are mean  $\pm$  SEM (n=3-4). Results with the same letter are not significantly different.

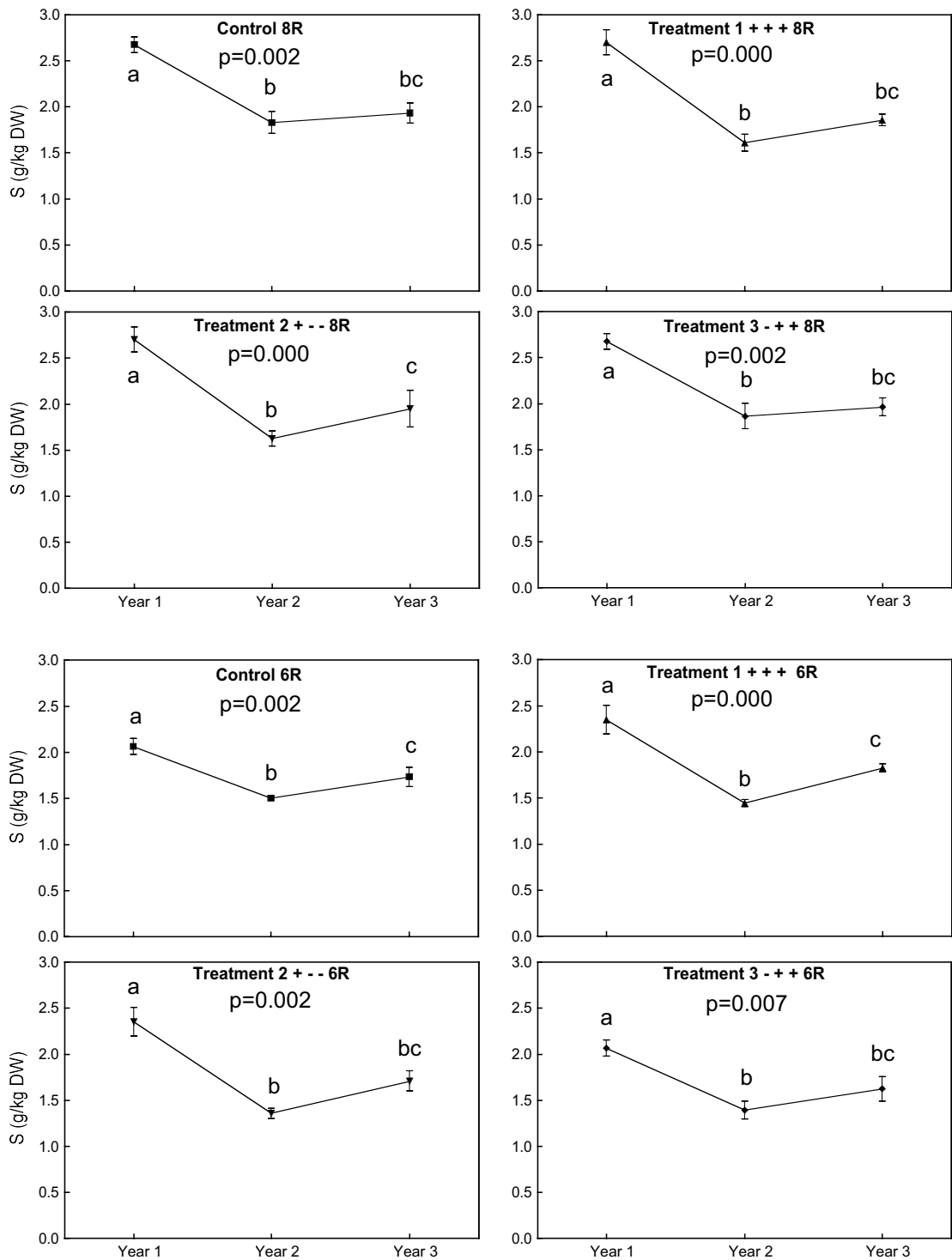


**Figure 5.18 Mean S (g/kg DW) concentration in petioles at 50 – 80% flowering for clones 8R and 6R over the 3 years of the trial.**

Values are mean  $\pm$  SEM (n=3-4). Results with the same letter are not significantly different.



**Table 5. 5 Clonal differences between the treatments for sulfur petiole concentrations in year 1, 2 and 3 of the trial.**

Differences are at the 5% levels and only significant data is presented.

<b>Year</b>	<b>Treatment</b>	<b>Clone X is significantly different to clone Y</b>	<b>Clone Y is significantly different to clone X</b>	<b>P value (0.05 level)</b>
<b>Year 1</b>	Control	D3V14	8R	0.000
		Q45-14	8R	0.014
		6R	8R	0.001
	Treatment 1	8R	D3V14	0.006
	Treatment 2	D3V14	8R	0.006
	Treatment 3	D3V14	8R	0.000
		Q45-14	8R	0.014
		8R	6R	0.001
<b>Year 2</b>	Control	8R	6R	0.025
	Treatment 1	D3V14	8R	0.006
	Treatment 3	8R	6R	0.027
<b>Year 3</b>	Treatment 1	D3V14	Q45-14	0.015
			8R	0.008
			6R	0.013
	Treatment 3	D3V14	8R	0.012

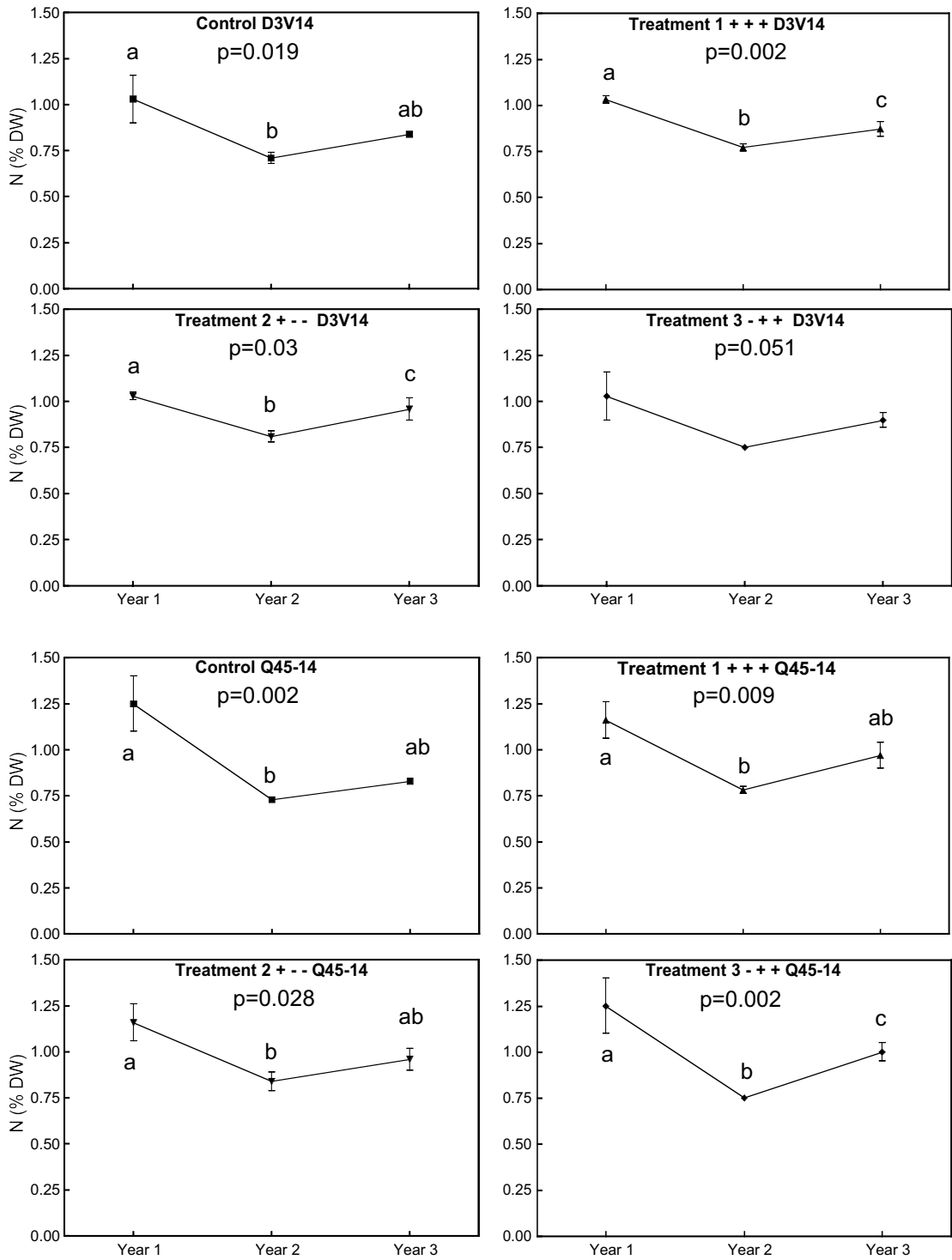


**Figure 5.19 Mean total N (% DW) concentration in petioles at 50 – 80% flowering for clones D3V14 and Q45-14 over the 3 years of the trial. Adequate levels of total N occur between 1.8 – 3% DW (Reuter and Robinson, 1997).**

Values are mean  $\pm$  SEM (n=3-4). Results with the same letter are not significantly different.

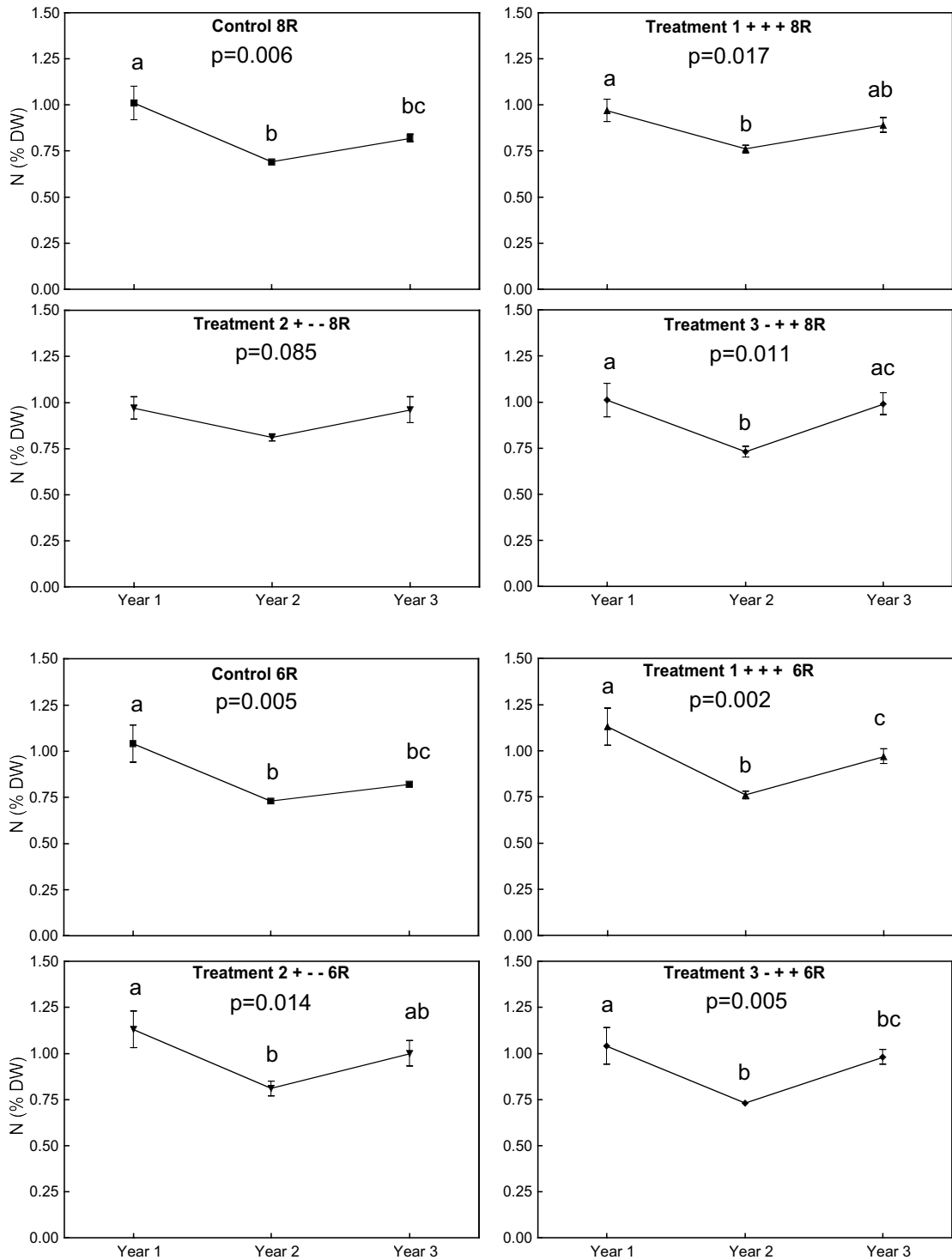


**Figure 5.20 Mean total N (% DW) concentration in petioles at 50 – 80% flowering for clones 8R and 6R over the 3 years of the trial. Adequate levels of total N occur between 1.8 – 3% DW (Reuter and Robinson, 1997).**

Values are mean  $\pm$  SEM (n=3-4). Results with the same letter are not significantly different.

**Table 5.6 Treatment differences between the treatments for nitrogen petiole concentrations in years 2 and 3 of the trial.**

Differences are at the 5% level and only significant data is presented.

<b>Year</b>	<b>Clone</b>	<b>Treatment X is significantly different to treatment Y</b>	<b>Treatment Y is significantly different to treatment X</b>	<b>P value (0.05 level)</b>
<b>Year 2</b>	D3V14	Control	Treatment 2	0.007
	Q45-14	Control	Treatment 2	0.017
		Treatment 2	Treatment 3	0.044
	8R	Control	Treatment 1	0.047
			Treatment 2	0.004
	Treatment 2	Treatment 3	0.028	
<b>Year 3</b>	Q45-14	Control	Treatment 3	0.038
	8R	Control	Treatment 3	0.030
	6R	Control	Treatment 1	0.045
			Treatment 2	0.014
			Treatment 3	0.019

**Table 5.7 Clonal differences between the treatments for nitrogen petiole concentrations in year 1, 2 and 3 of the trial.**

Differences are at the 5% levels and only significant data is presented.

<b>Year</b>	<b>Treatment</b>	<b>Clone X is significantly different to clone Y</b>	<b>Clone Y is significantly different to clone X</b>	<b>P value (0.05 level)</b>
<b>Year 1</b>	Treatment 1	Q45-14	8R	0.035
		6R	8R	0.006
	Treatment 2	Q45-14	8R	0.035
		6R	8R	0.006
<b>Year 3</b>	Treatment 1	Q45-14	8R	0.026

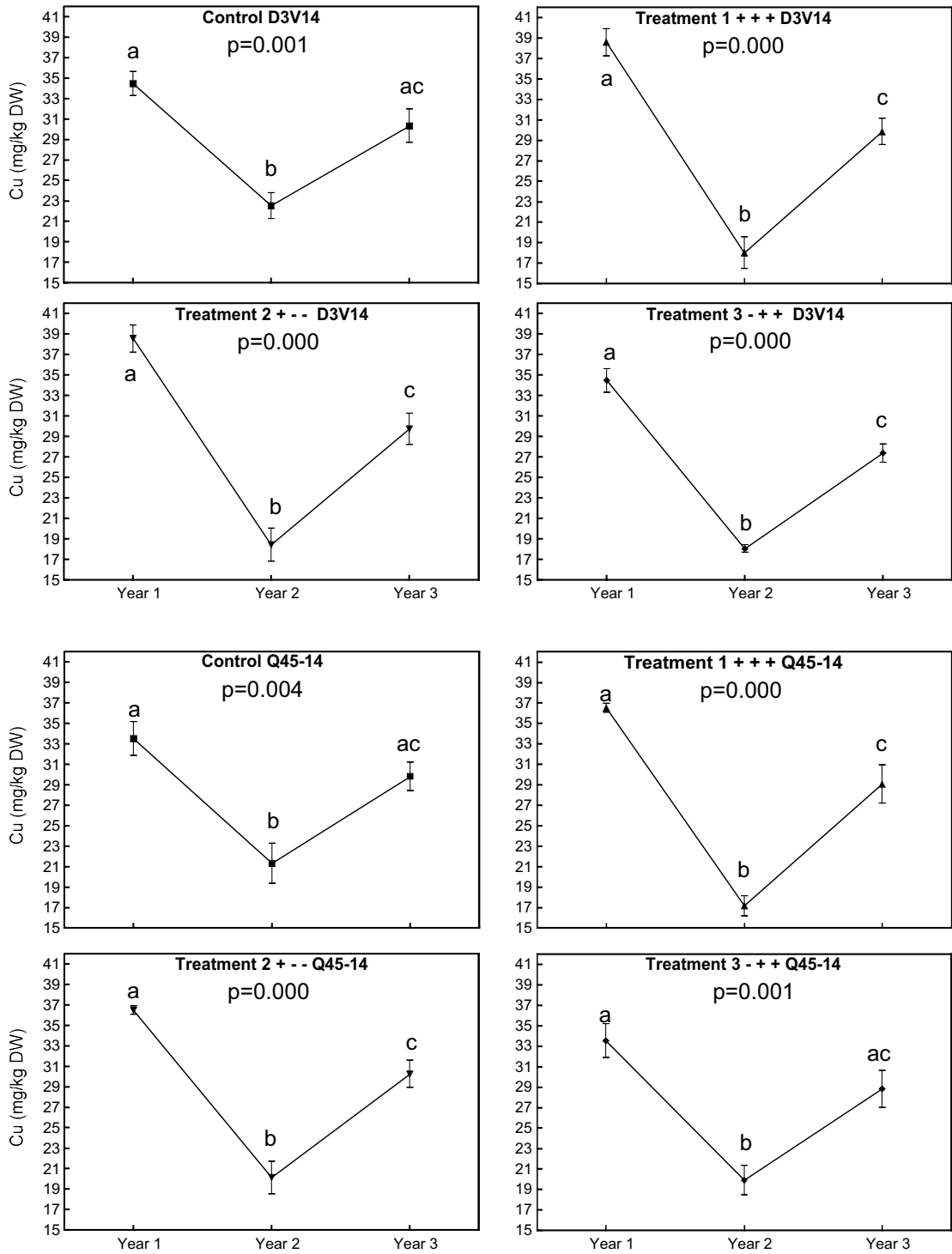


**Figure 5.21 Mean Cu (mg/kg DW) concentration in petioles at 50 – 80% flowering for clones 8R and 6R over the 3 years of the trial. Adequate levels of Cu occur between 6 – 11 mg/kg DW (Reuter and Robinson, 1997).**

Values are mean  $\pm$  SEM (n=3-4). Results with the same letter are not significantly different.

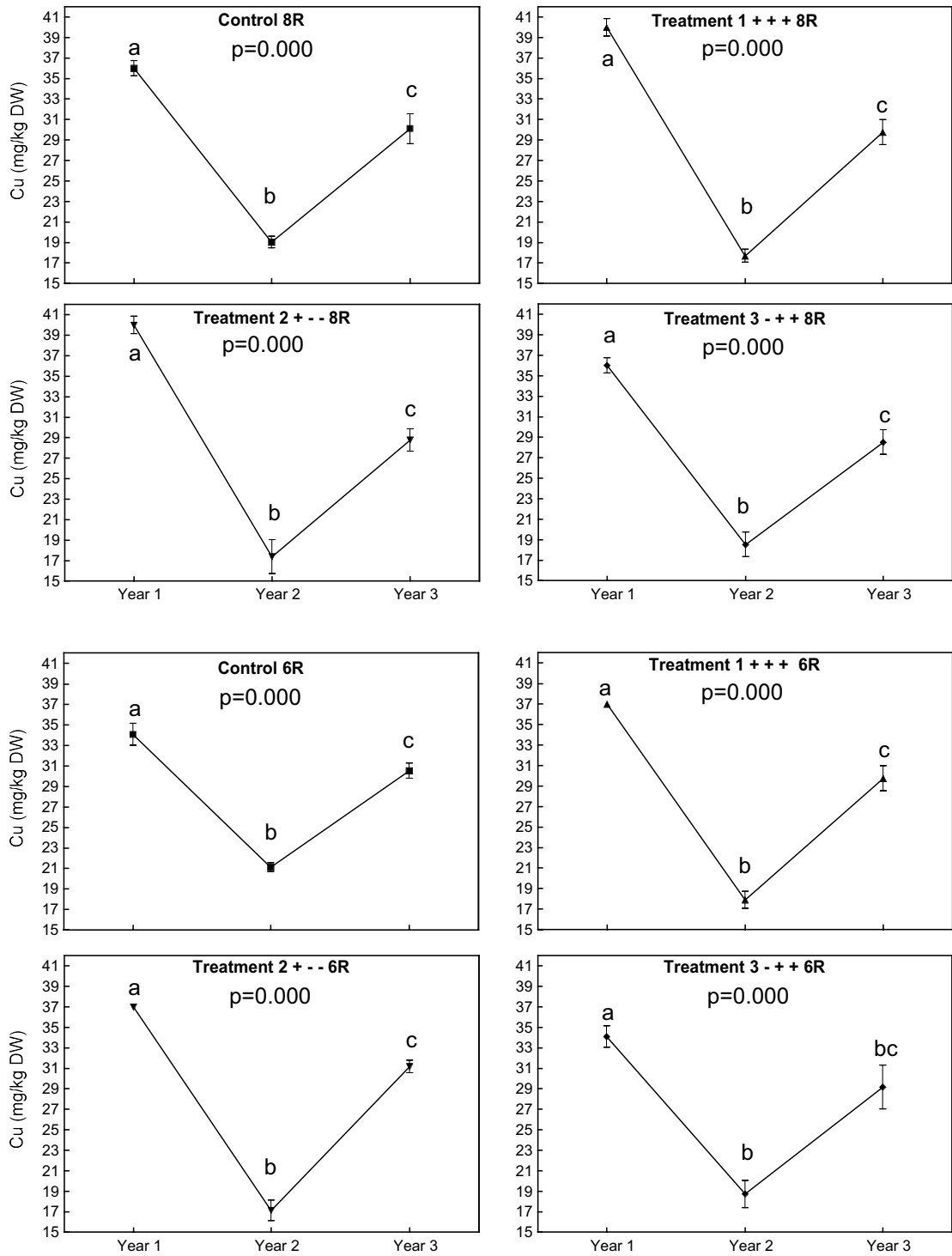


**Figure 5.22 Mean Cu (mg/kg DW) concentration in petioles at 50 – 80% flowering for clones 8R and 6R over the 3 years of the trial. Adequate levels of Cu occur between 6 – 11 mg/kg DW (Reuter and Robinson, 1997).**

Values are mean  $\pm$  SEM (n=3-4). Results with the same letter are not significantly different.

**Table 5.8 Treatment differences between the year and clones for copper petiole concentrations in years 1 and 2 of the trial.**

Differences are at the 5% levels and only significant data is presented.

<b>Year</b>	<b>Clone</b>	<b>Treatment X is significantly different to Treatment Y</b>	<b>Treatment Y is significantly different to Treatment X</b>	<b>P value (0.05 level)</b>
<b>Year 1</b>	D3V14	Control	Treatment 1	0.043
			Treatment 2	0.043
		Treatment 1	Treatment 3	0.043
		Treatment 2	Treatment 3	0.043
	8R	Control	Treatment 1	0.004
			Treatment 2	0.004
		Treatment 1	Treatment 3	0.004
		Treatment 2	Treatment 3	0.004
	6R	Control	Treatment 1	0.019
			Treatment 2	0.019
		Treatment 1	Treatment 3	0.019
		Treatment 2	Treatment 3	0.019
<b>Year 2</b>	D3V14	Control	Treatment 1	0.028
			Treatment 2	0.045
			Treatment 3	0.030
	6R	Control	Treatment 1	0.028
			Treatment 2	0.013



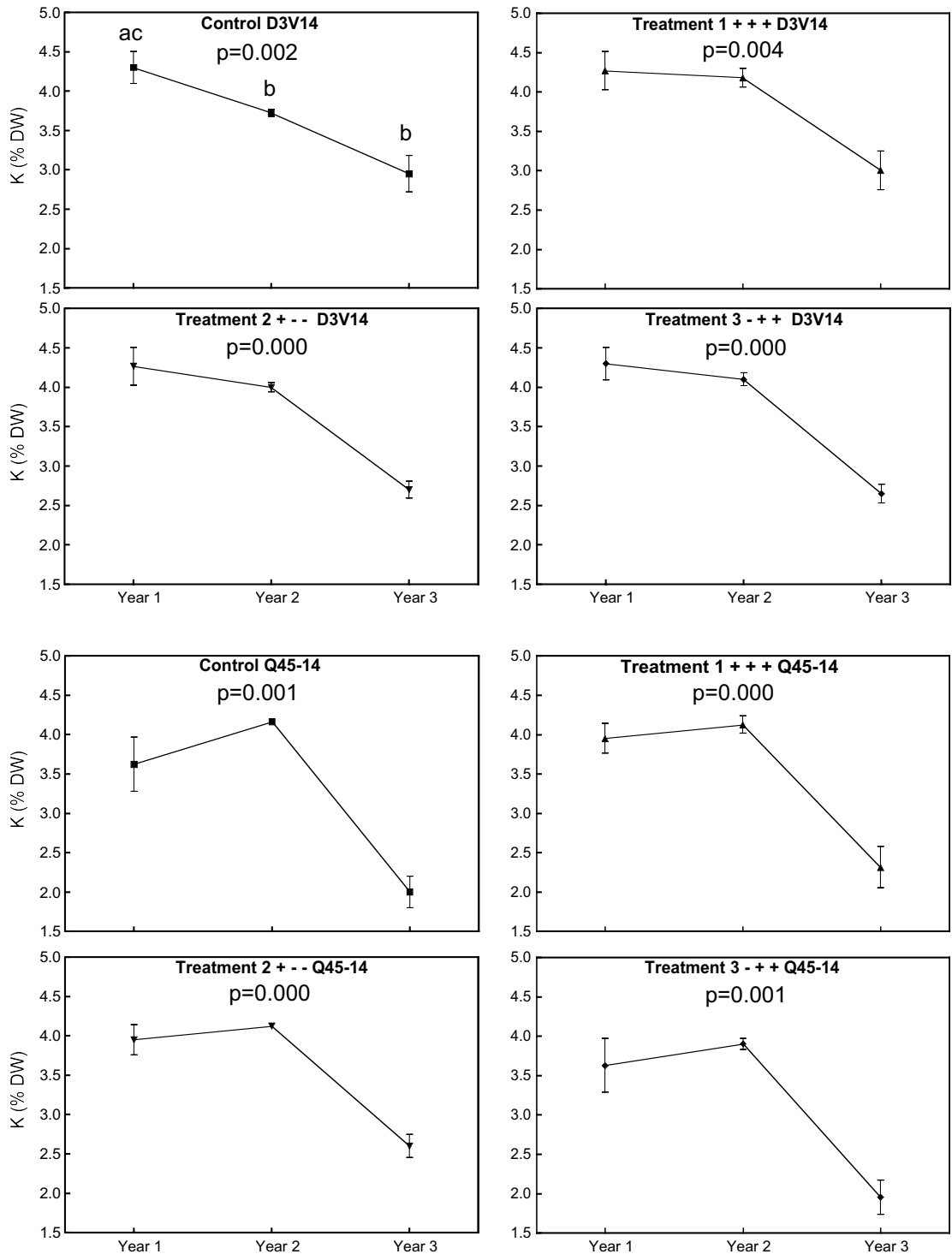


**Figure 5.23 Mean K (% DW) concentration in petioles at 50 – 80% flowering for clones D3V14 and Q45-14 over the 3 years of the trial. Adequate levels of K occur between 1.8 – 3% DW (Reuter and Robinson, 1997).**

Values are mean  $\pm$  SEM (n=3-4). Results with the same letter are not significantly different.

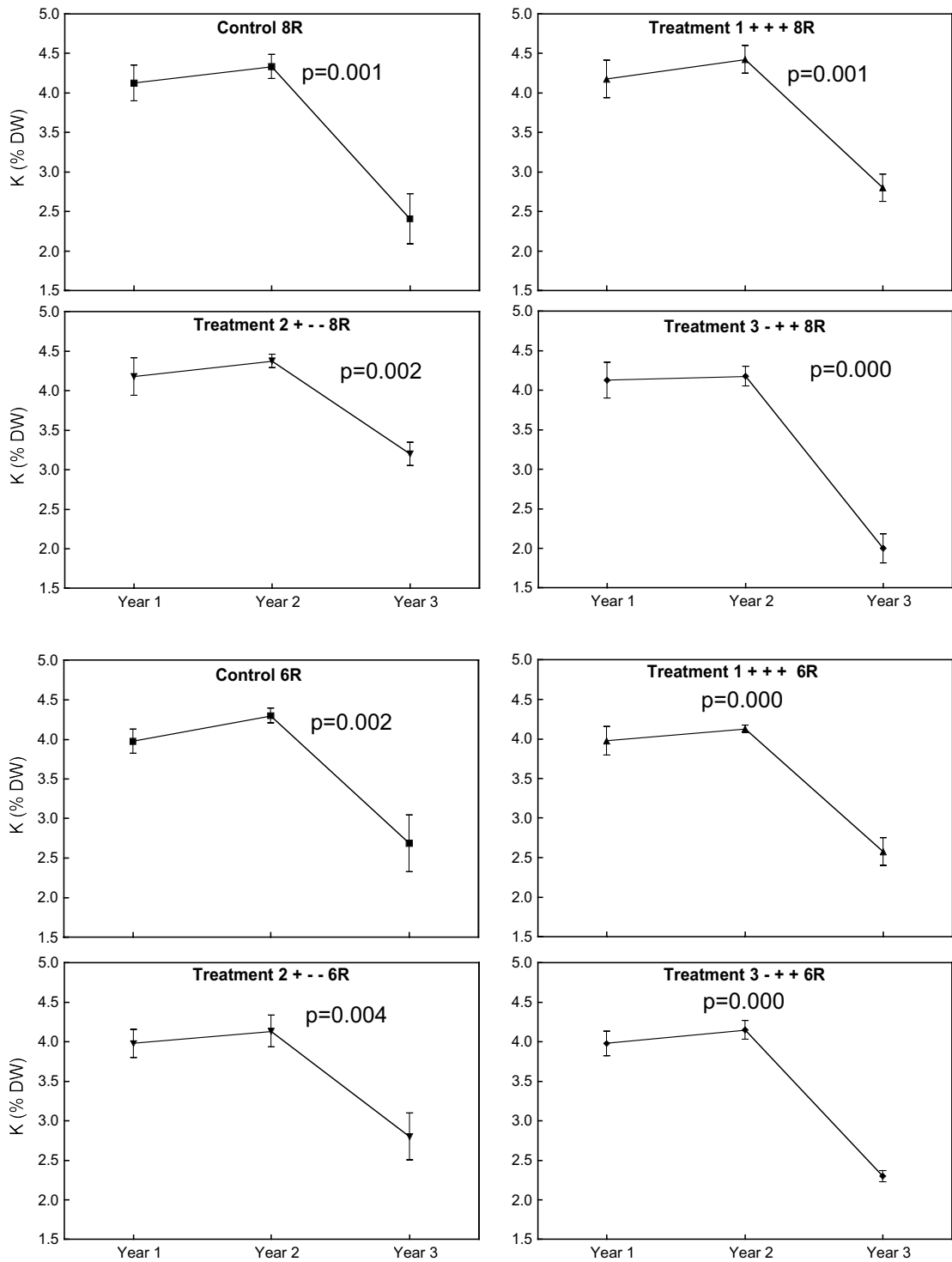


**Figure 5.24 Mean K (% DW) concentration in petioles at 50 – 80% flowering for clones 8R and 6R over the 3 years of the trial. Adequate levels of K occur between 1.8 – 3% DW (Reuter and Robinson, 1997).**

Values are mean  $\pm$  SEM (n=3-4). Results with the same letter are not significantly different.

**Table 5.9 Treatment differences between the years and clones for potassium petiole concentrations in years 2 and 3 of the trial.**

Differences are at the 5% levels and only significant data is presented.

<b>Year</b>	<b>Clone</b>	<b>Treatment X is significantly different to treatment Y</b>	<b>Treatment Y is significantly different to treatment X</b>	<b>P value (0.05 level)</b>
<b>Year 2</b>	D3V14	Control	Treatment 1	0.002
			Treatment 2	0.033
			Treatment 3	0.007
	Q45-14	Control	Treatment 3	0.032
			Treatment 1	0.047
			Treatment 3	0.047
<b>Year 3</b>	Q45-14	Treatment 3	Treatment 2	0.050
	8R	Control	Treatment 2	0.023
		Treatment 1	Treatment 3	0.022
		Treatment 2	Treatment 3	0.002

**Table 5.10 Treatment differences between the years and clones for potassium petiole concentrations in years 2 and 3 of the trial.**

Differences are at the 5% levels and only significant data is presented.

<b>Year</b>	<b>Treatment</b>	<b>Clone X is significantly different to clone Y</b>	<b>Clone Y is significantly different to clone X</b>	<b>P value (0.05 level)</b>
<b>Year 2</b>	Control	D3V14	Q45-14	0.009
			8R	0.001
			6R	0.001
	Treatment 2	D3V14	8R	0.020
<b>Year 3</b>	Control	D3V14	Q45-14	0.036
	Treatment 1	Q45-14	D3V14	0.046
	Treatment 2	Q45-14	8R	0.045

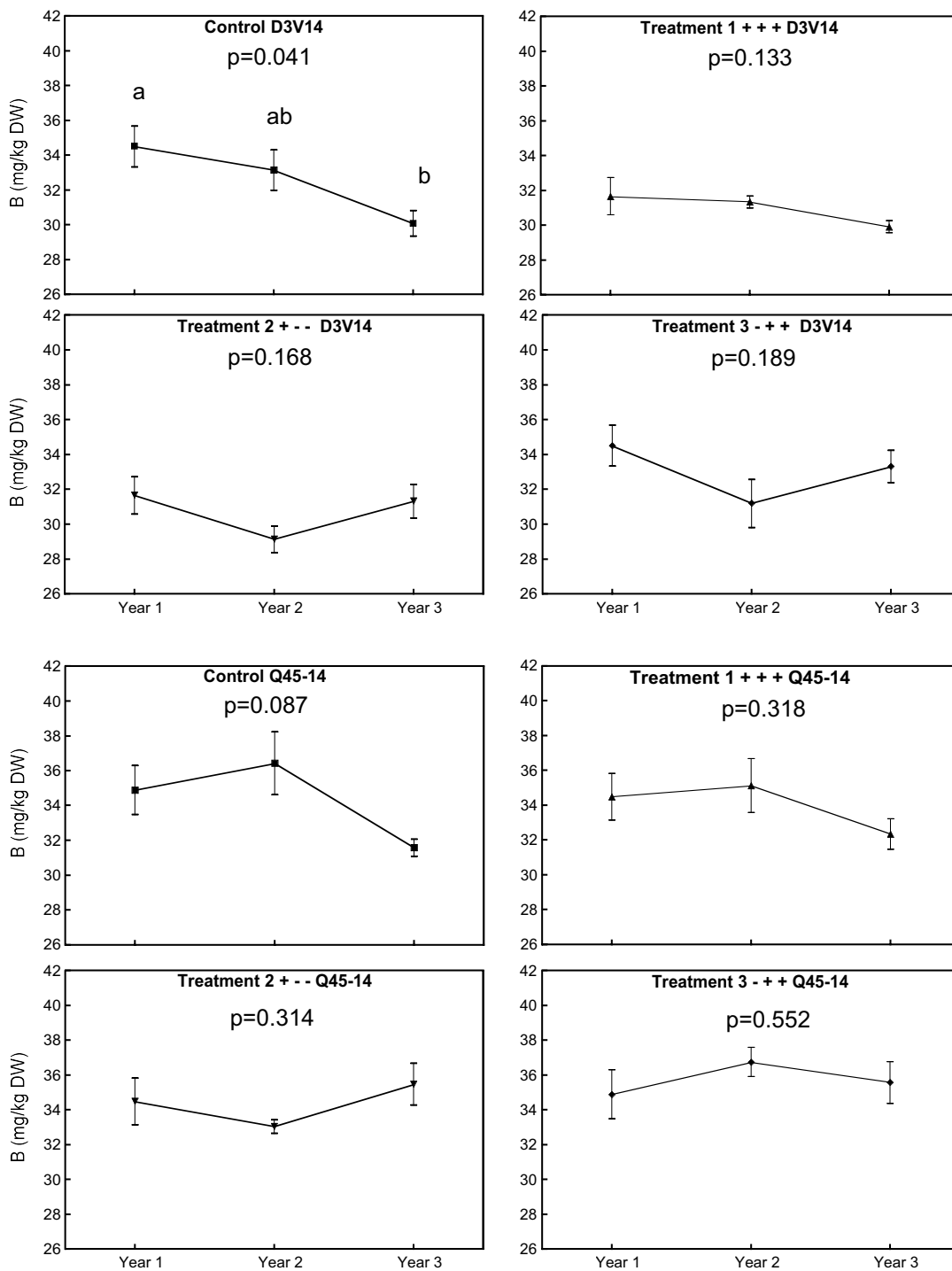


**Figure 5.25 Mean B (mg/kg DW) concentration in petioles at 50 – 80% flowering for clones D3V14 and Q45-14 over the 3 years of the trial. Adequate levels of B occur between 35 – 70 mg/kg DW (Reuter and Robinson, 1997).**

Values are mean  $\pm$  SEM (n=3-4). Results with the same letter are not significantly different.

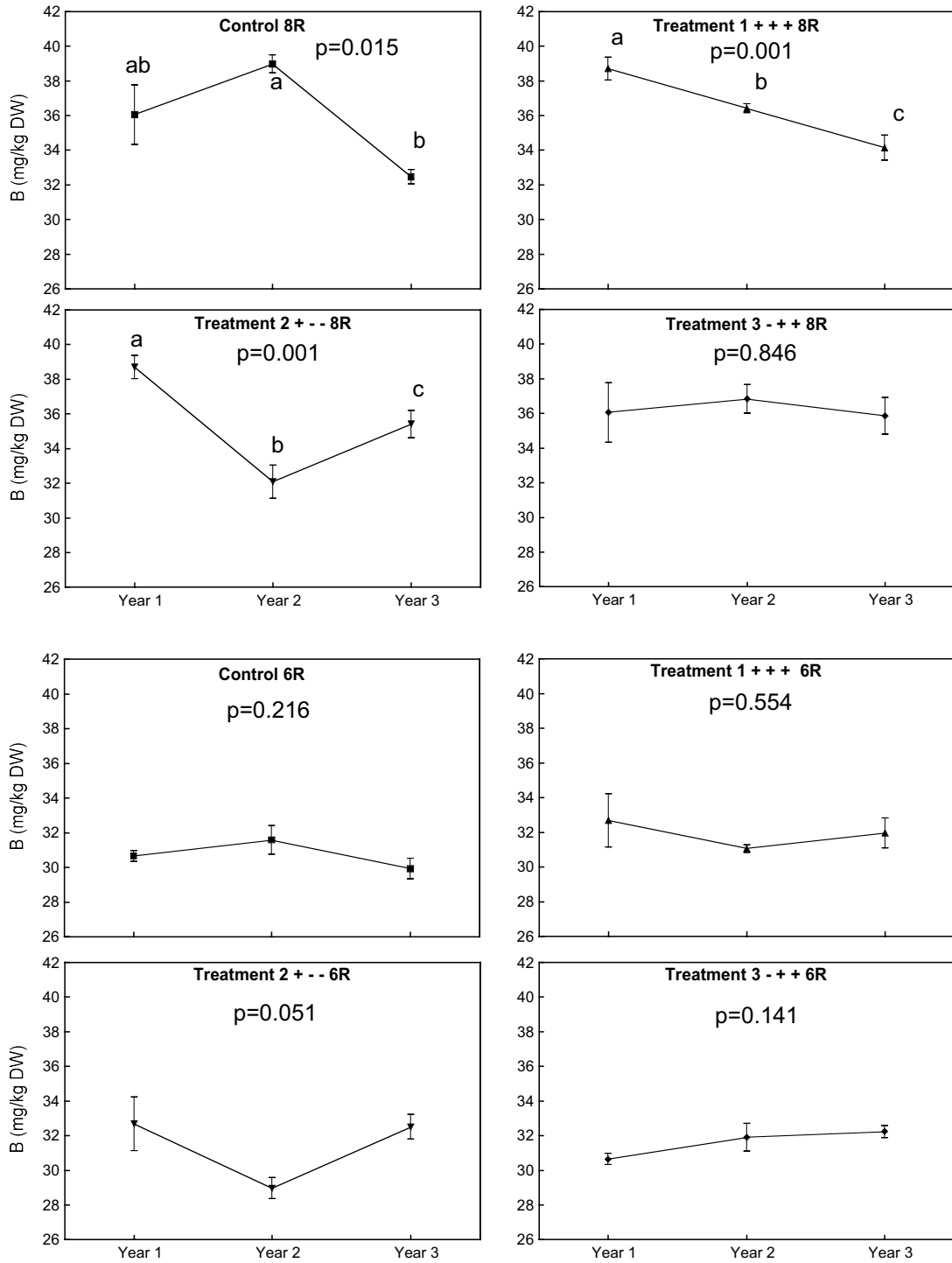


**Figure 5.26 Mean B (mg/kg DW) concentration in petioles at 50 – 80% flowering for clones 8R and 6R over the 3 years of the trial. Adequate levels of B occur between 35 – 70 mg/kg DW (Reuter and Robinson, 1997).**

Values are mean  $\pm$  SEM (n=3-4). Results with the same letter are not significantly different.

**Table 5. 11 Treatment differences between the years and clones for boron petiole concentrations in years 2 and 3 of the trial.**

Differences are at the 5% levels and only significant data is presented.

<b>Year</b>	<b>Clone</b>	<b>Treatment X is significantly different to treatment Y</b>	<b>Treatment Y is significantly different to treatment X</b>	<b>P value (0.05 level)</b>
<b>Year 2</b>	<b>D3V14</b>	Treatment 1	Treatment 2	0.015
		Control	Treatment 2	0.038
	<b>8R</b>	Control	Treatment 1	0.000
			Treatment 2	0.038
		Treatment 1	Treatment 2	0.001
	<b>6R</b>	Treatment 3	Treatment 2	0.001
		Control	Treatment 2	0.013
		Treatment 1	Treatment 2	0.039
		Treatment 2	Treatment 3	0.007
	<b>Year 3</b>	<b>D3V14</b>	Control	Treatment 3
Treatment 1			Treatment 3	0.009
<b>Q45-14</b>		Control	Treatment 2	0.016
			Treatment 3	0.014
		Treatment 1	Treatment 2	0.044
<b>8R</b>		Control	Treatment 3	0.039
			Treatment 2	0.020
		Treatment 3	0.009	
<b>6R</b>		Control	Treatment 2	0.017
		Treatment 3	Control	0.029

**Table 5. 12 Clonal differences between the years and treatment for boron petiole concentrations in years 1, 2 and 3 of the trial.**

Differences are at the 5% levels and only significant data is presented.

<b>Year</b>	<b>Treatment</b>	<b>Clone X is significantly different to clone Y</b>	<b>Clone Y is significantly different to clone X</b>	<b>P value (0.05 level)</b>	
<b>Year 1</b>	Control	Q45-14	6R	0.035	
		8R	6R	0.011	
	Treatment 1	D3V14	8R	0.003	
		Q45-14	8R	0.029	
		8R	6R	0.004	
	Treatment 2	D3V14	8R	0.003	
		Q45-14	8R	0.029	
		8R	6R	0.004	
	Treatment 3	Q45-14	6R	0.035	
		8R	6R	0.011	
	<b>Year 2</b>	Control	D3V14	8R	0.008
			Q45-14	6R	0.020
6R			8R	0.002	
Treatment 1		D3V14	Q45-14	0.006	
			8R	0.001	
		Q45-14	6R	0.004	
			8R	0.001	
Treatment 2		D3V14	Q45-14	0.002	
			8R	0.011	
		Q45-14	6R	0.001	
			8R	0.008	
Treatment 3		D3V14	Q45-14	0.002	
			8R	0.002	
		Q45-14	6R	0.005	
			8R	0.004	
<b>Year 3</b>	Control	D3V14	8R	0.012	
		8R	6R	0.009	
	Treatment 1	D3V14	Q45-14	0.038	
			8R	0.002	
	Treatment 2	D3V14	Q45-14	0.009	
			8R	0.010	
		Q45-14	6R	0.044	
	Treatment 3	Q45-14	6R	0.049	
8R			0.027		
8R6R			0.018		



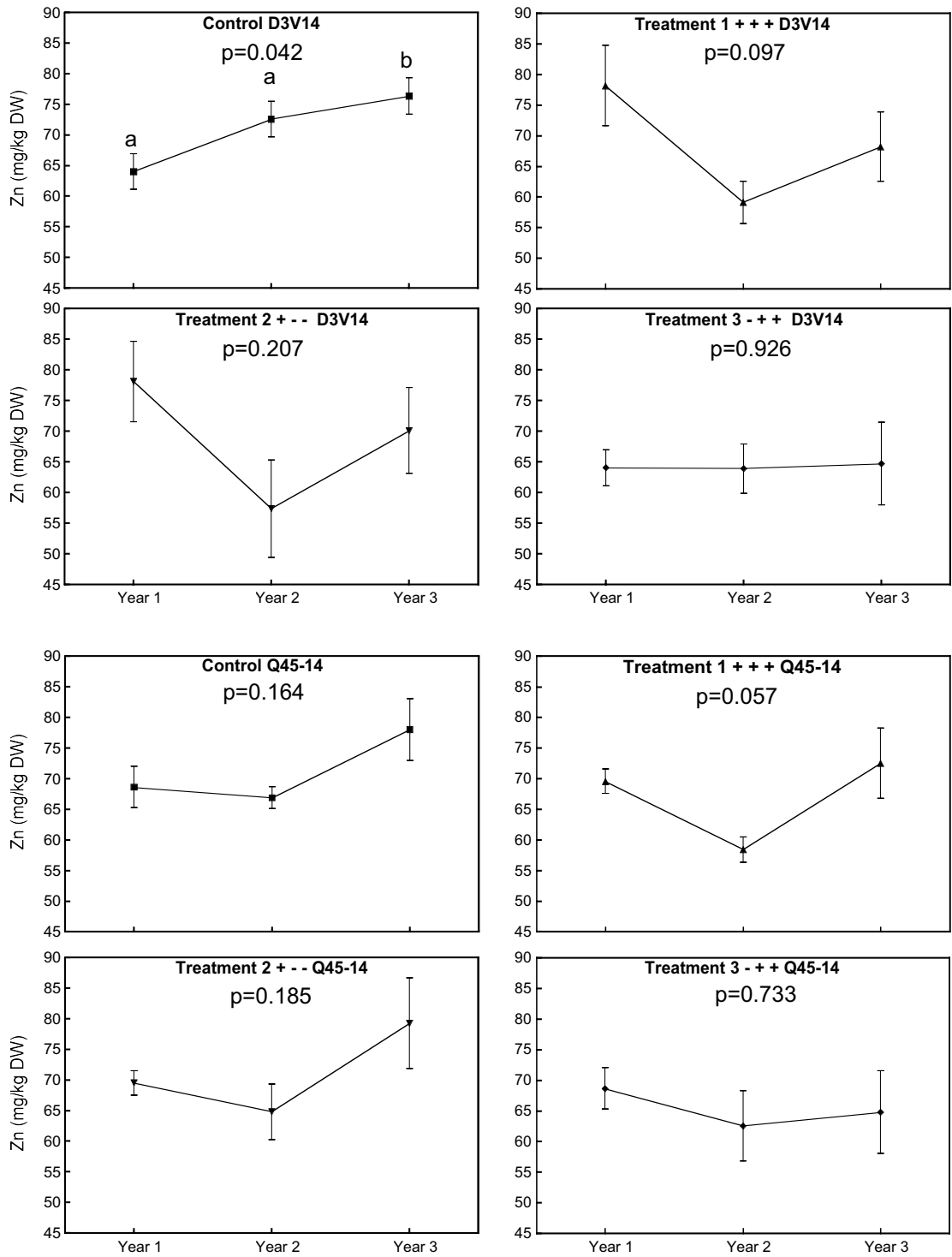


**Figure 5.27 Mean Zn (mg/kg DW) concentration in petioles at 50 – 80% flowering for clones D3V14 and Q45-14 over the 3 years of the trial. Adequate levels of Zn occur at >26 mg/kg DW (Reuter and Robinson, 1997).**

Values are mean  $\pm$  SEM (n=3-4). Results with the same letter are not significantly different.

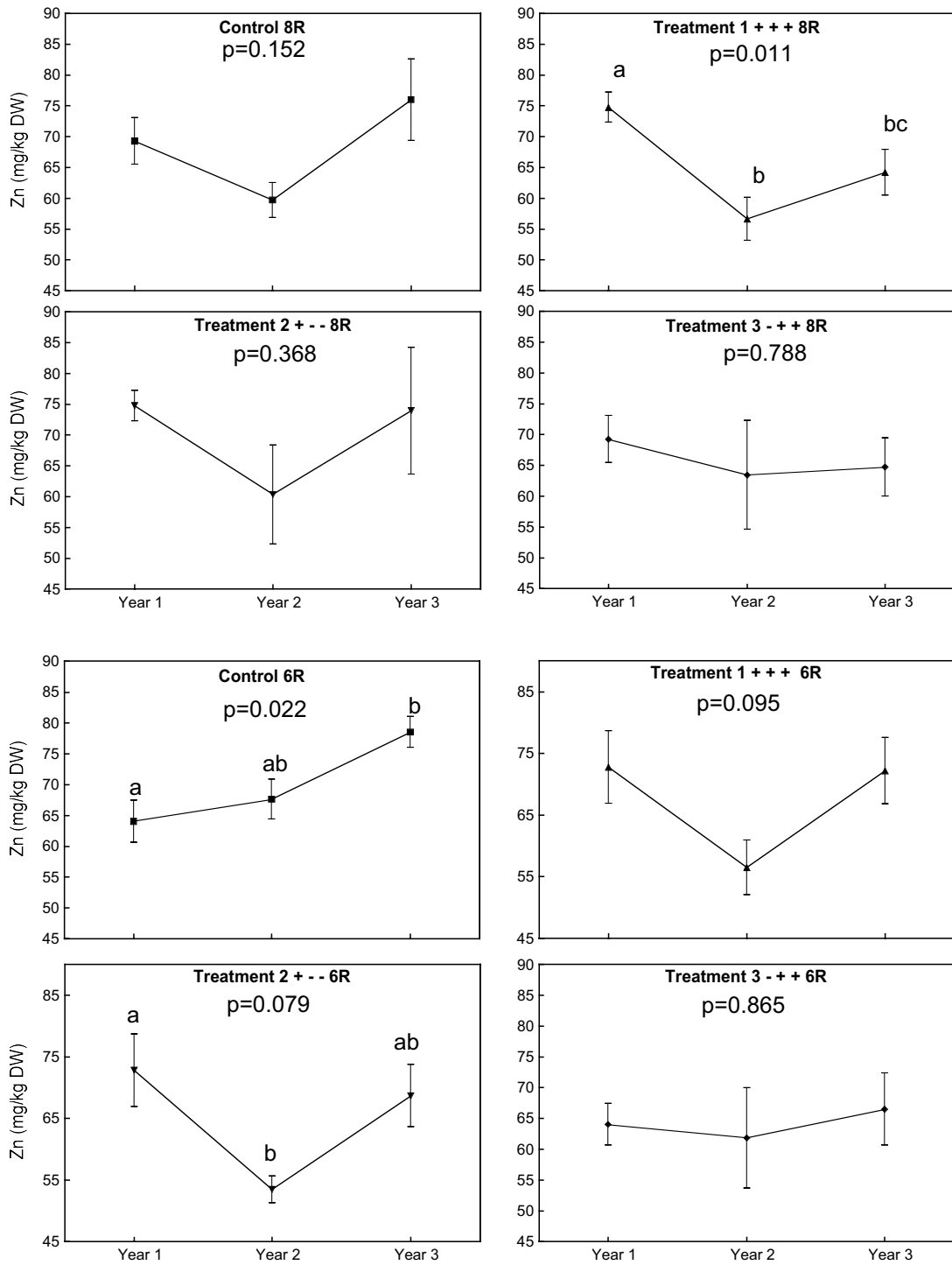


**Figure 5.28 Mean Zn (mg/kg DW) concentration in petioles at 50 – 80% flowering for clones 8R and 6R over the 3 years of the trial. Adequate levels of Zn occur at >26 mg/kg DW (Reuter and Robinson, 1997).**

Values are mean  $\pm$  SEM (n=3-4). Results with the same letter are not significantly different.

## Chapter 6

### General discussion

---

#### 6.1 Identification of plant molybdenum transporters

Despite molybdenum being of critical importance to plants as a metal cofactor (Mendel and Hansch, 2002; Mendel and Bittner, 2006; Mendel, 2007), little research has been conducted into how it is accessed from the soil and its subsequent distribution within the plant. Over the last 50 years, little headway has been made into the field where research into molybdenum transport has predominantly focussed on lower order prokaryotic organisms, where molybdenum transport systems are well defined. The original aims of this project were to identify a specific *V. vinifera* molybdenum transporter and test for its involvement in the molybdenum deficiency phenotype observed in the cultivar Merlot. Based on current knowledge of molybdate transport in *E.coli*, it was assumed that a plant molybdenum transporter would involve a high-affinity system due to the small concentrations required by plants and most likely functionally similar to the prokaryotic systems. Unfortunately, there were no homologs of any prokaryote molybdate transport gene found in eukaryotes, which forced a re-think about the mechanisms operating in plants, and the strategy required to identify them.

## **6.2 Functional complementation in yeast to identify novel molybdenum transport proteins in *Vitis vinifera***

Since molybdenum transport at the physiological and molecular level is a poorly defined system in plants, a forward genetic approach was adopted to identify putative unknown molybdenum transporters operating in grapevines. Previous research had shown that molybdenum transport is influenced by the sulfur status of a plant (Stout et. al., 1951; Tweedi and Segel, 1970; Mendel and Hansch, 2002; Alhendawi et. al., 2005). Similarly in prokaryotic systems sulfate is widely known as an effective competitor of molybdenum uptake (Self et. al., 2001). The close physiological interaction between sulfate and molybdenum transport was used to develop a working hypothesis that membrane transport proteins capable of sulfate transport are also responsible for molybdenum transport in plants and other organisms.

To help test this hypothesis, a yeast functional complementation screen was developed which utilised the sulfate transport mutant YSD1. YSD1 is deficient in its native sulfate transporter *SUL1* (Smith et. al., 1995b). Initial experiments with the yeast strain YSD1 indicated that cell growth could be reduced when grown on galactose and when molybdenum or sulfate levels were maintained at low concentrations (< 80 nM and 100  $\mu$ M, respectively) (Figure 3.4 and 3.6). The poor growth of YSD1 on the Low Mo Gal media was surprising as this media contains sulfate at concentrations normally found in complete yeast media preparations. When glucose was used as the carbon source instead of galactose, the growth patterns of YSD1 were improved on both the low molybdenum (data not shown) and sulfate media preparations (Figure 3.4). It would appear the reduced growth rate in galactose media allows for the deficiencies in molybdenum availability to be evaluated in YSD1 and when better growing conditions exist (glucose containing media). Other remaining systems, such as other non-specific anion transporters capable of providing sufficient molybdenum and sulfate to meet cell demand. Although the growth response was slight between the two carbon sources, it was sufficient to depress cell growth to allow a yeast complementation study to be used to identify and characterise plant molybdenum transporters.

A grapevine root cDNA library was synthesised from mRNA isolated from molybdenum starved plants. The cDNAs were cloned into a yeast expression vector and transformed into the yeast mutant YSD1 where a functional complementation screen was carried out on both Low S and Low Mo media. Unfortunately, no specific genes were identified that

could be linked to molybdenum transport *per se* (identified as *bona fide* sulfate or molybdate membrane transport proteins). Surprisingly, no sulfate transporters were identified in the screen even though Smith et. al. (1995b) had originally isolated SHST1 through this method. This may possibly be explained by the cDNA library not being enriched for these proteins as no sulfate starvation was allowed to occur. However, plants were starved of molybdenum, as molybdenum was omitted from the nutrient solution and other nutrients were not replenished within this 10 day time period. Given this fact alone, it is surprising that any putative sulfate transport cDNA's were not isolated as after 3 days as it has been shown that unregulated expression of SHST1 occurs after this time (Smith et. al., 1995a). There was also significant difficulty in confirming a number of the first round putative positives when retransformed back into YSD1 and re-screened and it is unknown as to why this occurred. Although the screen was initially encouraging, the level of complementation necessary to rescue cell growth on Low S Gal or Low Mo Gal media was small contributing to a large number of potential false positives.

### **6.3 SHST1 - the new molybdenum transport system**

Previous research has suggested that molybdenum may also be transported through sulfate transport proteins (Stout et. al., 1951; Marschner, 1995; Mendel and Schwarz, 1999; Mendel and Bittner, 2006) mainly due to chemical similarities of anion size, net charge, geometry and hydrogen bonding properties (Dudev and Lim, 2004). There are many reports of molybdate and sulfate interaction throughout the literature including research on *Clostridium pasteurianum* (Elliot and Mortenson, 1975; Elliot and Mortenson, 1976), *E.coli* (Self et. al., 2001), filamentous fungi (Tweedi and Segel, 1970) Rat ileum (Cardin and Mason, 1975), and both human and rat placental tissue (Dawson et. al., 2005; Miyauchi et. al., 2006). The lack of any success in identifying a sulfate transporter in the previous functional yeast complementation experiments was a disappointment. However, this failure did allow a different more directed approach to be developed. The original yeast screen based on poor growth of YSD1 on Low Mo Gal was still an attractive assay that could be used in a candidate gene approach where pre-characterised genes encoding transport proteins are tested for their ability to accumulate molybdenum and sulfate in YSD1.

The sulfate transporter, SHST1, was used as a candidate gene to determine whether molybdenum could be transported through a recognised sulfate transporter. There have been no previous attempts to do this type of experiment and surprisingly, no direct

evidence from functional analysis of identified sulfate transporters that molybdenum can be a potential substrate. Initial experiments in the yeast strain YSD1 indicated that SHST1 when expressed in the presence of galactose was capable of restoring growth on media containing low amounts of molybdenum (Figure 3.6). This growth response was most evident when molybdenum was provided at a concentration up to 80 nM. Using  $^{99}\text{MoO}_4^{2-}$  as a tracer for molybdenum uptake, time course experiments demonstrated SHST1 significantly increased the accumulation of molybdenum 3-fold compared to empty vector controls (Figure 3.12). As the external concentration of molybdenum increased from 1 to 1000 nM, the rate of  $^{99}\text{MoO}_4^{2-}$  uptake increased in a linear fashion showing no sign of saturation (Figure 3.14). Higher concentrations were not tested as molybdenum would rarely exceed these concentrations naturally. This transport phenotype was also observed with  $^{35}\text{SO}_4^{2-}$  at similar concentrations albeit the rate was significantly larger (Figure 3.15). There was evidence with SHST1 that at higher concentrations (25  $\mu\text{M}$ ), molybdate could compete with sulfate uptake (Figure 3.9 and 3.10). Competition was found to be strongest when cells were grown on 2XTL Gal over that of Low Mo Gal. At 25  $\mu\text{M}$   $\text{SO}_4^{2-}$  the predicted  $K_i$  of  $\text{MoO}_4^{2-}$  inhibition was 34  $\mu\text{M}$  (Figure 3.11). In contrast, no competition was evident between  $^{99}\text{MoO}_4^{2-}$  uptake and external sulfate. It would thus appear that SHST1 is primarily a sulfate transport protein at external sulfate concentrations of at least 25  $\mu\text{M}$ . However, SHST1 is capable of selective transport of low concentrations of molybdate irrespective of whether sulfate is present. The pH response of SHST1 indicated a pH dependence with increased molybdate uptake occurring in more acidic conditions (Figure 3.17). This result indicates that SHST1 is also acting as a  $\text{H}^+/\text{MoO}_4^{2-}$  cotransporter similar to the hypothesised  $\text{H}^+/\text{SO}_4^{2-}$  cotransporter originally suggested by Smith et. al. (1995a). Interestingly, a similar pH profile for sulfate uptake has also been demonstrated in isolated *Brassica napus* plasma membrane vesicles (Hawkesford et. al., 1993).

A great deal of research has been conducted into the similarities between the sulfate and molybdate anions and subsequent binding pockets of the ModA and SBP in *E.coli* (Lawson et. al., 1998; Self et. al., 2001; Pau and Lawson, 2002; Dudev and Lim, 2004). Anion size is postulated to dictate selectivity between molybdate and sulfate transport proteins in prokaryotic systems (Dudev and Lim, 2004). ModA binds molybdate and tungstate with high affinity, but not sulfate, phosphate, arsenate, nitrate, chlorate, selenate, metavanadate, perchlorate or permanganate (Pau and Lawson, 2002; Dudev and Lim, 2004) whereas SBP binds sulfate with high affinity but molybdate with very low affinity (Dudev and Lim, 2004). As molybdate is slightly larger than sulfate ( $\text{Mo-O} = 1.75 - 1.78$

Å vs. S-O = 1.47 – 1.49 Å (Dudev and Lim, 2004)) it is unclear how molybdate is able to fit into the SPB active site and be readily transported at low concentrations (< 1 μM) (Self et. al., 2001).

The role of SHST1 in molybdate transport *in planta* is relatively unknown. SHST1 has been primarily characterised in *Stylosanthes hamata* where its expression in roots is elevated under sulfur starvation conditions (Smith et. al., 1995a). Recently, *Brassica juncea* L. Czern (Indian Mustard) plants were transformed with SHST1 to investigate its role in mediating heavy metal tolerance and accumulation (Lindblom et. al., 2006). Plants transformed with SHST1 showed reduced growth compared to the wild type controls. Over expressing lines showed no changes in shoot molybdenum compared to the wild-type controls. However, over expression of SHST1 did lead to enhanced accumulation of chromium, cadmium vanadate and tungstate. Since tungstate and molybdate (W-O =1.78-1.79 Å vs. Mo-O =1.75-1.78 Å (Dudev and Lim, 2004)) are similar in size it is possible that molybdate can also be transported into the root system through SHST1. Unfortunately, insufficient root material was available to determine whether the molybdenum content within the roots increased in the study conducted by Lindblom et. al. (2006).

There has been a report of a putative molybdate transporter being cloned and characterised in *A. thaliana* (T. Fujiwara cited in Mendel, 2007). MoTR1 was identified through QTL analysis in the progeny of a cross between Col-O and Ler. A QTL identified on chromosome 2 was found to be linked to the accumulation of molybdenum in leaves. Within this region, the MoTR1 gene has been identified and surprisingly identified as a putative sulfate transporter. Unpublished reports also indicate that a T-DNA knock-out of MoTR1 disrupts molybdenum accumulation in Arabidopsis shoots, however there is no information on how this effects root molybdenum accumulation. This work supports our findings that sulfate transporters may be involved in molybdenum transport. This report has been confirmed with the discovery of a root specific molybdate transporter MOT1 (Tomatsu et. al., 2007) and simultaneous finding of MOT1 in *C. reinhardtii* (Tejada-Jimenex et. al., 2007) and a mitochondrially localised transporter (Baxter et. al., 2008).

## **6.4 Molybdenum transport and translocation of plants**

### **6.4.1 Molybdenum uptake in *Vitis vinifera***

Molybdenum uptake by roots and subsequent translocation to shoot tissues is poorly understood with most studies in plants having focussed at the shoot level (Stout and Meagher, 1948; Kannan and Ramani, 1978; Jongruaysup et. al., 1994). Kannan and Ramani (1978) demonstrated that when  $^{99}\text{MoO}_4^{2-}$  was fed onto a *P. vulgaris* primary leaf, most of the  $^{99}\text{MoO}_4^{2-}$  was transported towards the stem and into the root demonstrating that molybdenum was mobile. However, in *O. sativa* seedlings, the absorption and transport of molybdenum was influenced by the nutrient media culture with copper, chloride and sulfate inhibiting the absorption of molybdenum. Stout and Meagher (1948) also investigated molybdenum transport using  $^{99}\text{MoO}_4^{2-}$ . It was demonstrated using tomato plants that the roots accumulated molybdenum rapidly from the nutrient solution with translocation from the roots to the upper plant also taking place rapidly.

In Merlot, molybdenum deficiency is common amongst vines grown on own roots and in acid soils which limits molybdenum availability in the soil solution (Robinson and Burne, 2000; Gridley, 2003; Williams et. al., 2003; Williams et. al., 2004). Although this deficiency phenotype can be readily corrected by foliar molybdenum application, there has been little interest in determining the mechanism that initially causes the problem. It was originally hypothesised that Merlot may have a reduced or impaired root molybdenum transport system or alternatively problems in molybdenum translocation from root to shoot (Gridley, 2003). Little differences were found in molybdenum uptake between Merlot and Chardonnay (Figure 4.1 and 4.2), however both plants did accumulate more molybdenum when plants had previously been grown in the absence of molybdenum. As a result, there was no general trend of Merlot having reduced capacity to uptake molybdenum. It remains unclear exactly why Merlot suffers more predominantly from molybdenum deficiency compared to other varieties of grapevine. Although transport into the roots may not be a problem, a secondary transport mechanism may be involved such as loading into the xylem and translocation to the shoots and developing organs. This may also explain why grafting Merlot onto rootstocks overcomes molybdenum deficiency phenotypes (Gridley, 2003). Previous evidence suggests that in both Merlot and Chardonnay, molybdenum can be readily transported to other regions of the canopy (Brady, 2004). Brady (2004) observed that leaves painted with molybdenum could induce nitrate reductase activity in distant leaves on the same cane after a 24-hour period. This observation also confirms that a Moco mutation in Merlot can also be ruled out as Moco deficient plants show the pleiotropic loss of all Moco related enzymes, NR, XDH, SOX and AO which would result in plant death (Mendel and Schwarz, 1999). Previous work has demonstrated that molybdenum is mobile



within the plant system (Kannan and Ramani, 1978) however the 30-minute influx experiments completed in this study provided no evidence of root translocated  $^{99}\text{MoO}_4^{2-}$  in the shoot tissue above the woody cane. Other work has demonstrated that there is variability in phloem molybdenum mobility, which is dependent on the molybdenum status of the plant (Jongruaysup et. al., 1994). In molybdenum deficient *Vigna mungo* (Black gram) plants, molybdenum tended to be phloem immobile but then phloem mobile in all plant parts (except the stem) when plants were provided adequate amounts of molybdenum (Jongruaysup et. al., 1994).

#### **6.4.2 Molybdenum uptake in *Glycine max* symbiosomes**

Molybdenum is an essential element required for symbiotic nitrogen fixation. Nitrogen fixing bacterioids located in the nodules of legume species can fix atmospheric nitrogen ( $\text{N}_2$ ) to ammonia ( $\text{NH}_3$ ) through the activity of the bacterial enzyme nitrogenase. Nitrogenase is a two-component protein consisting of individual Fe and FeMo components. The FeMo component consists of at least 28 ions of Mo and is therefore a significant sink for molybdenum within the plant due to the large quantity of bacterioids per nodule. The plant mechanism supplying molybdenum to bacterioids is currently unknown. It is assumed that the process must rely upon molybdate import into symbiosomes through a transporter located on the PBM. Once in the PBS, bacterioids are assumed to readily take up molybdate using the *ModABC* molybdate transport system similar to that found in *E.coli* (Maier et. al., 1987; Maier and Graham, 1988; Delgado et. al., 2006). In the free-living state, the *ModABC* system is active however, little is known about whether this system still functions in the symbiotic state (Delgado et. al., 2006). Nevertheless, the supply of molybdenum from the plant to the bacterioids will be an important step to meet bacterioid nutritional requirements and to maintain nitrogen fixation to support plant growth.

Soybean symbiosomes were isolated from nodules of plants grown in the presence or absence of molybdenum from germination. In the minus molybdenum grown plants there was a clear increase in molybdenum uptake into symbiosomes compared to those grown normally in a full nutrient solution containing molybdenum (Figure 4.3). Uptake of  $^{99}\text{MoO}_4^{2-}$  was evident across both nM and  $\mu\text{M}$  ranges (Figure 4.4). This data may indicate a possible that a high-affinity molybdenum transport system is found on the PBM and most likely responsible for molybdenum flux into the PBS however the molecular mechanism for molybdenum transport across the PBM is unknown. Likely candidates for the transport

of molybdenum across the PBM include anion transporters such as those similar to SHST1. Recently, a sulfate transporter LjSST1 was identified in lotus nodules which is presumed responsible for sulfate transport across the PBM (Krusell et. al., 2005). As molybdenum can be transported by SHST1, it not unreasonable to expect that similar activities may also exist in SST1. In conclusion, molybdenum is transported across the PBM where the rate appears to be dependent on plant molybdenum status. It will be important to re-evaluate sulfate transporters found in nodules such as SST1 to examine their capacity for molybdenum transport especially since the discovery of MOT1.

### **6.5 The effects of foliar applied molybdenum on yield, yield components, quality parameters and petiole nutrient content in *Vitis vinifera* cv. Merlot**

Merlot grown on own roots in acidic soils frequently suffers from molybdenum deficiencies, which result in not only leaf size reduction, necrosis of the leaf edge, general chlorosis and stunted growth, but also altered berry development (Smart, 1992; Robinson and Burne, 2000) which results in reduced yields and profits for growers. Recent research has shown that these problems can be remedied by grafting Merlot onto rootstocks and also by applying molybdenum foliar sprays in spring prior to flowering (Robinson and Burne, 2000; Gridley, 2003; Williams et. al., 2003; Williams et. al., 2004). However little is known about the long-term consequences of repeated molybdenum application in the field over consecutive seasons and the impact it may have on plant growth, fruit yield and fruit quality.

#### **6.5.1 Molybdenum fertilisation and its effect on productivity in *Vitis vinifera* cv. Merlot**

A three-year field study was conducted to evaluate the growth and yield response of four Merlot cultivars to repeated and alternate year molybdenum spray applications. Previous research had determined that the vines chosen for this study were suffering from molybdenum deficiency as described in Williams et. al. (2004) and no corrective molybdenum foliar sprays had ever been applied to this site (Gridley, 2003). All control vines had molybdenum levels within the 0.05-0.09 mg/kg deficiency range throughout the trial (Figure 5.15 and 5.16) indicating that no new pools of molybdenum were being accessed by the plant roots within the soil profile. Application of molybdenum over 3 years (treatment 1) resulted in no cumulative effects of molybdenum within the vine (Figure 5.15 and 5.16). Subsequent treatments that did not receive molybdenum treatments each year resulted in decreasing molybdenum levels (Figure 5.15 and 5.16). This indicates that to

maintain adequate levels of molybdate within the plant system to remedy a molybdenum deficiency, the application of molybdenum will be required each year as redistribution from other plant parts including roots, trunk and cordon does not appear to occur.

### **6.5.2 Petiole nutrient content**

Petioles opposite developing flowers and/or bunches are commonly used as a measure of grapevine mineral nutrition status. Across the treatments in this study there were large fluctuations in petiole nitrogen (Figure 5.19 and 5.20), copper (Figure 5.21 and 5.22), iron, magnesium, phosphorous, and sodium (Appendix 3). Generally, levels were high in the first year, before decreasing in the second year and increasing again in the third year. It is unclear what exactly caused the large fluctuations in nutrient levels over the 3-year period, as changes were not correlated with molybdate foliar application. However, environmental conditions such as the reduction in rainfall and drought, which affected the field trial in years two and three (Figure 5.10) most likely contributed to the observed changes. Interestingly, no single Merlot clone showed different petiole nutrient profiles or changes in response to molybdenum application that could be related to an improved response to foliar molybdate application.

### **6.5.3 Yield and yield components responses to molybdenum sprays**

The foliar application of molybdenum to 4 clones of Merlot (D3V14, 8R, 6R and Q45-14) at E-L Stage 12 (Appendix 2) resulted in no significant yield increase over the 3-year trial. The general trend was actually an overall reduction in yields over the 3 years regardless of treatment which was most likely the result of increasing episodes of drought across the Kuyto area over this period (Figure 5.10). The only significant yield increase was measured in year 1 in clone D3V14 (Figure 5.4). D3V14 had an increase in bunch weight (Figure 5.6) despite control vines in all years being deficient in molybdenum. A small yield increase was also measured in year 3 in clone Q45-14 (Figure 5.4) and again was a result of an increase in bunch weight (Figure 5.6), but also an increase in berries per bunch (Figure 5.7) and rachis weight (Figure 5.9).

It is believed that the drought was an overriding factor in vine response to molybdenum treatments in this study. Previously it was thought that pre-existing molybdenum deficiency was a primary indicator for a potential positive yield response to molybdate foliar sprays (Williams et. al., 2003; Williams et. al., 2004). Clearly, this was not the case in this study and other parameters may be as equally important as the molybdenum status

of the plant, such as soil type, soil temperature, soil pH, climate and water availability when deciding whether molybdenum sprays are appropriate. As a result of this study it is important for growers to consider all factors when deciding to use molybdate sprays and pre-existing molybdenum deficiency may not be as a reliable indicator for yield increase as once thought.

#### **6.5.4 Quality parameters**

The application of molybdenum sprays had no effect on the quality parameters of sugars, colours, and pH of the grape juice. This study also indicated that there was no superior clone of Merlot amongst the four examined in terms of sugar, colour and pH that would be preferentially used in winemaking compared to others.

#### **6.6 Future research directions**

With the recent cloning of MOT1, a molybdate specific transporter with high homology what was originally thought to be the Group 5 sulfate transporters has opened the door to further research in this area. Although SHST1 has proved to be an effective molybdenum transport in a functional yeast screen, other sulfate transporters from plants are likely candidates for investigating molybdenum transport, such as those from Group 2, 3 and 4. A site-directed mutagenesis approach to mutagenise target amino acids could be used to determine if the same amino acid residues responsible for sulfate transport are also responsible for molybdenum transport could be considered for future work. Also further work characterising SHST1 *in planta* in order to determine how SHST1 contributes to plant molybdenum transport is required. However, initial research has suggested that SHST1 contributes little to molybdenum accumulation in Indian mustard transformed with the SHST1 gene (Lindblom et. al., 2006). LjSST1 may also be a likely candidate gene to investigate molybdenum transport across the PBM

Research into molybdenum transport may have been restricted due to necessity of using the radioactive isotope  $^{99}\text{Na}_2\text{MoO}_4^{2-}$  and the high costs associated with ICP-MS. This isotope is not only difficult to work with due to a short half-life and high  $\beta$  and  $\lambda$  emitting radiation, but also the extreme amounts of lead shielding required. However,  $^{99}\text{Na}_2\text{MoO}_4^{2-}$  is relatively inexpensive and accessible due to the large amounts produced for medical imaging. The use of a stable isotope of molybdate such as  $^{100}\text{Mo}$  or  $^{97}\text{Mo}$  as used by Turnland et. al. (1995) in relation to human molybdenum nutrition may also be helpful for experimental use. However, it is unclear as to the availability and costs of these isotopes

within Australia. The use of stable molybdenum isotopes will not only eliminate radiation but also allow for experiments that are more complex where short half-life and radiation dosage can hamper experimental progress. The use of stable isotopes would be especially useful in whole plant uptakes where plants may be kept for long periods of time and movement can be easily traced.

The discovery of MOT1 will further enhance our knowledge of molybdenum transport in plants. Future experiments may also focus on the expression of MOT1 homologues in *Vitis*. Q-PCR experiments could examine the expression of MOT1 in Merlot compared to other varieties that do not suffer with molybdenum deficiency. This could possibly confirm whether Merlot has a molybdenum transport problem.

### **6.7 Conclusion**

This research has contributed to our understanding plant molybdenum transport at both the gene and whole plant level. Though a specific molybdenum transporter was not identified, a pre-characterised gene, SHST1 proved to be an effective transporter of molybdenum at nM concentrations. This is the first known report of a plant sulfate transporter also transporting molybdenum in higher plants. Secondly, a high-affinity molybdenum transport system allowing molybdenum to cross the PBM has also been characterised. Although specific soybean genes were not identified, it is highly probable through the evidence gained with SHST1, that a sulfate transport protein may also be involved to facilitate the movement of molybdenum across the PBM.

Merlot does not lack the capacity to transport molybdenum, but problems with subsequent translocation may exist resulting in limited molybdenum within the upper sections of the plant system. This was also demonstrated when redistribution of molybdenum was not found to occur from storage organs such as trunks and roots after foliar applications of molybdenum.

Although this research has contributed to the overall understanding of molybdenum transport and nutrition in plants, additional questions remain as to existence of specific molybdenum transporters within grapevine.

## Bibliography

---

Adams, J., Burmester, C. and Mitchell, C. (1990). Long-term fertility treatments and molybdenum availability. *Fertilizer Research* 21: 167-179.

Agarwala, S., Chatterjee, C., Sharma, P., Sharma, C. and Nautiyal, N. (1979). Pollen development in maize plants subjected to molybdenum deficiency. *Canadian Journal of Botany* 57: 1946-1950.

Alhendawi, R. A., Kirkby, E. A. and Pilbeam, D. J. (2005). Evidence that sulfur deficiency enhances molybdenum transport in xylem sap of tomato plants. *Journal of Plant Nutrition* 28: 1347-1353.

Anderson, J., Huprikar, S., Kochian, L., Lucas, W. and Gaber, R. (1992). Functional Expression of a Probable *Arabidopsis thaliana* Potassium Channel in *Saccharomyces cerevisiae*. *PNAS* 89(9): 3736-3740.

Anderson, L. A., McNairn, E., Lubke, T., Pau, R. N. and Boxer, D. H. (2002). ModE-dependent, molybdate regulation of the molybdenum cofactor operon *moa* in *Escherichia coli* (vol 182, pg 7035, 2000). *Journal of Bacteriology* 184(15): 4326-4326.

Antipov, A., Lyalikova, N., Khijniak, T. and L'vov, N. (1998). Molybdenum-free nitrate reductases from vanadate-reducing bacteria. *Febs Letters* 441: 257-260.

Aravind, L. and Koonin, E. V. (2000). The STAS domain-a link between anion transporters and antisigma-factor antagonists. *Current Biology* 10(2): R53-R55.

Baxter, I. R., Muthukumar, B., Park, H., Buchner, P., Lahner, B., Danku, J., Lee, J., Hawkesford, M. J., Guerinot, M. L. and Salt, D. E. (2008). Variation in molybdenum content across broadly distributed populations of *Arabidopsis thaliana* is controlled by a mitochondrial molybdenum transporter (*MOT1*). *PLoS Genetics* 4(2): e1000004. doi:10.1371/journal.pgen.1000004.

Benedito, V. A., Dai, X., He, J., Zhao, P. and Udvardi, M. K. (2006). Functional genomics of plant transporters in legume nodules. *Functional Plant Biology* 33: 731-736.

- Brady, J. N. (2004). The uptake and assimilation of nitrate in *Vitis vinifera* cv. Merlot. School of Agriculture and Wine. Adelaide, The University of Adelaide.
- Breton, A. and Surdin-Kerjan, Y. (1977). Sulfate uptake in *Saccharomyces cerevisiae*: Biochemical and genetic study. *Journal of Bacteriology* 132(1): 224-232.
- Buchner, P., Takahashi, H. and Hawkesford, M. J. (2004). Plant sulphate transporters: coordination of uptake, intracellular and long distance transport. *Journal of Experimental Botany* 55(404): 1765-1773.
- Campbell, W. H. (1999). Nitrate reductase structure, function and regulation: bridging the gap between biochemistry and physiology. *Annual Review of Plant Physiology and Plant Molecular Biology* 50: 277-303.
- Cardin, C. J. and Mason, J. (1975). Sulphate transport by rat ileum-effect of molybdate and other anions. *Biochimica Et Biophysica Acta* 394: 46-54.
- Chatterjee, C. and Nautiyal, N. (2001). Molybdenum stress affects viability and vigour of wheat seeds. *Journal of Plant Nutrition* 24(9): 1377-1386.
- Cherest, H., Davidian, J., Thomas, D., Benes, V., Anson, W. and Surdin-Kerjan, Y. (1997). Molecular characterization of two high affinity sulfate transporters in *Saccharomyces cerevisiae*. *Genetics* 145: 627-635.
- Chipmann, E. W., Mackay, D., Gupta, U. and Cannon, H. B. (1970). Response of cauliflower cultivars to molybdenum deficiency. *Canadian Journal of Plant Science* 50: 163-167.
- Christiansen, J., Dean, D. R. and Seefeldt, L. C. (2001). Mechanistic features of the Mo-containing nitrogenase. *Annual Review of Plant Physiology and Plant Molecular Biology* 52(269-295).
- Cox, D. A. (1992a). Foliar applied molybdenum for preventing or correcting molybdenum deficiency of Poinsettia. *HortScience* 27(8): 894-895.

- Cox, D. A. (1992b). Poinsettia cultivars differ in their response to molybdenum deficiency. *HortScience* 27(8): 892-893.
- Crawford, N. M. (1995). Nitrate: nutrient and signal for plant growth. *The Plant Cell* 7: 859-868.
- Dawson, P. A., Pirlo, K. J., Steane, S. E., Nguyen, K. A., Kunzelmann, K., Chien, Y. J. and Markovich, D. (2005). The rat Na<sup>+</sup>-sulfate cotransporter rNaS2: functional characterization, tissue distribution and gene (*scl13a4*) structure. *Pflungers Arch* 450: 262-268.
- Day, D. A. and Udvardi, M. K. (1997). Metabolite transport across symbiotic membranes of legume nodules. *Annual Review of Plant Physiology and Plant Molecular Biology* 48: 493-523.
- Delgado, M. J., Tresierra-Ayala, A., Talbi, C. and Bedmar, E., J (2006). Functional characterisation of the *Bradyrhizobium japonicum* *modA* and *modB* genes involved in molybdenum transport. *Microbiology* 152: 199-207.
- Deng, M., Moureaux, T. and Caboche, M. (1989). Tungstate, a molybdate analogue inactivating nitrate reductase, deregulates the expression of the nitrate reductase structural gene. *Plant Physiology* 91: 304-309.
- Dudev, T. and Lim, C. (2004). Oxyanion selectivity in sulfate and molybdate transport proteins; An ab Initio/CDM study. *Journal of the American Chemical Society* 126: 10296-10305.
- Eilers, T., Gunter, S., Brinkmann, H., Witt, C., Richter, T., Nieder, J., Koch, B., Hille, R., Hansch, R. and Mendel, R. (2001). Identification and biochemical characterisation of *Arabidopsis thaliana* sulfite oxidase. *Journal of Biological Chemistry* 276(50): 46989-46994.
- Elliot, B. and Mortenson, L. (1975). Transport of molybdate by *Clostridium pasteurianum*. *Journal of Bacteriology* 124(3): 1295-1301.



- Elliot, B. and Mortenson, L. (1976). Regulation of molybdate transport by *Clostridium pasteurianum*. *Journal of Bacteriology* 127(3): 770-779.
- Frommer, W. B. and Ninnemann, O. (1995). Heterologous expression of genes in bacterial, fungal, animal, and plant cells. *Annual Reviews of Plant Physiology and Plant Molecular Biology* 46: 419-444.
- Gartrell, J. W. (1966). Field responses of cereals to molybdenum. *Nature* 209: 1050.
- Graham, L. and Maier, J. A. (1987). Variability in molybdenum uptake activity in *Bradyrhizobium japonicum* strains. *Journal of Bacteriology* 169(6): 2555-2560.
- Gridley, K. L. (2003). Honours thesis. The effects of molybdenum as a foliar spray on fruit set and berry size in *Vitis vinifera* cv. Merlot. School of Agriculture and Wine. Adelaide, The University of Adelaide.
- Grunden, A. M., Self, W. T., Villain, M., Blalock, J. E. and Shanmugam, K. T. (1999). An analysis of the binding of repressor protein ModE to modABCD (Molybdate transport) operator/promoter DNA of *Escherichia coli*. *Journal of Biological Chemistry* 274(34): 24308-24315.
- Gupta, U., Ed. (1997). Introduction to molybdenum in agriculture. Molybdenum in Agriculture. Cambridge, Cambridge University Press.
- Habili, N., Bongfiglioli, R. and Symons, B. (1998). The trouble with Merlot. *The Australian Grapegrower and Winemaker* Annual technical issue: 29-32.
- Hale, K. L., McGrath, S. P., Lombi, E., Stack, S. M., Terry, N., Pickering, I. J., George, G. N. and Pilon-Smits, E. A. H. (2001). Molybdenum sequestration in Brassica species. A role for anthocyanins? *Plant Physiology* 126(4): 1391-1402.
- Hathaway, S. (2006). 2006 South Australian winegrape utilisation and pricing survey, Phylloxera and Grape Industry Board of South Australia.

- Hawkesford, M. J., Davidian, J. and Grignon, C. (1993). Sulphate/proton cotransport in plasma-membrane vesicles isolated from roots of *Brassica napus* L.: increased transport in membranes isolated from sulphur-starved plants. *Planta* 190: 297-304.
- Heimer, Y., Wray, J. and Filner, P. (1969). The effect of tungstate on nitrate assimilation in higher plant tissues. *Plant Physiology* 44: 1197-1199.
- Herridge, D. J. (1977). Carbon and nitrogen nutrition of two annual legumes. Perth, University of Western Australia.
- Heuwinkel, H., Kirkby, E., Le Bot, J. and Marschner, H. (1992). Phosphorus deficiency enhances molybdenum uptake by Tomato plants. *Journal of Plant Nutrition* 15(5): 549-568.
- Hewitt, E. and Gundry, C. (1970). The molybdenum requirement of plants in relation to nitrogen supply. *Journal of Horticultural Science* 45: 351-358.
- Hille, R. (2003). Plants have SOX: The structure of sulfite oxidase from *Arabidopsis thaliana*. *Structure* 11: 1189-1197.
- Hoaglands, D. R. and Arnon, D. I. (1938). The water culture method for growing plants without soil. *Univ. Calif. Coll. Agric. Exp. Sta. Circ. Berkeley*: 347-353.
- Iland, P., Ewart, A., Sitters, J., Markides, A. and Bruer, N. (2000). *Techniques for chemical analysis and quality monitoring during winemaking*. Adelaide, Patrick Iland Wine Promotions.
- Imperial, J., Hadi, M. and Amy, N. K. (1998). Molybdate binding by ModA, the periplasmic component of the *Escherichia coli* mod molybdate transport system. *Biochimica Et Biophysica Acta-Biomembranes* 1370(2): 337-346.
- Invitrogen (2003). CloneMiner cDNA Library Construction Kit Manual. Version B.
- Invitrogen (2006). pDONR222 Vector map, Invitrogen Corporation. 2006.

- Jahn, T. P. and Moller, A. L. B. (2004). Aquaporin homologues in plant and mammals transport ammonia. *Febs Letters* 574(1-3): 31-36.
- Jongruaysup, S., Dell, B. and Bell, R. W. (1994). Distribution and redistribution of molybdenum in Black Gram (*Vigna mungo* L. Hepper) in relation to molybdenum supply. *Annals of Botany* 73: 161-167.
- Kaiser, B. N., Finnegan, P. M., Tyerman, S. D., Whitehead, L. F., Bergersen, F. J., Day, D. A. and Udvardi, M. K. (1998). Characterisation of an ammonium transport protein from the peribacteroid membrane of soybean nodules. *Science* 281(5380): 1202-1206.
- Kaiser, B. N., Gridley, K. L., Ngaire Brady, J., Phillips, T. and Tyerman, S. D. (2005). The role of molybdenum in agricultural plant production. *Annals of Botany (London)* 96(5): 745-754.
- Kannan, S. and Ramani, S. (1978). Studies on molybdenum absorption and transport in bean and rice. *Plant Physiology* 62: 179-181.
- Kouchi, H. and Shingo, H. (1993). Isolation and characterisation of novel nodulin cDNAs representing genes expressed at early stages of soybean development. *Molecular & General Genetics* 238: 106-119.
- Krusell, L., Krause, K., Ott, T., Desbrosses, G., Kramer, U., Sata, S., Nakamura, Y., Tabata, S., James, E. K., Sandal, N., Stougaars, J., Masayoshi, M., Miyamoto, A., Sugauma, N. and Udvardi, M. K. (2005). The sulfate transporter SST1 is crucial for symbiotic nitrogen fixation in *Lotus japonicus* root nodules. *The Plant Cell* 34: 454.
- Lawrence, C. (1991). Classical mutagenesis techniques. *Methods in enzymology* 194: 273-281.
- Lawson, D. M., Willimas, C. E. M., Mitchenall, L. A. and Pau, R. N. (1998). Ligand size is a major determinant of specificity in periplasmic oxyanion-binding proteins: the 1.2Å resolution crystal structure of *Azobacter vinelandii* ModA. *Structure* 6: 1529-1539.

- Leustek, T., Martin, M. N., Bick, J. and Davies, J. P. (2000). Pathways and regulation of sulfur metabolism revealed through molecular and genetic studies. *Annual Review of Plant Physiology and Plant Molecular Biology* 51: 141-165.
- Lindblom, S. D., Abdel-Ghany, S., Hanson, B. R., Hwang, S., Terry, N. and Pilon-Smits, E. A. H. (2006). Constitutive expression of a high-affinity sulfate transporter in Indian Mustard affects metal tolerance and accumulation. *Journal of Environmental Quality* 35: 726-733.
- Llamas, A., Kalakoutskii, K. L. and Fernandez, E. (2000). Molybdenum cofactor amounts in *Chlamydomonas reinhardtii* depend on the Nit5 gene function related to molybdate transport. *Plant Cell and Environment* 23(11): 1247-1255.
- Lyon, C. B. and Beeson, K. C. (1948). Influence of toxic concentrations of micro-nutrient elements in the nutrient medium on vitamin content of tomatoes and turnip. *Botanical Gazette*: 506-520.
- Maier, J. A., Graham, L., Keefe, R. G., Pihl, T. and Smith, E. (1987). *Bradyrhizobium japonicum* mutants defective in nitrogen fixation and molybdenum metabolism. *Journal of Bacteriology* 169(6): 2548-2554.
- Maier, R. J. and Graham, L. (1988). Molybdate transport by *Bradyrhizobium japonicum* bacteroids. *Journal of Bacteriology* 170(12): 5613-5619.
- Markovich, D., Regeer, R. R., Kunzelmann, K. and Dawson, P. A. (2005). Functional characterization and genomic organization of the human Na<sup>+</sup>-sulfate cotransporter hNaS2 gene (*SLC13A4*). *Biochemical and Biophysical Research Communications* 326: 729-734.
- Marschner, H. (1995). *Mineral nutrition of higher plants*. New York, Academic Press.
- Maruyana-Nakahita, A., Nakamura, Y., Yamaya, T. and Takahashi, H. (2004). Regulation of high-affinity sulfate transporters in plants: towards systematic analysis of sulphur signalling and regulation. *Journal of Experimental Botany* 55(404): 1843-1849.

- Maupin-Furlow, J., Rosentel, J., Lee, J., Deppenmeier, U., Gunsalus, R. and Shanmugan, K. (1995). Genetic analysis of the *modABCD* (molybdate transport) operon of *Escherichia coli*. *Journal of Bacteriology* 177(17): 4851-4856.
- McNicholas, P. M. and Gunsalus, R. P. (2002). The molybdate-responsive *Escherichia coli* ModE transcriptional regulator coordinates periplasmic nitrate reductase (napFDAGHBC) operon expression with nitrate and molybdate availability. *Journal of Bacteriology* 184(12): 3253-3259.
- McNicholas, P. M., Mazzotta, M. M., Rech, S. A. and Gunsalus, R. P. (1998). Functional dissection of the molybdate-responsive transcription regulator, ModE, from *Escherichia coli*. *Journal of Bacteriology* 180(17): 4638-4643.
- Mendel, R. (2007). Biology of the molybdenum cofactor. *Journal of Experimental Botany* Advance Access published March 9, 2007, doi:10.1093/jxb/erm024.
- Mendel, R. and Schwarz, G. (1999). Molybdoenzymes and molybdenum cofactor in plants. *Critical Reviews in Plant Sciences* 18(1): 33-69.
- Mendel, R. R. (1997). Molybdenum cofactor of higher plants: biosynthesis and molecular biology. *Planta* 203(4): 399-405.
- Mendel, R. R. and Bittner, F. (2006). Cell biology of molybdenum. *Biochimica Et Biophysica Acta* 1763: 621-635.
- Mendel, R. R. and Hansch, R. (2002). Molybdoenzymes and molybdenum cofactor in plants. *Journal of Experimental Botany* 53(375): 1689-1698.
- Miyauchi, S., Srinivas, S. R., Fei, Y.-J., Gopal, E., Umapathy, N. S., Wang, H., Conway, S. J., Ganapathy, V. and Prasad, P. D. (2006). Functional characteristics of NaS2, a placenta-specific Na<sup>+</sup>-coupled transporter for sulfate and oxyanions of the micronutrients selenium and chromium. *Placenta* 27: 550-559.
- Mouncey, N. J., Mitchenall, L. A. and Pau, R. N. (1995). Mutational analysis of genes of the *mod* locus involved in molybdenum transport, homeostasis and processing in *Azobacter vinelandii*. *Journal of Bacteriology* 177(18): 5294-5302.

- Nagarajah, S. (1999). A petiole sap test for nitrate and potassium in Sultana grapevines. *Australian Journal of Grape and Wine Research* 5: 56-60.
- Neubauer, H., Pantel, I., Lindgren, P. E. and Gotz, F. (1999). Characterization of the molybdate transport system ModABC of *Staphylococcus carnosus*. *Archives of Microbiology* 172(2): 109-115.
- Palmgren, M. and Harper, J. (1999). Pumping with plant P-type ATPases. *Journal of Experimental Botany* 50(Special issue): 883-893.
- Pasricha, N. S., Nayyar, V. K., Randhawa, N. S. and Sinha, M. K. (1977). Influence of sulphur fertilization on suppression of molybdenum uptake by berseem (*Trifolium alexandrinum* L.) and oats (*Avena sativa* L.) grown on molybdenum toxic soils. *Plant and Soil* 46: 245-250.
- Pateman, J. A., Cove, D. J., Rever, B. M. and Roberts, D. B. (1964). A common co-factor for nitrate reductase and xanthine dehydrogenase which also regulates the synthesis of nitrate reductase. *Nature* 201: 58-60.
- Pau, R. N. and Lawson, D. M. (2002). Transport, homeostasis, regulation and binding of molybdate and tungstate to proteins. *Metal Ions Biological System* 30: 31-74.
- Peterson, G. L. (1977). *Analytical Biochemistry* 83(346-356).
- Phillips, T. (2004). Molybdenum nutrition of *Vitis vinifera* cv. Merlot-foliar absorption, translocation and an enzymic assay for deficiency. School of Agriculture and Wine. Adelaide, The University of Adelaide.
- Rae, A. L., Cybinski, D. H., Jarmey, J., M. and Smith, F. W. (2003). Characterization of two phosphate transporters from barley; evidence for diverse function and kinetic properties among members of the Pht1 family. *Plant Molecular Biology* 53: 27-36.
- Rech, S. A., Wolin, C. and Gunsalus, R. (1996). Properties of the periplasmic ModA molybdate-binding protein of *Escherichia coli*. *Journal of Biological Chemistry* 271(5): 2557-2562.

Reddy, K., Munn, L. and Wang, L., Eds. (1997). Chemistry and mineralogy of molybdenum in soils. Molybdenum in agriculture. Cambridge, Cambridge University Press.

Reuter, D. and Robinson, B. (1997). *Plant analysis - an interpretation manual*. Australia, CSIRO publishing.

Robinson, B. and Burne, P. (2000). Another look at the Merlot problem-could it be a molybdenum deficiency? *The Australian Grapegrower and Winemaker Annual Technical Issue 2000*: 21-22.

Rosentel, J., Healy, F., Maupin-Furlow, J., Lee, J. and Shanmugam, K. (1995). Molybdate and regulation of *mod* (molybdate transport) *fdhF*, and *hyc* (formate hydrogenlyase) operons in *Echerichia coli*. *Journal of Bacteriology* 177(17): 4857-4864.

Rouached, H., Berthomieu, P., Kassis, E. E., Cathala, N., Catherinot, V., Labesse, G., Davidian, J. and Fourcroy, P. (2005). Structural and functional analysis of the C-terminal STAS (Sulfate Transporter and Anti-sigma Antagonist) domain of the *Arabidopsis thaliana* sulfate transporter SULTR1.2. *Journal of Biological Chemistry* 280(16): 15976-15983.

Saito, K. (2004). Sulfur assimilatory metabolism. The Long and smelling road. *Plant Physiology* 136: 2443-2450.

Schneider, K., Muller, A., Johannes, K., Diemann, E. and Kottmann, J. (1991). Selective removal of molybdenum traces from growth media of N<sub>2</sub>-fixing bacteria. *Analytical Biochemistry* 193: 292-298.

Self, W. T. (2002). Regulation of purine hydroxylase and xanthine dehydrogenase from *Clostridium purinolyticum* in response to purines, selenium, and molybdenum. *Journal of Bacteriology* 184(7): 2039-2044.

Self, W. T., Grunden, A. M., Hasona, A. and Shanmugam, K. T. (1999). Transcriptional regulation of molybdoenzyme synthesis in *Escherichia coli* in response to molybdenum: ModE-molybdate, a repressor of the modABCD (molybdate transport) operon is a

secondary transcriptional activator for the hyc and nar operons. *Microbiology-Uk* 145: 41-55.

Self, W. T., Grunden, A. M., Hasona, A. and Shanmugam, K. T. (2001). Molybdate transport. *Research in Microbiology* 152(3-4): 311-321.

Shaked, A. and Bar-Akiva, A. (1967). Nitrate reductase activity as an indication of molybdenum level and requirement of citrus plants. *Phytochemistry* 6: 347-350.

Sharma, S., Pareek, O. P. and Kaushik, R. A. (1995). Shot berry development in grapes-a review. *Agricultural Review* 16(4): 175-185.

Shelden, M. C., Loughlin, P., Tierney, M. L. and Howitt, S. M. (2001). Proline residues in two tightly coupled helices of the sulfate transporter, SHST1, are important for sulfate transport. *Biochemistry Journal* 356: 589-594.

Shelden, M. C., Loughlin, P., Tierney, M. L. and Howitt, S. M. (2003). Interactions between charged amino acid residues within transmembrane helices in the sulfate transporter SHST1. *Biochemistry* 42: 12941-12949.

Shibagaki, N. and Grossman, A. R. (2004). Probing the function of STAS domain of the Arabidopsis sulfate transporters. *Journal of Biological Chemistry* 279(29): 30791-30799.

Shibagaki, N. and Grossman, A. R. (2006). The role of the STAS domain in the function and biogenesis of a sulfate transporter as probed by random mutagenesis. *Journal of Biological Chemistry* 281(32): 22964-22973.

Silva, A. P., Rosa, A. and Hanklaus, S. H. (2003). Influence of foliar boron application in fruit set and yield of Hazelnut. *Journal of Plant Nutrition* 26(3): 561-569.

Smart, R. (1992). Merlot disorder in the Hunter Valley. *The Australian Grapegrower and Winemaker Annual Technical Issue*: 122-126.

Smith, F. W. (2002). The phosphate uptake mechanism. *Plant and Soil* 245: 105-114.



Smith, F. W., Ealing, P. M., Hawkesford, M. J. and Clarkson, D. T. (1995a). Plant members of sulfate transporters reveal functional subtypes. *Proceeding of the National Academy of Sciences USA* 92(9373-9377).

Smith, F. W., Hawkesford, M. J., Prosser, I. M. and Clarkson, D. T. (1995b). Isolation of a cDNA from *Saccharomyces cerevisiae* that encodes a high affinity sulphate transporter at the plasma membrane. *Molecular General Genetics* 247: 709-715.

Smith, F. W., Mudge, S., R., Rae, A. L. and D, G. (2003). Phosphate transport in plants. *Plant and Soil* 248: 71-83.

Smith, F. W., Rae, A. L. and Hawkesford, M. J. (2000). Molecular mechanisms of phosphate and sulphate transport in plants. *Biochimica Et Biophysica Acta-Biomembranes* 1465(1-2): 236-245.

Smith, K. S., Balistrieri, L. S., Smith, S. M. and Severson, R. C., Eds. (1997). Distribution and mobility of molybdenum in the terrestrial environment. Molybdenum in Agriculture. Cambridge, Cambridge University Press.

Srivastava, P. C., Ed. (1997). Biochemical significance of molybdenum in crop plants. Molybdenum in agriculture. Cambridge, Cambridge University Press.

Stout, P. R. and Meagher, W. R. (1948). Studies of the molybdenum nutrition of plants with radioactive molybdenum. *Science* 108: 471-473.

Stout, P. R., Meagher, W. R., Pearson, G. A. and Johnson, C. M. (1951). Molybdenum nutrition of crop plants. *Plant and Soil III* 1: 51-87.

Takahashi, H., Wantanabe-Takahashi, A., Smith, F. W., Blake-Kalff, M., Hawkesford, M. J. and Saito, K. (2000). The roles of 3 functional sulphate transporters involved in uptake and translocation of sulphate in *Arabidopsis thaliana*. *The Plant Journal* 23(2): 171-182.

Tassie, E. and Freeman, B. M. (1992). Pruning. Viticulture - Practices. Coombe, B. and Dry, P. Adelaide, Winetitles. Vol 2: 85-103.

- Tejada-Jimenez, M., Llamas, A., Sanz-Laue, E., Galvan, A. and Fernandez, E. (2007). A high-affinity molybdate transporter in eukaryotes. *Proceeding of the National Academy of Sciences USA* 104(50): 20126-20130.
- Thiel, T., Pratte, B. and Zahalak, M. (2002). Transport of molybdate in the cyanobacterium *Anabaena variabilis* ATCC 29413. *Archives of Microbiology* 179(1): 50-56.
- Tomatsu, H., Takano, J., Takahashi, H., Wantanabe-Takahashi, A., Shibagaki, N. and Fujiwara, T. (2007). An *Arabidopsis thaliana* high-affinity molybdate transporter required for efficient uptake of molybdate from soil. *Proceeding of the National Academy of Sciences USA* 104(47): 18807-18812.
- Turnland, J. R., Keyes, W. R., Peiffer, G. L. and Chiang, G. (1995). Molybdenum absorption, excretion, and retention studies with stable isotopes in young men during depletion and repletion. *American Journal of Clinical Nutrition* 61: 1102-1109.
- Tweedi, J. W. and Segel (1970). Specificity of transport process for sulfur, selenium and molybdenum anions by filamentous fungi. *Biochimica Et Biophysica Acta* 196: 95-106.
- Vieira, R. F., Cardoso, E., Vieira, C. and Cassini, S. T. A. (1998a). Foliar application of molybdenum in common bean. III. Effect on nodulation. *Journal of Plant Nutrition* 21(10): 2153-2161.
- Vieira, R. F., Vieira, C., Cardoso, E. and Mosquim, P. R. (1998b). Foliar application of molybdenum in common bean. II. Nitrogenase and nitrate reductase activities in a soil of low fertility. *Journal of Plant Nutrition* 21(10): 2141-2151.
- Villora, G., Moreno, D. A. and Romero, L. (2002a). Phosphorous supply influences the molybdenum, nitrate and nitrate reductase activity in eggplant. *Journal of Horticultural Science and Biotechnology* 77(3): 305-309.
- Villora, G., Moreno, D. A. and Romero, L. (2002b). Response of eggplant to nitrogen supply: molybdenum-nitrate relationships. *Biologia Plantarum* 45(4): 621-623.

- Wang, G., Angermuller, S. and Klipp, W. (1993). Characterization of *Rhodobacter capsulatus* genes encoding a molybdenum transport system and putative molybdenum-pterin-binding proteins. *Journal of Bacteriology* 175(10): 3031-3042.
- Weig, A. R. and Jakob, C. (2000). Functional identification of glycerol permease activity of *Arabidopsis thaliana* NLM1 and NLM2 protein by heterologous expression in *Saccharomyces cerevisiae*. *Febs Letters* 481(3): 293-298.
- Weinkoop, S. and Saalbach, G. (2003). Proteome analysis. Novel proteins identified at the peribacteroid membrane of *Lotus japonicus* root nodules. *Plant Physiology* 131: 1080 - 1090.
- Williams, C. M. J., Bartlett, L. and Lange, C. (2003). Molybdenum may improve fruit set. *Australian Viticulture* March-April: 31-33.
- Williams, C. M. J., Maier, N. A. and Bartlett, L. (2004). Effect of molybdenum foliar sprays on yield, berry size, seed formation and petiolar nutrient composition of 'Merlot' grapevines. *Journal of Plant Nutrition* 27: 1891-1916.
- Williams, R. J. P. and Frausto da Silva, J. J. R. (2002). The involvement of molybdenum in life. *Biochemical and Biophysical Research Communications* 292: 293-299.
- Yu, M., Hu, C. and Wang, Y. (1999). Influences of seed molybdenum and molybdenum application on nitrate reductase activity, shoot dry matter, and grain yields of winter wheat cultivars. *Journal of Plant Nutrition* 22(9): 1433-1441.
- Yu, M., Hu, C. and Wang, Y. (2002). Molybdenum efficiency in winter wheat cultivars as related to molybdenum uptake and distribution. *Plant and Soil* 245: 287-293.
- Zahalak, M., Pratte, B., Werth, K. J. and Thiel, T. (2004). Molybdate transport and its effect on nitrogen utilization in the cyanobacterium *Anabaena variabilis* ATCC 29413. *Molecular Microbiology* 51(2): 539-549.

## Appendix 1 – cDNA inserts identified in the library screen on Low S and Low Mo media

**Table 1. cDNA inserts which complemented YSD1 on Low S Gal media.**

Plasmid DNA was isolated from YSD1 cells and transformed into *E.coli* and then purified. Isolated cDNA's were then transformed back into new YSD1 cells and re-plated onto Low S media containing either galactose or glucose media to regulate gene expression. cDNA inserts were then sequenced and putative homologous proteins identified using BlastX (NCBI). NS= not sequenced due to size similarity to other cDNA's.

Plasmid #	cDNA insert size after BsrG1 digest	Sequence ID	# of times isolated	Putative function /homology	Accession number	E value
LS KG1	850 bp	KG27	1	<i>Helianthus annuus</i> GTP binding protein	AAM12880	5e-99
LS KG3	1.65 Kb	KG28	1	<i>A. thaliana</i> ABNORMAL SUPPRESSOR SUS2	NP_178124	1e-138
LS KG 4 LS KG 7 LS KG 15 LS KG17 LS KG18 LS KG 21 LS KG 22 LS KG 23 LS KG 24 LS KG 26	750 bp 750 bp 750 bp 800 bp 800 bp 800 bp 800 bp 800 bp 800 bp 800 bp	KG30 KG34 NS KG40 NS NS NS NS NS NS	10	<i>Quercus suber</i> Metallothionine like protein	CAC39481	6e-11
LS KG 5 LSKG 8 LS KG 9 LS KG 10 LS KG 11 LS KG 12 Ld KG 13 LS KG 34	1.9 Kb 900 bp 1.9Kb 1.35 Kb 1.95 Kb 1.95 Kb 1.95 Kb 1.35 Kb	KG33 KG35 KG37 KG38 NS NS NS NS	8	<i>A. thaliana</i> Amino acid permease LHT1	NP_851109	2e-101
LS KG 6	1.55 Kb	KG31	1	<i>Oryza sativa</i> Os02g0557300 HRD ubiquitin ligase complex ER membrane	NP_001047138	2e-37

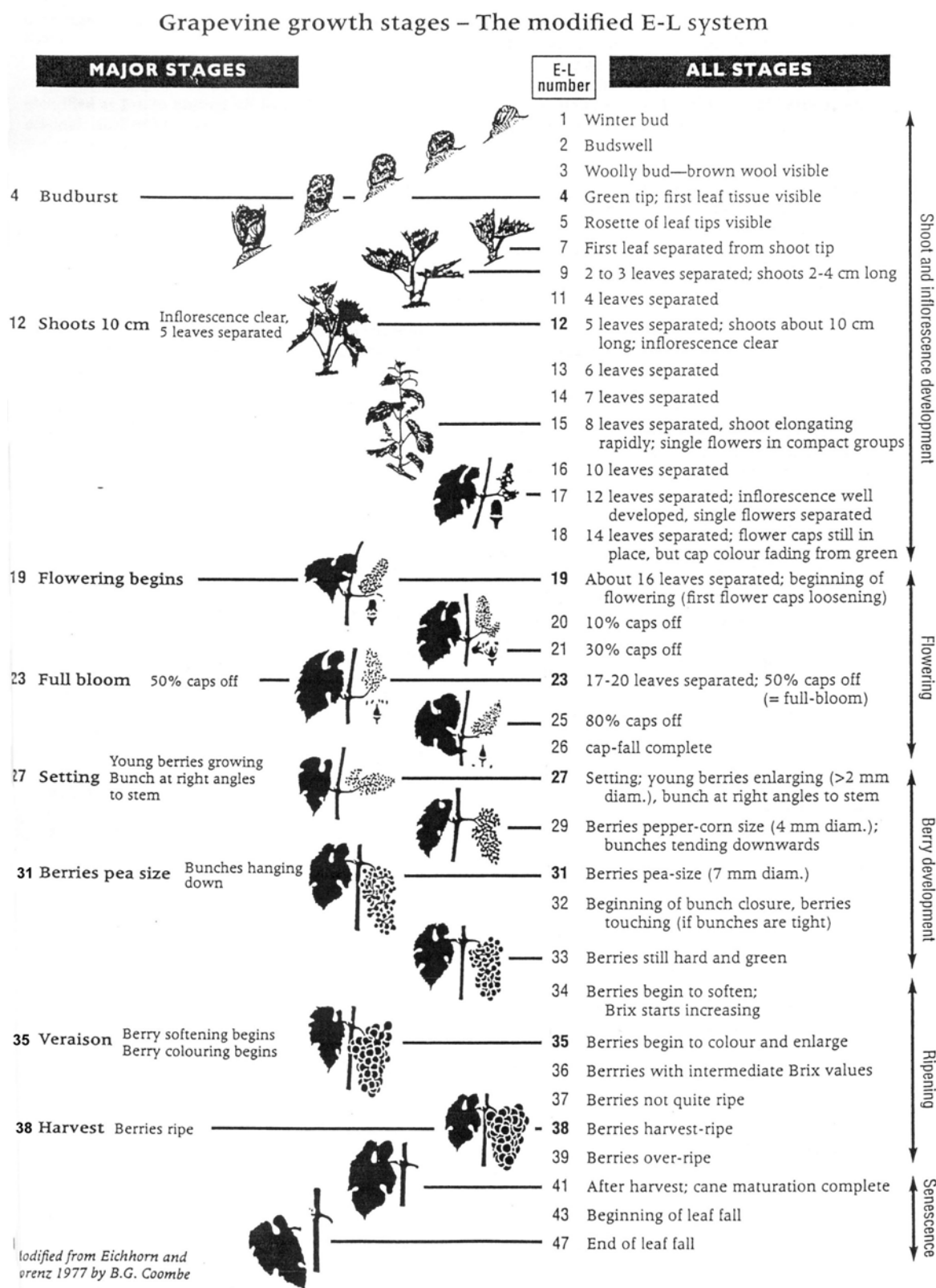
				RING-finger domain compenent		
LS KG 14	2.65 Kb	KG39	1	<i>Nicoitiana tabacum</i> Cellulose synthase like protein Cs1G	AAZ79231	2e-67
LS KG 20	600 bp	KG41	1	<i>Medicago truncatula</i> RING-type/Zinc finger	ABE82278	5e-36
LS KG 25	1.25 Kb	KG44	1	<i>Theobroma cacao</i> preprotein translocase SedY	DQ448876.1	5e-61
LS KG 29	950 bp	KG45	1	<i>A. thaliana</i> unknown protein	AAM65942.1	4e-53
LS KG 30	1.05 Kb	KG46	1	<i>N. tabacum</i> mRNA for protein kinase Ck2 regulatory sub unit 2 (ck2 beta 2 gene)	AJ488194.1	7e-94
LS KG 31 LS KG 35	1.75 Kb 1.75 Kb	KG48 NS	2	<i>Populus tremula</i> x <i>Populus tremuloides</i> sinapyl alcohol dehydrogenase like protein	AAW45741	7e-91
LS KG 36	1.65 Kb	-	1	<i>M. trunculata</i> Conserved hypothetical protein	ABE81298	1e-17
LS KG 38	750 bp	KG50	1	<i>M. trunculata</i> Pathogenesis related protein	ABE85366	8e-63
LS KG 39	1 Kb	KG51	1	<i>A. thaliana</i> unknown protein	NP_566709	2e-28

**Table 2. cDNA inserts which complemented YSD1 on Low Mo Gal media.**

Plasmid DNA was isolated from YSD1 cells and transformed into *E.coli* and then purified. Isolated cDNA's were then transformed back into new YSD1 cells and re-plated onto Low Mo media containing either galactose or glucose media to regulate gene expression. cDNA inserts were then sequenced and putative homologous proteins identified using BlastX (NCBI). NS= not sequenced due to size similarity to other cDNA's.

Plasmid #	cDNA insert size after BsrG1 digest	Sequence ID	Putative function /homology	Accession number	E score
LMO KG 1	1 Kb	KG55	<i>M. truncatula</i> Cyclin-like F-box; Galactosidoxidase, central	ABE907081	6e-45
LMO KG 4	1.15 Kb	KG56	<i>Prunus persica</i> major latex-like protein (PP-MLP1)	AAK14060.1	2e-38
LMO KG 5	250 bp	NS	-	-	-
LMO KG 7	1.45 Kb	KG58	<i>M. truncatula</i> Zinc finger;RING type PHD type	ABE80612	4e-42
LMO KG 9	1.1 Kb	KG59	<i>Arachis hypogaea</i> Translationally controlled tumor like protein	AB184255	3e-78
LMO KG 10	1 Kb	KG60	<i>Z. mays</i> PCO063017 mRNA sequence	AY105916	1.4e
LMO KG 11	1.15 Kb	KG61	<i>V.vinifera</i> osmotin-like protein	CAA71883.1	4e-113
LMO KG 12	750 bp	KG62	<i>O. sativa</i> hypothetical protein OsI-014741	EAY93508	2e-22

## Appendix 2. Modified E-L growth stages of grapevine.



### Appendix 3. Additional petiole nutrient data.

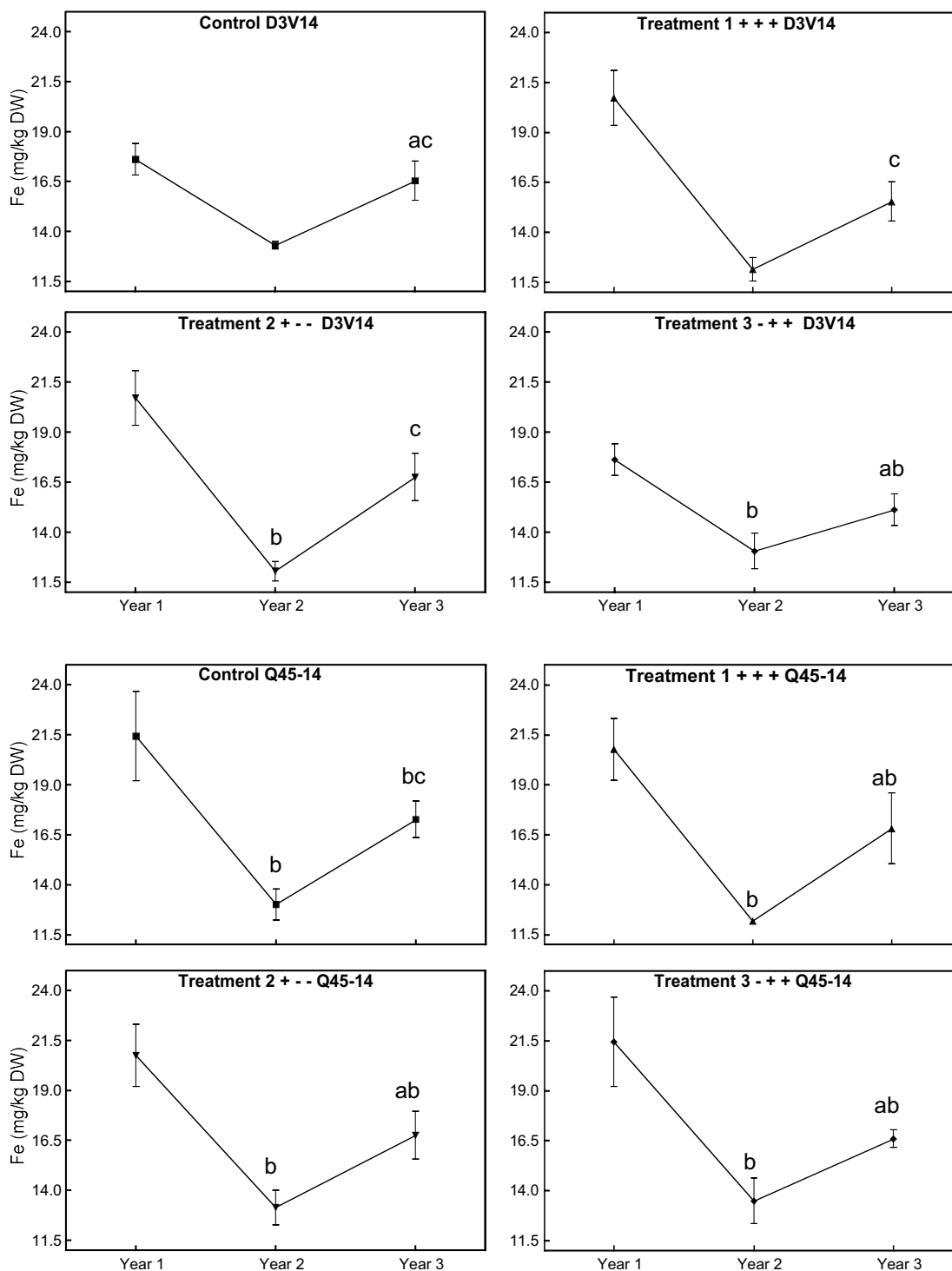


**Figure A3.1 Mean Fe (mg/kg DW) concentration in petioles at 50 – 80% flowering for clones D3V14 and Q45-14 over the 3 years of the trial. Adequate levels of Fe occur at >30 mg/kg Dw (Reuter and Robinson, 1997).**

Values are mean  $\pm$  SEM (n=3-4). Results with the same letter are not significantly different.



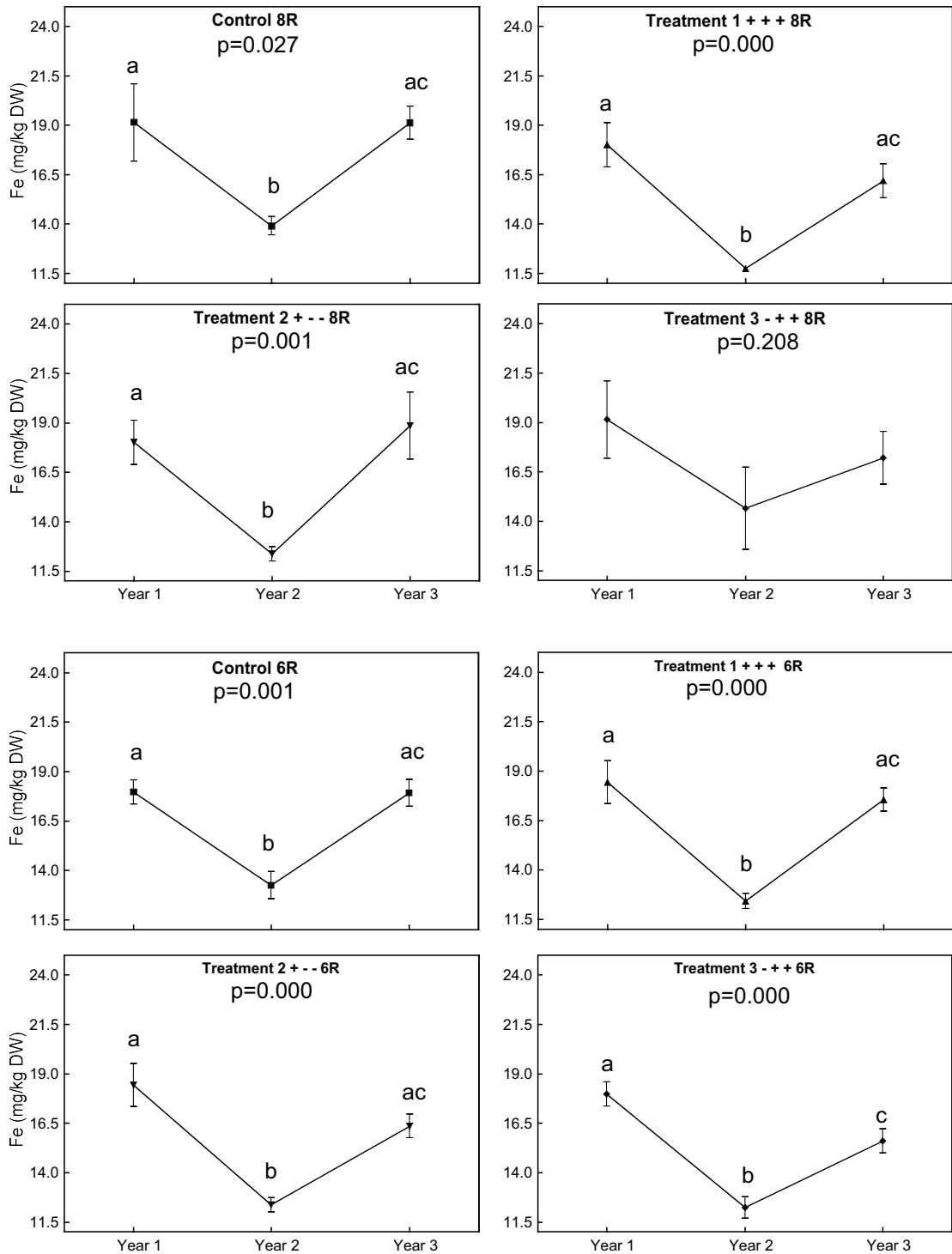


**Figure A3.2 Mean Fe (mg/kg DW) concentration in petioles at 50 – 80% flowering for clones 8R and 6R over the 3 years of the trial. Adequate levels of Fe occur at >30 mg/kg DW (Reuter and Robinson, 1997).**

Values are mean  $\pm$  SEM (n=3-4). Results with the same letter are not significantly different.

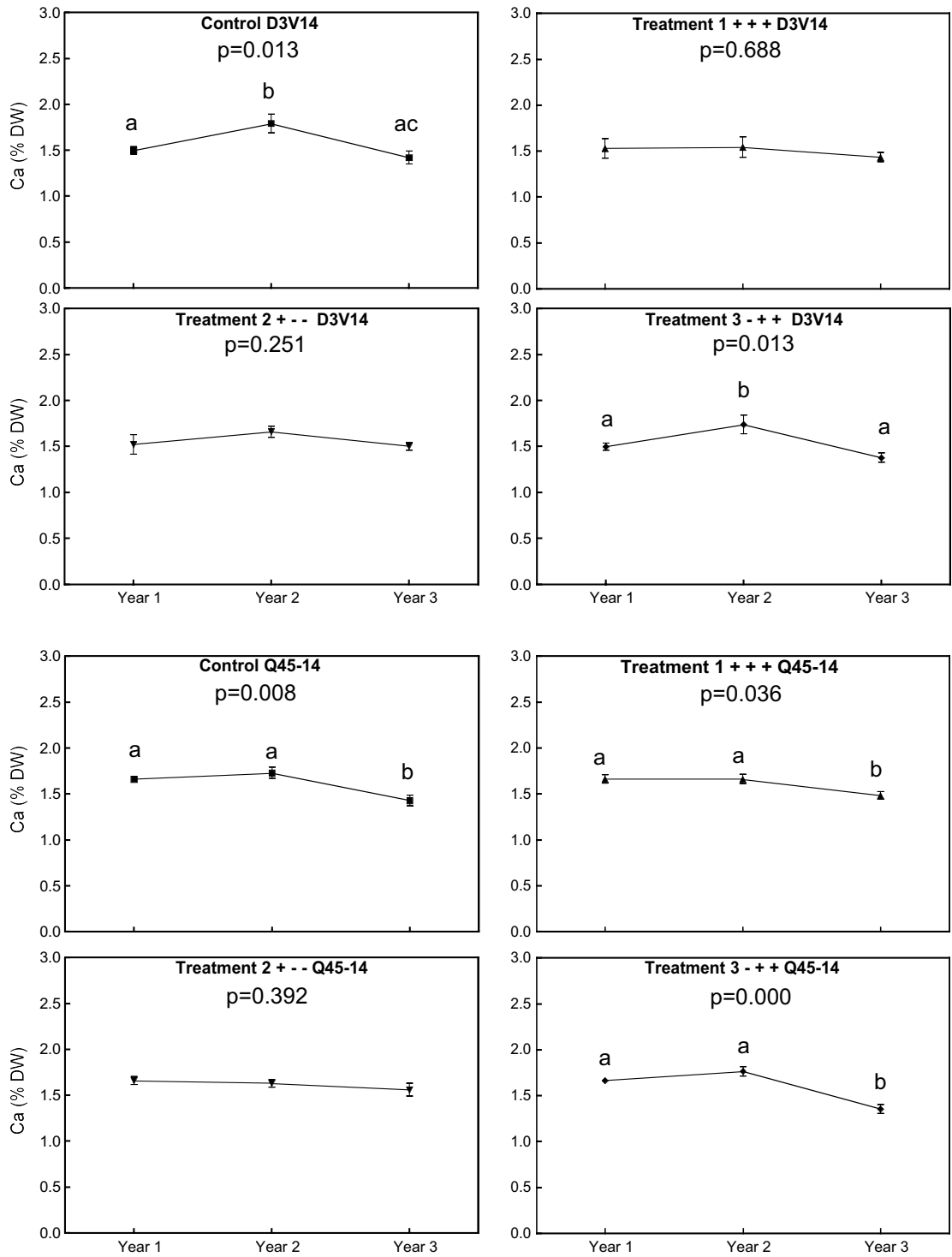


**Figure A3.3 Mean Ca (% DW) concentration in petioles at 50 – 80% flowering for clones D3V14 and Q45-14 over the 3 years of the trial. Adequate levels of Ca occur between 1.2 – 2.5% DW (Reuter and Robinson, 1997).**

Values are mean  $\pm$  SEM (n=3-4). Results with the same letter are not significantly different.

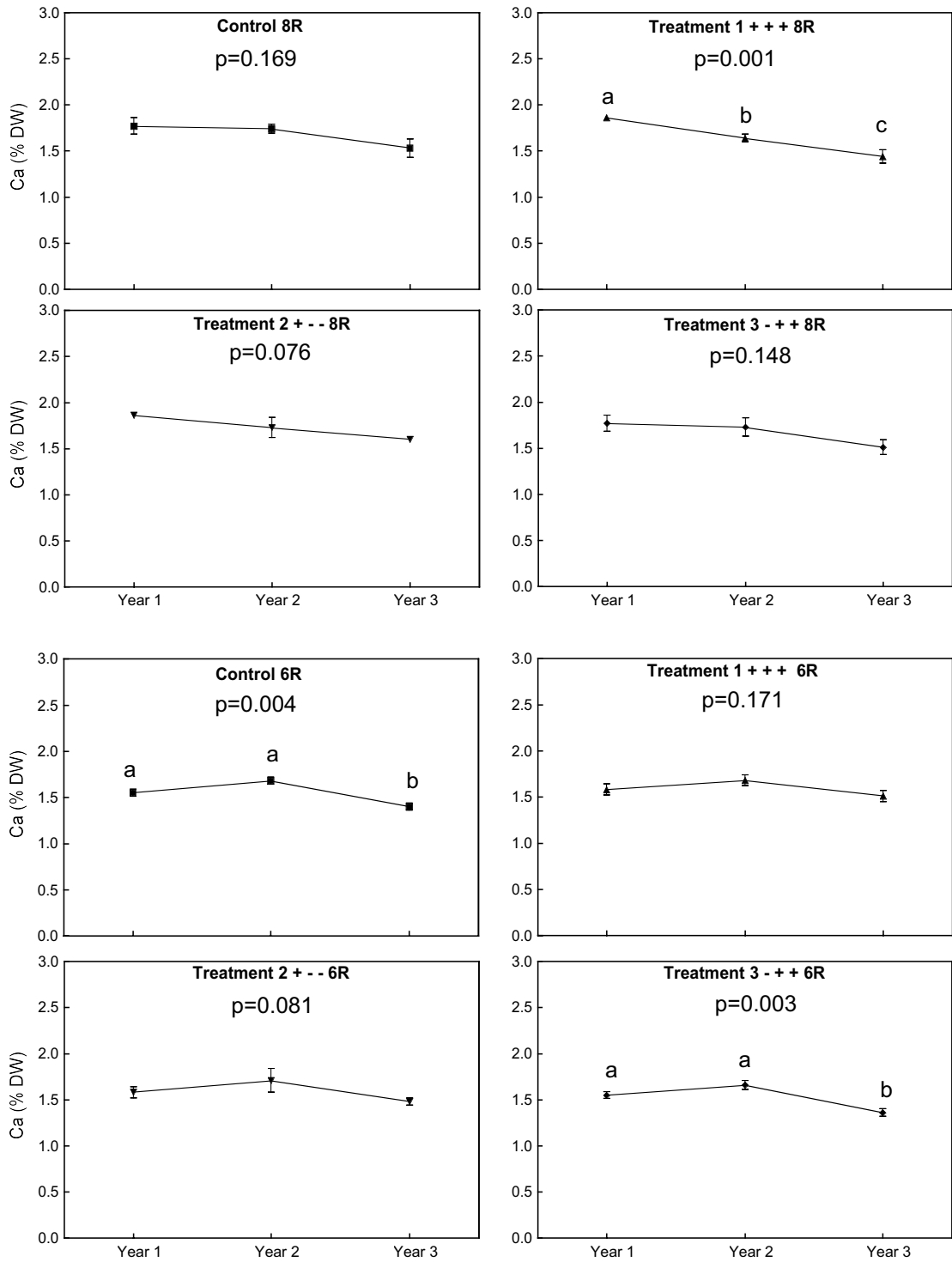


**Figure A3.4 Mean Ca (% DW) concentration in petioles at 50 – 80% flowering for clones 8R and 6R over the 3 years of the trial. Adequate levels of Ca occur between 1.2 – 2.5% DW (Reuter and Robinson, 1997).**

Values are mean  $\pm$  SEM (n=3-4). Results with the same letter are not significantly different.

**Table A3.1 Clonal differences between the treatments for calcium petiole concentrations in year 1 of the trial.**

Differences are at the 5% levels and only significant data is presented.

<b>Year</b>	<b>Treatment</b>	<b>Clone X is significantly different to clone Y</b>	<b>Clone Y is significantly different to clone X</b>	<b>P value (0.05 level)</b>
<b>Year 1</b>	Control	D3V14	Q45-14	0.048
			8R	0.003
		Q45-14	D3V14	0.045
		8R	D3V14	0.003
	Treatment 1	D3V14	8R	0.033
			Q45-14	8R
		8R	D3V14	0.003
			Q45-14	0.033
	Treatment 2	D3V14	8R	0.003
			Q45-14	8R
		8R	D3V14	0.003
			Q45-14	0.033
	Treatment 3	D3V14	Q45-14	0.048
			8R	0.003
		6R	8R	0.011

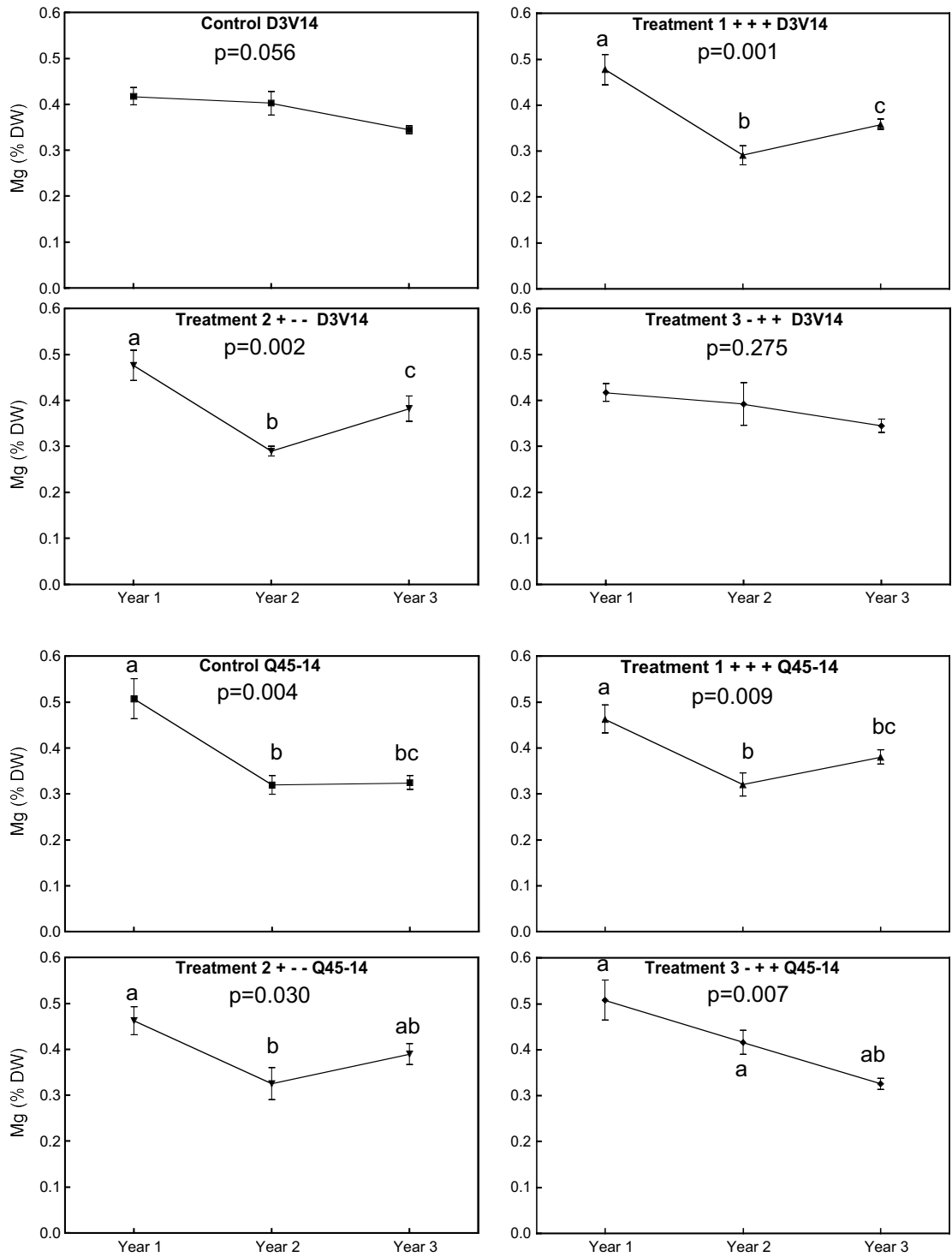


**Figure A3.5 Mean Mg (% DW) concentration in petioles at 50 – 80% flowering for clones D3V14 and Q45-15 over the 3 years of the trial. Adequate levels of Mg occur between at >0.4 % DW (Reuter and Robinson, 1997).**

Values are mean  $\pm$  SEM (n=3-4). Results with the same letter are not significantly different.

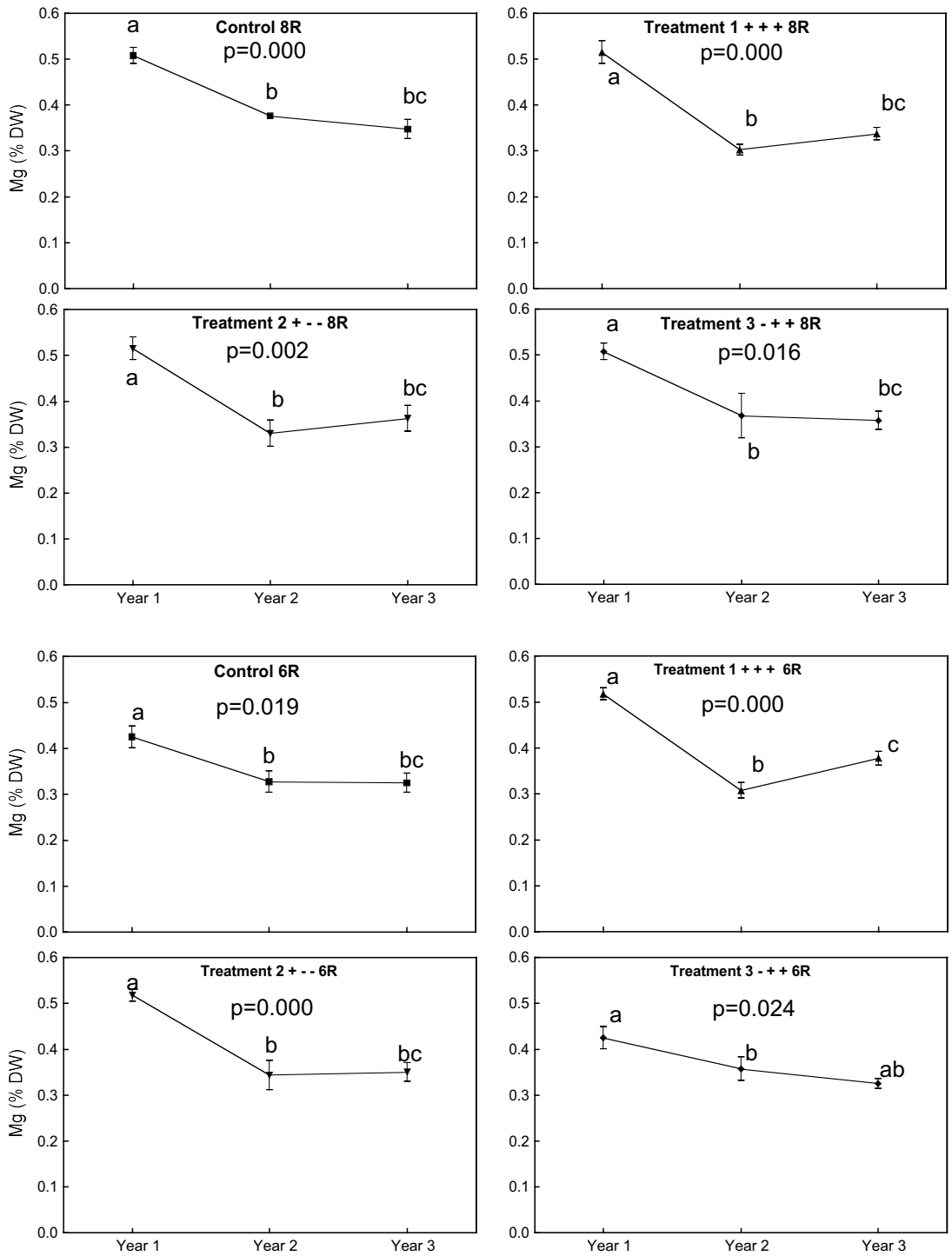


**Figure A3.6 Mean Mg (% DW) concentration in petioles at 50 – 80% flowering for clones 8R and 6R over the 3 years of the trial. Adequate levels of Mg occur between at >0.4 % DW (Reuter and Robinson, 1997).**

Values are mean  $\pm$  SEM (n=3-4). Results with the same letter are not significantly different.

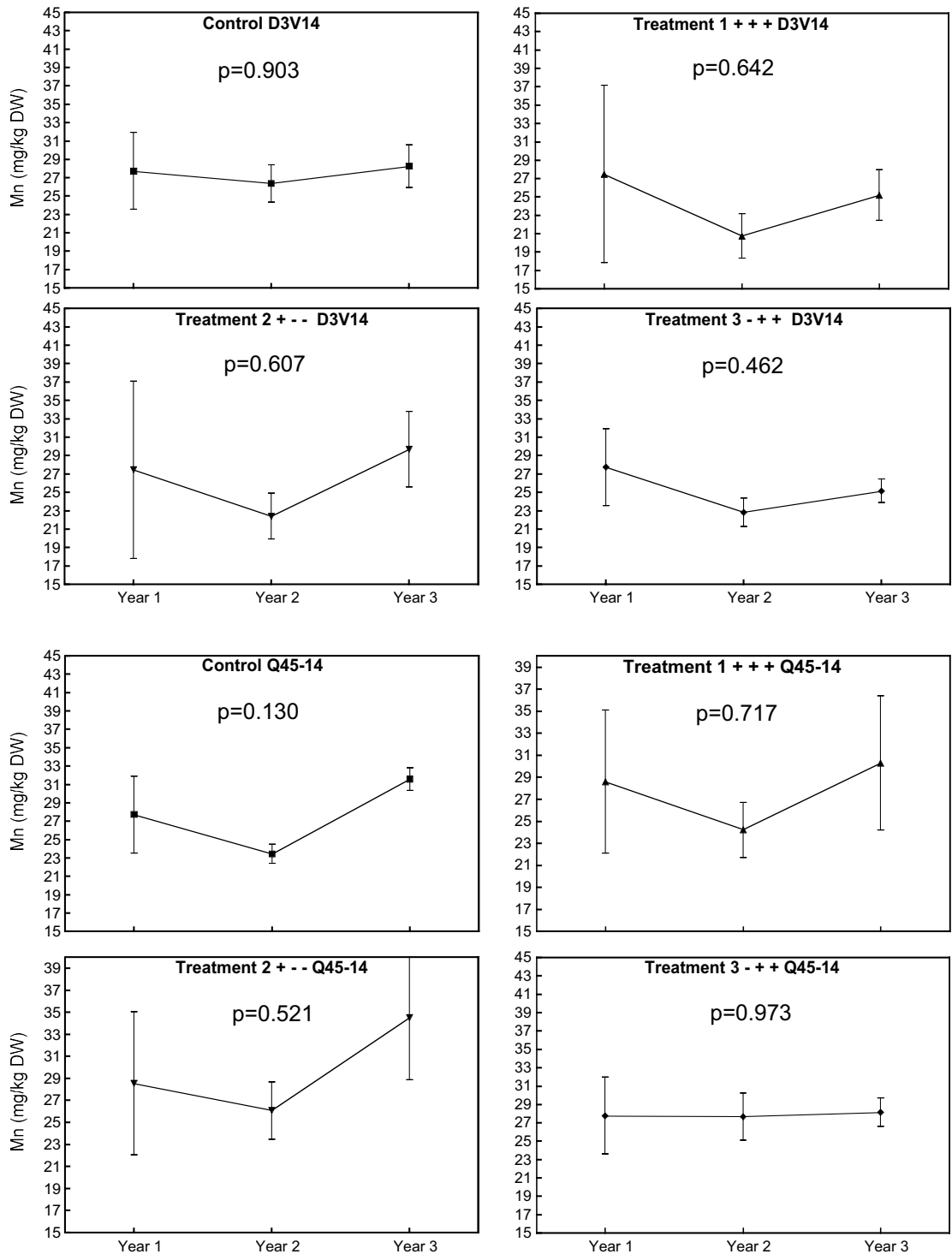


**Figure A3.7 Mean Mn (% DW) concentration in petioles at 50 – 80% flowering for clones D3V14 and Q45-14 over the 3 years of the trial. Adequate levels of Mn occur between 30 – 60 mg/kg DW (Reuter and Robinson, 1997).**

Values are mean  $\pm$  SEM (n=3-4). Results with the same letter are not significantly different.

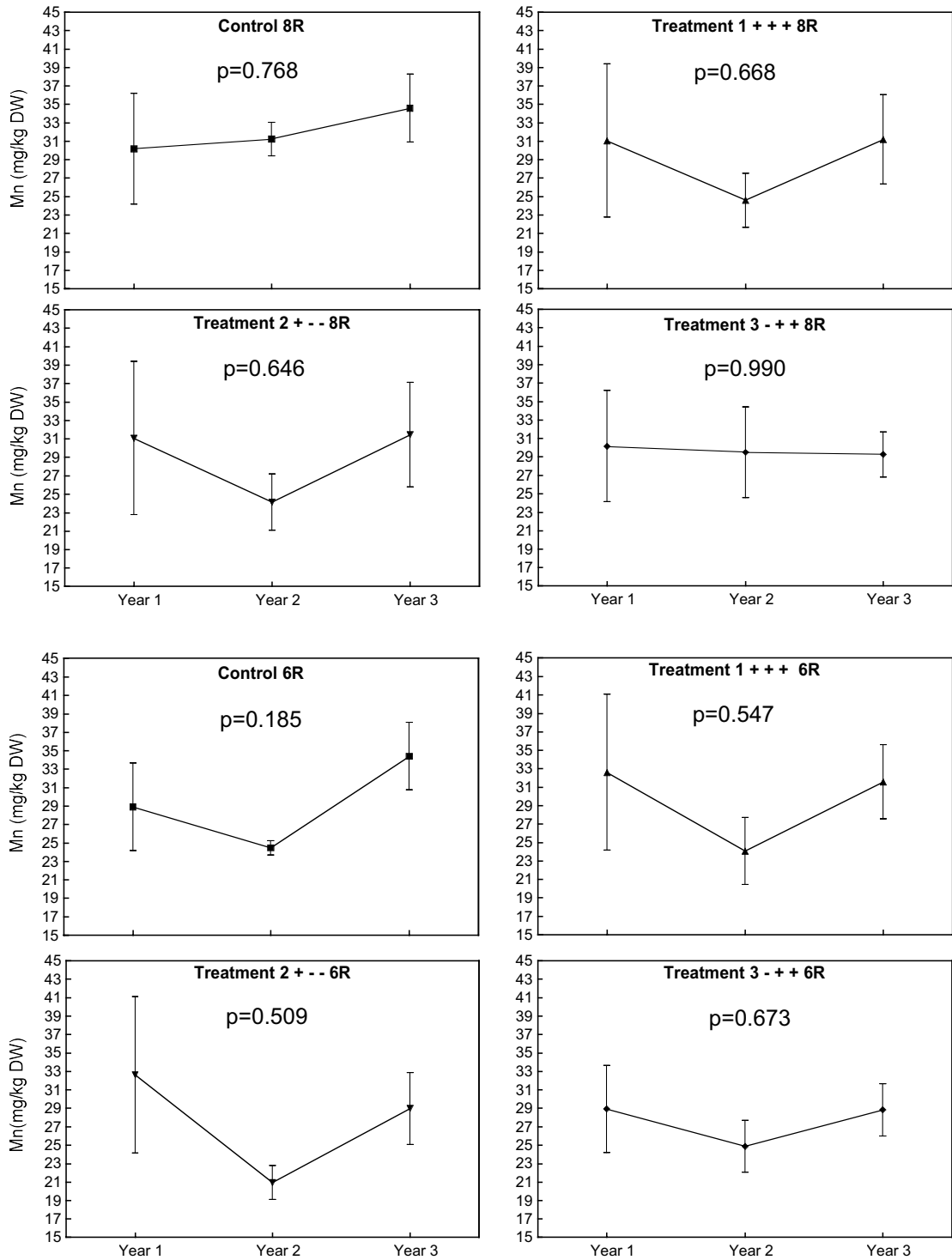


**Figure A3.8 Mean Mn (mg/kg DW) concentration in petioles at 50 – 80% flowering for clones 8R and 6R over the 3 years of the trial. Adequate levels of Mn occur between 30 – 60 mg/kg DW (Reuter and Robinson, 1997).**

Values are mean  $\pm$  SEM (n=3-4). Results with the same letter are not significantly different.



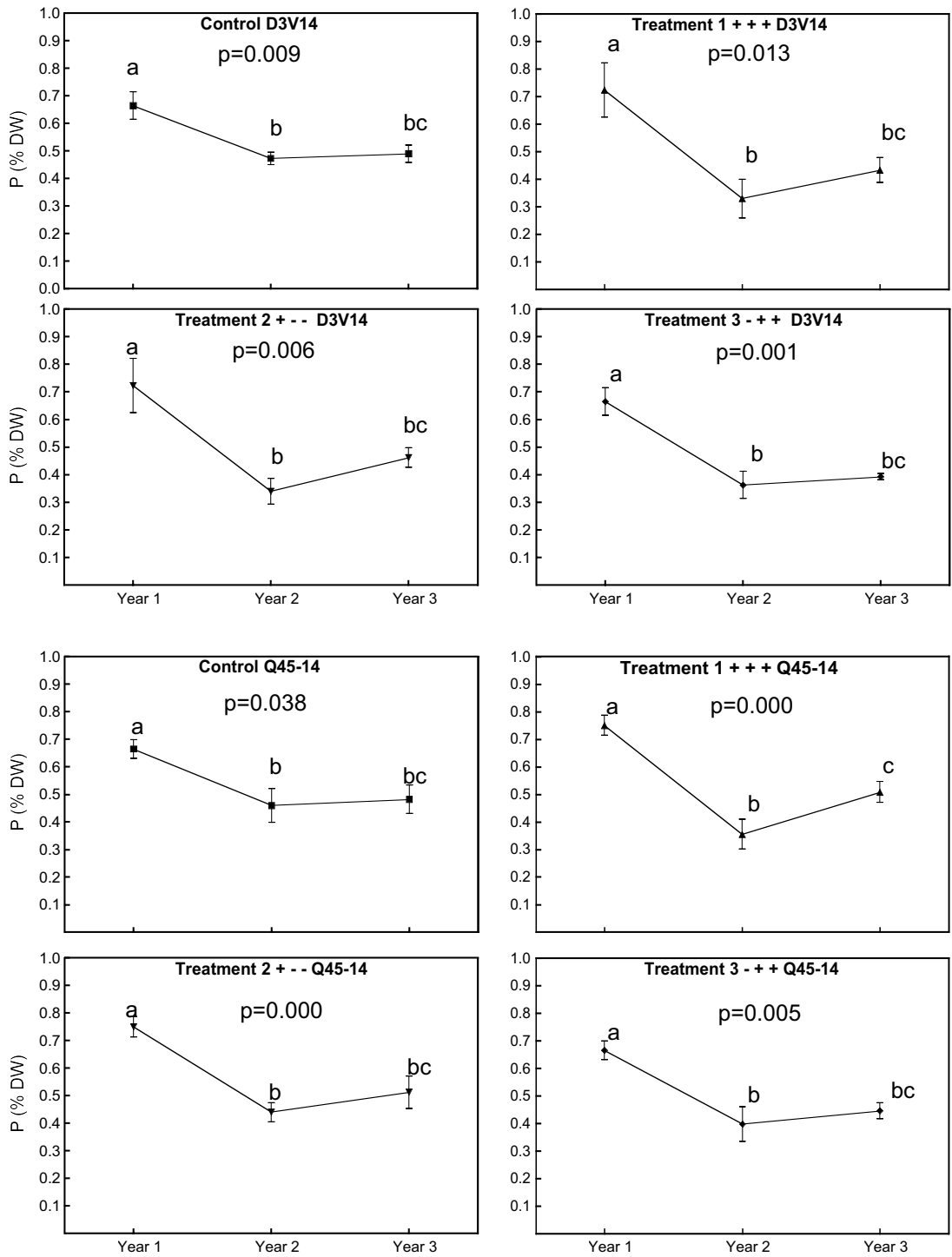


**Figure A3.9 Mean P (% DW) concentration in petioles at 50 – 80% flowering for clones D3V14 and Q45-14 over the 3 years of the trial. Adequate levels of P occur at between 0.25 – 0.5 % DW (Reuter and Robinson, 1997).**

Values are mean  $\pm$  SEM (n=3-4). Results with the same letter are not significantly different.

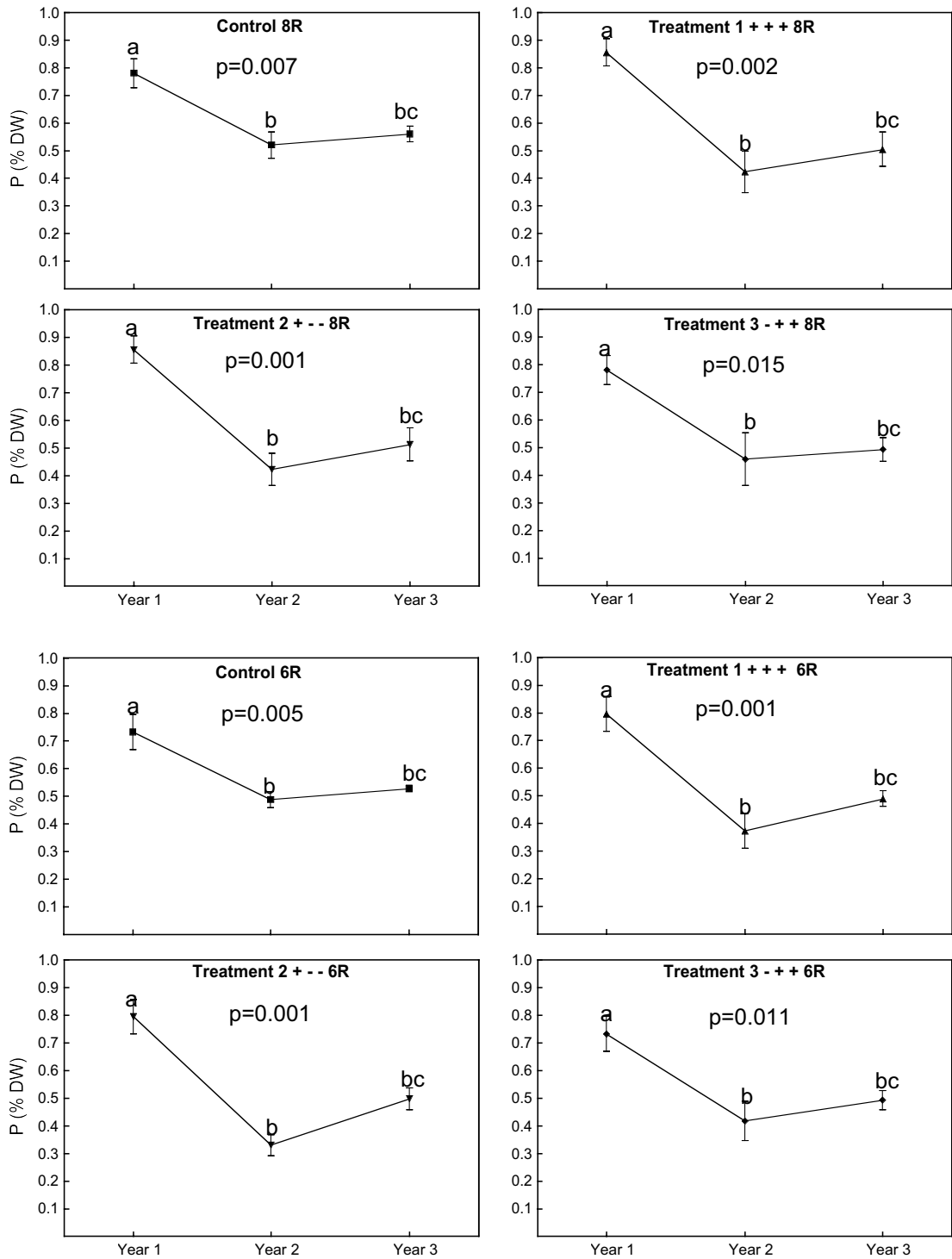


**Figure A3.10 Mean P (% DW) concentration in petioles at 50 – 80% flowering for clones 8R and 6R over the 3 years of the trial. Adequate levels of P occur at between 0.25 – 0.5 % DW (Reuter and Robinson, 1997).**

Values are mean  $\pm$  SEM (n=3-4). Results with the same letter are not significantly different.

**Table A3.2 Clonal differences between the years and treatment for phosphorous petiole concentrations in year 3 of the trial.**

<b>Year</b>	<b>Treatment</b>	<b>Clone X is significantly different to clone Y</b>	<b>Clone Y is significantly different to clone X</b>	<b>P value (0.05 level)</b>
<b>Year 3</b>	Treatment 3	D3V14	8R	0.045
			6R	0.045

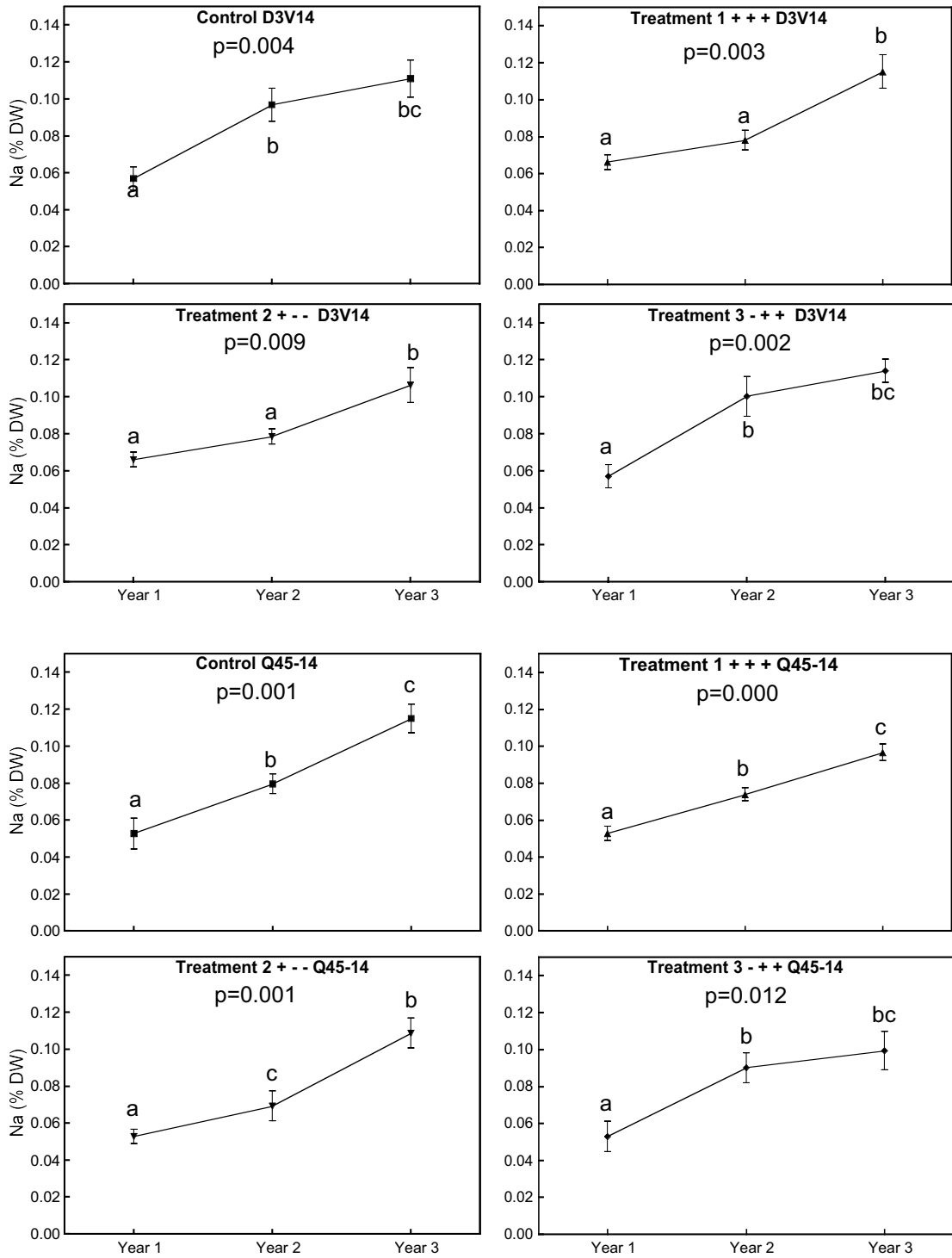


**Figure A3.11 Mean Na (% DW) concentration in petioles at 50 – 80% flowering for clones D3V14 and Q45-14 over the 3 years of the trial. Toxic levels of Na occur at 0.5 % DW (Reuter and Robinson, 1997).**

Values are mean  $\pm$  SEM (n=3-4). Results with the same letter are not significantly different.

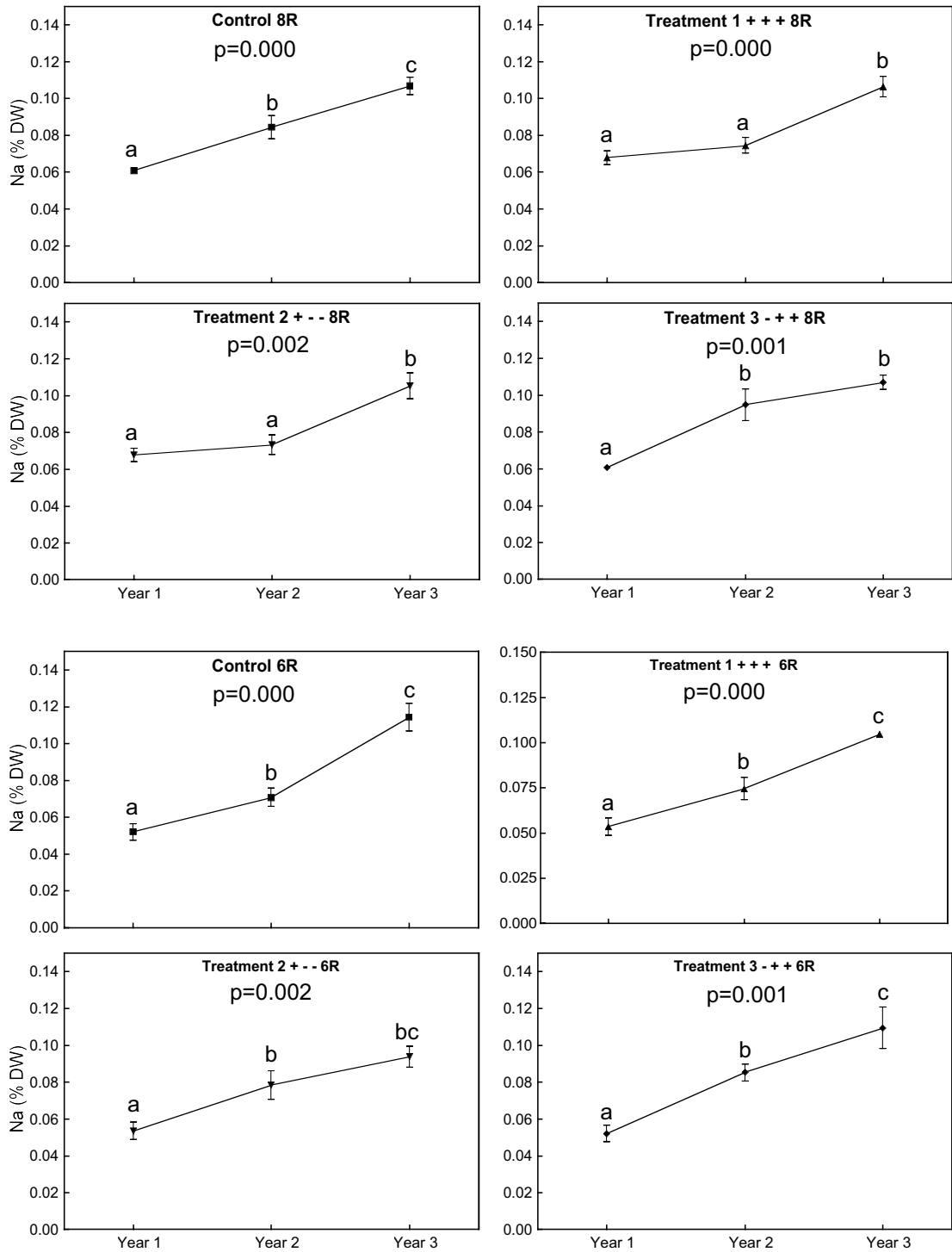


**Figure A3.12 Mean Na (% DW) concentration in petioles at 50 – 80% flowering for clones 8R and 6R over the 3 years of the trial. Toxic levels of Na occur at 0.5 % DW (Reuter and Robinson, 1997).**

Values are mean  $\pm$  SEM (n=3-4). Results with the same letter are not significantly different.

**Table A3.3 Clonal differences between the years and treatment for sodium petiole concentrations in years 1, 2 and 3 of the trial.**

<b>Year</b>	<b>Treatment</b>	<b>Clone X is significantly different to clone Y</b>	<b>Clone Y is significantly different to clone X</b>	<b>P value (0.05 level)</b>
<b>Year 1</b>	Treatment 1	Q45-14	8R	0.023
		8R	6R	0.029
	Treatment 2	Q45-14	8R	0.023
		6R	8R	0.029
<b>Year 2</b>	Control	D3V14	6R	0.021
<b>Year 3</b>	Control	D3V14	Q45-14	0.044

**Appendix 4. Scientific soil classification for the McLaren Vale Vine Improvement Society cv. Merlot clonal trial site by David Maschmedt (PIRSA) (Gridley, 2003).**

**Soil profile descriptions**

In the absence of information, it is assumed that all horizon boundaries are clear or sharper (i.e. the change from one layer to the next occurs over a vertical interface of less than 5 cm). pH estimates made using a Inoculo Field pH Test Kit. Profiles are classified according to the Australian Soil Classification (ASC) (Isbell, 1996)

**General description**

Self mulching? Black vertosol (if soil cracks to the surface) or Eutrophic, Black Dermosol; medium, non-gravelly, clayey/clayey, deep (if soil does not crack to the surface).

**Table A4.1 General soil description by David Maschmedt (PIRSA).**

NOTE: This table is included on page 238 of the print copy of the thesis held in the University of Adelaide Library.

**Table A4.2 Soil chemical properties David Maschmedt (PIRSA).**

NOTE: This table is included on pages 238-239 of the print copy of the thesis held in the University of Adelaide Library.